

4913

NATIONAL LIBRARY
OTTAWA



BIBLIOTHÈQUE NATIONALE
OTTAWA

NAME OF AUTHOR... *NEIL S. ANGELMAN*

TITLE OF THESIS... *NUCLEAR MAGNETIC RESONANCE
AND ELECTRON PARAMAGNETIC
RESONANCE STUDIES IN INORGANIC SYSTEMS*

UNIVERSITY... *OF ALBERTA*

DEGREE FOR WHICH THESIS WAS PRESENTED... *PH. D.*

YEAR THIS DEGREE GRANTED... *1967*

Permission is hereby granted to THE NATIONAL LIBRARY
OF CANADA to microfilm this thesis and to lend or sell copies
of the film.

The author reserves other publication rights, and
neither the thesis nor extensive extracts from it may be
printed or otherwise reproduced without the author's
written permission.

(Signed) *N.S. Angelman*

PERMANENT ADDRESS:

Box 204

Evansburg, Alberta

.....

DATED *August 6,* 1967.

THE UNIVERSITY OF ALBERTA

NUCLEAR MAGNETIC RESONANCE AND
ELECTRON PARAMAGNETIC RESONANCE LINE WIDTH
STUDIES IN INORGANIC SYSTEMS

by



Neil Stanley Angerman

A THESIS

SUBMITTED TO THE FACULTY OF GRADUATE STUDIES
IN PARTIAL FULFILMENT OF THE REQUIREMENTS FOR THE DEGREE
OF DOCTOR OF PHILOSOPHY

Department of Chemistry

Edmonton, Alberta

Fall, 1969

THE UNIVERSITY OF ALBERTA
FACULTY OF GRADUATE STUDIES

The undersigned certify that they have read, and
recommend to the Faculty of Graduate Studies for acceptance,
a thesis entitled

NUCLEAR MAGNETIC RESONANCE AND ELECTRON
PARAMAGNETIC RESONANCE LINE WIDTH STUDIES
IN INORGANIC SYSTEMS

submitted by Neil Stanley Angerman in partial fulfilment of the
requirements for the degree of Doctor of Philosophy.

Robert B. Jordan.....
Supervisor

H.B. Duff.....

A. Darwin.....

Ronald G. Howell.....

D.G. Hughes.....

Robert E. Cornwell.....
External Examiner

..August..1,.... 1969.

ACKNOWLEDGMENTS

I would like to express my sincere gratitude to Dr. Robert B. Jordan for his constant advice throughout the course of this work.

I am also grateful for the secretarial assistance of Mrs. Gladys Whittal.

Financial assistance from the University of Alberta and the National Research Council of Canada was greatly appreciated.

ABSTRACT

Chapter I which is divided into three sections serves as an introduction to this thesis. Section 1 discusses previous studies which use the Nuclear Magnetic Resonance (NMR) and Electron Paramagnetic Resonance (EPR) techniques in inorganic kinetics. Section 2 deals briefly with the theory of NMR line broadening as applied to exchange reactions; the modifications to the general theory which have been used in this thesis are indicated in this section. Section 3 deals with the theory necessary to extract tumbling correlation times from the line widths in an EPR spectrum.

Chapter II discusses the preparation and characterization of the complexes studied here. Methods of purification of all the reagents and discussion of the instrumentation are also included in this chapter.

Chapter III contains six sections which discuss the various systems on which the NMR line broadening technique was used. Section 1 deals with the proton NMR line broadenings caused by the paramagnetic vanadyl ion in the solvents N,N-dimethylformamide, acetonitrile, dimethylsulfoxide, trimethylphosphate and trimethylphosphite. Activation enthalpies, entropies and exchange rates were obtained for the N,N-dimethylformamide and acetonitrile systems; however, only limits on the exchange rates could be obtained for the other systems. Exchange was too fast to measure by the NMR technique in dimethylsulfoxide and

trimethylphosphate and too slow in trimethylphosphite. Solvent proton relaxation in these latter cases was best accounted for by a dipolar interaction between the unpaired electron on the vanadyl ion and the protons of one rapidly exchanging inner sphere molecule plus a similar interaction with a continuum of outer sphere molecules.

Section 2 discusses the behavior of the vanadyl ion, vanadyl acetylacetonate and vanadyl trifluoroacetylacetonate in various alcohols. Differences in the hydroxy and methyl proton exchange rates for the vanadyl ion in methanol can be accounted for by proton dissociation and exchange of whole solvent molecules, respectively. Results on the chelated systems were explained by rapid exchange of one solvent molecule on the complex with intramolecular proton transfer to the oxygen of the chelating ligand.

Section 3 outlines the results of a study of the NMR line broadening of the methanol resonances by copper acetylacetonate and the solvated copper(II) ion. Line broadening in the former system was attributed to a dipolar interaction process involving two rapidly exchanging inner sphere molecules and a continuum of outer sphere molecules. In the latter system the line broadening was accounted for by rapid exchange of methanol molecules and a labile equilibrium forming a species with a hydroxy proton dissociated from a methanol molecule in the first coordination sphere of the copper(II) ion.

Section 4 discusses the NMR line broadening of solvent methanol and trimethylphosphate protons by solvated chromium(II) and vanadium(II) ions. The results for the chromium(II) systems can be explained by either rapid exchange of the bulk solvent or by ligand interchange between the axial and equatorial positions on the Jahn-Teller distorted chromium(II) ion. In the case of vanadium(II), methanol exchange was too slow and trimethylphosphate exchange too fast to measure by the NMR line broadening technique.

Section 5 deals with the line broadening of the dimethylsulfoxide and trimethylphosphate proton resonances by nickel(II) and cobalt(II). The nickel(II)-dimethylsulfoxide system is the only one that yielded all the kinetic parameters for solvent molecule exchange. Only limits on the exchange rates could be obtained for the other systems. The cobalt(II)-trimethylphosphate system was unique in that an octahedral-tetrahedral equilibrium existed between the cobalt(II) and the coordinating trimethylphosphate.

In section 6 the results of a NMR study on vanadium(III) in *N,N*-dimethylformamide are reported. It was found that an octahedral-tetrahedral equilibrium also exists in this system. All the kinetic parameters for ligand exchange were obtained for both the octahedral and tetrahedral complexes.

An Electron Paramagnetic Resonance line width study of the vanadyl ion in various solvents is discussed in Chapter IV. It was found that the EPR theory of Kivelson could be used to

extract tumbling correlation times of the solvated complexes from the hyperfine resonance line widths. These tumbling correlation times were used in the interpretation of the NMR data. A residual line width was observed which could not be accounted for by Kivelson's theory or by a spin-rotational relaxation mechanism. The origin of this excess line width is discussed.

Chapter V is a general discussion on the factors affecting ligand exchange on transition metal ions. A survey of the available exchange data indicates that the main contributions to ligand exchange activation enthalpies are a crystal field factor and a solvation factor.

TABLE OF CONTENTS

	<u>Page</u>
Acknowledgements	iii
Abstract	iv
List of Figures	xi
List of Tables	xvi
I INTRODUCTION	1
1. General Comments	1
2. Nuclear Magnetic Resonance Theory	3
3. Electron Paramagnetic Resonance Theory	17
II THE PREPARATION AND CHARACTERIZATION OF COMPLEXES, PURIFICATION OF REAGENTS AND INSTRUMENTATION	24
1. Purification of Solvents	24
2. Preparation of penta-N,N-dimethylformamidovanadyl perchlorate	25
3. Preparation of pentaquovanadyl perchlorate and pentaquovanadyl tetrafluoroborate	26
4. Preparation of vanadyl tetrafluoroborate complexes with acetonitrile, trimethylphosphate, trimethyl- phosphite and dimethylsulfoxide	26
5. Preparation of pentamethanol vanadyl perchlorate	28
6. Preparation of bisacetylacetonato-oxovanadium(IV)	29

	<u>Page</u>
7. Preparation of bistrifluoroacetylacetonato-oxovanadium(IV)	29
8. Preparation of trisacetylacetonatovanadium(III)	29
9. Preparation of bisacetylacetonatocopper(II) and hexamethanol copper(II) perchlorate	30
10. Preparation of chromium(II) and vanadium(II) tetrafluoroborate complexes in methanol and trimethylphosphate	31
11. Preparation of nickel(II) and cobalt(II) perchlorate complexes of dimethylsulfoxide and trimethylphosphate	33
12. Preparation of hexa-N,N-dimethylformamidovanadium(III) perchlorate	34
13. Instrumentation	35
14. The preparation of NMR and EPR samples and the determination of their spectra	36
III NUCLEAR MAGNETIC RESONANCE LINE BROADENING STUDIES OF NONAQUEOUS SOLVENTS CONTAINING TRANSITION METAL IONS	37
1. Line Broadening of the Nuclear Magnetic Resonances of N,N-Dimethylformamide, Acetonitrile, Dimethylsulfoxide, Trimethylphosphate and Trimethylphosphite by the Vanadyl Ion	37
2. Line Broadening of the Nuclear Magnetic Resonances of Methanol, Trichloroethanol and Trifluoroethanol by Vanadyl Complexes	56

	<u>Page</u>
3. Nuclear Magnetic Resonance Line Broadenings of Nonaqueous Methanol by Copper(II) Complexes	93
4. Nuclear Magnetic Resonance Line Broadening of Methanol and Trimethylphosphate by Chromium(II) and Vanadium(II)	109
5. Proton Relaxation in Dimethylsulfoxide and Trimethylphosphate by Nickel(II) and Cobalt(II) Perchlorates	122
6. Nuclear Magnetic Resonance Line Broadening of N,N-dimethylformamide Resonances by Vanadium(III). . .	150
 IV ELECTRON PARAMAGNETIC RESONANCE LINE WIDTH STUDY OF THE VANADYL ION IN VARIOUS SOLVENTS.	 159
 V GENERAL DISCUSSION ON LIGAND EXCHANGE ON TRANSITION METAL IONS	 190
 Literature Cited	 203
Appendix A - Tables of Data for the Figures in the Text . .	211
Appendix B - Electron Paramagnetic Resonance Computer Programme	253

LIST OF FIGURES

<u>Figure</u>		<u>Page</u>
1	Temperature dependence of $\log (T_{2p}')^{-1}$ for the formyl proton resonance of N,N-dimethylformamide containing vanadyl perchlorate.	41
2	Temperature dependence of $\log (T_{2p}')^{-1}$ for the methyl proton resonance at 60 MHz of acetonitrile containing vanadyl perchlorate.	42
3	Temperature dependence of $\log (T_{2p}')^{-1}$ for the proton resonances of trimethylphosphite at 60 MHz, dimethylsulfoxide at 60MHz and trimethylphosphate at 100 MHz, all containing vanadyl tetrafluoroborate.	43
4	Temperature dependence of $\log (T_{2p}')^{-1}$ at 60 MHz for the protons of methanol containing vanadyl perchlorate.	58
5	Temperature dependence of $\log (T_{2p}')^{-1}$ at 60 MHz for the protons of methanol containing vanadyl acetylacetonate.	59
6	Temperature dependence of $\log (T_{2p}')^{-1}$ at 60 MHz for the protons of methanol containing vanadyl trifluoroacetylacetonate.	60
7	Temperature dependence of $\log (T_{2p}')^{-1}$ at 60 MHz for the protons of trichloroethanol containing vanadyl acetylacetonate.	61

<u>Figure</u>		<u>Page</u>
8	Temperature dependence of $\log (T_{2p}^{-1})$ at 60 MHz for the protons of trifluoroethanol containing vanadyl acetylacetonate.	62
9	A proposed mechanism for the exchange of the hydroxy proton of methanol for the system of vanadyl acetylacetonate in methanol.	76
10	Temperature dependence of $\log (T_{2p}^{-1})$ at 60 MHz for the protons of methanol containing copper acetylacetonate.	94
11	Temperature dependence of $\log (T_{2p}^{-1})$ at 60 MHz for the protons of methanol containing copper(II) perchlorate and copper(II) perchlorate in 1.5 molar hexafluorophosphoric acid.	98
12	Temperature dependence of the shift normalized to 1 molal at 60 MHz for the protons of methanol containing copper(II) perchlorate and copper(II) perchlorate in 1.5 molar hexafluorophosphoric acid.	99
13	Due to reanalysis of the data in Chapter III, section 3 with a computer programme this figure has been omitted.	
14	Temperature dependence of $\log (T_{2p}^{-1})$ at 60 MHz for the protons of methanol containing chromium(II) tetrafluoroborate.	111

<u>Figure</u>		<u>Page</u>
15	Temperature dependence of the shift normalized to 1 molal at 60 MHz for the protons of methanol containing chromium(II) tetrafluoroborate.	112
16	Temperature dependence of $\log (T_{2p}')^{-1}$ at 60 MHz for the protons of methanol containing vanadium(II) tetrafluoroborate.	113
17	Temperature dependence of $\log (T_{2p}')^{-1}$ at 60 MHz for the protons of trimethylphosphate containing chromium(II) tetrafluoroborate.	114
18	Temperature dependence of $\log (T_{2p}')^{-1}$ at 60 MHz for the protons of trimethylphosphate containing vanadium(II) tetrafluoroborate.	115
19	Temperature dependence of $\log (T_{2p}')^{-1}/P_M$ for the protons of dimethylsulfoxide at 60 MHz containing nickel(II) perchlorate, and at 60 MHz containing cobalt(II) perchlorate.	123
20	Temperature dependence of the shift of the protons of dimethylsulfoxide at 100 MHz and at 60 MHz containing nickel(II) perchlorate, and at 60 MHz containing cobalt(II) perchlorate.	124
21	Temperature dependence of $\log (T_{2p}')^{-1}$ at 60 MHz for the protons of trimethylphosphate containing nickel(II) perchlorate.	131

<u>Figure</u>		<u>Page</u>
22	Temperature dependence of the shift at 60 MHz for the protons of trimethylphosphate containing nickel(II) perchlorate.	132
23	Temperature dependence of $\log (T_{2p}')^{-1}$ at 60 MHz and at 100 MHz for the formyl proton of N,N-dimethylformamide containing vanadium(III) perchlorate.	152
24	Temperature dependence of the shift normalized to 1 molal for the formyl proton of N,N-dimethylformamide containing vanadium(III) perchlorate.	153
25	Glass EPR spectrum of 10^{-2} molal vanadyl perchlorate in N,N-dimethylformamide at -173°C .	164
26	Solution EPR spectrum of 10^{-2} molal vanadyl perchlorate in N,N-dimethylformamide at 25°C .	165
27	Temperature and quantum number dependence of the EPR hyperfine line width of a solution spectrum of 10^{-3} molal vanadyl perchlorate in water.	169
28	Temperature dependence of the average g-value for a solution of 10^{-3} molal vanadyl perchlorate in water.	181
29	Temperature dependence of the average hyperfine coupling constant of a solution of 10^{-3} molal vanadyl perchlorate in water.	182

FigurePage

30 Temperature dependence of the residual line
width for a solution of 10^{-3} molal vanadyl
perchlorate in water.

185

LIST OF TABLES

<u>Table</u>		<u>Page</u>
I	Spectral properties of vanadyl ion in various solvents	40
II	Kinetic parameters for solvent exchange on the solvated vanadyl ion	49
III	Interaction distances for inner (r_1) and outer (r_o) sphere dipole-dipole broadening	52
IV	Rate parameters for solvent exchange with vanadyl complexes	83
V	Inner and outer sphere parameters for various vanadyl complex-alcohol systems	88
VI	The least squares parameters which best fit the broadening data for the $Ni(ClO_4)_2$ -dimethylsulfoxide broadening	127
VII	Calculated and observed NMR results for the cobalt(II)-trimethylphosphate system	134
VIII	Spectrophotometric results for the cobalt(II)-trimethylphosphate system	139
IX	Exchange rates and hyperfine coupling constants for nickel(II) and cobalt(II) in dimethylsulfoxide (DMSO) and trimethylphosphate (TMPA)	146
X	EPR parameters for vanadyl complexes in various solvents	163

<u>Table</u>		<u>Page</u>
XI	Temperature dependence of the viscosity and density for trichloroethanol and trifluoroethanol	167
XII	Parameters obtained from the EPR study of vanadyl acetylacetonate-alcohol systems	170
XIII	EPR parameters for vanadyl perchlorate in water	171
XIV	EPR parameters for vanadyl acetylacetonate in ethanol	172
XV	EPR parameters for vanadyl acetylacetonate in n-propanol	173
XVI	EPR parameters for vanadyl acetylacetonate in isopropanol	174
XVII	EPR parameters for vanadyl acetylacetonate in n-butanol	175
XVIII	EPR parameters for vanadyl acetylacetonate in t-butanol	176
XIX	EPR parameters for vanadyl acetylacetonate in trifluoroethanol	177
XX	EPR parameters for vanadyl acetylacetonate in trichloroethanol	178
XXI	EPR parameters for vanadyl trifluoroacetylacetonate in methanol	179

<u>Table</u>		<u>Page</u>
XXII	Parameters obtained from the excess residual EPR line widths for the vanadyl ion-solvent systems at 25°C	189
XXIII	Kinetic exchange parameters and spectroscopic parameters for nickel(II) in various solvents	199
XXIV	Kinetic exchange parameters and spectroscopic parameters for cobalt(II) in various solvents	200
XXV	Kinetic exchange parameters and spectroscopic parameters for the vanadyl ion in various solvents	201
XXVI	Physical properties for some solvents	202
XXVII	Temperature dependence of the water proton line width at 60 MHz	212
XXVIII	Temperature dependence of the formyl proton line width of N,N-dimethylformamide at 60 MHz	213
XXIX	Temperature dependence of the hydroxy and methyl proton line widths of methanol at 60 MHz	214
XXX	Temperature dependence of the methyl proton line width of acetonitrile at 60 MHz	215
XXXI	Temperature dependence of the methyl proton line width of dimethylsulfoxide at 60 MHz	216
XXXII	Temperature dependence of the methyl proton line width of trimethylphosphate at 60 MHz	217

<u>Table</u>	<u>Page</u>	
XXXIII	Temperature dependence of the methyl proton line width of trimethylphosphite at 60 MHz	218
XXXIV	Proton line broadening for 0.0907 molal, 0.0276 molal, and 0.0547 molal solutions of $\text{VO}(\text{ClO}_4)_2$ in N,N-dimethylformamide. Frequency: 60 MHz and 100 MHz.	219
XXXV	Proton line broadening of a 0.0851 molal solution of $\text{VO}(\text{ClO}_4)_2$ in acetonitrile. Frequency: 60 MHz.	221
XXXVI	Proton line broadening of a 0.1563 molal solution of $\text{VO}(\text{BF}_4)_2$ in trimethylphosphite. Frequency: 60 MHz.	222
XXXVII	Proton line broadening of a 0.0632 molal solution of $\text{VO}(\text{BF}_4)_2$ in dimethylsulfoxide. Frequency: 60 MHz.	223
XXXVIII	Proton line broadening of 0.0726 molal and 0.0363 molal solutions of $\text{VO}(\text{BF}_4)_2$ in trimethylphosphate. Frequency: 100 MHz.	224
XXXIX	Proton line broadening of 0.123 molal and 0.101 solutions of $\text{VO}(\text{ClO}_4)_2$ in methanol. Frequency: 100 MHz and 60 MHz.	225
XL	Proton line broadening of a 0.067 molal solution of $\text{VO}(\text{acac})_2$ in methanol. Frequency: 60 MHz.	226
XLI	Proton line broadening of a 0.2186 molal solution of $\text{VO}(\text{tfac})_2$ in methanol. Frequency: 60 MHz.	227

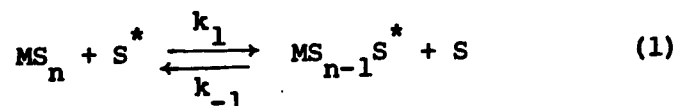
<u>Table</u>		<u>Page</u>
XLII	Proton line broadening of a 0.0073 molal solution of VO(acac) ₂ in trichloroethanol. Frequency: 100 MHz.	228
XLIII	Proton line broadening of a 0.0613 molal solution of VO(acac) ₂ in trifluoroethanol. Frequency: 60 MHz.	229
XLIV	Proton line broadening of 0.175 molal and 0.069 molal solutions of copper acetylacetonate in methanol. Frequency: 60 MHz.	230
XLV	Proton line broadening and shift for a 0.0175 molal solution of Cu(ClO ₄) ₂ and 1.56 molar H ₃ PF ₆ in methanol. Frequency: 60 MHz.	231
XLVI	Proton line broadening of 0.0151 molal and 0.00999 molal solutions of Cu(ClO ₄) ₂ in methanol. Frequency: 60 MHz.	232
XLVII	Proton line shift of 0.0151 molal and 0.00999 molal solutions of Cu(ClO ₄) ₂ in methanol. Frequency: 60 MHz.	233
XLVIII	Proton line broadening and shift for a 0.1503 molal solution of Cr(BF ₄) ₂ in methanol. Frequency: 60 MHz.	234
XLIX	Proton line broadening of a 0.1523 molal solution of V(BF ₄) ₂ in methanol. Frequency: 60 MHz.	235

<u>Table</u>		<u>Page</u>
L	Proton line broadening of a 0.5285 molal solution of $\text{Cr}(\text{BF}_4)_2$ in trimethylphosphate. Frequency: 60 MHz.	236
LI	Proton line broadening of a 0.967 molal solution of $\text{V}(\text{BF}_4)_2$ in trimethylphosphate. Frequency: 60 MHz.	237
LII	Proton line broadening of 0.219 molal and 0.181 molal solutions of $\text{Ni}(\text{ClO}_4)_2$ in dimethylsulfoxide	238
LIII	Proton line shift of 0.219 molal and 0.181 molal solutions of $\text{Ni}(\text{ClO}_4)_2$ in dimethylsulfoxide	240
LIV	Proton line broadening and shift of 0.413 molal and 0.356 molal solutions of $\text{Co}(\text{ClO}_4)_2$ in dimethylsulfoxide. Frequency: 60 MHz.	242
LV	Proton line broadening and shift of 0.137 molal, 0.244 molal and 0.432 molal solutions of $\text{Ni}(\text{ClO}_4)_2$ in trimethylphosphate. Frequency: 60 MHz.	243
LVI	Proton line broadening and shift of a 0.495 molal solution of $\text{Co}(\text{ClO}_4)_2$ in trimethylphosphate. Frequency: 60 MHz.	246
LVII	Proton line broadening of 0.150, 0.160 molal and 0.120 molal solutions of $\text{V}(\text{ClO}_4)_3$ in N,N-dimethylformamide	248
LVIII	Proton line shift of a 0.085 molal solution of $\text{V}(\text{ClO}_4)_3$ in N,N-dimethylformamide	252

CHAPTER I: INTRODUCTION

1. General Comments

The nuclear magnetic resonance (NMR) line broadening technique is a very useful tool for determining kinetic parameters for exchange reactions. Of particular interest in inorganic solution kinetics are the rates of solvent exchange from the first coordination sphere of a metal ion. This exchange process is commonly denoted as:



where S and S* are chemically the same and n is the number of solvent molecules in the first coordination sphere of the metal, M.

Comparisons of the rates for the above reaction and the rates of ligand substitution processes determined by various flow and fast relaxation techniques have led to some useful conclusions about the mechanism of ligand exchange. These results, which are summarized in recent reviews (1-4), indicate that substitution generally occurs by an S_N1 ion pair type mechanism. It has also been found that the variation of the water exchange rate for various first row transition metal ions may be correlated by crystal or ligand field theory. This theory should also predict the variation of the exchange rate with varying solvent ligands.

A number of studies on cobalt(II) and nickel(II) in various aqueous and nonaqueous solvents (6-16) indicate that crystal field effects may be important in ligand exchange processes; however,

it is difficult to separate this factor from a general solvent effect. The vanadyl ion, being a d^1 -system, should show relatively small variation in exchange rate due to crystal field effects because the lone electron is in a π -type, d_{xy} orbital. Therefore, studies of the vanadyl ion in various solvents should permit some estimation of general solvent effects on ligand exchange rates. These effects may then be compared to cobalt(II) and nickel(II) to help sort out the solvent and crystal field effects.

In addition to the NMR study an Electron Paramagnetic Resonance (EPR) line broadening study of the vanadyl complexes in various solvents was also undertaken. The variation in line width of the vanadyl ion hyperfine EPR lines has been interpreted in terms of the theory developed by Kivelson (17). The fitting of the EPR line widths to this theory provides a value for the rotational tumbling time of the vanadyl complex. The values for the tumbling times have been used in the interpretation of the NMR line broadening.

The temperature dependence of the EPR line broadening was also studied in several vanadyl-alcohol systems to test the predictions of Kivelson's theory about the variation in the EPR hyperfine line widths with the viscosity of the solvent, and to determine if the tumbling times of the complexes obeyed the Debye formula for the rotation of solid spheres in solution. It was generally found in this work that the theory provided

an adequate description of the EPR hyperfine line widths and that the Debye formula, with a suitable hydrodynamic radius, does describe the tumbling motion of the vanadyl complexes.

Studies similar to this have been undertaken by a number of other workers (17-28). Wilson and Kivelson (24,26) have shown that Kivelson's theory predicts the proper dependence of the EPR hyperfine lines in vanadyl acetylacetonate on solvent viscosity, and that the motion of this complex can be adequately explained by the Debye formula using a radius of 3.28\AA in noncoordinating solvents. McCain and Myers (27) found that Kivelson's theory did not give an adequate description of the EPR hyperfine line widths of the vanadyl ion in aqueous solution. However, on the basis of the EPR work presented in this thesis it was concluded that Kivelson's theory will adequately predict the hyperfine line widths of the aquo vanadyl ion if appropriate experimental errors are assigned to the measured line widths.

2. Nuclear Magnetic Resonance Theory

The variation in magnetization of a system is adequately described for the purpose of this work by the Bloch phenomenological equations which were first presented in two papers by Wanagsness and Bloch (29) and Bloch (30) and later were modified by McConnell (31) to include exchange. The modified Bloch equations give the change in magnetization (M) of the bulk solvent molecules (S), which are

exchanging with a site on the metal ion (M), as:

$$\frac{dM_x^S}{dt} = \gamma \left\{ M_y^S H_0 + M_z^S H_1 \sin \omega t \right\} - \frac{M_x^S}{T_{2S}} - \frac{M_x^S}{\tau_S} + \frac{M_x^M}{\tau_M} \quad (2-a)$$

$$\frac{dM_y^S}{dt} = \gamma \left\{ M_z^S H_1 \cos \omega t - M_x^S H_0 \right\} - \frac{M_y^S}{T_{2S}} - \frac{M_y^S}{\tau_S} + \frac{M_y^M}{\tau_M} \quad (2-b)$$

$$\begin{aligned} \frac{dM_z^S}{dt} = \gamma \left\{ -M_x^S H_1 \sin \omega t - M_y^S H_1 \cos \omega t \right\} + \\ \frac{M_0^S}{T_{1S}} - \frac{M_z^S}{T_{1S}} - \frac{M_z^S}{\tau_S} + \frac{M_z^M}{\tau_M} \end{aligned} \quad (2-c)$$

The corresponding equations for the change of magnetization of molecules in the site adjacent to the metal ion (M) can be obtained by interchanging the S's for M's in the above equations. In these equations M_0 is the equilibrium magnetization, $2H_1$ is the magnitude of the sinusoidally varying magnetic field perpendicular to the main magnetic field, M_z is the magnetization induced in the system in an arbitrarily defined z-direction usually taken in the direction of the external magnetic field, M_x and M_y are magnetizations perpendicular to M_z and to each other, γ is the magnetogyric ratio of the species of interest and is the proportionality between the resonance frequency in radians per sec for the magnetic species and

the magnetic field in gauss, ω is the frequency associated with the sinusoidally varying H_1 , T_1 is the longitudinal (spin-lattice) relaxation time which is dependent on the interaction between the magnetic species and the lattice (solvent), T_2 is the transverse (spin-spin) relaxation time which depends upon the phase correlation of the magnetic species in the different sites, t is the time, τ_S and τ_M are the lifetimes of the magnetic species in the bulk solvent and in the first coordination sphere of the metal ion, respectively. The superscripts, M and S, have been dropped in the above definitions of the symbols since the definitions apply for either site S or site M.

The modified Bloch equations can be transformed, for mathematical convenience, into rotating coordinates moving at the same angular velocity as the radio frequency field (H_1) by the following relationships:

$$u = M_x \cos \omega t - M_y \sin \omega t \quad (3)$$

and

$$v = M_x \sin \omega t - M_y \cos \omega t \quad (4)$$

where the parameters have the same definition as above. With the additional definition

$$G = u + i v \quad (5)$$

equations (2-a) and (2-b) reduce to

$$\frac{dG_S}{dt} + \left\{ \frac{1}{\tau_S} + \frac{1}{T_{2S}} - i(\omega_S - \omega) \right\} G_S - \frac{G_M}{T_M} = -i \gamma H_1 M_o^S \quad (6)$$

This equation gives the rate of change of magnetization in the x and y directions in the bulk solvent. Similarly, the rate of change of magnetization for a magnetic species in the first coordination sphere of the metal ion is given as

$$\frac{dG_M}{dt} + \left\{ \frac{1}{\tau_M} + \frac{1}{T_{2M}} - i(\omega_M - \omega) \right\} G_M - \frac{G_S}{\tau_S} = -i \gamma H_1 M_O^M \quad (7)$$

ω_S and ω_M are the resonance frequencies for the magnetic species in the bulk solvent and in the first coordination sphere of the metal ion, respectively.

If the condition of slow passage through all resonances is established, then a steady state of magnetization exists in the system in which case $dG_S/dt = dG_M/dt = 0$. Equations (6) and (7) can then be written as:

$$\left\{ \frac{1}{\tau_S} + \frac{1}{T_{2S}} - i\Delta\omega_S \right\} G_S - \frac{G_M}{\tau_M} = -i \gamma H_1 M_O^S \quad (8)$$

and

$$\left\{ \frac{1}{\tau_M} + \frac{1}{T_{2M}} - i\Delta\omega_M \right\} G_M - \frac{G_S}{\tau_S} = -i \gamma H_1 M_O^M \quad (9)$$

respectively, where $\Delta\omega_S = \omega_S - \omega$ and $\Delta\omega_M = \omega_M - \omega$. The approximation that $M_O^M \ll M_O^S$ is now made because the concentration of M is usually small compared to the concentration of S. Solving equations (8) and (9) for G_S and comparing this result to the general solution of the Bloch equations which are not modified for chemical exchange

{equation (10-4) of reference (32)} it can be shown that the imaginary part corresponding to the absorption mode yields:

$$\frac{1}{T_{2p}} = \frac{1}{T_{2OBS}} - \frac{1}{T_{2S}} = \frac{\{(\tau_{2M}^{-1})^2 + (\tau_{2M}\tau_M)^{-1} + \Delta\omega_M^2\}}{\tau_S\{[(\tau_{2M}^{-1}) + (\tau_M^{-1})]^2 + \Delta\omega_M^2\}} \quad (10)$$

and

$$\Delta\omega_p = -\Delta\omega_S = \frac{\Delta\omega_M}{\tau_M\tau_S\{[(\tau_{2M}^{-1}) + (\tau_M^{-1})]^2 + \Delta\omega_M^2\}} \quad (11)$$

where T_{2OBS} is the transverse relaxation time observed for the bulk solvent in a solution containing a small concentration of M in S and $\Delta\omega_S$ is the observed chemical shift from some reference point for the bulk solvent in this same solution. In order to determine the parameters in the above equations from the experimental data it is necessary to first look at the line shape function $\{g(\nu)\}$ for a Lorentzian curve which may be derived from the Bloch equations (32):

$$g(\nu) = \frac{2T_2}{1 + 4\pi^2 T_2^2 (\nu_0 - \nu)^2 + \gamma^2 H_1^2 T_1 T_2} \quad (12)$$

If the magnitude of the oscillating magnetic field is small so that saturation does not occur, then

$$\gamma^2 H_1^2 T_1 T_2 \ll 1. \quad (13)$$

Equation (12) then becomes

$$g(\nu) = \frac{2T_2}{1 + 4\pi^2 T_2^2 (\nu_0 - \nu)^2} \quad (14)$$

From this equation it can be shown that the full width at half maximum height $\{\Delta\nu_{\frac{1}{2}} \text{ Hz}\}$ is related to the transverse relaxation time T_2 by

$$\frac{1}{T_2} = \pi \Delta\nu_{\frac{1}{2}}. \quad (15)$$

Therefore, $1/T_{2\text{OBS}}$ and $1/T_{2\text{S}}$ can be obtained by measuring the full width at half height of the resonance signal for a solution of M in S, and for pure S, respectively. $\Delta\omega_{\text{S}}$ in radians per sec can be obtained by measuring the shift in Hz from some internal standard for the solution of M in S ($\Delta\nu_{\text{OBS}}$) and for the pure solvent ($\Delta\nu_{\text{S}}$), respectively, and using the relationship

$$\Delta\omega = 2\pi\Delta\nu. \quad (16)$$

From the general relationship for τ :

$$\frac{1}{\tau} = \frac{\text{Rate of disappearance of a species}}{\text{Concentration of the same species}} \quad (17)$$

the following expressions for τ_{S} and τ_{M} can be obtained upon consideration of equation (1):

$$\frac{1}{\tau_{\text{S}}} = k_1 \{n[\text{MS}_n]\} \quad (18\text{-a})$$

and

$$\frac{1}{\tau_{\text{M}}} = k_{-1} \{[\text{S}] - n[\text{MS}_n]\}; \quad (18\text{-b})$$

where [S] is the total solvent molality of pure solvent. Then, the following relationship exists between the two life times above if

$$k_1 = k_{-1}:$$

$$\frac{1}{\tau_S} = \{n[MS_n]/([S]-n[MS_n])\} \frac{1}{\tau_M} = \frac{P_M}{\tau_M} \quad (19)$$

P_M is the probability of S being in the first coordinate sphere of M. All concentrations are taken in molal units, m, throughout this study.

It is usual practice to express the temperature dependence of $\frac{1}{\tau_M}$ using the transition state theory expression

$$\frac{1}{\tau_M} = \frac{kT}{h} \exp(-\Delta H^\ddagger/RT + \Delta S^\ddagger/R) \quad (20)$$

where k is Boltzmann's constant, h is Planck's constant, T is the absolute temperature, R is the gas constant, ΔH^\ddagger and ΔS^\ddagger are the reaction enthalpy and entropy, respectively. The expression for $\Delta\omega_M$ was developed by Bloembergen (7) from consideration of the hyperfine interaction between the unpaired electrons on M and the magnetic nuclei on S. This expression is given as:

$$\Delta\omega_M = -2\pi \left(\frac{A}{h}\right) \frac{\omega_o \mu_{eff} \beta \sqrt{S(S+1)}}{3k T \gamma_I} \quad (21)$$

If the spin only value for μ_{eff} is assumed then

$$\Delta\omega_M = -\frac{\omega_o S(S+1)h}{3k T} \left(\frac{A}{h}\right) \frac{\gamma_e}{\gamma_I} \quad (22)$$

where ω_o is the operating frequency in radians, k, h and T have their usual meanings, A/h is the hyperfine coupling constant, S is the sum of the spins of the unpaired electrons on M, γ_e and γ_I are the magnetogyric ratios of the electron and the magnetic nucleus,

respectively, and μ_{eff} is the effective magnetic moment of M.

The evaluation of a theoretical expression for the T_{2M} relaxation mechanism in equation (10) has been treated in detail by Solomon in a review article on "*Relaxation Processes in a System of Two Spins*" (33). The interaction considered is between two species, the unpaired electrons on the metal ion (M) and the magnetic particle on the coordinated solvent (S). These spins are denoted as \vec{S} and \vec{I} , respectively. The total Hamiltonian for these spins along the z-direction in a magnetic field, H_0 , is:

$$H = H_0 - \hbar \gamma_I H_0 I_z - \hbar \gamma_e H_0 S_z + H' \quad (23)$$

where $\hbar = h/2\pi$, H_0 is the external magnetic field, I_z and S_z are the z-components taken in the direction of H_0 for \vec{I} and \vec{S} , respectively, and H_0 is the Hamiltonian for the motion of particles. Similar equations can be written for the Hamiltonian in the x and y directions. The second two terms on the right of equation (23) are the Zeeman energies of the spins in a constant magnetic field. H' is a perturbation Hamiltonian necessary to describe the interactions between the two spins. This interaction can be of two types: the dipole-dipole interaction in which case the magnetic fields of the spins interact through space causing the spins to be relaxed or the hyperfine interaction which is an indirect interaction between the spins due to spin polarization of the electrons through the bonds in the complex. The perturbing

Hamiltonian then has the following form

$$H' = H_{DD}' + H_{HF}'$$

where H_{DD}' is the dipole-dipole interaction Hamiltonian given by

$$H_{DD}' = \{h \gamma_I \gamma_e / r_i^3\} \{3(\vec{I} \cdot \vec{r})(\vec{S} \cdot \vec{r}) - \vec{I} \cdot \vec{S}\} \quad (24)$$

and H_{HF}' is the hyperfine interaction Hamiltonian given by

$$H_{HF}' = h \left(\frac{A}{h} \right) \vec{I} \cdot \vec{S} \quad (25)$$

\vec{r} represents the vector which may be constructed between the two interacting spins and r_i is its magnitude; A/h is the isotopic hyperfine coupling constant which is a measure of the degree of interaction between the magnetic species.

The interactions between the two spins \vec{I} and \vec{S} create a time dependent perturbation on the system which causes various transitions between spin states to take place. However, if the fluctuations of the perturbation are rapid as in liquids, then the result is a time independent transition probability per unit time. By treating a system of unlike spins in this manner Solomon has obtained the following expression for $(T_{2M})^{-1}$ due to a dipole-dipole interaction (33):

$$(T_{2M})_{DD}^{-1} = \frac{1}{15} \frac{S(S+1)\gamma_I^2 g^2 \beta^2}{r_i^6} \left\{ 4(\tau_C)_1 + \frac{(\tau_C)_2}{1+(\omega_I - \omega_e)^2 (\tau_C)_2^2} + \frac{3(\tau_C)_1}{1+\omega_I^2 (\tau_C)_1^2} + \frac{6(\tau_C)_2}{1+\omega_e^2 (\tau_C)_2^2} + \frac{6(\tau_C)_2}{1+(\omega_I + \omega_e)^2 (\tau_C)_2^2} \right\} \quad (26)$$

Solomon and Bloembergen (34) obtained the following expression for $(T_{2M})^{-1}$ if a hyperfine interaction is considered:

$$(T_{2M})_{HF}^{-1} = \frac{1}{3} S(S+1) \left(\frac{A}{\hbar}\right)^2 \left\{ (\tau_e)_1 + \frac{(\tau_e)_2}{1 + (\omega_I - \omega_e)^2 (\tau_e)_2^2} \right\} \quad (27)$$

where ω_I and ω_e are the resonance frequencies of the magnetic nucleus and electron, respectively, and $(\tau_C)_1$ and $(\tau_C)_2$ are the longitudinal and transverse correlation times for the dipole-dipole interaction with the electron, respectively, and $(\tau_e)_1$ and $(\tau_e)_2$ are the longitudinal and transverse correlation times for the hyperfine interaction with the electron, respectively (15). It is general practice to assume that the longitudinal and transverse correlation times for these two interactions are equal and have the following definition:

$$(\tau_C)^{-1} = (\tau_S)^{-1} + (\tau_M)^{-1} + (\tau_R)^{-1} \quad (28)$$

and

$$(\tau_e)^{-1} = (\tau_S)^{-1} + (\tau_M)^{-1} \quad (29)$$

where τ_S , τ_M and τ_R are the correlation times for electron relaxation, for the lifetime of S on M, and for the complex tumbling. It is easily seen that the shortest correlation time in equation (28) equals τ_C and the shorter correlation time in equation (29) equals τ_e .

The expressions given in equations (26) and (27) can be simplified by noting that $\omega_I \ll \omega_e$, $\omega_I^2 \tau_e^2 \ll 1$ and $\omega_I^2 \tau_C^2 \ll 1$,

then the total equation:

$$\frac{1}{T_{2M}} = \left(\frac{1}{T_{2M}} \right)_{DD} + \left(\frac{1}{T_{2M}} \right)_{HF} \quad (30)$$

can be reduced to:

$$\frac{1}{T_{2M}} = \frac{1}{15} \frac{S(S+1)\gamma_I^2 g^2 \beta^2}{r_i^6} \left\{ 7\tau_C + \frac{13\tau_C}{1+\omega_e^2 \tau_C^2} \right\} + \quad (31)$$

$$\frac{1}{3} S(S+1) \left(\frac{A}{\hbar} \right)^2 \left\{ \tau_e + \frac{\tau_e}{1+\omega_e^2 \tau_e^2} \right\} .$$

Up to this point the T_{2M} relaxation process has dealt only with the interaction of the unlike spins for solvent molecules in the first coordination sphere of the paramagnetic centre. There is the possibility that this interaction may extend beyond the first coordination sphere and cause relaxation of spins in second and more remote spheres of the paramagnetic centre. Since the solvent molecules beyond the first coordination sphere undergo very weak interactions with the paramagnetic centre the hyperfine coupling constant for these molecules would be expected to be small; therefore, the hyperfine contribution to $(T_{2M})^{-1}$ is neglected in consideration of outer sphere relaxation. However, the dipole-dipole interaction through space cannot be neglected in consideration of outer sphere interactions. Two possibilities exist for this type of interaction (41):

(1) The lifetime of the solvent molecules in the second coordination sphere of the paramagnetic centre may be long with respect to the complex tumbling time; this results in a well defined second coordination sphere. The first term of equation (31) can then be used to calculate the contribution to $(T_{2M})^{-1}$ from this second coordination sphere by taking a reasonable interaction distance and assuming that very little contribution comes from more remote spheres because of the inverse sixth power dependence on the interaction distance.

(2) The lifetimes of the solvent molecules in spheres beyond the first coordination sphere are short with respect to the tumbling time of the complex in which case the solvent distribution can be approximated as a continuum and the $(T_{2M})^{-1}$ expression can be integrated over this continuum (68). The result of this integration gives $(T_{2p})^{-1}$ directly, that is:

$$(T_{2p})^{-1} = \frac{1}{15} \int_{r_0}^{\infty} \frac{4\pi r^2 nS(S+1) \gamma_I^2 g^2 \beta^2}{r^6} \left\{ 7\tau_c + \frac{13\tau_c}{1 + \omega_e^2 \tau_c^2} \right\} dr \quad (32-a)$$

$$(T_{2p})^{-1} = \frac{4\pi nS(S+1) \gamma_I^2 g^2 \beta^2}{45 r_0^3} \left\{ 7\tau_c + \frac{13\tau_c}{1 + \omega_e^2 \tau_c^2} \right\} \quad (32-b)$$

where all the symbols have their usual meaning and n is the number of paramagnetic centres per cubic centimeter of solution which is related to their concentration, $[M]$, Avogadro's number, N , and the

density of the solvent, ρ , by:

$$n = \rho N[M]/1000 . \quad (33)$$

This outer sphere relaxation process is independent of the inner sphere relaxation processes, therefore, equation (32-b) can be added directly to equation (10) as a separate term.

In order to simplify the interpretation of the temperature dependence of $(T_{2p})^{-1}$ and $\Delta\omega_p$ it is necessary to recognize certain limiting conditions in equations (10) and (11). The four limiting conditions noted by Swift and Connick (8) are:

$$\Delta\omega_M^2 \gg \left(\frac{1}{T_{2M}}\right)^2, \left(\frac{1}{\tau_M}\right)^2; \quad \frac{1}{T_{2p}} = \frac{P_M}{\tau_M} = \frac{1}{\tau_S} \text{ and}$$

$$\Delta\omega_p = \frac{P_M}{\Delta\omega_M \tau_M^2}, \quad (34-a)$$

relaxation occurs by a change in the precessional frequency between the two available sites and $(T_{2p})^{-1}$ is controlled by chemical exchange and $\Delta\omega_p$ is small.

$$\left(\frac{1}{\tau_M}\right)^2 \gg \Delta\omega_M^2 \gg \frac{1}{T_{2M} \tau_M}; \quad \frac{1}{T_{2p}} = P_M \tau_M \Delta\omega_M^2 \text{ and}$$

$$(34-b)$$

$$\Delta\omega_p = P_M \Delta\omega_M,$$

relaxation occurs by a change in precessional frequency which controls $(T_{2p})^{-1}$ and chemical exchange is fast. $\Delta\omega_p$ is appreciable and approaches $P_M \Delta\omega_M$ when τ_M becomes sufficiently short to make

$$\tau_M^2 \Delta\omega_M^2 < 1.$$

$$\left(\frac{1}{T_{2M}}\right)^2 \gg \Delta\omega_M^2, \left(\frac{1}{\tau_M}\right)^2, \quad \frac{1}{T_{2p}} = \frac{P_M}{\tau_M} = \frac{1}{\tau_S} \quad \text{and} \quad (34-c)$$

$$\Delta\omega_p = P_M \Delta\omega_M \left(\frac{T_{2M}}{\tau_M}\right)^2,$$

relaxation by a T_{2M} mechanism is fast causing $(T_{2p})^{-1}$ to be controlled by chemical exchange and $\Delta\omega_p$ is small since $(1/T_{2M}) \gg (1/\tau_M)$.

$$\frac{1}{T_{2M} \tau_M} \gg \left(\frac{1}{T_{2M}}\right)^2, \Delta\omega_M^2, \quad \frac{1}{T_{2p}} = \frac{P_M}{T_{2M}} \quad \text{and} \quad (34-d)$$

$$\Delta\omega_p = P_M \Delta\omega_M,$$

rapid chemical exchange occurs and $(T_{2p})^{-1}$ is controlled by an inner sphere dipole-dipole or hyperfine T_{2M} relaxation process and $\Delta\omega_p$ may be appreciable.

A fifth possibility may occur if the chemical exchange is slow and $(T_{2p})^{-1}$ is controlled by an outer sphere dipolar interaction. In this case $\Delta\omega_p$ is small because of the small coupling constant for the outer sphere. The theoretical expression for $(T_{2p})^{-1}$ is given by equation (32-b).

Since all the parameters in the general expression for $(T_{2p})^{-1}$ are dependent differently on the absolute temperature as shown by equations (20), (21), (22), (31) and (32), (the last two equations are dependent on correlation times which are assumed to have

exponential temperature dependences) a plot of $\log (T_{2p})^{-1}$ versus the inverse absolute temperature will give a good indication of the type of mechanism which controls $(T_{2p})^{-1}$. After having identified the relaxation mechanism it is then possible to obtain the magnitude of the various parameters which control the relaxation by using a graphical fitting procedure and the theoretical expressions for these parameters.

In this study a nonlinear least squares computer programme (37) was used to fit the general expression for $(T_{2p})^{-1}$ {equation (10)} to the temperature dependence of the NMR line broadening data. In analyzing the data in this manner it was still necessary to apply the limiting conditions given above in order to determine initial guesses for the adjustable parameters. It was generally found that the parameters obtained by the limiting conditions method agreed within the 95% confidence limits for the parameters obtained by the nonlinear least squares method. A copy of this programme and the directions for its use appear in reference (38).

3. Electron Paramagnetic Resonance Theory

The general theory for the factors which control the electron paramagnetic resonance (EPR) line widths has been developed and discussed by Kivelson (17). The theory applies to free radicals in diamagnetically dilute crystals or in dilute liquid solutions. The main assumptions made by Kivelson are that spin-orbital

interactions are negligible because of the quenching of orbital angular momentum, a strong applied magnetic field is used, there is small anisotropy in the radical, and negligible relaxation occurs by chemical exchange processes or intermolecular interactions. The modulation of the interaction between the free electron(s) and the nucleus due to the tumbling of the complex is taken to be the major contribution to the relaxation process.

EPR spectra of vanadyl complexes show eight hyperfine lines which result from the interaction of the one unpaired electron with the vanadium nucleus which has a spin of $7/2$. The variation in these hyperfine line widths can be analyzed by the above theory after they are related to the various quantum numbers of vanadium ($m_i = 7/2$ to $-7/2$) by the following expression

$$\frac{\sqrt{3}}{2} \left(\frac{g\beta}{h} \right) \Delta H_i = \alpha + \beta m_i + \gamma m_i^2 + \delta m_i^3 + \epsilon m_i^4. \quad (35)$$

ΔH_i is the peak to peak width of the m_i th component of the derivative spectrum of the complex, m_i is the i th quantum number, $\alpha = \alpha' + \alpha''$ where α'' is the residual line width which will be discussed subsequently, α' is the line width contribution due to modulation of the anisotropic hyperfine tensor and the anisotropic g-tensor, β is the line width contribution due to the cross correlation between these two modulations, γ is the portion of the line width due to additional modulation of the anisotropic hyperfine tensor, δ contributes to the line width because of the modulation of the

anisotropic dipolar tensor and g-tensor, and ϵ contributes because of quadrupolar relaxation and is usually essentially zero.

The residual line width (α'') has been treated most successfully in terms of a spin-rotational relaxation mechanism (25). Spin-rotational relaxation results from the inability of the electrons to rigidly follow the motion of the nuclear framework as the complex rotates. The imbalance of rotating charge creates a magnetic moment which can interact with the electron spin in the molecule. A mechanism of this type would be expected to depend on the anisotropy in the complex and on the solvent in which the complex is dissolved but not on the magnetic field. An expression for the spin-rotational interaction has been given by Hubbard (39):

$$\alpha'' = 2\sqrt{3} (\hbar/g\beta) (I^2/12\pi r^3 \hbar^2) \{ (2C_{\perp}^2 + C_{\parallel}^2) kT/\eta \} \quad (36-a)$$

where α'' is given in gauss, I is the moment of inertia, C_{\parallel} and C_{\perp} are the diagonalized components of \tilde{C} (the spin-rotational interaction tensor) along the unique molecular axis and perpendicular to it, respectively, r is the effective hydrodynamic radius of the complex, and η is the bulk solvent viscosity in poise. Now, since C_{\parallel} and C_{\perp} are not readily available, the following approximate relationship can be used (73):

$$(2C_{\perp}^2 + C_{\parallel}^2) I^2/\hbar^2 \approx (2\Delta g_{\perp}^2 + \Delta g_{\parallel}^2) \quad (36-b)$$

where $\Delta g_{\perp} = g_{\perp} - 2.0023$ and $\Delta g_{\parallel} = g_{\parallel} - 2.0023$. Combining equations (36-a) and (36-b) gives an expression which is independent of the moment of inertia, that is:

$$\alpha'' = 2\sqrt{3} (\hbar/g\beta) (12\pi r^3)^{-1} (2\Delta g_{\perp}^2 + \Delta g_{\parallel}^2) kT/\eta \quad (36-c)$$

In analyzing the EPR spectra of the vanadyl complexes the hyperfine line widths from the derivative solution spectrum were measured and fitted to equation (35) by a least squares method. This analysis yielded values for α , β , γ and δ . Theoretical expressions for α' , β , γ and δ which depend on the complex tumbling time (τ_R) have been given in Table III of reference (26). These expressions were programmed to run on an IBM 360/67 computer. This programme calculated a value of τ_R from the γ derived from the least squares fit (the latter was found to be least sensitive to experimental errors in the measurement of line widths). Then this τ_R was used to calculate β and δ from the theoretical expressions. The individual hyperfine line widths were recalculated from these parameters and the least squares value for α , and were found to agree within experimental error with the observed line widths. α'' was calculated from the theoretical expression for α' and the total value (α) obtained from the least squares fit. This value of α'' was then compared to the value predicted by the spin-rotational theory. Details of the operation of the computer programme are given in Chapter IV and a copy of the programme appears in Appendix B.

The value of τ_R was analyzed with the Debye equation

$$\tau_R = \frac{4\pi r^3 \eta}{3kT} \quad (37)$$

for the rotation of spherical particles in solution and was found to be reasonably well explained by this relationship if a suitable r was chosen.

In order to carry out the above calculations in the computer programme it was necessary to know the anisotropic components of the coupling constant (A_x, A_y, A_z) and g-value (g_x, g_y, g_z) as well as the average values, $\langle A \rangle$ and $\langle g \rangle$, respectively. The latter quantities could be obtained from the solution spectra by using the following equations (26):

$$\langle A \rangle = - \langle g \rangle \beta \{H_i - H_{-i}\} / 2m_i \hbar \quad (38-a)$$

and

$$\begin{aligned} \langle g \rangle = & g_S + g_S \{ [H_S - \frac{1}{2} (H_i - H_{-i})] / \frac{1}{2} (H_i - H_{-i}) \} \\ & - 2\langle A \rangle^2 \hbar^2 [I(I+1) - m_i^2] / g_S \beta^2 (H_i + H_{-i})^2 \end{aligned} \quad (38-b)$$

where H_i and H_{-i} are the magnetic fields of the $m_{i\text{th}}$ and $m_{-i\text{th}}$ quantum numbers (I), respectively, g_S and H_S are the g-value and resonant magnetic field of a standard of known g-value and all the other parameters have their usual meaning.

In the determination of $\langle A \rangle$ the four values for $(H_i - H_{-i}) / m_i$ were determined from the eight hyperfine lines in the vanadyl hyperfine EPR spectrum and the average of these values was

used in determining $\langle A \rangle$. Since $\langle A \rangle$ and $\langle g \rangle$ are not independent of one another, $\langle g \rangle = g_s$ was used in determining $\langle A \rangle$. This value of $\langle A \rangle$ along with the average of the values $(H_1 - H_{-1})$ and $(H_1 + H_{-1})$ was used to determine $\langle g \rangle$. $\langle g \rangle$ was generally found to be less than 2% different than g_s , therefore, no correction was made to $\langle A \rangle$.

The anisotropic components for the coupling constant and g-value were obtained by rapidly freezing the solution of vanadyl complex in liquid nitrogen in order to form a glass and then the EPR spectrum of the glass was run at -173°C . Either two or three overlapping spectra with eight hyperfine components each were obtained for this vitreous state. The spectrum with the largest coupling constant was identified with A_z and g_z , and was used to obtain these two parameters by taking the average separation between hyperfine components and by using the relationship

$$h\nu_0 = g_z \beta H_z$$

where ν_0 is the operating frequency and H_z is the magnetic field midway between the $m_1 = +\frac{1}{2}$ and $m_1 = -\frac{1}{2}$ hyperfine components. It was difficult to obtain the other anisotropic components accurately; therefore, the relationships between the average components and the anisotropic components:

$$\langle A \rangle = \frac{1}{3} \{A_x + A_y + A_z\} \quad (39)$$

and

$$\langle g \rangle = \frac{1}{3} \{g_x + g_y + g_z\} \quad (40)$$

were used to obtain A_x , A_y , g_x and g_y .

In the case where only two overlapping spectra occur, $A_x = A_y$ and $g_x = g_y$, and these parameters can be easily obtained if the average values of $\langle A \rangle$ and $\langle g \rangle$ are known from the solution spectra and A_z and g_z are known from the glass spectrum. However, if $A_x \neq A_y$ and $g_x \neq g_y$ three overlapping spectra are obtained from which the differences, $A_x - A_y$ and $g_x - g_y$, can be obtained. Knowing these differences the individual parameters can again be calculated from equations (39) and (40). The computer programme handles all of these calculations if suitable input parameters are used.

CHAPTER II: THE PREPARATION AND CHARACTERIZATION OF COMPLEXES,
PURIFICATION OF REAGENTS AND INSTRUMENTATION

1. Purification of Solvents

N,N-dimethylformamide (DMF) (Fisher Reagent Grade) was purified by vacuum distillation (40°C) from barium oxide (Fisher Reagent Grade) onto Linde 3A molecular sieves; only the middle portion was retained. The DMF was stored under vacuum over the molecular sieves until it was used in sample preparation when it was again vacuum distilled onto the complex.

Acetonitrile (Baker Reagent), trimethylphosphate (Aldrich), trimethylphosphite (Matheson, Coleman and Bell), dimethylsulfoxide (Fisher Reagent) and methanol (Fisher Reagent) were purified and dried by double vacuum distillation from Linde 3A molecular sieves; only the middle fraction was retained in each case. The solvents were stored under vacuum and on molecular sieves.

Ethanol, 1-propanol, 2-propanol, 1-butanol (all Fisher reagent), tertiary butyl alcohol (Eastman), 2,2,2-trichloroethanol (Aldrich Chemical Co.), and 2,2,2-trifluoroethanol (Eastman Organic Chemicals) were all vacuum distilled two consecutive times through a 12 inch fractionating column from Linde 3A molecular sieves. The middle portion of each distillation was retained and stored under vacuum over molecular sieves. Subsequent transfers of the alcohols for preparation of the EPR samples were made by vacuum distillation.

2. Preparation of penta-N,N-dimethylformamidovanadyl perchlorate $\{VO(DMF)_5(ClO_4)_2\}$

Vanadyl sulfate (A.D. MacKay Inc.) and barium perchlorate which was prepared by neutralization of barium carbonate (Fisher Reagent) with 60 percent perchloric acid (Baker and Adamson) were added in stoichiometric amounts to redistilled water. The barium sulfate was removed by filtration; a 0.22 μ Millipore filter (Millipore Filter Corp., Bedford, Mass.) was used. The filtrate was concentrated by vacuum distilling the water at room temperature. A large excess of benzene and N,N-dimethylformamide was added to the remaining concentrated solution. This mixed solvent was vacuum distilled, the water being removed as an azeotrope with benzene. The DMF was allowed to evaporate slowly leaving blue crystals. This procedure was repeated three consecutive times. In the final treatment purified DMF was used. Finally a concentrated DMF solution was cooled to $-10^{\circ}C$ and blue crystals of $VO(DMF)_5(ClO_4)_2$ formed and were collected by vacuum filtration.

Anal. Calc'd. for $VO(DMF)_5(ClO_4)_2$: C, 28.60; H, 5.60; N, 11.10.

Found: C, 28.86; H, 5.69; N, 11.02.

All subsequent handlings were done in either a dry nitrogen atmosphere or in suitable vacuum apparatus.

A known amount of $VO(DMF)_5(ClO_4)_2$ was put into a weighed

container and the purified DMF was vacuum distilled onto the solid. NMR and EPR samples were prepared by pouring the solution into sample tubes attached to the flask through a side arm and sealed under vacuum. Thus, all samples were prepared and stored under vacuum and in the absence of water.

3. Preparation of pentaquovanadyl perchlorate $\{VO(H_2O)_5(ClO_4)_2\}$ and pentaquovanadyl tetrafluoroborate $\{VO(H_2O)_5(BF_4)_2\}$

Hydrated vanadyl perchlorate or vanadyl tetrafluoroborate were prepared by adding barium perchlorate or barium tetrafluoroborate and stoichiometric amounts of vanadyl sulfate (Fisher Reagent) to redistilled water. Barium perchlorate and barium tetrafluoroborate were prepared by neutralization of barium carbonate (Fisher Reagent) with perchloric acid (Baker and Adamson) and tetrafluoroboric acid (Baker and Adamson), respectively. The barium sulfate was removed by filtration using a Millipore filter and the filtrate was concentrated by vacuum distillation of the water at 25°C to yield blue crystals of the hydrated vanadyl perchlorate or tetrafluoroborate. These crystals were used in all subsequent preparations without further purification.

4. Preparation of vanadyl tetrafluoroborate complexes with acetonitrile, trimethylphosphate, trimethylphosphite, and dimethylsulfoxide

Vanadyl tetrafluoroborate complexes with the above solvents were prepared by adding 5 gms each of hydrated vanadyl tetrafluoro-

borate and Linde 3A molecular sieves to approximately 100 mls of freshly distilled solvent. *Note: the reaction with trimethylphosphite is very exothermic and reagents must be mixed slowly or the solvent may ignite and explode.* The mixture was stored under vacuum for 5-6 hours and then the molecular sieves were filtered under vacuum from the solution; the solvent was removed by vacuum distillation. The oil which remained was redissolved in a minimum amount of solvent and filtered. The solution was cooled to -10°C in an attempt to obtain a crystalline product. All operations were carried out under vacuum.

Crystals were obtained for the acetonitrile and dimethylsulfoxide complexes.

Anal. Calc'd. for $\text{VO}(\text{CH}_3\text{CN})_5(\text{BF}_4)_2$: C, 26.9; H, 3.39; N, 15.7

Found: C, 25.9; H, 3.28; N, 15.7

Calc'd. for $\text{VO}[(\text{CH}_3)_2\text{SO}]_5(\text{BF}_4)_2$: C, 19.1; H, 4.81.

Found: C, 19.4; H, 4.99.

The trimethylphosphite and trimethylphosphate complexes could not be obtained in crystalline form. Trimethylphosphite was removed from the vanadyl tetrafluoroborate by prolonged vacuum distillation leaving a viscous oil which was analysed directly.

Anal. Calc'd. for $\text{VO}[\text{P}(\text{OCH}_3)_3]_8(\text{BF}_4)_2$: C, 23.4; H, 5.88.

Found: C, 23.7; H, 5.85.

Vanadyl concentrations were subsequently determined on the basis of the 8:1 mole ratio of trimethylphosphite to vanadyl tetrafluoroborate indicated by the analysis.

The concentrations of the vanadyl ion in the trimethylphosphate system were determined spectrophotometrically using the extinction coefficients given in reference (40).

The complexes were all stored under vacuum and all transfers were made in a dry nitrogen atmosphere or under vacuum. NMR samples were prepared and transferred to 5 mm o.d. tubes and sealed under vacuum. EPR samples were sealed under vacuum in 3 mm o.d. flattened quartz tubes.

5. Preparation of pentamethanol vanadyl perchlorate $\{VO(CH_3OH)_5(ClO_4)_2\}$

Crystalline hydrated vanadyl perchlorate (5 gms) was treated with excess purified methanol and two mole equivalents of 2,2 -dimethoxypropane. The solution was stirred for two hours at room temperature and the solvent was then removed by vacuum distillation. The green crystals which separated were analyzed for carbon and hydrogen.

Anal. Calc'd. for $VO(CH_3OH)_5(ClO_4)_2$: C, 14.05; H, 4.73.

Found: C, 13.91; H, 4.70.

Subsequent handlings for preparation of the NMR and EPR samples were carried out under dry nitrogen or in suitable vacuum apparatus to exclude atmospheric water.

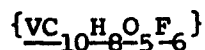
6. Preparation of bisacetylacetonato-oxovanadium(IV) $\{VC_{10}H_{14}O_5\}$

This complex $\{VO(acac)_2\}$ was obtained from Aceto Chemical Company Inc. and recrystallized twice from reagent grade chloroform (Shawinigan) and stored under vacuum.

Anal. Calc'd. for $VC_{10}H_{14}O_5$: C, 45.3; H, 5.32

Found: C, 44.9; H, 5.23.

7. Preparation of bistrifluoroacetylacetonato-oxovanadium(IV)



This complex $\{VO(tfac)_2\}$ was prepared by adding stoichiometric amounts of hydrated vanadyl perchlorate and trifluoroacetylacetone (Peninsular Chemical Research Inc.) to slightly acidic (H_2SO_4) redistilled water. The solution was slowly neutralized by the addition of sodium carbonate. The greenish precipitate which separated from the aqueous solution was extracted into chloroform (Shawinigan) and recrystallized from this solvent.

Anal. Calc'd. for $VC_{10}H_8O_5F_6$: C, 32.2; H, 2.16.

Found: C, 32.7; H, 2.22.

8. Preparation of trisacetylacetonatovanadium(III) $\{VC_{15}H_{21}O_6\}$

Trisacetylacetonate vanadium(III) was prepared under vacuum by the slow addition of dilute aqueous ammonia to a solution containing vanadium trichloride and acetylacetone in a mole ratio 1:3. The entire operation was carried out under vacuum.

The light brown product was extracted into chloroform and recrystallized from this solvent.

Anal. Calc'd. for $\text{VC}_{15}\text{H}_{21}\text{O}_6$: C, 51.7; H, 6.06.

Found: C, 50.1; H, 5.95.

9. Preparation of bisacetylacetonatocopper(II) $\{\text{CuC}_{10}\text{H}_{14}\text{O}_4\}$
and hexamethanol copper(II) perchlorate $\{\text{Cu}(\text{CH}_2\text{OH})_6(\text{ClO}_4)_2\}$

Hydrated cupric sulfate (BDH) and acetylacetonone (Eastman) were added in a 1:2 mole ratio to redistilled water. When a saturated solution of Na_2CO_3 (Matheson, Coleman and Bell) was added to the well-stirred aqueous solution a dark blue precipitate formed. This precipitate was extracted into chloroform (Shawinigan) and crystallized from this solvent.

Anal. Calc'd. for $\text{Cu}(\text{C}_{10}\text{H}_{14}\text{O}_4)$: C, 46.0; H, 5.41.

Found: C, 45.8; H, 5.45.

Hydrated cupric perchlorate was prepared by treating an aqueous solution of cupric sulfate (BDH) with barium perchlorate. The barium sulfate was filtered from the solution using a 0.22 μ Millipore filter. The filtrate was evaporated to dryness under vacuum. The resulting blue crystals were dissolved in purified methanol in the presence of about 10 grams of Linde 3A molecular sieves. This mixture was allowed to stand for 24 hours and the

molecular sieves were filtered off under vacuum. Three successive treatments with methanol and molecular sieves in the above manner with the subsequent vacuum distillation of excess methanol yielded light blue crystals.

Anal. Calc'd. for $\text{Cu}(\text{CH}_3\text{OH})_6(\text{ClO}_4)_2$: C, 16.0; H, 5.38.

Found: C, 15.5; H, 5.35

10. Preparation of chromium(II) and vanadium(II) tetrafluoroborate complexes in methanol and trimethylphosphate

Chromium(II) tetrafluoroborate was prepared in aqueous solution by treating chromium metal of 99.999 percent purity (United Mineral and Chemical Corp.) with degassed 1 molar tetrafluoroboric acid (Baker and Adamson). The water from the blue solution was vacuum distilled at room temperature until only a small residual volume remained. This solution was treated under vacuum with about 20 mls. of degassed, purified methanol or degassed, purified trimethylphosphate. The solvents from the chromium(II) tetrafluoroborate solutions were then allowed to evaporate slowly under vacuum. The addition and subsequent removal of methanol or trimethylphosphate was carried out three times. The final solutions were then analyzed for chromium(II) by oxidation to chromium(III) with standardized ferric ammonium sulfate (Mallinckrodt Chemicals) solution; excess iron(III) was reduced by iodide, the iodine produced being determined with standard sodium thiosulfate. These solutions contained greater than 99.0 percent of the chromium(II) that was expected from the weighed amount of chromium metal

used. Chromium(II) solutions of methanol and trimethylphosphate for the NMR line broadening study were prepared by transferring known weights of standard solutions under vacuum to containers into which purified solvent was vacuum distilled.

Vanadium(II) tetrafluoroborate was prepared in aqueous solution by the electrolytic reduction of vanadyl tetrafluoroborate using a Model D-612T D.C. Power Supply from Electro Products Laboratories, Inc.

The aqueous solution of vanadium(II) tetrafluoroborate was then treated in the same manner as the chromium(II) tetrafluoroborate solutions. The concentrations of the final standard $V(BF_4)_2$ - methanol and trimethylphosphate solutions were determined by the reduction of the silver ion in a standard $Ag(BF_4)$ solution by the vanadium(II) to give vanadium(III). The silver precipitate was filtered with a 0.22 μ Millipore filter, dried and weighed; three determinations were made on each solution. The concentrations of the standard solutions were 0.101 molal and 0.0975 molal, respectively, in good agreement with the amount of vanadium expected from the weighed amount of vanadyl tetrafluoroborate used in the electrolysis. NMR solutions were prepared by diluting the standard solutions in a manner analogous to the chromium(II) solutions.

11. Preparation of nickel(II) and cobalt(II) perchlorate complexes in dimethylsulfoxide and trimethylphosphate

Hydrated nickel(II) and cobalt(II) perchlorate were prepared by neutralization of the respective carbonates with perchloric acid.

The complexes of $\text{Ni}(\text{ClO}_4)_2$ and $\text{Co}(\text{ClO}_4)_2$ with dimethylsulfoxide (DMSO) and trimethylphosphate (TMPA) were prepared by mixing the appropriate hydrated perchlorate salt (~ 10 gm), solvent (~ 50 ml) and Linde 3A molecular sieves. The solution was stirred for 24 hours and the molecular sieves were removed by filtration. This process was repeated three times; all operations were carried out under vacuum. The solvent volume was then reduced by vacuum distillation to an amount suitable to permit crystallization of the metal ion complex. The absence of water was established from the lack of an infrared band in the 3500 cm^{-1} region of the infrared spectrum of the complex crystals. The spectra were determined in a nujol mull between pressed sodium chloride disks on a Perkin Elmer 337 infrared spectrophotometer. Carbon and hydrogen analyses further serve to characterize the compounds.

Anal. Calc'd. for $\text{Ni}(\text{DMSO})_6(\text{ClO}_4)_2$: C, 19.84; H, 4.99

Found: C, 19.40; H, 4.79.

Calc'd. for $\text{Ni}(\text{TMPA})_6(\text{ClO}_4)_2$: C, 19.68; H, 4.96.

Found: C, 19.63; H, 4.78.

Anal. Calc'd. for $\text{Co}(\text{DMSO})_6(\text{ClO}_4)_2$: C, 19.84; H, 4.99.

Found: C, 20.09; H, 5.18.

Calc'd. for $\text{Co}(\text{TMPA})_6(\text{ClO}_4)_2$: C, 19.68; H, 4.96.

Found: C, 19.45; H, 5.07.

The complexes were stored under vacuum and subsequent handling was done in a suitable vacuum apparatus or under a dry nitrogen atmosphere.

12. Preparation of hexa-N,N-dimethylformamidovanadium(III)

perchlorate $\{\text{V}(\text{DMF})_6(\text{ClO}_4)_3\}$

Hexa-N,N-dimethylformamidovanadium(III) perchlorate was prepared by adding vanadium trichloride (~ 0.5 gm) (Stauffer Chemical Co.) and anhydrous thallos perchlorate in a mole ratio of 1:3 to purified DMF (10 mls.) under vacuum. The precipitated thallos chloride was removed by vacuum filtration. The DMF from the green filtrate was evaporated under vacuum at room temperature to a suitable volume (5 mls.) for crystallization and cooled at -10°C overnight. The green crystals which formed were collected by filtration under vacuum.

Anal. Calc'd. for $\text{V}(\text{DMF})_6(\text{ClO}_4)_3$: C, 27.47; H, 5.52; N, 10.78.

Found: C, 27.49; H, 5.38; N, 10.68.

All subsequent transfers of the complex were carried out under vacuum. NMR samples were prepared by vacuum distillation of purified DMF onto a weighed amount of complex.

Leaf 35 omitted in page numbering.

Visible and ultraviolet spectra of the complexes were recorded on a Cary model 14 spectrophotometer using either 1 cm quartz cells or 1 cm i.d. pyrex cells. The pyrex cells could be sealed under vacuum. Infrared spectra were determined on Perkin Elmer model 337 and 421 spectrophotometers using pressed NaCl disks.

14. The preparation of NMR and EPR samples and the determination of their spectra

The first step in the general method used for preparing the NMR and EPR samples was to transfer the complex to a weighed vacuum flask. This operation was carried out under a nitrogen atmosphere. The flask was reweighed and then evacuated. The appropriate solvent was vacuum distilled onto the complex. The amount of solvent transferred was determined by weighing the flask again. The solution was then transferred to a 5 mm o.d. pyrex NMR tube or a 3 mm o.d. flattened quartz EPR tube; this operation was also carried out under vacuum.

Spectra were determined on the machines mentioned above. Temperatures were controlled by standard Varian variable temperature probes which are cooled below room temperature by nitrogen gas passing through a copper coil immersed in liquid nitrogen. The nitrogen gas is reheated by a thermostatically controlled heating element in the probe. The temperature ranges covered are shown in the tables in Appendix A.

CHAPTER III NUCLEAR MAGNETIC RESONANCE LINE BROADENING
STUDIES OF NONAQUEOUS SOLVENTS CONTAINING TRANSITION METAL IONS

1. Line Broadening of the Nuclear Magnetic Resonances of
N,N-Dimethylformamide, Acetonitrile, Dimethylsulfoxide,
Trimethylphosphate and Trimethylphosphite by the Vanadyl Ion

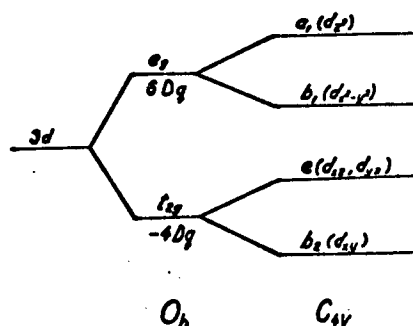
The NMR line broadening technique has been applied previously to a number of systems to determine ligand exchange rates on metal ion complexes as discussed in Chapter I. This section describes the application of this technique to the solvated vanadyl ion in N,N-dimethylformamide (DMF), acetonitrile (AN), dimethylsulfoxide (DMSO), trimethylphosphate (TMPA) and trimethylphosphite (TMPI). The results of this section are discussed in Chapter V in relation to previous work on the water exchange rate on the vanadyl ion (41,42) and the rate of exchange of several solvents on cobalt(II) and nickel(II) (6,9,10,11,12).

In the vanadyl-dimethylformamide and -acetonitrile systems the solvent exchange rate is determined from the NMR line broadening. However, in the other systems studied here: the vanadyl ion in dimethylsulfoxide, trimethylphosphate and trimethylphosphite, chemical exchange never becomes the controlling relaxation mechanism. In order to decide whether exchange is faster or slower than the observed relaxation it is necessary to determine if relaxation is occurring in the inner or outer coordination spheres of the vanadyl ion. The criteria for distinguishing between these two alternatives are discussed.

The absorption spectra of the vanadyl complexes studied show the typical long wavelength absorption and the accompanying shoulder; however, only the trimethylphosphate and trimethylphosphite complexes show the short wavelength absorption. The spectra for the dimethylsulfoxide, trimethylphosphate and acetonitrile complexes agree with those previously reported by Gutmann and Lausegger (40).

The values of Dq are calculated from the crystal field theory spectral assignments made by Ballhausen and Gray (43) who assumed that for $\{VOSO_4 \cdot 5H_2O\}$ a compressed tetragonal, C_{4v} structure was most appropriate for assigning the spectral bands. The separation of free ion d-orbitals in the octahedral field and then the tetragonal field is shown below.

Energy level diagram used to make spectral assignments for vanadyl complexes (43)



The long wavelength absorption is associated with the $b_2 \rightarrow e$ transition and the accompanying shoulder with the $b_2 \rightarrow b_1$ transition which gives $10 Dq$. The higher energy transition which is observed for some of the vanadyl complexes and not others as mentioned above is taken to be the $b_2 \rightarrow a_1$ transition.

Molecular orbital theory which leads to energy levels analogous to those shown above could be used to interpret the visible spectra more explicitly but Dq-values seem to provide a simple parameter for comparison to other systems. The order of the Dq-values for water, methanol, dimethylformamide and dimethylsulfoxide (Table I) is typical of that found in nickel(II) complexes (44). From previous work, the Dq-values of acetonitrile (12,44) and trimethylphosphate (45) are expected to be higher than that of water, whereas they are definitely lower than water in the vanadyl systems. However, the former results are based on nickel(II) and cobalt(II) complexes, respectively, and the Dq-values may be high due to metal-ligand π -bonding, which apparently is not so important in the vanadyl complexes (43).

The molal NMR relaxation time (T'_{2p}) was determined from the NMR line broadening using a slight modification of equation (16):

$$(T'_{2p})^{-1} = \frac{(T_{2p})^{-1}}{[M]} = \frac{(\Delta U_{OBS} - \Delta U_{SOL})}{[M]} \text{ sec}^{-1} \text{ molal}^{-1} \quad (41)$$

where ΔU_{OBS} is the full line width at half height of the bulk solvent resonance in an [M] molal vanadyl solution, and ΔU_{SOL} is the line width of pure solvent. Plots of $\log (T'_{2p})^{-1}$ versus the reciprocal of the absolute temperature are shown for the vanadyl ion in N,N-dimethylformamide in Figure 1, in acetonitrile in Figure 2, and in dimethylsulfoxide, trimethylphosphate and trimethylphosphite in Figure 3.

TABLE I
Spectral properties of vanadyl ion in various solvents

Compound	Solvent ^(c)	Spectral Band Maxima cm ⁻¹			Dq cm ⁻¹
VO(BF ₄) ₂	DMSO	12,100	14,300	-	1430
VO(BF ₄) ₂	TMPA	12,200	13,900	26,300	1390
VO(BF ₄) ₂	TMPI	12,500	14,500	24,100	1450
VO(BF ₄) ₂	CH ₃ CN	12,750	14,800	-	1480
VO(ClO ₄) ₂	DMF	12,680	15,400	-	1540
	CH ₃ OH ^(a)	13,000	15,500	27,400	1550
VO(SO ₄) ₂	H ₂ O ^(b)	13,000	16,000	-	1600

(a) Chapter III, Section 2.

(b) Reference (43).

(c) The solvent name abbreviations are:

DMSO - dimethylsulfoxide,
 TMPA - trimethylphosphate,
 TMPI - trimethylphosphite,
 DMF - N,N-dimethylformamide.

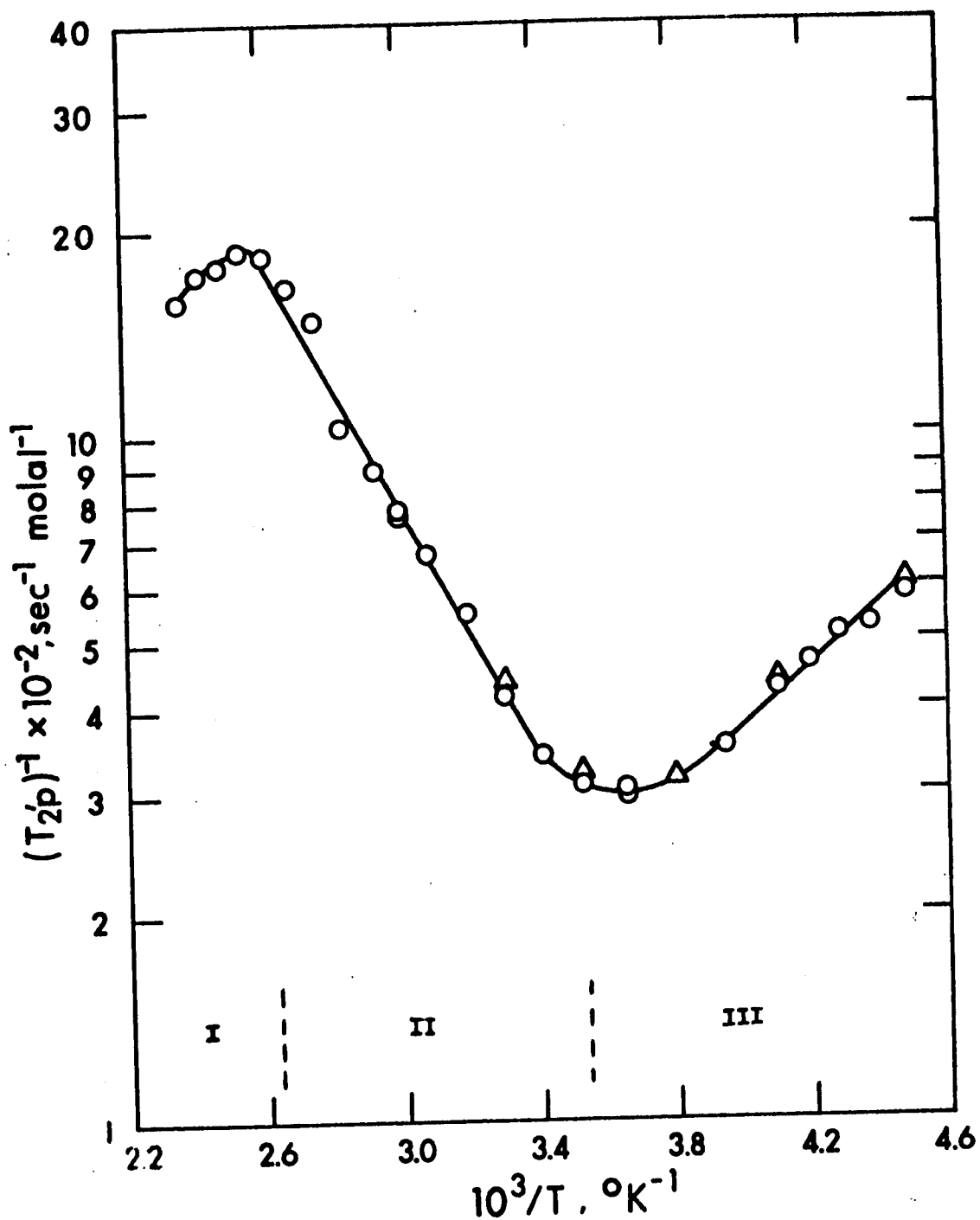


Figure 1: Temperature dependence of $\log (T_{2p}^{-1})^{-1}$ for the formyl proton resonance of N,N-dimethylformamide containing vanadyl perchlorate.
 O - 60 MHz Δ - 100 MHz

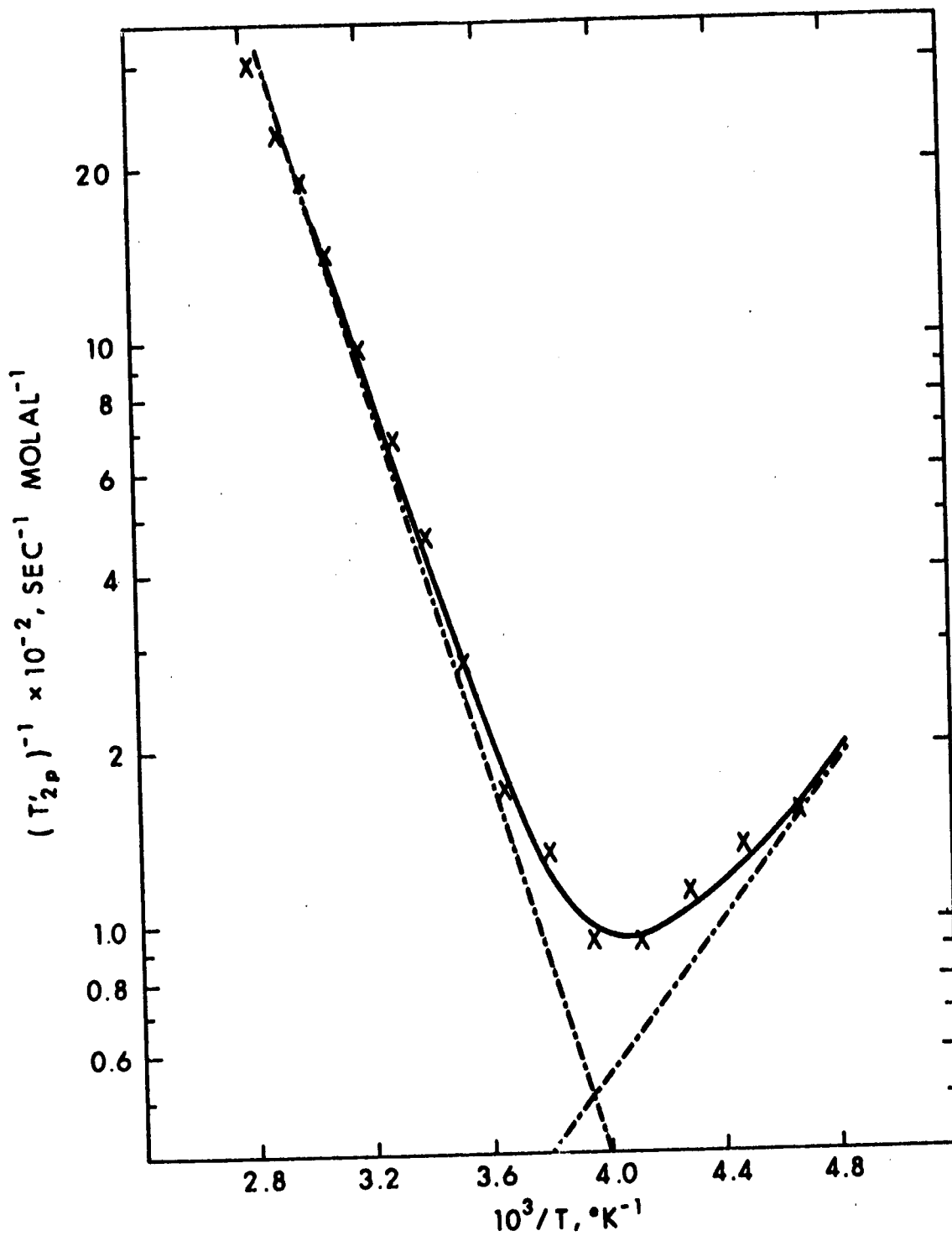


Figure 2: Temperature dependence of $\log (T_{2p}')^{-1}$ for the methyl proton resonance at 60 MHz of acetonitrile containing vanadyl perchlorate.

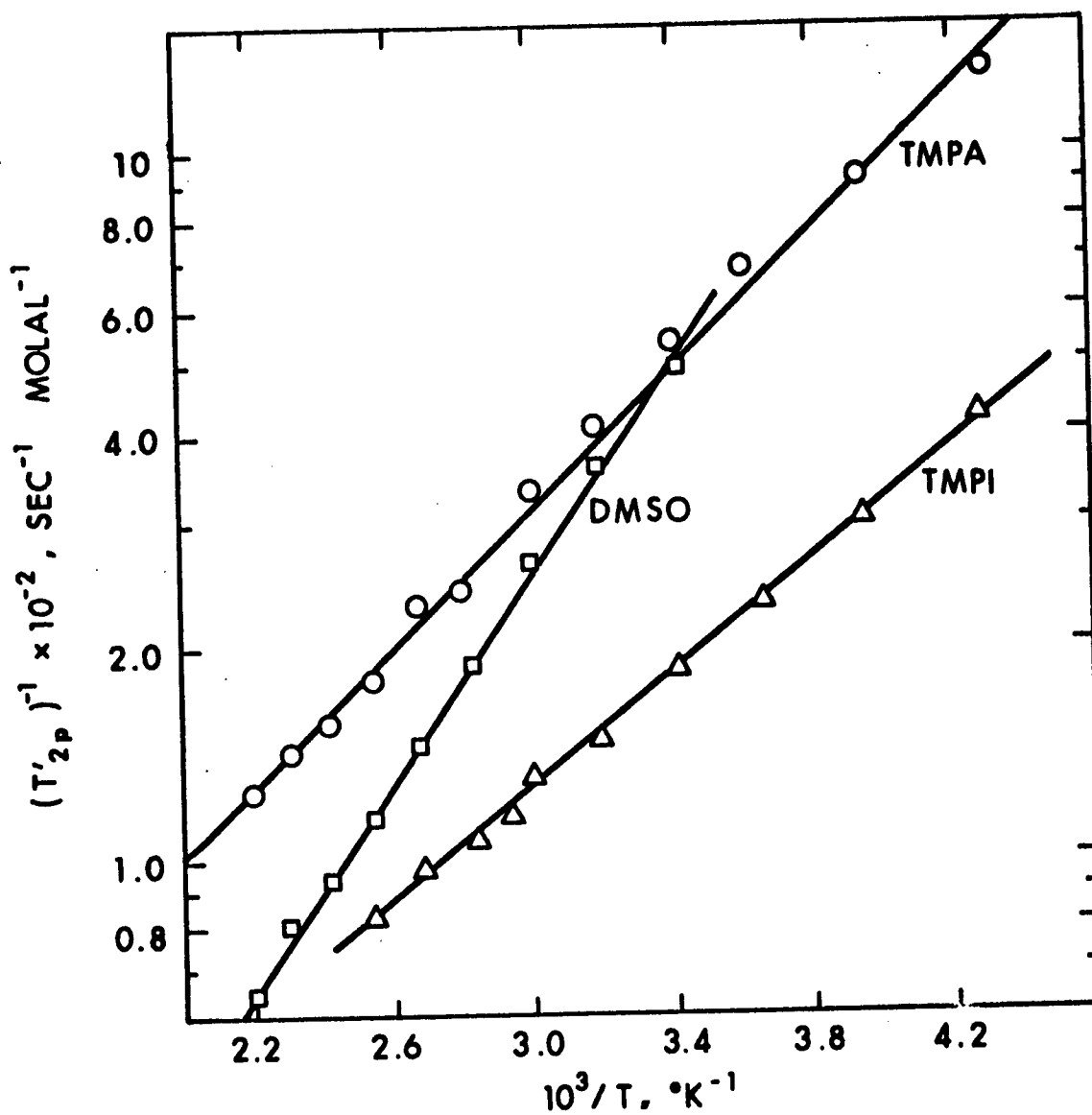


Figure 3: Temperature dependence of $\log (T'_{2p})^{-1}$ for the proton resonances of trimethylphosphite at 60 MHz, dimethyl sulfoxide at 60 MHz and trimethylphosphate at 100 MHz, all containing vanadyl tetrafluoroborate.

There was no frequency dependence of the formyl proton line width of bulk solvent N,N-dimethylformamide containing vanadyl ion when the samples were run at 60 MHz and 100 MHz and $\Delta\omega_p = 0$. Therefore it was concluded that a combination of conditions (34-a) and (34-d) would explain the broadening data for this system in regions (I) and (II) of Figure I. That is, $T_{2M}^{-1}, \tau_M^{-1} > \Delta\omega_M$ in which case equation (10) reduces to

$$(T'_{2p})^{-1} = P_M / (\tau_M + T_{2M}). \quad (42)$$

In region (I) chemical exchange is fast (τ_M is short) and $(T'_{2p})^{-1}$ is controlled by an inner sphere relaxation which has a small temperature dependence; however, in region (II) the lifetime for inner sphere exchange, τ_M , becomes longer than T_{2M} and $(T'_{2p})^{-1}$ is controlled by an exchange process with a large temperature dependence. In region (III) inner sphere exchange becomes slow and relaxation is controlled by a dipolar interaction of the unpaired electron on vanadium with solvent molecules in the outer coordination spheres of the vanadyl complex. This process was relatively easy to identify in the vanadyl-dimethylformamide system because an outer sphere dipolar interaction is expected to have a small and negative temperature dependence as observed in region (III).

For the vanadyl-dimethylformamide system the data was fitted to the following function:

$$(T'_{2p})^{-1} = P_M / (\tau_M + T_{2M}) + C_1 \exp(E_a/RT) \quad (43)$$

by a nonlinear least squares programme (37). The first term on the right comes from equation (42) and the second term results from consideration of the outer sphere contribution to the broadening as shown below. It follows from the definition of P_M in Chapter I that:

$$P_M = \frac{n[M]}{[S] - n[M]} \quad (44)$$

where $[M]$ and $[S]$ refer to the vanadyl ion and solvent molal concentrations, respectively, and n is the number of exchanging solvent molecules in the first coordination sphere of the metal ion.

For this system a simplified form of equation (31) is used for the inner sphere T_{2M} relaxation broadening since $\omega_e^2 \tau_c^2 \gg 1$:

$$(T_{2M})_{\text{Inner}}^{-1} = \frac{7}{15} \left\{ \frac{\gamma_I^2 g^2 \beta^2 S(S+1)}{r_i^6} \right\} \tau_c \quad (45-a)$$

$$= \frac{11.5 \times 10^{16}}{r_i^6} S(S+1) \tau_o \exp(E_a/RT) \quad (45-b)$$

$$= C_2 \exp(E_a/RT) \quad (45-c)$$

The hyperfine term of equation (31) was assumed to be negligible because of the apparent small isotropic hyperfine coupling constant as indicated by the lack of shift. The corresponding expression for the outer sphere dipolar broadening is:

$$(\tau'_{2p})_{\text{Outer}}^{-1} = \frac{7}{45} \left\{ \frac{\gamma_I^2 g^2 \beta^2 s(s+1) 4 \pi \eta}{r_o^3} \right\} \tau_C \quad (46-a)$$

$$= \frac{2.90 \times 10^{14} \rho s(s+1) \tau_o}{r_o^3} \exp(E_a/RT) \quad (46-b)$$

$$= C_1 \exp(E_a/RT). \quad (46-c)$$

This equation follows from equation (33) if $\omega_e^2 \tau_c^2 \gg 1$ and τ_c has an exponential temperature dependence with an apparent activation energy E_a . The activation energy appearing in the inner and outer sphere expressions given above has been assumed equal because, as noted later, this activation energy is interpreted to be associated with a tumbling process for the vanadyl complex. The solvent diffusion time (τ_d) may be shorter than the tumbling time (τ_R) and be the dominant relaxation time beyond the second coordination sphere; however, it has been found (116) that $\tau_d \approx \tau_R$ which makes these two processes indistinguishable.

In the interpretation of the broadening data for the vanadyl-acetonitrile system an analysis similar to that in the vanadyl-dimethylformamide system was carried out. However, since there was no evidence (that is, bend over in the data for this system at the highest temperatures) that an inner sphere relaxation process was contributing to the line broadening (Figure 2), the T_{2M} in the first term on the right in equation (43) was omitted. A nonlinear least squares fit of the $(\tau'_{2p})^{-1}$ data was then carried out on the following expression:

$$(\tau'_{2p})^{-1} = P_M/\tau_M + C_1 \exp(E_a/RT). \quad (47)$$

Before equations (43) and (47) could be fit to the vanadyl-dimethylformamide and vanadyl-acetonitrile $(T_{2p}')^{-1}$ versus $(T^\circ K)^{-1}$ data, respectively, the transition state theory expression for τ_M {equation (20)} and the appropriate expressions for inner and outer sphere dipolar broadening {equations (45-c) and (46-c)} were substituted into equations (43) and (47). Initial guesses for ΔH^\ddagger , ΔS^\ddagger , C_1 , C_2 and E_a were obtained by a graphical fitting of the data. The least squares results for ΔH^\ddagger , ΔS^\ddagger , and E_a are given in Table II.

The obvious difficulty in interpreting the values obtained for C_1 and C_2 from the nonlinear least squares method is that τ_c is not known and the interaction distances cannot be estimated to better than about $\pm 0.2 \text{ \AA}$ for the outer sphere distances. It has been found that the correlation time (τ_c) can be calculated from the EPR line widths of the vanadium hyperfine lines of the solvated vanadyl ion. This procedure, which will be discussed more fully in Chapter IV, makes use of the theory developed by Kivelson, *et al* (17,24) to explain the variation in the EPR hyperfine line widths with the variation in quantum number of vanadium. The values for τ_c at 25°C for all the complexes studied here, as obtained from the EPR studies of these complexes, are given in Table III and justified in Chapter IV. The value of τ_c for the vanadyl-dimethylformamide system can be used in conjunction with the least squares values of C_1 and C_2 to

calculate outer and inner sphere interaction distances, respectively, as will be discussed later. Similarly, the outer sphere interaction distance for the vanadyl-acetonitrile complex can be calculated from the value of C_1 obtained for this system. However, it will be shown in the second section of this chapter on the vanadyl-methanol system and later in this section on other vanadyl-nonaqueous solvent systems that the most reasonable estimates of the interaction distances, as compared to models, are obtained by considering the low temperature dipolar broadening as due to the outer sphere contribution along with the inner sphere contribution of one rapidly exchanging molecule trans to the vanadyl oxygen.

The value of C_1 obtained for the vanadyl-acetonitrile system and E_a , as given in Table II, predict a dipolar contribution of $16.5 \text{ sec}^{-1} \text{ molal}^{-1}$ to $(T'_{2p})^{-1}$ at 25°C . If all this broadening is attributed to outer sphere dipolar broadening and if the τ_c value in Table III is used, then an outer sphere interaction distance of 8.6_5 \AA is obtained. This distance appears to be too short from consideration of a model of this complex in which bond lengths were taken from reference (46); a value of 9.9_0 \AA is more reasonable. However, if there is one rapidly exchanging inner sphere solvent molecule with an interaction distance of 5.3_0 \AA , then it will contribute $10.1 \text{ sec}^{-1} \text{ molal}^{-1}$ to $(T'_{2p})^{-1}$. The remainder of the broadening, $6.4 \text{ sec}^{-1} \text{ molal}^{-1}$, can be

TABLE II
Kinetic parameters for solvent exchange
on the solvated vanadyl ion

Solvent ^(c)	$10^{-3} \times k$ sec ⁻¹ @ 25°C	ΔH^\ddagger kcal mole ⁻¹	ΔS^\ddagger (a) cal deg ⁻¹ mole ⁻¹	E_a kcal mole ⁻¹
DMSO	> 1.52			3.44 ± 0.20
TMPI	< 0.35			1.87 ± 0.35
TMPA	> 0.84			2.25 ± 0.15
CH ₃ CN	2.97	6.65 ± 0.29	-20.3 ± 0.9	3.44 ± 0.62
DMF	0.76	6.77 ± 1.94	-22.6 ± 5.7	2.26 ± 0.68
CH ₃ OH ^(b)	0.55	9.46 ± 0.68	-14.2 ± 0.21	2.91 ± 0.30
H ₂ O ^(b)	0.50	13.7	-0.6	

(a) Calculated assuming a coordination number of 4.

(b) Data for CH₃OH and H₂O are taken from Chapter III, section 2 and reference (43), respectively.

(c) Solvent abbreviations are listed in footnote (c) of Table I.

(c) Errors are quoted as the 95% confidence limits on the parameters from the nonlinear least squares fit to the data.

attributed to an outer sphere interaction for which an interaction distance of 11.8 \AA is calculated. This latter value is somewhat longer than expected; however, the expected value of 9.9 \AA is obtained if the inner sphere distance is taken as 5.9 \AA . The latter value may be longer than that originally predicted from the copper(II) model complex (46) because of weaker bonding in the position trans to the vanadyl oxygen.

In the vanadyl-dimethylformamide system the inner sphere interaction distance for the formyl proton can be determined by using C_2 from the least squares fit to the broadening data and equation (45-b). This interaction distance was found to be 2.9 \AA if four exchanging inner sphere molecules are assumed. If the number of inner sphere molecules is taken as five, then r_i only changes by five percent. The interaction distance obtained for this system is reasonable in view of the model used by Matwiyoff (6) for cobalt(II) and nickel(II) in N,N-dimethylformamide. The value calculated for $(T'_{2p})^{-1}$ at 25°C is $1.6_0 \times 10^3 \text{ sec}^{-1} \text{ molal}^{-1}$; therefore, one rapidly exchanging inner sphere molecule would be expected to contribute one fifth of this value or $320 \text{ sec}^{-1} \text{ molal}^{-1}$ to $(T'_{2p})^{-1}$ at 25°C . The value obtained for $(T'_{2p})^{-1}$ at 25°C from C_1 for this system is $168.5 \text{ sec}^{-1} \text{ molal}^{-1}$. Therefore, it must be assumed that the dimethylformamide molecule trans to the vanadyl oxygen does not form a normal inner sphere bond and has a much longer interaction distance.

An outer sphere interaction distance for the formyl proton was then calculated under the assumption that there was no inner sphere contribution to the low temperature broadening and was found to be 5.7_5°\AA . This value is reasonable, judging from molecular models.

In the other three systems studied here: vanadyl ion in dimethylsulfoxide, in trimethylphosphate and in trimethylphosphite, it can be seen from Figure 3 that no chemical exchange controlled line broadening was observed and it is not known whether exchange is fast and $(T'_{2p})^{-1}$ is controlled by inner sphere dipole-dipole relaxation, or if exchange is slow and the observed broadening is due to outer sphere dipole-dipole relaxation. In principle, using equations (45-a) and (46-a), the inner and outer sphere broadening can be calculated and the results compared to the observed value to decide whether one is observing inner or outer sphere relaxation. Again it was necessary to use the correlation times, which were obtained from the EPR line widths of the solvated vanadyl ion in the corresponding solvent, along with the observed $(T'_{2p})^{-1}$ at 25°C to calculate interaction distances. The results are shown in Table III. It should be noted that in the calculation of r_o the observed $(T'_{2p})^{-1}$ values have been corrected for the dipolar broadening resulting from one rapidly exchanging solvent molecule undergoing inner sphere dipolar broadening as discussed above for the acetonitrile system.

TABLE III

Interaction distances for inner (r_i) and
outer (r_o) sphere dipole-dipole broadening

Solvent ^(c)	$(T'_{2p})^{-1}$ sec ⁻¹ molal ⁻¹ @ 25°C	r_i (a) Å	$(T'_{2p})^{-1}$ (b) corr sec ⁻¹ molal ⁻¹ @ 25°C	$10^{10} \chi \tau_c$ sec @ 25°C	r_i Å	r_o Å
CH ₃ CN	16.5	5.3 (5.9)	6.4 (10.1)	0.62	6.3	11.8 (9.9)
TMPI	176	4.8	77	1.10	5.70	7.0
TMPA	460	4.9	343	1.32	5.13	4.8
DMSO	455	4.5	357	1.17	4.45	4.3

- (a) The r_i values for CH₃CN, TMPI, TMPA and DMSO are estimated from structures in references 46,47,48 and 49, respectively.
- (b) Corrected assuming one rapidly exchanging inner sphere solvent molecule. $(T'_{2p})^{-1}_{corr}$ is used to calculate r_o .
- (c) Solvent abbreviations are listed in footnote (c) of Table I.

The estimated interaction distances in Table III are based as much as possible on known structures from the literature (46,47, 48,49) in order to get the best values for the outer sphere interaction distances. However, because of free rotation about the ligand-metal bond and bonds in the ligand itself there is actually a range of interaction distances. Those given in Table III are the average of the estimated limits assuming free rotation about all single bonds in the ligand and about the metal-ligand bond.

It is apparent from the results in Table III that in the trimethylphosphate and dimethylsulfoxide systems the inner sphere interaction distance is reasonably close to the estimated interaction distance. In addition, the calculated outer sphere distances in these solvents are much too short to be reasonable. It seems unlikely in view of the results in acetonitrile, N,N-dimethylformamide and methanol (Chapter III, section 2) that the EPR method (Chapter IV) yields too short a correlation time in dimethylsulfoxide and trimethylphosphate; therefore, it is concluded that solvent exchange is fast in these two solvents leading to an inner sphere dipolar relaxation process. Thus, only a lower limit can be established for the exchange rate from the NMR line broadening.

The broadening in the trimethylphosphite system seems most consistent with outer sphere relaxation because the calculated outer sphere interaction distance ($7.0\overset{\circ}{\text{Å}}$) is reasonable, whereas

the inner sphere interaction distance (5.7\AA) is 0.9\AA longer than the estimated value. In the trimethylphosphate and dimethylsulfoxide systems the difference between estimated and calculated inner sphere interaction distances is 0.25\AA or less. The conclusion that outer sphere relaxation is dominant in the trimethylphosphite system is also indicated by comparison to the broadening in the trimethylphosphate systems; the solvent molalities, densities and estimated interaction distances are similar, however, the broadening is 2.6 times less in the trimethylphosphite system. Therefore, if outer sphere relaxation is being observed, then only an upper limit can be placed on the exchange rate of trimethylphosphite on the vanadyl ion as given in Table II.

It might also be mentioned at this point that an attempt to analyze the results for all the systems studied here in terms of a model where the second coordination sphere molecules are reasonably strongly coordinated and contribute to most of the dipolar outer sphere broadening (41) was generally unsuccessful. This lack of success may be due to the outer sphere molecules not retaining a specific orientation with respect to the complex. Therefore, the model which treats the solvent as a continuum (36) with labile outer sphere molecules has been used throughout this thesis to explain the outer sphere broadening.

It has also been observed that the values of E_a in Table III

are similar to those predicted from the temperature dependence of the viscosities of the solvents. This is consistent with the concept that the dipolar relaxation process is dependent on the tumbling of the complex in solution. The tumbling process will be discussed more fully in connection with the EPR results in Chapter IV. The exchange parameters for the vanadyl systems studied here will be discussed in more detail in Chapter V.

2. Line Broadening of the Nuclear Magnetic Resonances of Methanol, Trichloroethanol and Trifluoroethanol by Vanadyl Complexes

The line broadening of the methyl and hydroxy proton resonances of methanol caused by the vanadyl ion shows typical chemical exchange control above 0° with the hydroxyl protons exchanging faster than the methyl protons. These results are interpreted in terms of proton dissociation from the coordinated hydroxy group and solvent methanol molecule exchange; the low temperature line broadening is attributed to a dipolar relaxation process.

When vanadyl acetylacetonate is dissolved in methanol or trichloroethanol and vanadyl trifluoroacetylacetonate is dissolved in methanol, only the solvent hydroxy proton shows chemical exchange controlled NMR line broadening. The methyl or methylene solvent protons in these systems show only a T_{2M} controlled transverse relaxation time which is due to a dipolar-interaction. Vanadyl acetylacetonate causes only T_{2M} controlled nuclear relaxation of both the hydroxy and methylene protons of trifluoroethanol.

The proton exchange process occurring in the vanadyl acetylacetonate-methanol and -trichloroethanol systems and in the vanadyl trifluoroacetylacetonate-methanol system was interpreted as an internal proton transfer from the alcohol coordinated in the position trans to the vanadyl oxygen to the coordinated acetylacetonate or trifluoroacetylacetonate ligands, respectively. Since previous studies (18,42) indicate that solvent molecule exchange from the sixth position is very fast, it was necessary to treat these

results using a three site mechanism.

A spectrophotometric study of vanadyl perchlorate in methanol shows a typical absorption at $13,000 \text{ cm}^{-1}$ (ϵ , 17.0) with a shoulder at $15,500 \text{ cm}^{-1}$, and an additional band at $24,700 \text{ cm}^{-1}$ (ϵ , 117). The molecular orbital diagram given by Ballhausen and Gray (43) for $\text{VO}(\text{SO}_4) \cdot 5 \text{ H}_2\text{O}$ can be used as in Chapter III, section 1 to assign the spectral transitions observed in $\text{VO}(\text{CH}_3\text{OH})_5^{2+}$. The $13,000 \text{ cm}^{-1}$ and $15,500 \text{ cm}^{-1}$ absorptions are identified as the $b_2 \rightarrow e$ and $b_2 \rightarrow b_1$ transitions, respectively, and the $27,400 \text{ cm}^{-1}$ absorption is assigned to the $b_2 \rightarrow a_1$ transition. The value of Dq obtained directly from the $b_2 \rightarrow b_1$ transition is $1,550 \text{ cm}^{-1}$ which may be compared to $1,600 \text{ cm}^{-1}$ for $\text{VO}(\text{H}_2\text{O})_5^{2+}$. The kinetic significance of these relative Dq values will be more thoroughly discussed in Chapter V.

The variation of $\log (T_{2p}')^{-1}$ with the inverse absolute temperature for vanadyl perchlorate in methanol, vanadyl acetylacetonate in methanol, vanadyl trifluoroacetylacetonate in methanol, and vanadyl acetylacetonate in trichloroethanol and trifluoroethanol are shown in Figures 4 to 8, respectively. The values of $(T_{2p}')^{-1}$ were obtained from equation (42) where $[M]$ is the molal concentration of the corresponding complex. The curves that show two distinct regions were analyzed by the nonlinear least squares method discussed in Chapter III, section 1 using equation (47). The mechanism responsible for the exchange controlled line broadening

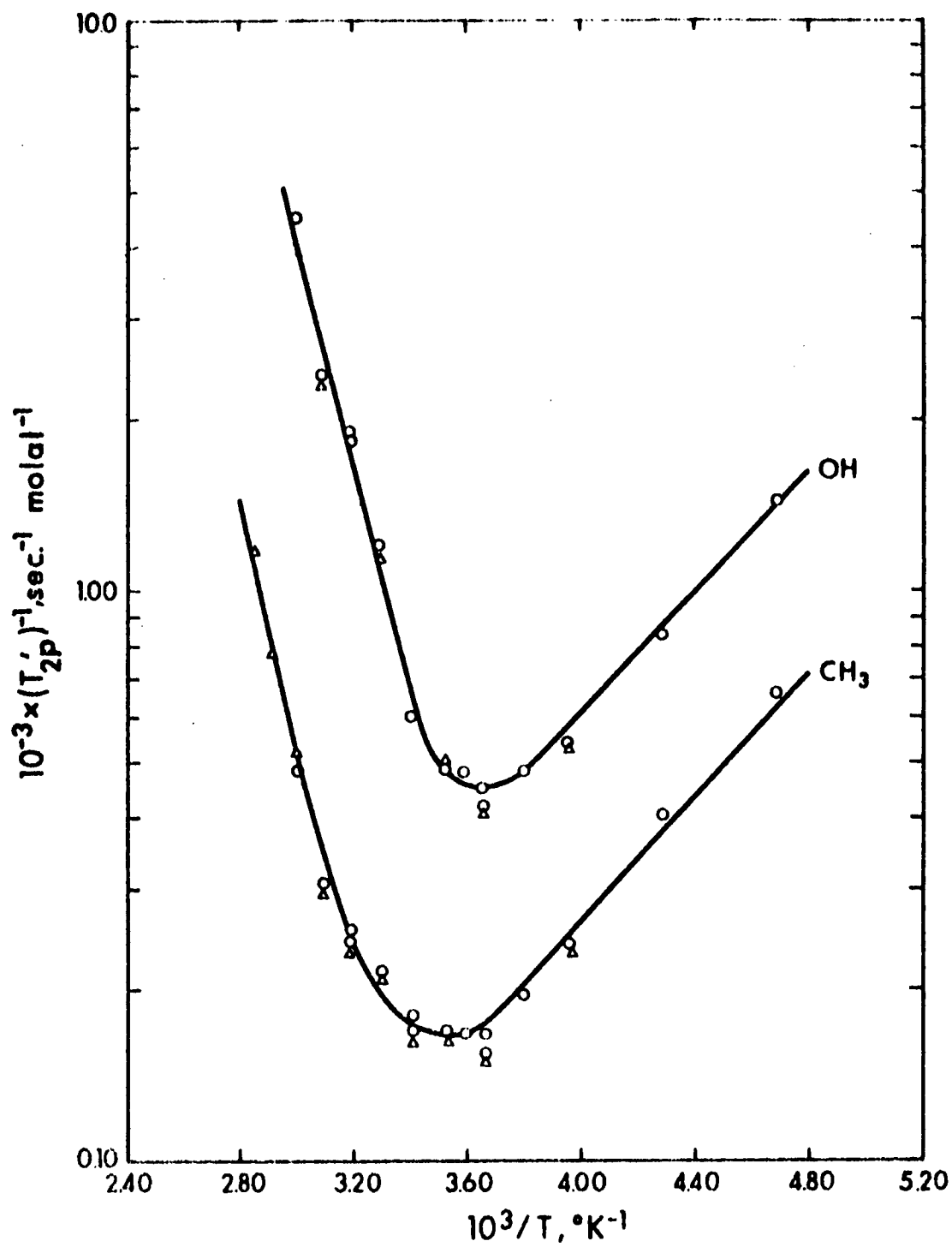


Figure 4: Temperature dependence of $\log (T_{2p}')^{-1}$ at 60 MHz for the protons of methanol containing vanadyl perchlorate.

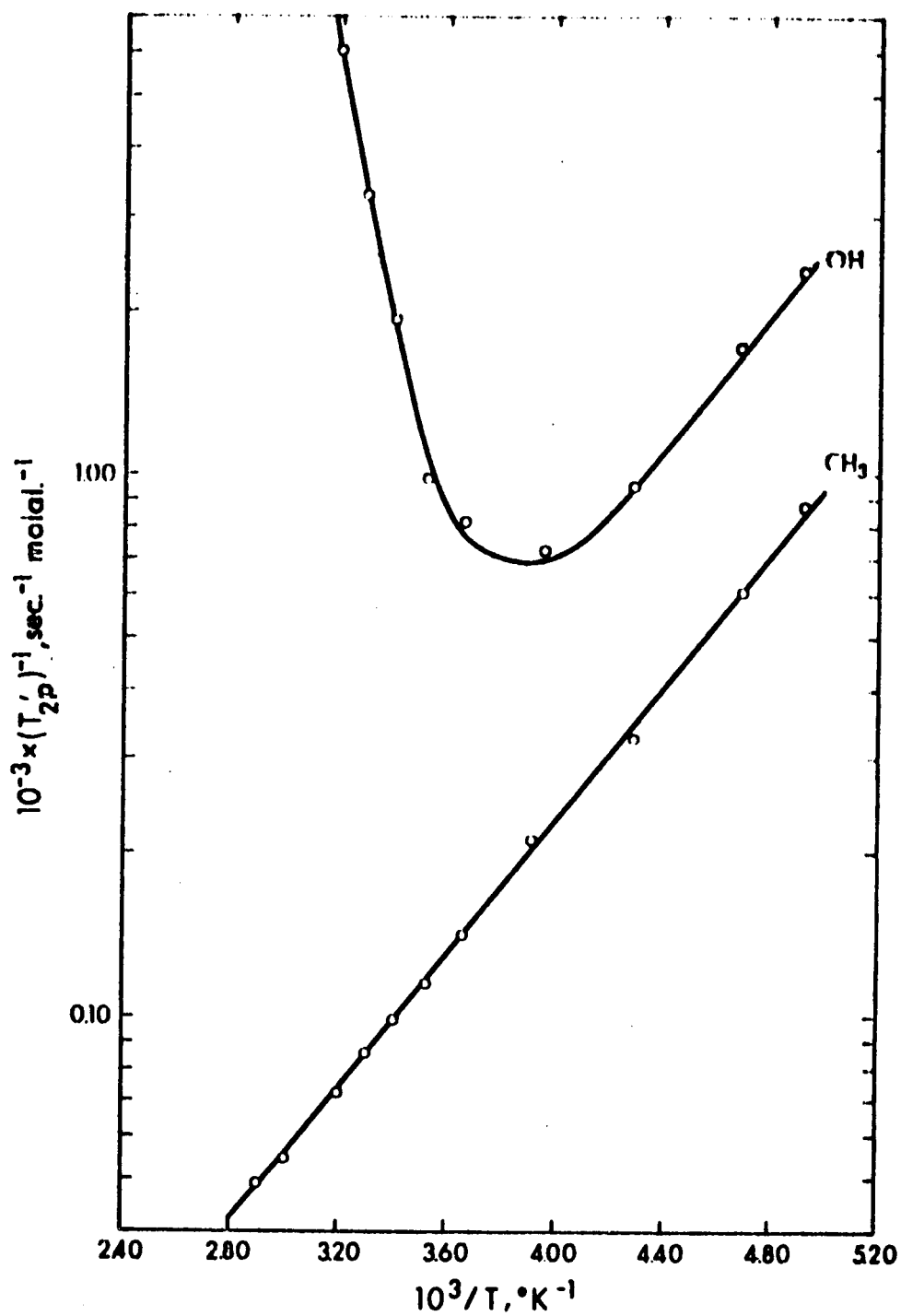


Figure 5: Temperature dependence of $\log (T_{2p}')^{-1}$ at 60 MHz for the protons of methanol containing vanadyl acetylacetonate.

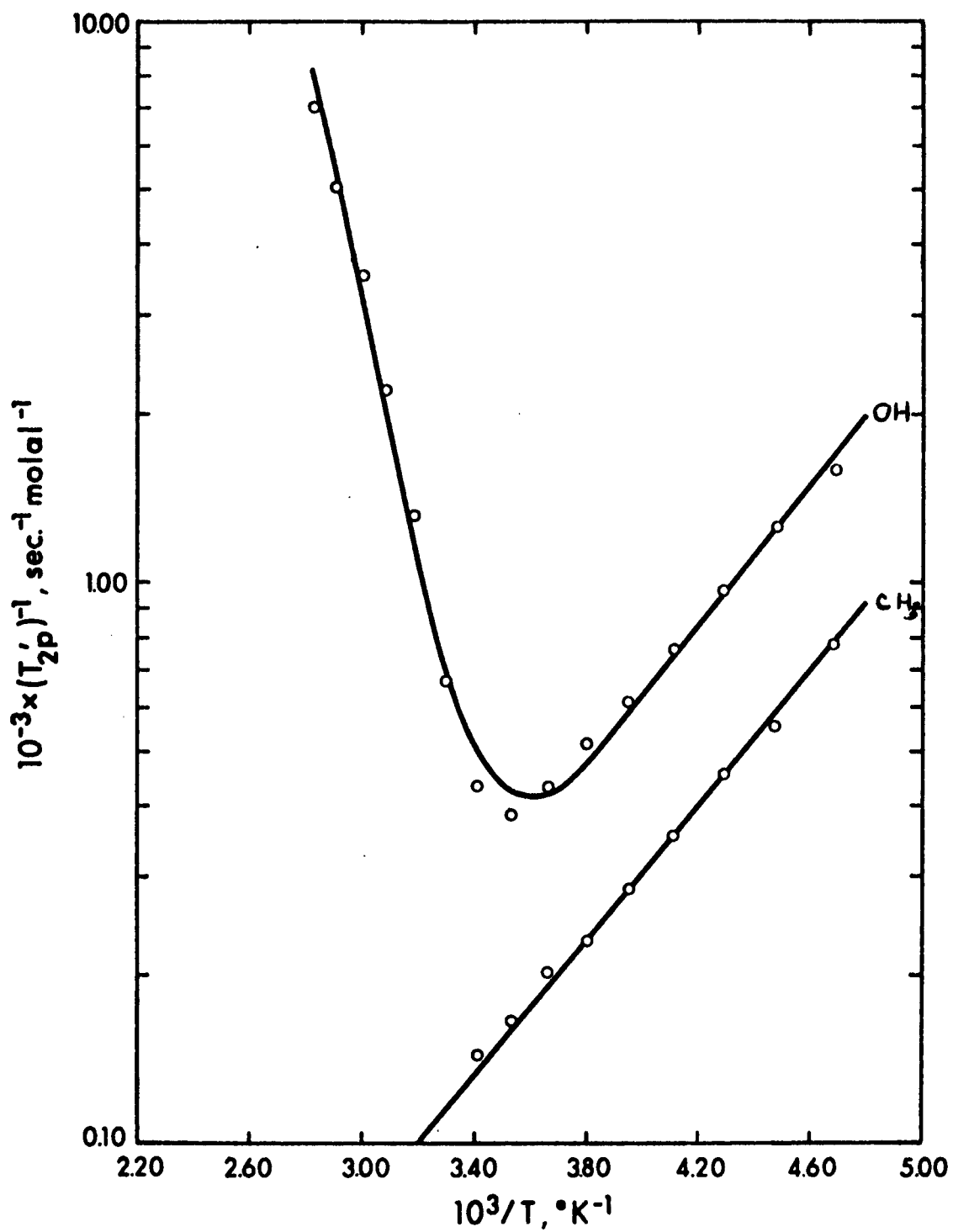


Figure 6: Temperature dependence of $\log (T_{2p}')^{-1}$ at 60 MHz for the protons of methanol containing vanadyl trifluoroacetylacetonate.

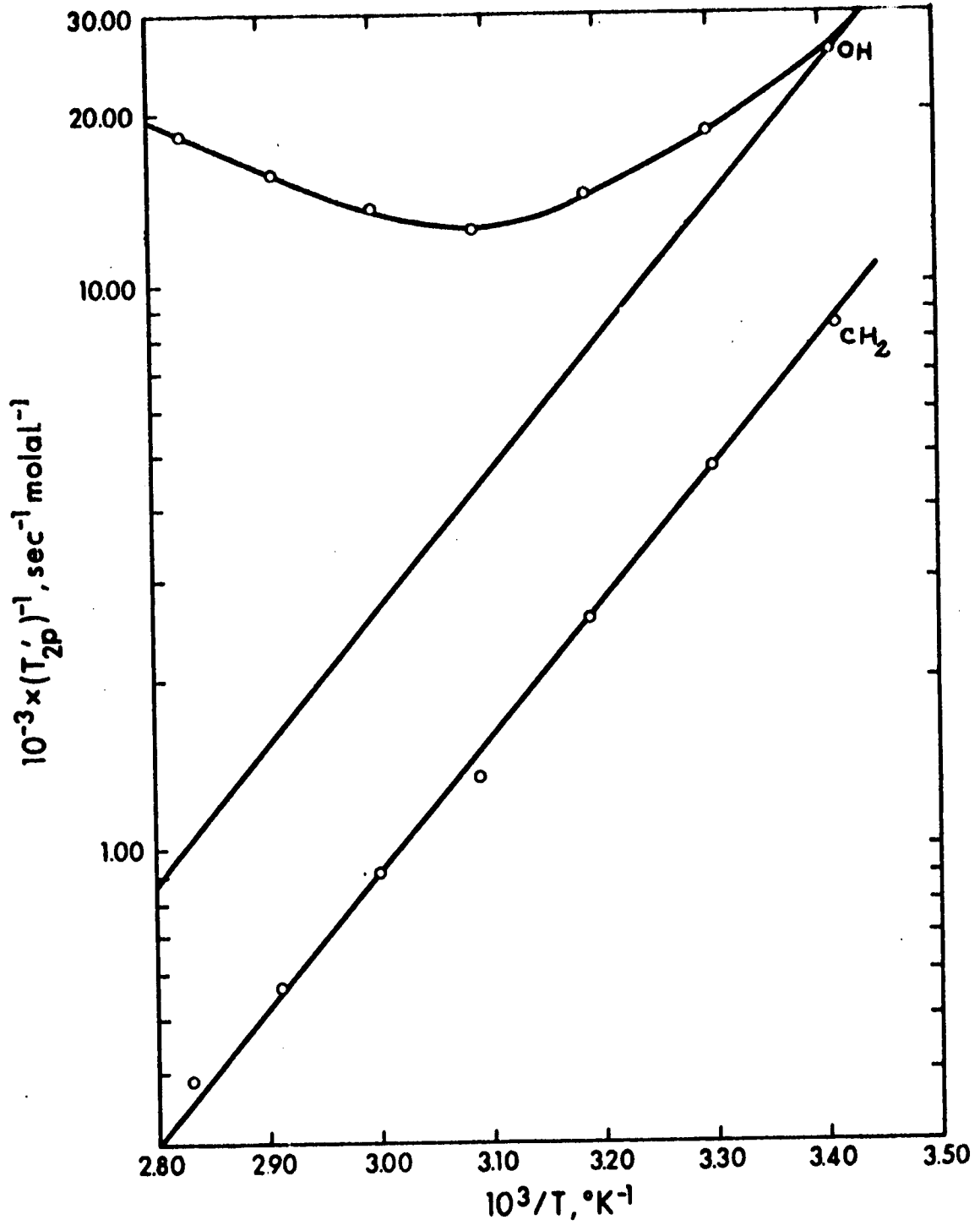


Figure 7: Temperature dependence of $\log (T_{2p}')^{-1}$ at 60 MHz for the protons of trichloroethanol containing vanadyl acetylacetonate.

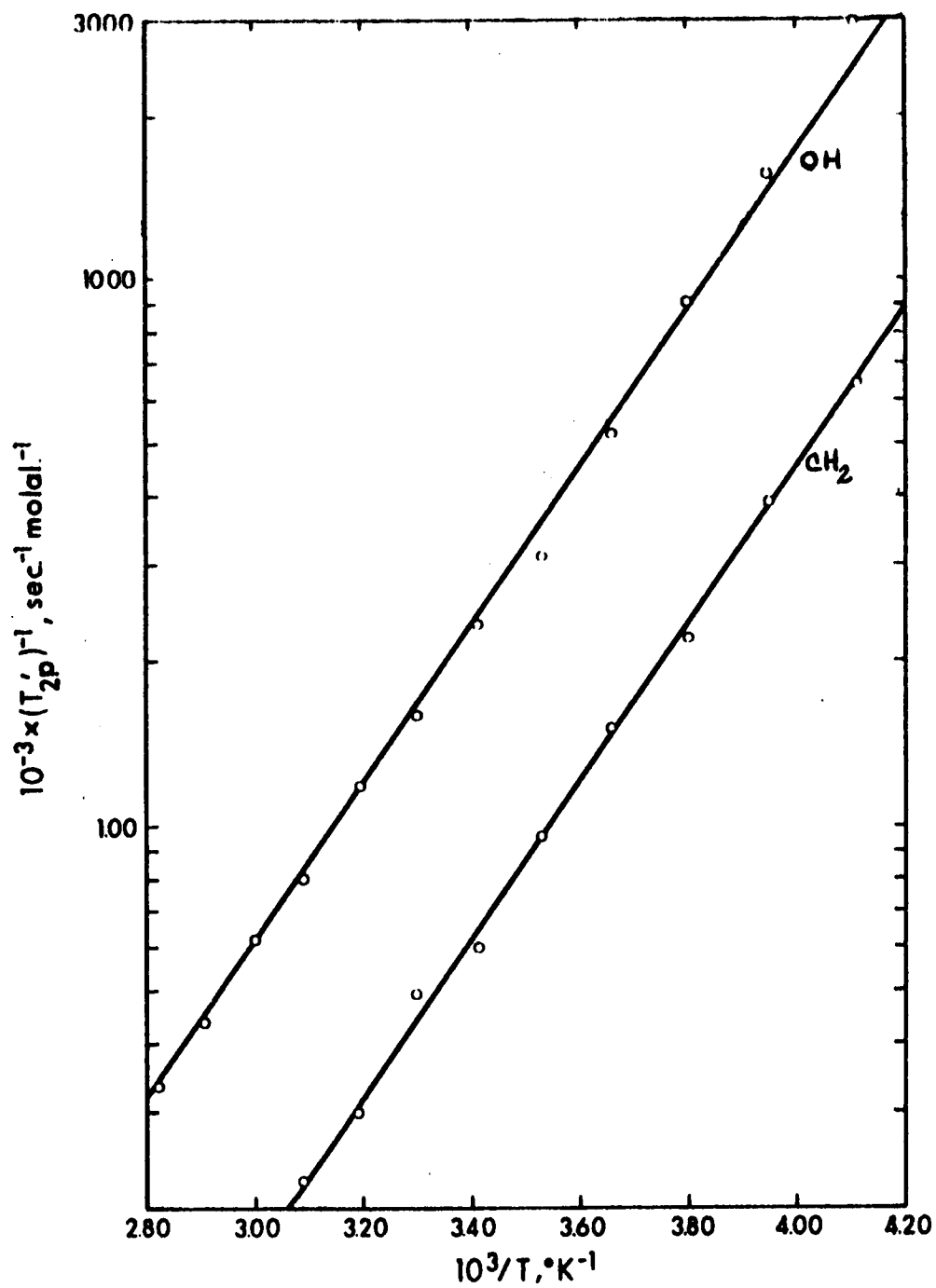


Figure 8: Temperature dependence of $\log (T_{2p}')^{-1}$ at 60 MHz for the protons of trifluoroethanol containing vanadyl acetylacetonate.

will be discussed subsequently for each system. Appropriate P_M values were used, along with guesses of ΔH^\ddagger , ΔS^\ddagger , C_2 and E_a which were obtained by resolving the two regions graphically. The values for ΔH^\ddagger and ΔS^\ddagger , obtained from the nonlinear least squares fit to the data and the exchange rate at 25°C are given in Table IV. When $\log (T_{2p}')^{-1}$ showed only a linear dependence on the inverse temperature the data was fit to a straight line by eye.

The constant, C_2 , obtained from the nonlinear least squares fit was used to calculate the dipolar relaxation broadening at 25°C whenever this constant was available. The value for this broadening could also be obtained directly from the line chosen to best fit the data for cases in which only a linear decrease of $\log (T_{2p}')^{-1}$ with decreasing $(T \text{ } ^\circ\text{K})^{-1}$ was observed. These broadenings can be analyzed by using equation (45-a) or (46-a) if the correlation time (τ_c) and the proper interaction distances are known.

There is evidence in these systems for a combined inner and outer sphere dipolar relaxation process controlling the broadening at the lower temperatures, as found for the vanadyl ion systems in Chapter III, section 1. It would be expected that for all transition metal ions dissolved in methanol the ratio of outer sphere broadening of the hydroxy proton compared to the methyl protons should be approximately constant. This generalization is based on the similarity in ionic radii of transition metal ions and on the assumption that the orientation of the outer sphere molecules is the same in all

cases. The validity of this proposal may be tested for nickel(II) (36), cobalt(II) (36), and vanadium(II) (Chapter III, section 4) for which the ratios are 1.64, 1.62, and 1.70, respectively. However, for the vanadyl ion in methanol this ratio is 2.6 and is similar for the other vanadyl complexes in methanol. Several alternatives to the inner-outer sphere dipolar relaxation process which may give rise to the anomalous ratio for systems containing a vanadyl complex might be noted. If two solvent molecules are hydrogen bonded to the vanadyl oxygen atom, then the two hydroxy protons would be about 2.8\AA from the vanadium atom provided the assumption is made that these two protons each make a 120° bond angle at the vanadyl oxygen atom. The methyl protons are at an average distance of about 6\AA for the same model. If this model is assumed in the vanadyl ion-methanol system and the EPR correlation time, $4.1_0 \times 10^{-11}$ sec, from Chapter IV is used along with the inner sphere dipolar expression {equation (45-a)}, since these two protons are actually in the first coordination sphere, a good estimate of $(T_{2p}')^{-1}$ for the hydroxy proton is obtained. However, the value for $(T_{2p}')^{-1}$ for the methyl protons is about twenty times smaller than the observed value. The difficulty lies in the fact that this model requires the interaction distances for the two types of protons to differ by about a factor of two and the expression for the predicted line broadening depends on the inverse sixth power of these distances. Therefore, the

predicted ratio of $(T_{2p}')_{OH}^{-1} / (T_{2p}')_{CH_3}^{-1}$ for this model will always be about 64 compared to the observed ratio of 2.6.

A similar difficulty arises if it is assumed that the dipolar broadening is due solely to a rapidly exchanging methanol in the sixth coordination position, which is trans to the vanadyl oxygen. Assuming the metal to solvent oxygen bond lengths to be the same as those in $VO(H_2O)_5^{2+}$ (50) and with normal covalent bond lengths and angles for methanol, the interaction distances are about 2.9\AA and 3.9\AA for the hydroxy and methyl protons, respectively. These values predict $(T_{2p}')_{OH}^{-1} / (T_{2p}')_{CH_3}^{-1} = 4.5$. This ratio is close to the value of 4.8₅ found for chromium(II) solutions in methanol where inner sphere dipolar broadening is expected to occur (Chapter III, section 4), but is not consistent with the observed ratio in the vanadyl systems.

It was assumed, therefore, that both normal outer sphere and inner sphere (due to one rapidly exchanging methanol trans to the vanadyl oxygen) dipolar processes were contributing to the observed line broadening. If the inner and outer sphere interaction distances are taken to be 3.9\AA and 4.8\AA , respectively, for the methyl protons as estimated from models and using $\tau_c = 4.1_0 \times 10^{-11}$ sec, then the inner and outer sphere contributions to $(T_{2p}')^{-1}$ are 33 and $74 \text{ sec}^{-1} \text{ molal}^{-1}$, respectively, at 25°C. Their sum is reasonably close to the observed value of $100 \text{ sec}^{-1} \text{ molal}^{-1}$ which was calculated from the constant (C_2) obtained from the least squares analysis.

Similarly for the hydroxy proton, using inner and outer sphere distances of 2.9_5°\AA and 4.0_0°\AA , respectively, the calculated broadening is $280 \text{ sec}^{-1} \text{ molal}^{-1}$ which is in better agreement than should be expected with the observed value of $275 \text{ sec}^{-1} \text{ molal}^{-1}$. The same analysis was used for the other systems studied here and the results are shown in Table V. The correlation time, τ_c , was determined from the EPR line widths of the vanadyl complex in the appropriate solvent using the theory developed by Kivelson (17). The method is described in Chapter IV. The values for τ_c were used to calculate the hydrodynamic radius of the ion, r , using equation (37). The outer sphere hydroxy and methyl distances were arbitrarily taken as $(r + 0.5)^{\circ}\text{\AA}$ and $(r + 1.3)^{\circ}\text{\AA}$, respectively. This procedure gives a consistent method for treating all the systems. The inner sphere interaction distance for the hydroxy proton was calculated from the observed broadening after subtracting off the outer sphere contribution. The methyl proton inner sphere line broadening was then calculated from equation (45-a) using $(r_i)_{\text{CH}_3} = (r_i)_{\text{OH}} + 0.95^{\circ}\text{\AA}$. The distance of 0.95°\AA between the methyl and hydroxy protons is derived from models of the methanol molecule. It can be seen that for all the systems listed in Table V the calculated and observed values of $(T_{2p}')_{\text{CH}_3}^{-1}$ or $(T_{2p}')_{\text{CH}_2}^{-1}$ are in good agreement. Therefore, it was concluded that only the inner and outer sphere dipolar interactions are contributing significantly to the low temperature line broadening.

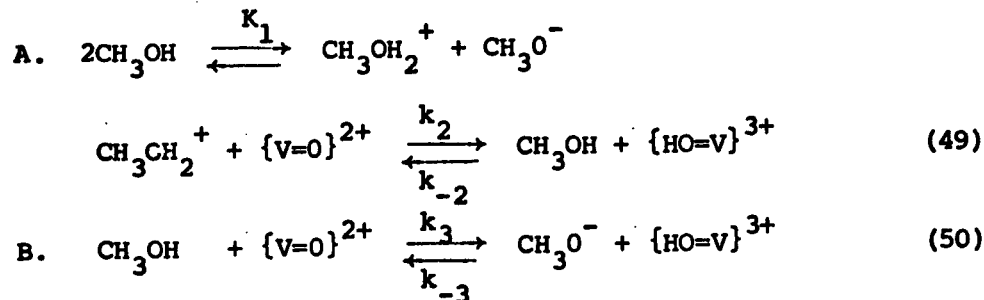
The rapid exchange of a fifth solvent molecule, presumably in the coordination position trans to the vanadyl oxygen, is consistent with the coordination number of four found for the vanadyl ion in water (42), the recent structure determination of $\{VO(H_2O)_4SO_4\} \cdot H_2O$ (50) and the H_2O^{17} NMR work on various vanadyl complexes (51).

The temperature dependence of $\log (T_{2p}')^{-1}$ for the methyl and hydroxy protons of methanol for the system containing vanadyl perchlorate in methanol is shown in Figure IV. It is apparent from the high temperature region that the hydroxy and methyl protons are exchanging at different rates. The kinetic parameters for the exchange processes are given in Table IV.

It is possible to estimate the limiting conditions which apply when chemical exchange is controlling $(T_{2p}')^{-1}$. In order for $\Delta\omega_M$ to be ten times greater than $(\tau_M)^{-1}$ ($0.6 \times 10^3 \text{ sec}^{-1}$ at 25°C) for the methyl protons the hyperfine coupling constant must be about $1 \times 10^6 \text{ Hz}$. If a value of 10^{-9} sec is used for the electron spin relaxation time, τ_e , then the value of $(T_{2M})^{-1}$ due to the hyperfine interaction is about $1.3 \times 10^4 \text{ sec}^{-1}$. This gives the conditions $\Delta\omega_M \approx (T_{2M})^{-1} \gg (\tau_M)^{-1}$ which, when used in the general two site expression for $(T_{2p}')^{-1}$ given by equation (10), gives $(T_{2p}')^{-1} = P_M (\tau_M)^{-1}$.

The methyl protons must be exchanging with the whole methanol molecule, whereas, the hydroxy proton can also exchange

by proton dissociation from coordinated methanol or possibly by protonation of the vanadyl oxygen. For the latter mechanism two paths have been considered:



The reciprocal lifetime of the hydroxy proton in a solvent methanol molecule for scheme A is given by

$$(\tau_{\text{S}})_{\text{OH}}^{-1} = (\tau_{2\text{p}})_{\text{OH}}^{-1} = k_{-2}[\text{V=OH}^{3+}] = k_2 \frac{[\text{V=O}^{2+}][\text{CH}_3\text{OH}_2^+]}{[\text{CH}_3\text{OH}]} \quad (51)$$

The value of $(\tau_{\text{S}})_{\text{OH}}^{-1}$ at 25°C is 500 molal⁻¹sec⁻¹ from Figure 4. The CH_3OH_2^+ concentration calculated from the autoprotolysis constant of methanol ($K_1 = 1.15 \times 10^{-17}$ molar) (52) is 3.3×10^{-9} molar, however, this value is likely to be about 10^{-3} molar due to the proton dissociation from coordinated methanol (assuming a $\text{p}K_{\text{a}}$ of 6 as found for the aquo vanadyl complex). This mechanism required that $(\tau_{2\text{p}})_{\text{OH}}^{-1}$ has a first order hydrogen ion dependence if it is assumed that $\{\text{V=OH}\}^{3+}$ is a strong acid as indicated by the study of Rossotti and Rossotti (53) in up to 2.9₅M perchloric acid; in this case the vanadyl ion is largely present in the unprotonated form. The acid dependence of $(\tau_{2\text{p}})_{\text{OH}}^{-1}$ was investigated in the vanadyl acetyl-

acetate-methanol system. This system also shows only hydroxy proton chemical exchange and because of the reduced charge of $\text{VO}(\text{acac})_2$ compared to $\text{VO}(\text{CH}_3\text{OH})_5^{2+}$, reaction A should be more favored for $\text{VO}(\text{acac})_2$. Four solutions were prepared containing 0.096 molal $\text{VO}(\text{acac})_2$ and 0.0, 0.01, 0.05 and 0.10 molal 2,4-dinitrobenzenesulfonic acid. No significant variation in the line widths in the four solutions was observed, proving that the hydroxy proton exchange rate in the $\text{VO}(\text{acac})_2$ system and also in the $\text{VO}(\text{CH}_3\text{OH})_5^{2+}$ system does not occur by reaction A.

In scheme B it is expected that k_{-3} will be diffusion controlled and

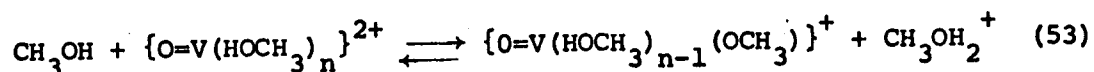
$$(\tau_{2p})^{-1} = (\tau_S)^{-1} = k_3 [\text{V}=\text{O}^{2+}] \quad (52)$$

Again it is assumed that the vanadium is mainly in the $\{\text{V}=\text{O}\}^{2+}$ form, in which case $[\text{V}=\text{O}^{2+}] = 1.0$ molal and $k_3 = 500 \text{ sec}^{-1}$ at 25° from Figure 4. It is then possible to calculate K_3 as follows

$$K_3 = \frac{k_3}{k_{-3}} \approx \frac{500}{10^{10}} = 5 \times 10^{-8}$$

This result implies that the vanadyl ion has the same basicity as the acetate ion (54) in anhydrous methanol which is again inconsistent with the lack of basicity of the aqueous vanadyl ion (53).

Therefore, it was concluded that the most reasonable path for hydroxy proton exchange is represented by the reaction:



where it is possible for $n=4$ or 5 ; from the conclusions about the dipolar relaxation it seems most likely that $n=4$. The rate constant for proton dissociation by reaction (53), assuming $n=4$, is $4.3_5 \times 10^3 \text{ sec}^{-1}$ at 25°C .

The variation of the proton relaxation time with temperature for solvent methanol containing vanadyl acetylacetonate is shown in Figure 5. In this system only the hydroxy protons show a chemical exchange controlled nuclear relaxation. The relative values of the methyl and hydroxy line broadening at low temperatures may be explained by a combination of inner and outer sphere dipolar relaxation as discussed previously. The parameters used and the results are given in Table IV.

The same considerations used previously may be applied to the vanadyl acetylacetonate complex to show that reactions A or B cannot explain the hydroxy proton exchange. There is the additional possibility that the CH proton of coordinated acetylacetonate may exchange with methanol. This possibility was tested by measuring the line width of the CH proton of trisacetylacetonatovanadium(III) dissolved in chloroform (no exchange) and in methanol. The spectrum in both solvents recorded at 100 MHz exhibited two peaks due to the CH and CH_3 resonances at 3948 and 4492 Hz, respectively, downfield from internal tetramethylsilane (TMS). The CH resonance was broadened by less than 10 Hz in methanol, indicating an exchange rate of less than 62 sec^{-1} at 40°C . Therefore, this type of exchange is too slow to account for the solvent hydroxy proton

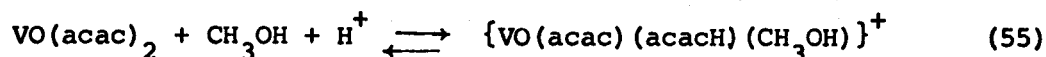
exchange.

Dissociation of one of the acetylacetonate ligands and substitution of solvent molecules could also explain the results:



The equilibrium constant is 10^{-2} for the reaction analogous to (54) in aqueous solution (55). Hydroxy proton exchange may occur by proton dissociation from $\text{VO}(\text{acac})(\text{CH}_3\text{OH})_2^+$ by a process analogous to reaction (53). If a hydrogen ion concentration of 10^{-3}M is assumed (due to proton dissociation from coordinated methanol) in the $\text{VO}(\text{acac})_2$ solution then there is about 10% of the dissociated species present. The addition of up to 0.10 molal acid should cause about 50% dissociation and, therefore, about a 5 fold increase in $P_M(\tau_M)^{-1}$ and in turn in $(\tau_{2p}')^{-1}$. It was noted above that the line widths did not change for the solutions which were 0.01, 0.05, or 0.10 molal in 2,4-dinitrobenzenesulfonic acid. Therefore, this mechanism cannot explain the exchange broadening except in the unlikely event that the complex is largely dissociated even in pure methanol solutions.

Partial dissociation of one of the chelate rings would also produce a species which would undergo hydroxy proton dissociation. Pearson and Moore (56) have found evidence for the reaction:



in the hydrolysis of vanadyl acetylacetonate. It is not possible to realistically estimate the equilibrium constant for reaction (55). However, as part of a general EPR line broadening study, as outlined in Chapter IV, the coupling constants in the plane, A_x and A_y , and g -values in the plane, g_x and g_y , for the $\text{VO}(\text{acac})_2$ complex have been determined in a number of alcohols. In the series of alcohols including methanol, trichloroethanol, and trifluoroethanol the value of $\Delta g = (g_x - g_y)$ is constant at 0.0100 and the value of $\Delta A = (A_x - A_y)$ is also constant at 6.5 ± 0.5 gauss. The temperature dependences of the line widths over a wide temperature range of the respective alcohols show no anomalies and are quantitatively consistent with the presence of only one vanadyl species. The EPR results of Wüthrich and Connick (51) indicate that it should be possible to observe a separate signal for a new species if it constitutes about 10% of the total species. Therefore, the EPR study discussed in Chapter IV establishes that there can only be a small concentration of the dissociated vanadyl acetylacetonate in the alcohol solutions. This conclusion, combined with the lack of acid dependence of the line broadening, makes it very unlikely that there is a partially dissociated species undergoing chemical exchange.

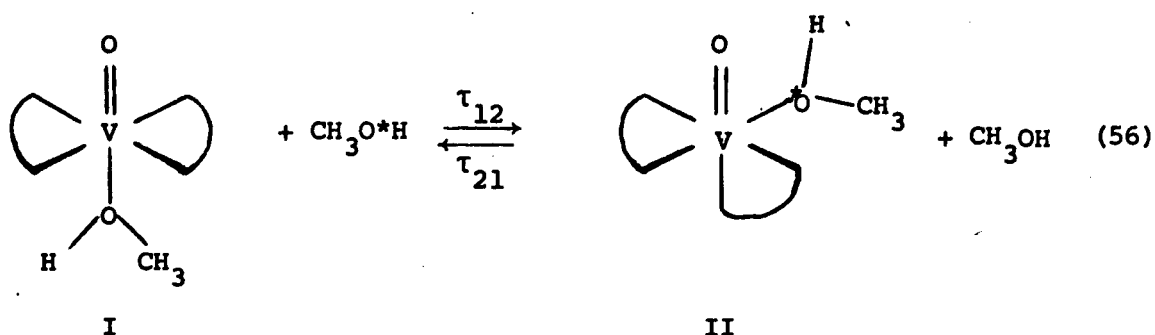
Several other points argue against a partially dissociated exchanging species. The study of Wüthrich and Connick (51) indicates that water exchange is about 10^3 times faster from various vanadyl chelates than from $\text{VO}(\text{OH}_2)_4^{2+}$ which indicates

that exchange rates are dependent on charge effects. The reduced charge on the $\text{VO}(\text{acac})(\text{CH}_3\text{OH})_2^+$ species is expected to give a slower rate of hydroxy proton dissociation than $\text{VO}(\text{CH}_3\text{OH})_n^{2+}$, not faster as observed. However, the observed chemical exchange might be due to whole methanol molecule exchange from $\text{VO}(\text{acac})(\text{CH}_3\text{OH})_2^+$. If this were the case then the methyl protons would also be expected to show chemical exchange controlled line broadening. The only alternative is to assume that the acetylacetonate ligand has decreased the coupling constant for the methyl protons by more than a factor of 10 compared to the value in $\text{VO}(\text{CH}_3\text{OH})_5^{2+}$, while not dramatically affecting the coupling constant for the hydroxy protons. Then the hydroxy protons would satisfy the limiting condition $(T_{2M}^{-1})^2 \gg (\tau_M^{-1})^2$, $\Delta\omega_M^2$, whereas the methyl protons would satisfy the condition $(T_{2M}\tau_M)^{-1} \gg (T_{2M}^{-1})^2$, $\Delta\omega_M^2$. Under these limiting conditions the hydroxy proton would show exchange control of $(T_{2p}')^{-1}$ but the methyl protons would not. However, this proposal seems unlikely since the coordination of an acetylacetonate ligand would not be expected to affect the coupling constant of the methyl protons dramatically without affecting that of the hydroxy proton.

It should also be noted that the line broadening in the chemical exchange controlled region is greater for $\text{VO}(\text{acac})_2$ than for $\text{VO}(\text{CH}_3\text{OH})_5^{2+}$. This result is the opposite of that expected when the higher charge on $\text{VO}(\text{CH}_3\text{OH})_5^{2+}$ is considered. A similar

comparison between $\text{VO}(\text{tfac})_2$ and $\text{VO}(\text{acac})_2$ is not very revealing since faster exchange in the latter system could be attributed to more dissociation.

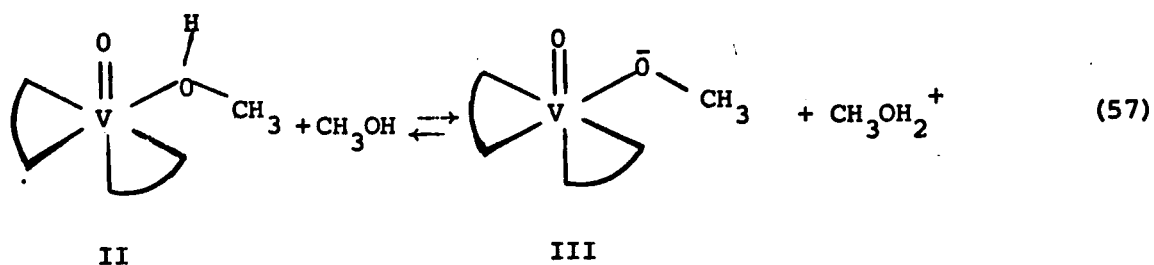
Another possible exchange mechanism may be represented by reaction (56).



The detailed mechanism may be either a direct substitution as implied in reaction (56) or an intramolecular interchange of species I, since direct exchange of methanol in species I with bulk solvent is fast. The latter condition is based on the results for the solvated vanadyl ion in water (42) and methanol. The transverse relaxation time of the hydroxy protons in species II, ($T_{2\text{II}}$), is assumed to be short due to a hyperfine interaction. The solvent proton T_2 will then be controlled by the rate of the I \rightarrow II interchange of the hydroxy proton. It is necessary to assume that $T_{2\text{II}}$ for the methyl protons is longer than the exchange lifetime. As noted previously this conclusion does

not seem very probable in view of the results on VO^{2+} in methanol.

If the I→II interchange lifetime is slower than $(T_{2\text{II}})^{\text{OH}}$ but faster than $(T_{2\text{II}})^{\text{CH}_3}$ then the hydroxy proton dissociation from species (II) may control the solvent hydroxy proton relaxation by the following mechanism:



The previous comparison of $\text{VO}(\text{CH}_3\text{OH})_5^{2+}$ and $\text{VO}(\text{acac})_2$ as well as slower exchange on $\text{VO}(\text{tfac})_2$ compared to $\text{VO}(\text{acac})_2$ make this an unlikely possibility. Another possible mechanism which was considered to explain the behavior of the acetylacetonate and trifluoroacetylacetonate complexes in methanol and trichloroethanol is pictured in Figure 9. This mechanism proposes a three site relaxation process for the hydroxy proton of the solvent methanol. The solution of the Bloch equations (Chapter I, section 2) for the three site case yields (58):

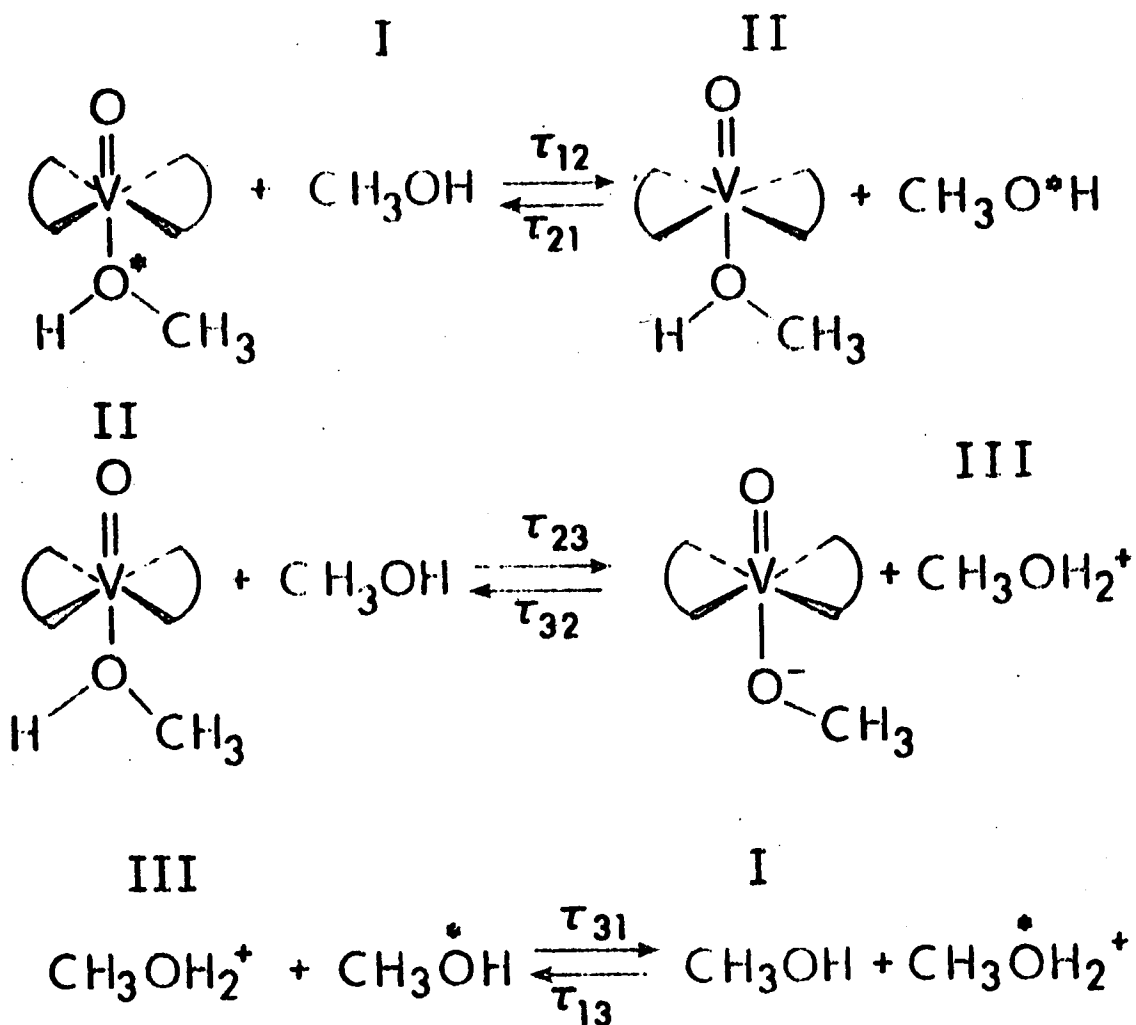


Figure 9: A proposed mechanism for the exchange of the hydroxy proton of methanol for the system of vanadyl acetylacetonate in methanol.

$$(\tau_{2p})^{-1} = (\tau_2)_{\text{OBS}}^{-1} - (\tau_{21})^{-1}$$

$$\begin{aligned} & \left(\left\{ \frac{1}{\tau_{22}} + \frac{1}{\tau_{21}} \right\} \lambda_3 + \frac{1}{\tau_{23}} \left\{ \frac{1}{\tau_{23}} + \frac{1}{\tau_{31}} \right\} \right) \left(\frac{1}{\tau_{12}} \left\{ \frac{\lambda_3}{\tau_{22}} + \frac{1}{\tau_{23}\tau_{23}} \right\} + \right. \\ & \left. \frac{1}{\tau_{13}} \left\{ \frac{\lambda_2}{\tau_{23}} + \frac{1}{\tau_{32}\tau_{22}} \right\} \right) + \frac{1}{\tau_{12}} \left((\lambda_3^2 + \Delta\omega_3^2) \Delta\omega_2^2 + \right. \\ & \left. \left\{ \frac{1}{\tau_{22}} + \frac{1}{\tau_{23}} \right\} \Delta\omega_3^2 \lambda_2 + \left\{ \frac{2}{\tau_{32}} + \frac{1}{\tau_{31}} \right\} \frac{\Delta\omega_2 \Delta\omega_3}{\tau_{23}} \right) + \frac{1}{\tau_{13}} \left(\left\{ \lambda_2^2 + \Delta\omega_2^2 \right\} \Delta\omega_3^2 + \right. \\ & \left. \left\{ \frac{1}{\tau_{23}} + \frac{1}{\tau_{32}} \right\} \Delta\omega_2^2 \lambda_3 + \left\{ \frac{2}{\tau_{23}} + \frac{1}{\tau_{21}} \right\} \frac{\Delta\omega_2 \Delta\omega_3}{\tau_{32}} \right) \end{aligned}$$

(58)

$$\begin{aligned} & \left(\left\{ \frac{1}{\tau_{22}} + \frac{1}{\tau_{21}} \right\} \lambda_3 + \frac{1}{\tau_{23}} \left\{ \frac{1}{\tau_{23}} + \frac{1}{\tau_{31}} \right\} \right)^2 + \lambda_2^2 \Delta\omega_3^2 + \lambda_3^2 \Delta\omega_2^2 + \\ & \frac{2 \Delta\omega_2 \Delta\omega_3}{\tau_{23}\tau_{32}} + \Delta\omega_2^2 \Delta\omega_3^2 \end{aligned}$$

where $\lambda_i = \tau_{2i}^{-1} + \tau_{ij}^{-1} + \tau_{ik}^{-1}$; τ_{2i} is the transverse relaxation time of the nucleus in the i th site and $\Delta\omega_i$ is the chemical shift of the nucleus in the i th site from that in a site on species (I) in the absence of exchange. The relationship $\tau_{12}\tau_{23}\tau_{31} = \tau_{13}\tau_{32}\tau_{21}$ has also been used to obtain equation (58). The equation developed by Swift and Connick can be obtained from equation (58) simply by setting $(\tau_{32})^{-1} = (\tau_{23})^{-1} = 0$ and collecting terms. It is obviously necessary to simplify equation (58) before it can be applied. A consideration of data in the literature gives the following values:

$$\begin{aligned} \frac{1}{\tau_{12}} &= 10^9 [\text{VO}]; & \frac{1}{\tau_{21}} &= 10^9 [\text{MeOH}] \\ \frac{1}{\tau_{13}} &= 10^9 [\text{MeOH}_2^+]; & \frac{1}{\tau_{31}} &= 10^9 [\text{MeOH}] \\ \frac{1}{\tau_{23}} &= 10^5 [\text{MeOH}]; & \frac{1}{\tau_{32}} &= 10^{10} [\text{OVOMe}] \end{aligned} \quad (59)$$

The rate constants for the II→III, I→II and I→III processes are estimated from references 59, 28 and 60, respectively. With these approximate values and assuming that $\lambda_1 > \Delta\omega_1$, the following expression for $(T_{2p})^{-1}$ is obtained:

$$\frac{1}{T_{2p}} = \frac{\frac{1}{\tau_{12}} \left\{ \frac{1}{T_{22}} \left\{ \frac{1}{T_{23}} + \frac{1}{\tau_{31}} + \frac{1}{\tau_{32}} \right\} + \frac{1}{\tau_{23} T_{23}} \right\} + \frac{1}{\tau_{13}} \left\{ \frac{1}{T_{23}} \left\{ \frac{1}{T_{22}} + \frac{1}{\tau_{21}} + \frac{1}{\tau_{23}} \right\} + \frac{1}{\tau_{32} T_{22}} \right\}}{\left\{ \frac{1}{T_{22}} + \frac{1}{\tau_{21}} \right\} \left\{ \frac{1}{T_{23}} + \frac{1}{\tau_{31}} \right\} + \frac{1}{T_{22} \tau_{32}} + \frac{1}{T_{23} \tau_{23}} + \frac{1}{\tau_{21} \tau_{32}} + \frac{1}{\tau_{23} \tau_{31}}} \quad (60-a)$$

The conditions that can be applied to equation (60-a) are

$\tau_{21}^{-1} \gg T_{22}^{-1}, \tau_{23}^{-1}$ and $\tau_{31}^{-1} \gg T_{23}^{-1}, \tau_{32}^{-1}$. The relative values of the τ 's given in equation (59) are consistent with these conditions.

The line width for the hydroxy proton in CH_3OH_2^+ is expected to be similar to that in methanol; therefore, the condition $\tau_{31}^{-1} \gg T_{23}^{-1}$ is certainly justified. If the T_{22} -relaxation is primarily due to the dipolar interaction, then the previous calculations of these values (Table V) confirm that τ_{21}^{-1} is larger than T_{22}^{-1} . Equation (60-a) then simplifies to:

$$\frac{1}{T_{2p}} = \frac{\tau_{21}}{\tau_{12}} \left\{ \frac{1}{T_{22} + \tau_{21}} \right\} + \frac{\tau_{31}}{\tau_{13}} \left\{ \frac{1}{T_{23} + \tau_{31}} \right\} \quad (60-b)$$

and in addition if $T_{22}^{-1} \ll \tau_{21}^{-1}$ and $T_{23} \ll \tau_{31}^{-1}$, then equation (60-b) yields:

$$\frac{1}{T_{2p}} = \frac{P_{2M}}{T_{22}} + \frac{P_{3M}}{T_{23}} \quad (60-c)$$

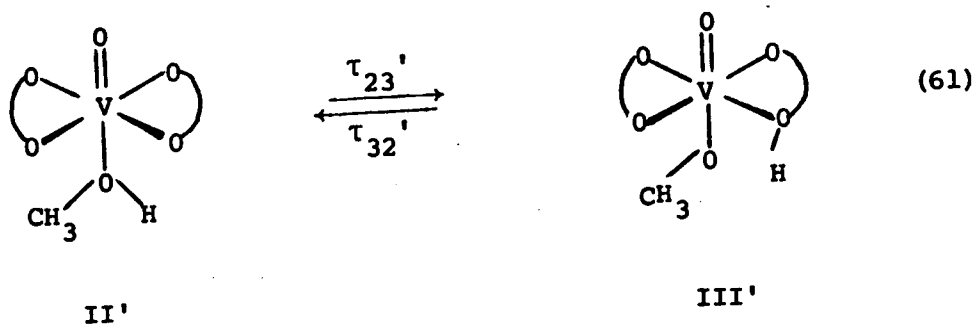
where $P_{2M} = \tau_{21}/\tau_{12}$ and $P_{3M} = \tau_{31}/\tau_{13}$. This final equation contains no exchange rates as expected because relaxation by fast exchange dominates over the slow exchange and leads to a T_{2M} relaxation process. This result does not explain the chemical exchange controlled region experimentally observed. However, if $T_{22}^{-1} \gg \tau_{21}^{-1}, \tau_{23}^{-1}$, because of considerable hyperfine interaction between the unpaired electron on vanadium and the protons, then from equation (60-b):

$$\frac{1}{T_{2p}} = \frac{1}{\tau_{12}} + \frac{P_M}{T_{23}} \quad (60-d)$$

Since the I \rightarrow II exchange in Figure 9 involves the whole methanol molecule, this result indicates that both the hydroxy and methyl protons should show chemical exchange controlled line broadening unless the methyl coupling constant is 10 times less than that of the hydroxy proton so that $(T_{22})_{OH}^{-1} \gg (\tau_{21})_{OH}^{-1}$ and $(T_{22})_{CH_3}^{-1} \ll (\tau_{21})_{CH_3}^{-1}$. As noted previously the latter condition seems unlikely and this mechanism cannot be correct. This conclusion is also

consistent with the work of Walker, *et al* (28) and Reuben and Fiat (42) who have established that exchange from the sixth position is much faster than the chemical exchange rate being measured in this case.

A mechanism which does seem to be consistent with the observations is an internal proton transfer to the coordinated acetylacetonate oxygen from an alcohol ligand coordinated to the sixth position. Again this relaxation process must be treated as a three site problem in which case the II→III step of Figure 9 is replaced by the following mechanism:



The limiting conditions applied to equation (60-a) to analyze this mechanism are $\tau_{21}^{-1} \gg \tau_{22}^{-1}, \tau_{23}^{-1}$ and $\tau_{32}^{-1} \gg \tau_{31}^{-1}$ which means that the reverse of reaction (61) is much faster than proton transfer from acetylacetone to solvent methanol. In this case the following expression is obtained:

$$(\tau_{2p})^{-1} = \frac{\tau_{21}'}{\tau_{12}} \left\{ \frac{1}{\tau_{22}'} + \frac{\tau_{32}'}{\tau_{23}'(\tau_{23}' + \tau_{32}')} \right\} \quad (62-a)$$

Now, if T_{23}' is very short due to the hyperfine interaction since the proton is now in the xy-plane in the III' site and T_{22}' is long because only the dipolar interaction can act on the proton in the II' site, then:

$$(T_{2p})^{-1} = \frac{\tau_{21}'}{\tau_{12}} \left\{ \frac{1}{\tau_{23}'} \right\} = P_M (\tau_{23}')^{-1} \quad (62-b)$$

It is also possible in the present system that only $\Delta\omega_2'$ and $(T_{22}')^{-1}$ are small relative to the other values in equation (58), but the $\Delta\omega_3'$ cannot be ignored. This would be more consistent with the condition that T_{23}' is short due to a hyperfine interaction since this interaction requires a finite electron-nuclear coupling constant and therefore some finite value for $\Delta\omega_3'$. If terms in $\Delta\omega_2'$ and $(T_{22}')^{-1}$ are dropped from equation (58) and noting that $\lambda_3' \tau_{21}'^{-1} + \tau_{23}'^{-1} (T_{23}'^{-1} + \tau_{31}'^{-1}) \approx \lambda_3' (\tau_{21}'^{-1} + \tau_{23}'^{-1})$ since $\lambda_3' (\tau_{21}'^{-1} + \tau_{23}'^{-1}) \gg (\tau_{32}' \tau_{23}')^{-1}$, then

$$(T_{2p})^{-1} = \frac{\left\{ \frac{1}{\tau_{12}\tau_{23}'} + \frac{1}{\tau_{13}} \left\{ \frac{1}{\tau_{21}'} + \frac{1}{\tau_{23}'} \right\} \right\} \left\{ \frac{\lambda_3'}{\tau_{23}'} + (\Delta\omega_3')^2 \right\}}{\left\{ \frac{1}{\tau_{21}'} + \frac{1}{\tau_{23}'} \right\} \left\{ (\lambda_3')^2 + (\Delta\omega_3')^2 \right\}}, \quad (63-a)$$

cancel under either of the probable conditions $(T_{23}')^{-1} \gg (\tau_{32}')^{-1}, (\tau_{31}')^{-1}$ or $\Delta\omega_3'^2 \gg \lambda_3'^2$. If it is also assumed that $(\tau_{21}')^{-1} \gg (\tau_{23}')^{-1} \gg (\tau_{13})^{-1}$ then

$$(T_{2p})^{-1} = \frac{\tau_{21}'}{\tau_{12}} \left\{ \frac{1}{\tau_{23}'} \right\} = P_M (\tau_{23}')^{-1} \quad (63-b)$$

The various limiting conditions which have been discussed correspond to easily recognized situations. If $(T_{23}')^{-1}$ is short then nuclear relaxation in site III' is very fast and the rate limiting step for the relaxation in site I is the exchange into III'. This might be either $I \rightarrow II'$ or $II' \rightarrow III'$ exchange and under the present circumstances it seems most likely that $I \rightarrow II'$ exchange is faster. Then, as long as $I \rightarrow II'$ exchange is faster than $II' \rightarrow III'$ exchange the nuclear relaxation in site I is controlled by the $II' \rightarrow III'$ exchange. Similar considerations apply when $\Delta\omega_3'$ is large but then the relaxation occurs through the change in precessional frequency or dephasing of nuclei from site I. The rate constants for $VO(acac)_2$ in methanol and trichloroethanol and $VO(tfac)_2$ in methanol are given in Table IV.

Substantiating proof for a mechanism involving coordination to the 6th position is the observation of a reduction in the value of $(T_{2p}')^{-1}$ from $3.4_0 \times 10^3 \text{ sec}^{-1} \text{ molal}^{-1}$ to $6.3_0 \times 10^2 \text{ sec}^{-1} \text{ molal}^{-1}$ (at 30°C) by adding a ten fold molar excess of trimethylphosphite to the $VO(acac)_2$ -methanol solution. Trimethylphosphite will coordinate in the 6th position (6l) and consequently decrease the concentration of methanol in this position.

The proton transfer, $II' \rightarrow III'$, is considered to be one of the electron pairs in an sp^2 hybrid orbital on the acetylacetonate ligand oxygen. The bonding of the acetylacetonate ligand to the metal in III' would certainly be weakened because of the reduced

TABLE IV
Rate parameters for solvent proton exchange with
vanadyl complexes

Vanadyl Complex	Solvent	Exchanging Protons	$k \times 10^{-3}$ sec^{-1}	$\Delta H^\ddagger(a)$ kcal mole^{-1}	$\Delta S^\ddagger(a)$ $\text{cal mole}^{-1} \text{deg}^{-1}$
VO^{2+}	CH_3OH	OH	4.35	10.90 (± 0.73)	-5.39 (± 2.3)
		CH_3	0.565	9.46 (± 0.68)	-14.2 (± 2.1)
$\text{VO}(\text{acac})_2$	CH_3OH	OH	66.6	11.79 (± 0.72)	3.1 (± 1.7)
$\text{VO}(\text{tfac})_2$	CH_3OH	OH	12.0	11.12 (± 0.70)	- 2.6 (± 2.1)
$\text{VO}(\text{acac})_2$	$\text{CCl}_3\text{CH}_2\text{OH}$	OH	401	6.41 (± 1.49)	-11.5 (± 4.2)

(a) Errors are quoted as the 95% confidence limits from the nonlinear least squares fit to the data.

charge on the oxygen, however neither the metal ligand σ -bonds, nor the ligand π -bonds are necessarily broken during the proton transfer process.

Several predictions of rate trends can be made on the basis of reaction (61). If the rate of internal proton transfer follows the normal pattern for intermolecular proton transfer (62), then increasing the acidity of the alcohol and the basicity of the acetylacetonate should increase the rate of proton transfer. The results described later show that these predictions do correspond to the observations.

The temperature dependence of $(T_{2p})^{-1}$ for the protons of methanol containing vanadyl trifluoroacetylacetonate is shown in Figure 6. It can be seen by comparison to Figure 5 that the line broadening behavior of $\text{VO}(\text{acac})_2$ and $\text{VO}(\text{tfac})_2$ are similar. The low temperature broadening of the hydroxy and methyl protons is attributed again to inner and outer sphere dipolar relaxation. The unusually long outer sphere interaction distance results from the longer tumbling time found for this complex which in turn gives a greater hydrodynamic radius from the Debye formula. If there is hydrogen bonding between the trifluoromethyl groups and solvent methanol then $\text{VO}(\text{tfac})_2$ may be a sticky, rather than a hard sphere and the Debye theory may not apply. Alternatively, if the hydrogen bonds have a lifetime longer than 10^{-10} sec, then the hydrogen bonded solvent molecules may be tumbling

with the $\text{VO}(\text{tfac})_2$ and the molecule would then have a larger hydrodynamic radius.

It should also be noted that the inner sphere distances $(r_i)_{\text{OH}}$ and $(r_i)_{\text{CH}_3}$ are longer in this system than for $\text{VO}(\text{acac})_2$. This change is in the opposite direction to that expected on electrostatic grounds since the perfluoromethyl groups should leave more positive charge on vanadium in $\text{VO}(\text{tfac})_2$ relative to that in $\text{VO}(\text{acac})_2$, and therefore give a stronger bond to the methanol. However, it must be remembered that the acetylacetone ligands in $\text{VO}(\text{acac})_2$ and probably in $\text{VO}(\text{tfac})_2$ are below the vanadium atom and the planes of each acetylacetonate ligand intersect at an angle of 163° in $\text{VO}(\text{acac})_2$ (63). The factors affecting this type of distortion are not well understood, but if it is greater in $\text{VO}(\text{tfac})_2$ than in $\text{VO}(\text{acac})_2$, then steric crowding may result in a longer bond length to methanol in $\text{VO}(\text{tfac})_2$.

As mentioned previously, the slower hydroxy proton exchange observed in this system compared to $\text{VO}(\text{acac})_2$ is as expected on the basis of the proton transfer mechanism because the trifluoroacetylacetonate oxygens will be less basic than those in acetylacetonate.

The temperature dependence of $(T_{2p}')^{-1}$ for the hydroxy and methylene protons of trichloroethanol solutions of $\text{VO}(\text{acac})_2$ are shown in Figure 7. The low temperature hydroxy and all the methylene proton broadening may be explained by the inner and outer sphere dipolar relaxation processes as discussed previously. The interaction distances and correlation time used are given in Table IV. The interaction distances generally show the expected changes when compared to the $\text{VO}(\text{acac})_2$ -methanol system. The high value for E_a appears unusual but actually corresponds closely to that expected from the temperature dependence of the viscosity of trichloroethanol (8.5 kcal, Chapter IV).

Chemical exchange control of the hydroxy proton $(T_{2p}')^{-1}$ is again observed at high temperature, but there is no exchange control of the nuclear relaxation of the methylene protons. The faster exchange in this system is consistent with either hydrolysis, equation (55), interchange, equation (56) or (57), or intramolecular proton transfer, equation (61). Since trichloroethanol is a stronger acid than methanol it is expected to show faster proton transfer. Although the equilibria would not be so favorable for hydrolysis or interchange, the faster proton transfer might compensate for the smaller concentration of exchanging species.

It is apparent from the temperature dependence of $(T_{2p}')^{-1}$ for the hydroxy and methylene protons of trifluoroethanol solutions of $\text{VO}(\text{acac})_2$ as shown in Figure 8 that no chemical

exchange controlled line broadening is observed for either of the protons. Examination of the interaction distances given in Table V reveals some rather unexpected values for this system. The inner sphere interaction distances are shorter than the values for $\text{VO}(\text{CH}_3\text{OH})_5^{2+}$, exactly the reverse of the expected trend as discussed for $\text{VO}(\text{acac})_2$ in trichloroethanol. The large errors given in the structural determination of trifluoroethanol (64), by electron diffraction, do not preclude the possibility that the bond angles are rather different from those in methanol and therefore, the relative interaction distances of the hydroxy and methylene protons may be different. Extrapolation of the results from the trichloroethanol system to the trifluoroethanol system would indicate that the hydroxy proton exchange lifetime may be shorter than T_{2M} in the latter and there may be some hyperfine contribution to the hydroxy proton broadening as well.

It may be useful to summarize the conclusions from the results in this section. Information obtained from the exchange parameters of the vanadyl perchlorate-methanol system will be discussed more completely in Chapter V. The NMR line broadening of solvent alcohol protons by various vanadyl complexes indicates that there is a rapidly exchanging solvent molecule in the coordination position trans to the vanadyl oxygen. This conclusion rests primarily on

TABLE V

Inner and outer sphere parameters for various vanadyl complex - alcohol systems

Complex	VO(ClO ₄) ₂ CH ₃ OH	VO(acac) ₂ CH ₃ OH	VO(tfac) ₂ CH ₃ OH	VO(acac) ₂ CCl ₃ CH ₂ OH	VO(acac) ₂ CF ₃ CH ₂ OH	
Hydroxy Protons	$\langle r_i \rangle \text{Å}$	2.95	2.95 (a)	3.38	3.22	2.83 (c)
	$\langle r_o \rangle \text{Å}$	4.00	4.00 (a)	6.00	4.30	4.16 (c)
	$\langle T_{2p} \rangle^{-1} \text{ cal, sec}^{-1}$	280	252	260	4350	2200
	$\langle T_{2p} \rangle^{-1} \text{ OBS, sec}^{-1}$	275	256	260	4350	2200
Methyl or Methylene Protons	$\langle r_i \rangle \text{Å}$	3.90	3.90 (a)	4.33	4.17	3.78 (c)
	$\langle r_o \rangle \text{Å}$	4.80	4.80 (a)	6.80	5.10	4.96 (c)
	$\langle T_{2p} \rangle^{-1} \text{ cal, sec}^{-1}$	107	96	98	1350	580
	$\langle T_{2p} \rangle^{-1} \text{ OBS, sec}^{-1}$	100	97	102	1360	583
$\tau_c \times 10^{11}, \text{sec.}$	4.10	3.60	9.35	27.0	10.8	
$E_a^{(b)}, \text{kcal mole}^{-1}$	2.91±0.30	2.60±0.21	3.01±0.29	8.15±1.27	6.50±1.00	

(a) Since no EPR work was done on this system the same values as those for VO(CH₃OH)₅²⁺ were assumed.

(b) Errors are quoted as the 95% confidence limits from the nonlinear least squares fit to the data.

(c) The values of $\langle r_i \rangle_{OH}$ and $\langle r_i \rangle_{CH_3}$ will be too short, and $\langle r_o \rangle_{OH}$ and $\langle r_o \rangle_{CH_3}$ too long, if there is fast hydroxy proton exchange with some hyperfine contribution to the observed T_{2M} relaxation.

the unusual ratio of hydroxy to methyl or methylene proton line broadenings. It is found that this ratio can be quantitatively explained by assuming one rapidly exchanging inner sphere solvent molecule plus the usual outer sphere molecules all interacting with the unpaired electron spin by a dipole-dipole mechanism.

Chemical exchange control of the NMR line broadening has been observed for the hydroxy alcohol proton in all systems except $\text{VO}(\text{acac})_2$ in trifluoroethanol. The methyl or methylene proton line broadening was controlled by chemical exchange only for $\text{VO}(\text{CH}_3\text{OH})_5^{2+}$ in methanol. In the latter system the methyl proton broadening is associated with whole solvent molecule exchange from the four coplanar positions. The faster hydroxy proton exchange is caused by proton dissociation from the coordinated methanol molecules, analogous to that observed for $\text{VO}(\text{H}_2\text{O})_5^{2+}$ in water (59).

Several mechanisms have been considered to explain the hydroxy proton exchange in the various vanadyl acetylacetonate chelate systems. Protonation of the vanadyl oxygen is not consistent with the expected low basicity of this site. A partially solvolysed species undergoing exchange is not consistent with the lack of acid dependence of the hydroxy proton exchange rate. This mechanism also requires that the inner sphere relaxation time for the hydroxy protons is 100 times greater than that for the methyl protons for $\text{VO}(\text{acac})_2$

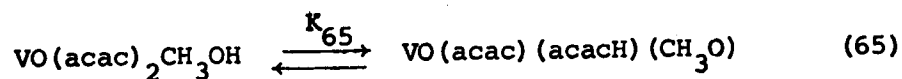
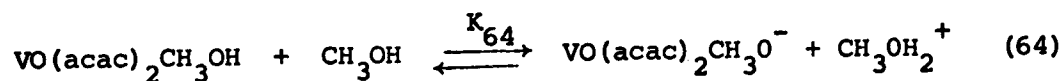
in methanol if whole solvent molecule exchange is much faster than in $\text{VO}(\text{CH}_3\text{OH})_5^{2+}$ as predicted from the results of Wüthrich and Connick (19). Proton dissociation from a solvent molecule trans to the vanadyl oxygen is eliminated because the whole solvent molecule exchange rate from this site is much greater than the observed rates. Finally two mechanisms designated "interchange" and "intramolecular proton transfer" have been considered and both are found to be reasonably consistent with the observations.

The interchange mechanism proposes that normal proton dissociation occurs from a species with one end of an acetylacetonate ligand in the position trans to the vanadyl oxygen and an alcohol molecule in the position vacated by the end of the acetylacetonate. The lack of chemical exchange controlled methyl or methylene proton line broadening requires that the hyperfine coupling constant for these protons is ten times less than that for the hydroxy protons. This mechanism does not seem consistent with the low and more favorable ΔS^\ddagger and faster exchange in the $\text{VO}(\text{acac})_2$ -methanol system compared to the $\text{VO}(\text{CH}_3\text{OH})_5^{2+}$ -methanol system but is otherwise consistent with the results.

The results may also be explained by an intramolecular proton transfer from the molecule trans to the vanadyl oxygen to one of the acetylacetonate oxygen atoms. This mechanism requires that proton relaxation in the trans position is slower

than chemical exchange but that relaxation of the proton on the acetylacetonate oxygen is faster than the chemical exchange. This condition seems reasonable since the electron nuclear hyperfine coupling constant is expected to be much greater for protons in the xy plane of the complex. This mechanism is consistent with the greater exchange rate and more favorable entropy for $\text{VO}(\text{acac})_2$ in methanol compared to $\text{VO}(\text{CH}_3\text{OH})_5^{2+}$ in methanol. The less favorable entropy for methanol hydroxy proton exchange with $\text{VO}(\text{tfac})_2$ compared to $\text{VO}(\text{acac})_2$ also is compatible with this mechanism.

An estimate of the relative basicity of solvent methanol and a coordinated acetylacetonate oxygen may be made by comparing equilibrium constants for the reactions:



Reasonable estimates based on the assumption that the reverse reactions are diffusion controlled would indicate that $K_{64} \approx 10^{-8}$ and $K_{65} \approx 5 \times 10^{-6}$. With due account for the difference in concentration of the bases this result indicates that coordinated acetylacetonate is from 10 to 100 times stronger a base than a solvent methanol molecule. This result does not seem intuitively reasonable but it is too approximate to constitute a strong

argument against the intramolecular proton transfer mechanism.
More knowledge on the charge distribution in these complexes
and the acidity of coordinated ligands is obviously required.

3. Nuclear Magnetic Resonance Line Broadenings of Nonaqueous Methanol by Copper(II) Complexes

It was proposed by Cotton and Wise (65) that the unpaired electron in copper(II) existed in the d_{xy} orbital as in the vanadyl ion. This proposal led to the study of copper(II) acetylacetonate $\{Cu(acac)_2\}$ and copper(II) perchlorate $\{Cu(ClO_4)_2\}$ in methanol, to determine if the same behavior was exhibited by the copper(II) and vanadyl systems.

Plots of $\log (T_{2p}')^{-1}$ versus the inverse of the absolute temperature for the two copper systems are shown in Figures 10 and 11. $(T_{2p}')^{-1}$ was obtained as before from equation (41) of Chapter III, section 1. In this study $[M]$ is the concentration in molal units of copper(II) acetylacetonate or copper(II) perchlorate. The small, linear decrease of $\log (T_{2p}')^{-1}$ with $(T^\circ K)^{-1}$ for $Cu(acac)_2$ in methanol (Figure 10) indicates that the broadening of the hydroxy and methyl proton resonances is due to a T_{2M} relaxation process. The lack of any shift of the methanol proton resonance signals in this system suggests that any hyperfine contact coupling between these protons and the unpaired electron on copper(II) is small. This is reasonable if solvated $Cu(acac)_2$ exists as a distorted octahedral complex with the methanol ligands in the two sites above and below the plane formed by the copper and the two acetylacetonate ligands. The Jahn-Teller distortion in the complex may make the copper-

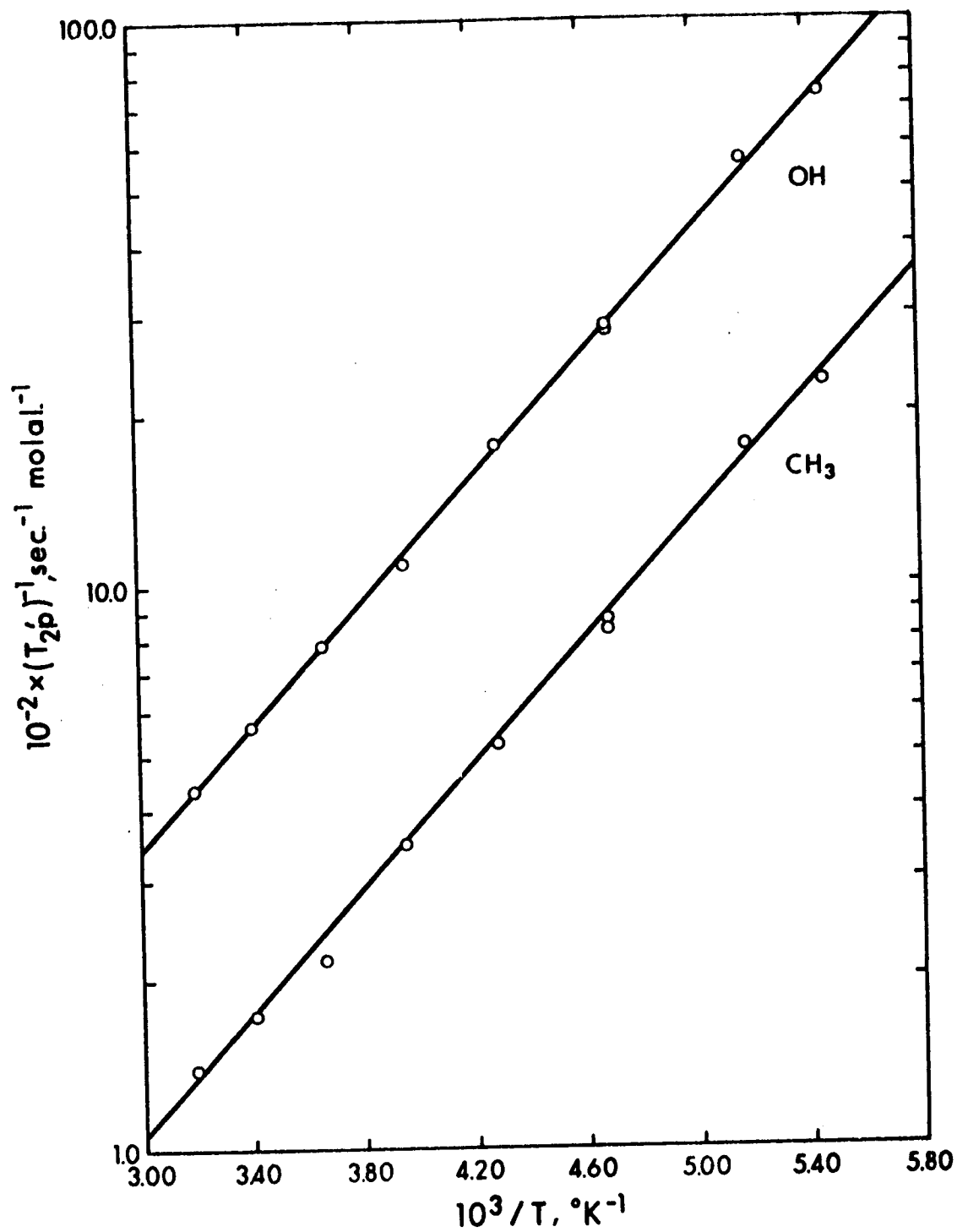


Figure 10: Temperature dependence of $\log (T_{2p})^{-1}$ at 60 MHz for the protons of methanol containing copper acetylacetonate.

methanol coordinate bonds somewhat weaker than in a regular octahedron and consequently the hyperfine coupling constant may be smaller.

The broadening (Figure 10) is assumed to be due to a dipole-dipole interaction which is dependent on a correlation time, τ_c , given by equation (28) of Chapter I, section 1. If the $\text{Cu}(\text{acac})_2$ has two axial methanol molecules exchanging rapidly with $\tau_M \ll T_{2M}$, then there is an inner sphere dipolar contribution to $(T_{2p}')^{-1}$ {equation(45-b)} in addition to the usual outer sphere contribution {equation (46-b)}. The respective amounts of inner and outer sphere broadening were calculated by an iterative method. The same interaction distances as those obtained for $\text{VO}(\text{acac})_2$ in methanol were used and the iteration was carried out until self-consistent values for τ_c were obtained. The resulting correlation time of $4.8_0 \times 10^{-11}$ sec at 25°C gives inner sphere and outer sphere contributions to $(T_{2p}')_{\text{OH}}^{-1}$ of $40_5 \text{ sec}^{-1} \text{ molal}^{-1}$ and $13_0 \text{ sec}^{-1} \text{ molal}^{-1}$, respectively, for the hydroxy proton. Of course the sum of these contributions agrees exactly with the observed $(T_{2p}')_{\text{OH}}^{-1}$ of $53_5 \text{ sec}^{-1} \text{ molal}^{-1}$. The methyl proton broadening may then be calculated using this value of τ_c obtained from $(T_{2p}')_{\text{OH}}^{-1}$ and the same methyl interaction distances as used in the $\text{VO}(\text{acac})_2$ -methanol system. The calculated inner and outer sphere methyl proton broadenings are $78.2 \text{ sec}^{-1} \text{ molal}^{-1}$

and $77.0 \text{ sec}^{-1} \text{ molal}^{-1}$, respectively; their sum is in reasonable agreement with the observed value for $(T_{2p}')_{\text{CH}_3}^{-1}$ of $165.0 \text{ sec}^{-1} \text{ molal}^{-1}$. There is also evidence that $\text{Cu}(\text{acac})_2$ coordinates to only one other ligand with distortion of the acetylacetonate ligands out of the plane (82). Therefore, this possibility was considered here and it was found that a correlation time of $7.6_5 \times 10^{-11} \text{ sec}$ gave an inner and outer sphere $(T_{2p}')_{\text{OH}}^{-1}$ at 25°C of $329.0 \text{ sec}^{-1} \text{ molal}^{-1}$ and $206.0 \text{ sec}^{-1} \text{ molal}^{-1}$, respectively, the sum of which is identical with the observed value. However, the corresponding values for the methyl protons are $60.7 \text{ sec}^{-1} \text{ molal}^{-1}$ and $120.0 \text{ sec}^{-1} \text{ molal}^{-1}$, respectively, the sum of which is in relatively poor agreement with the observed value of $165.0 \text{ sec}^{-1} \text{ molal}^{-1}$. The agreement of calculated and observed $(T_{2p}')_{\text{CH}_3}^{-1}$ is only slightly better if two inner sphere molecules are assumed, but the correlation time seems much more reasonable when compared to the value of $3.6_0 \times 10^{-11} \text{ sec}$ for $\text{VO}(\text{acac})_2$ in methanol.

There is also the possibility that $\text{Cu}(\text{acac})_2$ has a tumbling time identical to $\text{VO}(\text{acac})_2$ in methanol. If this possibility is assumed and the interaction distances for $\text{Cu}(\text{acac})_2$ in methanol are taken to be the same as in the $\text{VO}(\text{acac})_2$ -methanol system, then the inner and outer sphere dipolar relaxation mechanisms account for $402.0 \text{ sec}^{-1} \text{ molal}^{-1}$ of the observed $535.0 \text{ sec}^{-1} \text{ molal}^{-1}$ for the hydroxy proton and $113.0 \text{ sec}^{-1} \text{ molal}^{-1}$ of the

observed $165.0 \text{ sec}^{-1} \text{ molal}^{-1}$ for the methyl protons at 25°C . If the remainder of $(T_{2p}')_{\text{OH}}^{-1}$ and $(T_{2p}')_{\text{CH}_3}^{-1}$ is attributed to a hyperfine interaction, then assuming the approximate value for $\tau_e \approx 10^{-10} \text{ sec}$ (67) the coupling constant for the hydroxy proton would have to be $(A/h)_{\text{OH}} \approx 1.4_5 \times 10^6 \text{ cps}$ and for the methyl proton $(A/h)_{\text{CH}_3} \approx 9.1_0 \times 10^5 \text{ cps}$. These coupling constants indicate that a shift of approximately 15 Hz should have been seen at 25°C for the hydroxy proton and 10 Hz for the methyl protons. However, since no shift was observed, the coupling constants must be at least an order of magnitude less than those given above. These results indicate that any contribution to $(T_{2p}')_{\text{OH}}^{-1}$ and $(T_{2p}')_{\text{CH}_3}^{-1}$ from a hyperfine interaction must be negligible.

The correlation time, $\tau_c = 4.8_0 \times 10^{-11} \text{ sec}$, obtained for the distorted octahedral model may be the electron spin relaxation time, τ_s , the solvent exchange time, τ_M , or the complex tumbling time, τ_R , as shown by equation (28). The shortest of these three times will equal τ_c . Since copper(II) complexes are known to give reasonably sharp EPR spectra τ_s must be much larger than $4.8_0 \times 10^{-11} \text{ sec}$. τ_c may be the chemical exchange lifetime; however, it seems more consistent with $\tau_R = 3.6_0 \times 10^{-11} \text{ sec}$ for the $\text{VO}(\text{acac})_2$ -methanol system. The temperature dependence ($2.5_0 \text{ kcal mole}^{-1}$) also agrees with that of the latter system ($2.60 \pm 0.20 \text{ kcal mole}^{-1}$).

The temperature dependence of $\log (T_{2p}')^{-1}$ and the chemical

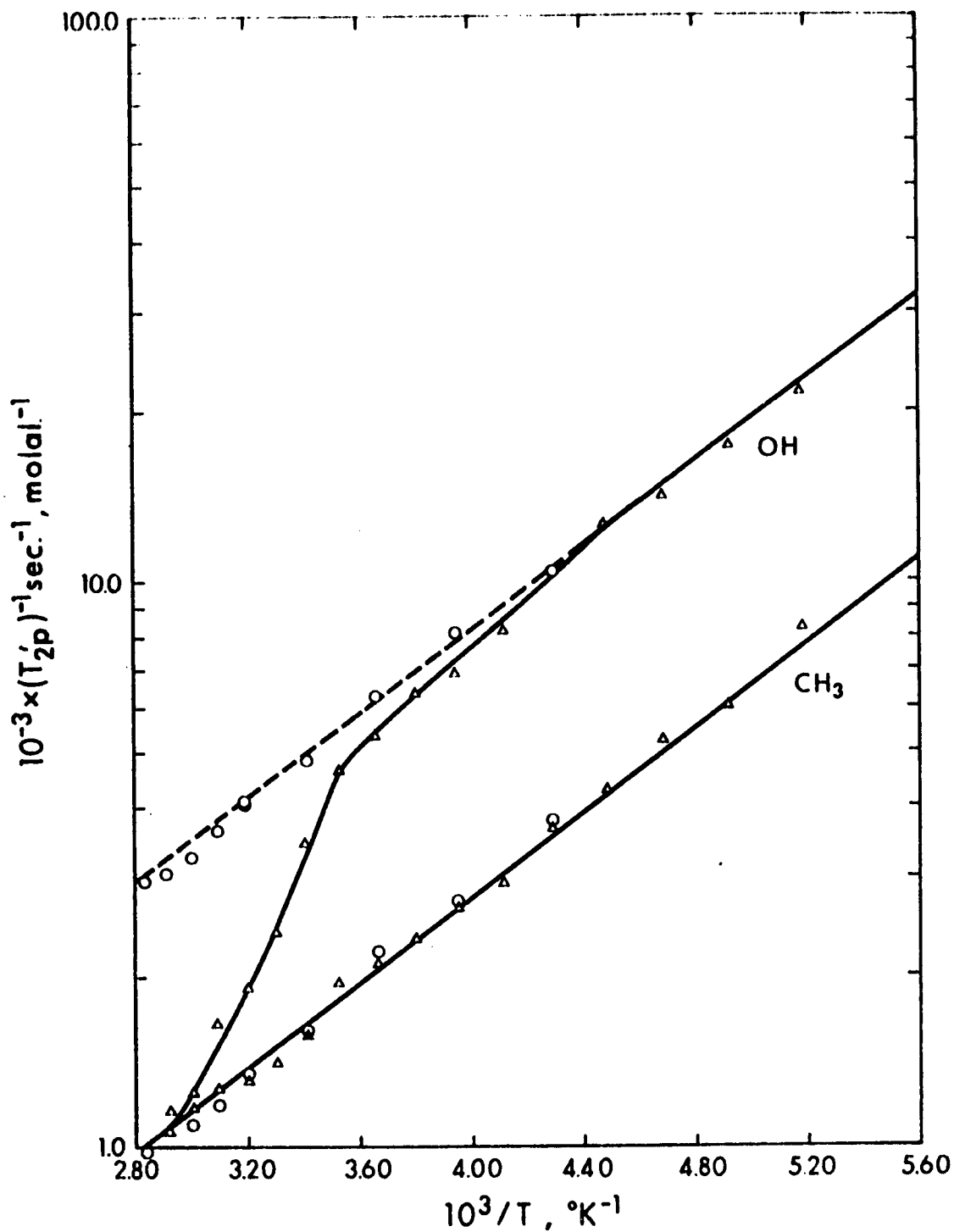


Figure 11: Temperature dependence of $\log (T_{2p}')^{-1}$ at 60 MHz for the protons of methanol containing copper (II) perchlorate - Δ , containing copper (II) perchlorate and 1.5 molar in hexafluorophosphoric acid - O.

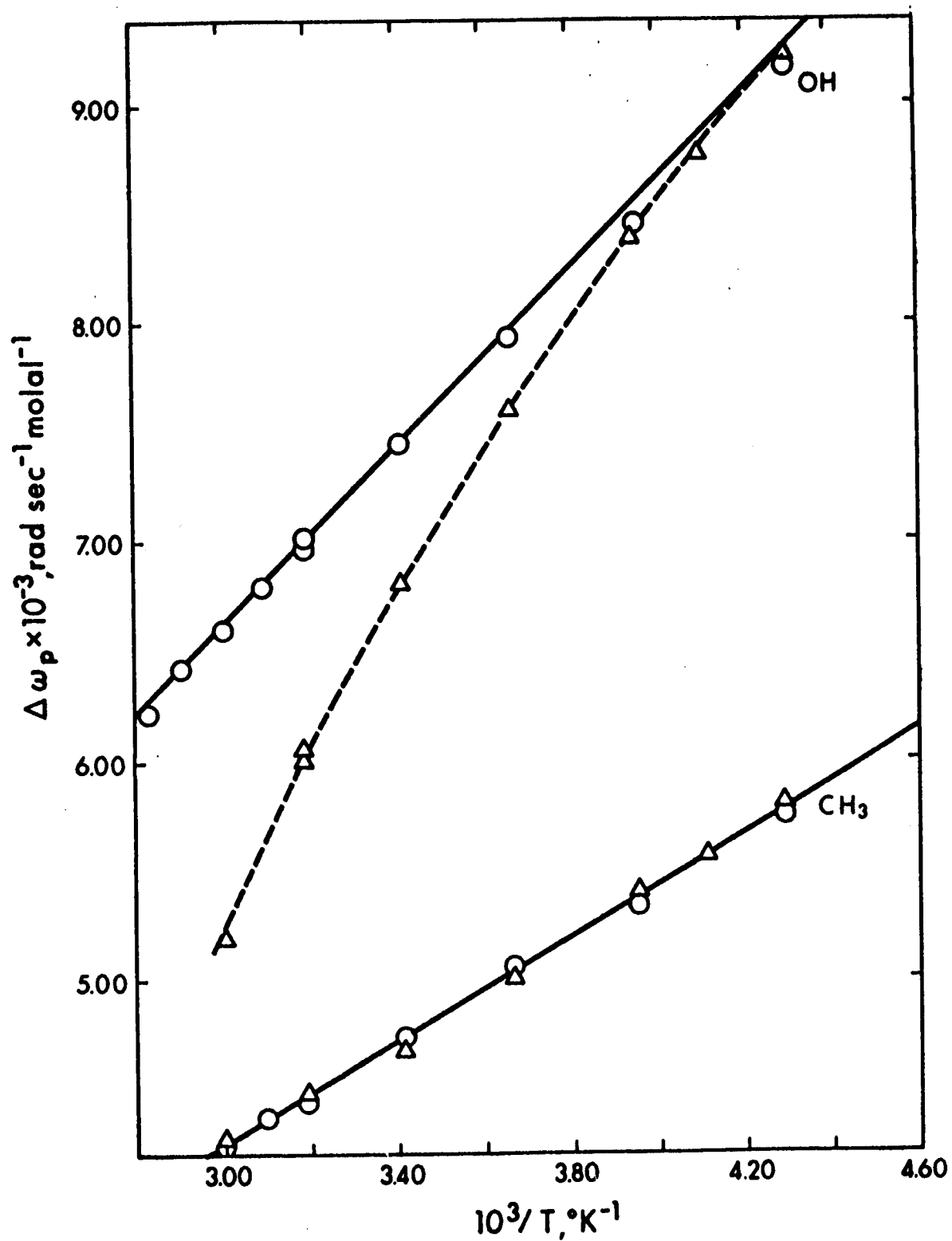
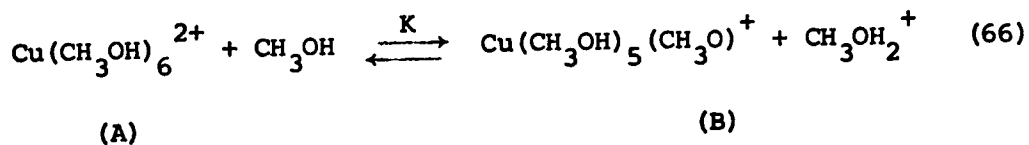


Figure 12: Temperature dependence of the shift normalized to 1 molal at 60 MHz for the protons of methanol containing copper(II) perchlorate - Δ , containing copper(II) perchlorate and 1.5 molar in hexafluorophosphoric acid - O.

shift, $\Delta\omega_p$, for the methanol protons in the copper(II) perchlorate-methanol system are shown in Figures 11 and 12, respectively. Both the hydroxy proton and methyl protons show a linear variation of $\log (T_{2p}')_{OH}^{-1}$ and $\Delta\omega_p$ with $(T^\circ K)^{-1}$ at low temperatures; the temperature dependence of these parameters is small. This behavior indicates rapid exchange and T_{2M} control of T_{2p} . However, at high temperatures $(T_{2p}')_{OH}^{-1}$ and $\Delta\omega_p$ for the hydroxy protons deviate dramatically from the low temperature linearity but the methyl protons appear to behave normally. This is the behavior expected if the hydroxy protons on the coordinated methanol are dissociating from the copper complex as indicated by equation (66).



where

$$K = \frac{[\text{B}] [\text{CH}_3\text{OH}_2^+]}{[\text{A}]} = \frac{[\text{B}]^2}{[\text{A}]} \quad (67)$$

The $(T_{2p}')_{OH}^{-1}$ data indicates that the undissociated form predominates at low temperatures. This proposal was verified by adding copper(II) perchlorate to anhydrous 1.5 molar hexafluorophosphoric acid in methanol. This solution was prepared by mixing $\text{Cu}(\text{CH}_3\text{OH})_6(\text{ClO}_4)_2$ and 60% H_3PF_6 in methanol and storing for four days over molecular sieves. The added acid prevents proton dissociation and $\log (T_{2p}')_{OH}^{-1}$

and $\Delta\omega_p$ for the hydroxy proton show only the expected linear dependence with $(T^\circ K)^{-1}$. The fact that $(T_{2p}')_{CH_3}^{-1}$ for the methyl protons is the same in both pure methanol and in the H_3PF_6 solution shows that no water has been left in the first coordination sphere of copper(II) in the latter solution.

Preliminary calculations indicated that inner and outer sphere dipolar and inner sphere hyperfine interactions, equation (31), are contributing to the low temperature $(T_{2p}')_{OH}^{-1}$ of the hydroxy proton and to the $(T_{2p}')_{CH_3}^{-1}$ of the methyl protons. The outer sphere dipolar contribution was assumed to be the same as that for copper(II) acetylacetonate in methanol, and the inner sphere dipolar contribution was taken as three times that for copper(II) acetylacetonate since the copper(II) ion probably has six rather than two inner sphere solvent molecules. These assumptions imply that the same interaction distances, tumbling time, and activation energy apply for $Cu(acac)_2(CH_3OH)_2$ and $Cu(CH_3OH)_6^{2+}$ in methanol. The assumptions made here are at least consistent with the results for $VO(acac)_2$ and $VO(CH_3OH)_5^{2+}$ in methanol.

Initially, the methyl proton $(T_{2p}')_{CH_3}^{-1}$ data was analyzed in Figure 11 by fitting it to the following expression:

$$(T_{2p}')_{CH_3}^{-1}(\text{OBS}) - (T_{2p}')_{CH_3}^{-1}(\text{DIPOLAR}) = P_M C_{CH_3}^{-1} \exp(E_a/RT) \quad (68)$$

by a nonlinear least squares method. This expression is a modification of equation (31); E_a is the temperature dependence

of the hyperfine interaction correlation time, C_{CH_3} contains, in addition to other known parameters, the product of the square of the isotropic hyperfine coupling constant and the hyperfine interaction correlation time at infinite temperature (τ_0). To separate these latter two parameters, it was necessary to obtain the isotropic coupling constant, $(A/h)_{\text{CH}_3} = 2.30 \pm 0.41 \times 10^6$ cps, from an analysis of the shift as discussed below. This analysis gives $\tau_0 = 8.22 \pm 0.30 \times 10^{-12}$ sec with a temperature dependence of 1.64 ± 0.02 kcal mole⁻¹; these parameters give a hyperfine interaction correlation time (τ_A) at 25°C of $1.3_1 \times 10^{-10}$ sec.

The isotropic coupling constant for the methyl protons can be obtained from the shift measurements. Extrapolation of the plot of $\Delta\omega_p$ versus $(T^\circ\text{K})^{-1}$ shows that $\Delta\omega_p$ is not zero when $(T^\circ\text{K})^{-1}$ is zero. This is contrary to the prediction of equation (22) and may be most simply interpreted by assuming that the magnetic moment is not given by the spin-only value and that it is temperature dependent. Griffith (74) has given an expression for the magnetic moment of copper(II):

$$\mu_{\text{eff}}^2 = \frac{3}{4} g^2 + \frac{12kT}{E(^2T_2) - E(^2E)} \quad (69)$$

where $g^2 = \frac{1}{3} (g_x^2 + g_y^2 + g_z^2)$ with $g_x = g_y = g_{\perp}$ and $g_z = g_{\parallel}$; g_{\parallel} and g_{\perp} can be obtained from a low temperature (-173°C) EPR spectrum of a dilute solution, 10^{-3} molal, of $\text{Cu}(\text{ClO}_4)_2$ in

anhydrous methanol. These parameters were determined from two well defined spectra and were found to be 2.39_3 and 2.05_5 , respectively. $E(^2T_2) - E(^2E)$ is the energy of the transition shown by the broad absorption band at $12,300 \text{ cm}^{-1}$ in the visible spectrum (75) for $\text{Cu}(\text{ClO}_4)_2$ in methanol. The last term in equation (69) results from so-called high frequency contributions due to mixing of ground and excited electronic states. Using this expression for μ_{eff} allows the isotropic hyperfine coupling constant to be calculated by a nonlinear least squares fit of equation (21) to the shift data.

The hydroxy proton $(T_{2p}')_{\text{OH}}^{-1}$ and $\Delta\omega_p$ data for the $\text{Cu}(\text{ClO}_4)_2$ methanol solution containing H_3PF_6 was also treated in the same manner as the methyl proton data. It was found that τ_0 and E_a agreed for the two analyses within the error which is quoted as the 95% confidence limits on the least squares fit. The isotropic coupling constant for the hydroxy protons was calculated to be $(A/h)_{\text{OH}} = 3.75 \pm 0.10 \times 10^6 \text{ cps}$.

It is possible, after making several reasonable approximations, to give a quantitative interpretation of the temperature variation of $(T_{2p}')_{\text{OH}}^{-1}$ and $\Delta\omega_p$ for the hydroxy protons in the copper-methanol system. It is assumed that the $\text{Cu}(\text{CH}_3\text{OH})_5(\text{CH}_3\text{O})^+$ species is less effective in broadening the hydroxy proton resonance because of a much reduced hyperfine contribution to the relaxation mechanism. If the dipolar (inner and outer sphere) contributions to $(T_{2p}')_{\text{OH}}^{-1}$

are assumed to be the same for $\text{Cu}(\text{CH}_3\text{OH})_6^{2+}$ and $\text{Cu}(\text{CH}_3\text{OH})_5(\text{CH}_3\text{O})^+$,
then

$$(\tau_{2p}')_{\text{OH(OBS)}}^{-1} - (\tau_{2p}')_{\text{OH(DIPOLAR)}}^{-1} = \left\{ (\tau_{2p}')_{\text{A}}^{-1} + (\tau_{2p}')_{\text{B}}^{-1} \right\} \text{HYPERFINE} \quad (70)$$

where A and B represent $\text{Cu}(\text{CH}_3\text{OH})_6^{2+}$ and $\text{Cu}(\text{CH}_3\text{OH})_5(\text{CH}_3\text{O})^+$, respectively.

The error in $(\tau_{2p}')_{\text{OH(DIPOLAR)}}^{-1}$ due to the approximation that the stoichiometric factor is the same for species A and B is less than 5%. The hyperfine contributions of A, $(\tau_{2p}')_{\text{A}}^{-1}$, may be represented by $[A] C_A \exp(E_a/RT)$ where [A] is the concentration of A, C_A is a constant containing the isotropic hyperfine coupling constant and the hyperfine interaction correlation time at infinite temperature. If an analogous expression is written for $(\tau_{2p}')_{\text{B}}^{-1}$, assuming the activation (E_a) is the same for both species, then

$$(\tau_{2p}')_{\text{OH(OBS)}}^{-1} - (\tau_{2p}')_{\text{OH(DIPOLAR)}}^{-1} = \left\{ P_{\text{MA}} [A] C_A + P_{\text{MB}} [B] C_B \right\} \exp(E_a/RT) \quad (71)$$

where $P_{\text{MA}} = 6/[\text{CH}_3\text{OH}]$ and $P_{\text{MB}} = 5/[\text{CH}_3\text{OH}]$. Now, [A] and [B] are related through the equilibrium constant given by equation (67) and

$$[A] + [B] = [\text{Cu}^{2+}]_{\text{TOTAL}} = 1.00\text{m} \quad (72)$$

Also, K is assumed to have the usual form

$$K = \exp(-\Delta H/RT + \Delta S/R) \quad (73)$$

Then substituting equations (67) and (73) into (72) gives

$$[B] = \exp(\Delta S/R) \left\{ -\exp(-\Delta H/RT) + \sqrt{\exp(-2\Delta H/RT) + 4 \exp(-\Delta H/RT)} \right\}; \quad (74)$$

[A] is obtained immediately from equation (72).

The expressions for [B] and [A] were substituted into equation (71) and the best fit of the data to this equation was obtained by varying ΔH , ΔS and C_B ; C_A was evaluated from the results of the $\text{Cu}(\text{ClO}_4)_2$ -methanol- H_3PF_6 system. ΔH , ΔS and C_B were found to be 5.6_3 kcal mole⁻¹, 8.7_0 e.u., and 33.3 sec⁻¹, respectively. The isotropic coupling constant and correlation time in C_B were separated by determining the coupling constant from a fit of equation (75) to the hydroxy proton shift data.

$$\Delta\omega_{\text{P(OBS)}} = P_{\text{MA}} \Delta\omega_{\text{MA}} [\text{A}] + P_{\text{MB}} \Delta\omega_{\text{MB}} [\text{B}] \quad (75)$$

All the parameters in equation (75) are known except the coupling constant of species B, which was found to be $(A/h)_{\text{OH(B)}} = 3.75 \pm 0.20 \times 10^6$ cps from the least squares fit. The correlation time (τ_0) could then be calculated from C_B giving $\tau_0 = 2.4_6 \times 10^{-12}$ sec or at 25°C, $\tau_B = 3.9_6 \times 10^{-11}$ sec. It may also be noted that μ_{eff} was taken to be the same for the dissociated and undissociated copper(II)-methanol complexes. This procedure assumes that $E(^2T_2) - E(^2E)$ does not vary significantly for the two species, and since the second term on the right in equation (69) only contributes about 4% to the total μ_{eff} , this is not considered to be a significant assumption. However, it is also assumed that g , the average g -value, is the same for both species. This assumption may be reasonable since it was found in the EPR study

on vanadyl complexes in Chapter IV that although g_{11} and g_1 may vary appreciably, g does not vary significantly. Therefore, the same behavior may be demonstrated by these two copper complexes.

It is now of interest to attempt to identify the correlation times which have been obtained for the two species A and B, that is, $\tau_A = 1.3_1 \times 10^{-10}$ sec and $\tau_B = 3.9_6 \times 10^{-11}$ sec at 25°C. τ_A for the undissociated species is very similar to the value obtained by Meredith (67) for the aquo-copper(II) system ($\tau_e = 1.44 \times 10^{-10}$ sec at 25°C) which he identified with the exchange of water on copper(II). It is quite possible that the value obtained here is the exchange rate of methanol on copper(II). However, for the dissociated species a shorter correlation time has been obtained. From the parameters obtained above the equilibrium constant for dissociation is $K = 7.6 \times 10^{-3}$ molal at 25°C. If $K = k_f/k_r$ and the reverse of reaction (66) is assumed to be diffusion controlled, that is, $k_r \approx 10^{10}$ sec⁻¹, then $k_f \approx 10^8$ sec⁻¹; therefore, the correlation time cannot be due to a intermolecular dissociation of the proton. However, it may be possible that intramolecular proton transfer to the coordinated methoxide in the dissociated species can proceed somewhat faster than 10^8 sec⁻¹. If the axial and equatorial hydroxy proton coupling constants differ this process would account for the change in the correlation time of this proton with no apparent change in that for the methyl protons.

In the analysis of the shift for the $\text{Cu}(\text{ClO}_4)_2$ -methanol system it should be noted that due to the anisotropy in the

copper(II) complexes, which is caused by Jahn-Teller distortions, the isotropic shift has contributions from a contact interaction and a psuedo-contact interaction (83). That is

$$\Delta\omega_p = \Delta\omega_c + \Delta\omega_{pc} \quad (76)$$

where $\Delta\omega_p$ is the total observed shift, $\Delta\omega_c$ is the contact shift, and $\Delta\omega_{pc}$ is the psuedo-contact shift.

McConnell and Robertson (66) have given an expression for the psuedo-contact shift:

$$\Delta\omega_{pc} = \frac{-\beta^2 S(S+1) (3 \cos^2 \phi - 1) \omega_o}{27r_i^3 kT} (g_{||} + 2g_{\perp}) (g_{||} - g_{\perp}) \quad (77)$$

where β is the Bohr magneton, S is the sum of the free spins, $g_{||}$ and g_{\perp} are the anisotropic g -values parallel and perpendicular to the crystal field axis, ϕ is the angle between the crystal field axis of the complex (taken in the axial direction for the copper(II) complexes) and the radius vector from the metal ion to the proton, r_i is the length of this vector, k is Boltzmann's constant, T is the absolute temperature and ω_o is the operating frequency. If the inner sphere interaction distances of the hydroxy and methyl are taken to be the same in this system as for the vanadyl ion-methanol complex as in Chapter III, section 2 and ϕ is taken as equal to 0° for the ligands in the axial positions and 90° for those in the equatorial positions, then a total psuedo-contact

contribution to the observed shift of a 1 Molal solution at 25°C for the hydroxy protons is 243.0 radians and for the methyl protons is 120.0 radians. This psuedo-contact shift contribution can then be calculated for any temperature and subtracted from the observed shift, thus allowing a contact coupling constant to be calculated. The isotropic hyperfine contact coupling constants for the hydroxy and methyl protons were found to be $(A/h)_{OH(CONTACT)} = 3.60 \pm 0.50 \times 10^6$ cps and $(A/h)_{CH_3(CONTACT)} = 2.25 \pm 0.45 \times 10^6$ cps, respectively. These coupling constants differ from the total hyperfine coupling constant by only about 4% which means that only 4% of the shift is caused by a psuedo-contact interaction due to anisotropy in the copper(II) complexes.

4. Nuclear Magnetic Resonance Line Broadening of Methanol and Trimethylphosphate by Chromium(II) and Vanadium(II)

The line broadening of the proton magnetic resonance of the solvents methanol (CH_3OH) and trimethylphosphate (TMPA) in the presence of chromium(II) and vanadium(II) has been studied in an extension of the previous studies on these ions in aqueous solution. Meredith and Connick (67) studied the 0^{17} line broadening in the chromium(II)-water system and Taube and co-workers (68) have reported a similar study on vanadium(II) in water.

Plots of $\log (T_{2p}')^{-1}$ versus the inverse of the absolute temperature are shown in Figures 14 and 16 for the chromium(II) and vanadium(II) - methanol systems and in Figures 17 and 18 for the chromium(II) and vanadium(II) - trimethylphosphate systems. The excess broadening of the bulk solvent proton magnetic resonances as shown in these plots are interpreted as due to a dipolar interaction of the protons with the paramagnetic centres. Equation (31) for the inner sphere broadening and equation (32) for the outer sphere broadening were used in the analyses of this data.

The inner sphere interaction distances required in equations (31) and (32) were taken from the estimated values for the vanadyl-trimethylphosphate system in Chapter III, section 1 (4.9_0°\AA) and the calculated values for the vanadyl-methanol system in Chapter III, section 2 (2.9_5°\AA and 3.9_0°\AA for the hydroxy and methyl protons, respectively). The outer sphere interaction distance for the trimethylphosphate system was taken as 7.5_5°\AA and for the methanol

systems as 4.0_0°\AA for the hydroxy proton and 4.8_0°\AA for the methyl protons.

It can easily be shown that the observed broadening in the chromium(II) - methanol system is not due to a hyperfine interaction. The hyperfine coupling constants which can be calculated from the temperature dependence of the shift (Figure 15) are $7.2_0 \times 10^4$ cps for the hydroxy proton and $1.0_3 \times 10^5$ cps for the methyl protons. These values substituted into the second term of equation (31) (assuming $\omega_e^2 \tau_e^2 \gg 1$) give $\tau_e = 1.2_5 \times 10^{-8}$ sec. However, the inability to observe an EPR resonance for chromium(II) puts an upper limit of approximately 6×10^{-11} sec. (67) on τ_s . Therefore, this large inconsistency shows that the broadening does not originate from a hyperfine interaction.

However, if the ligand exchange is rapid for the chromium(II) - methanol complex, then the excess broadening can be interpreted as an inner and outer sphere dipolar relaxation process. It was initially assumed that the excess broadening for the hydroxy proton was due entirely to an inner sphere dipolar relaxation process and a correlation time (τ_c) was calculated using equation (31) with $\omega_e^2 \tau_c^2 \gg 1$, then τ_c was substituted back into $\omega_e^2 \tau_c^2$ in equation (31) with no approximations and a new value for τ_c was obtained. This process was continued until a self consistent correlation time was obtained. The resultant value of τ_c

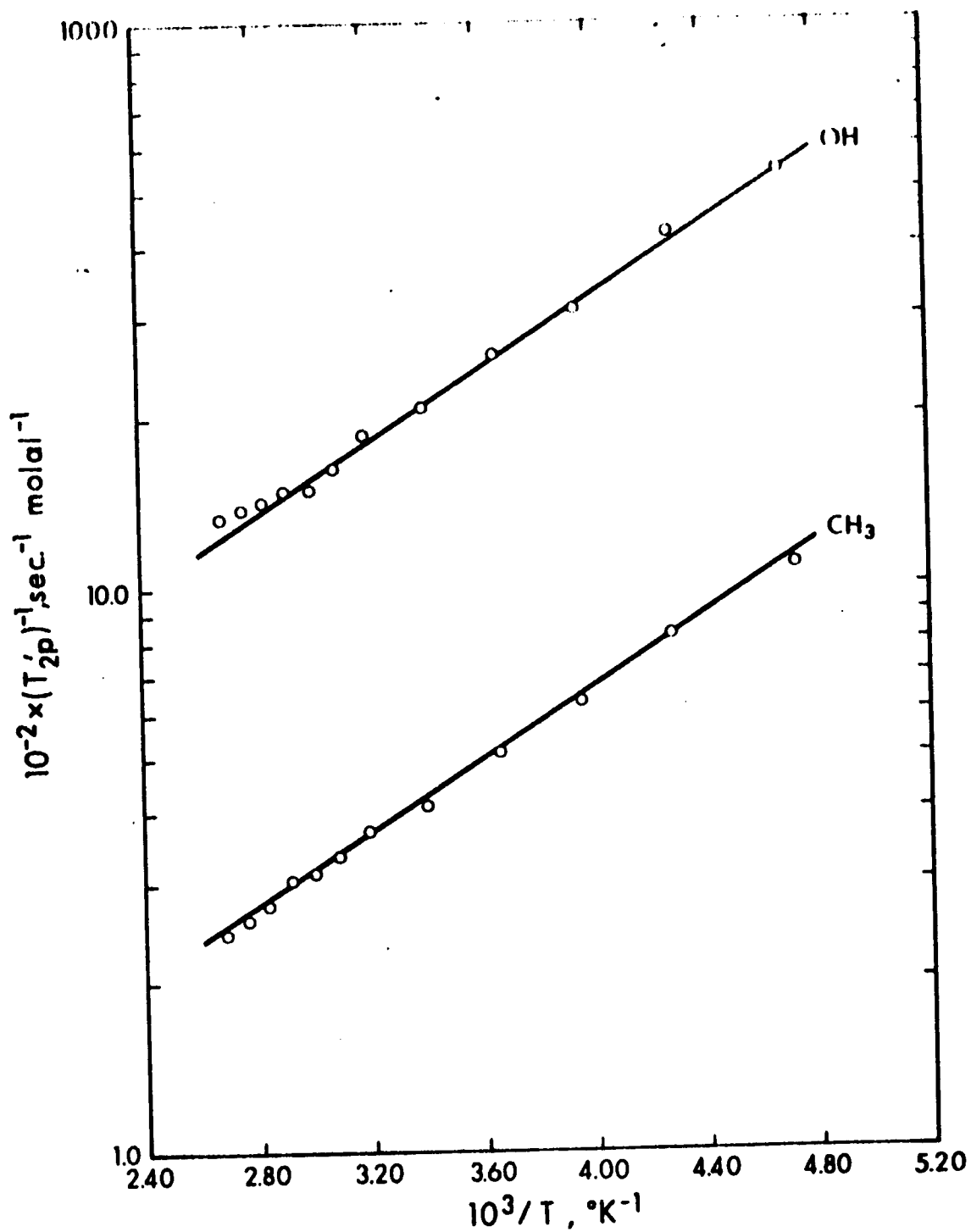


Figure 14: Temperature dependence of $\log (T_{2p}')^{-1}$ at 60 MHz for the protons of methanol containing chromium (II) tetrafluoroborate.

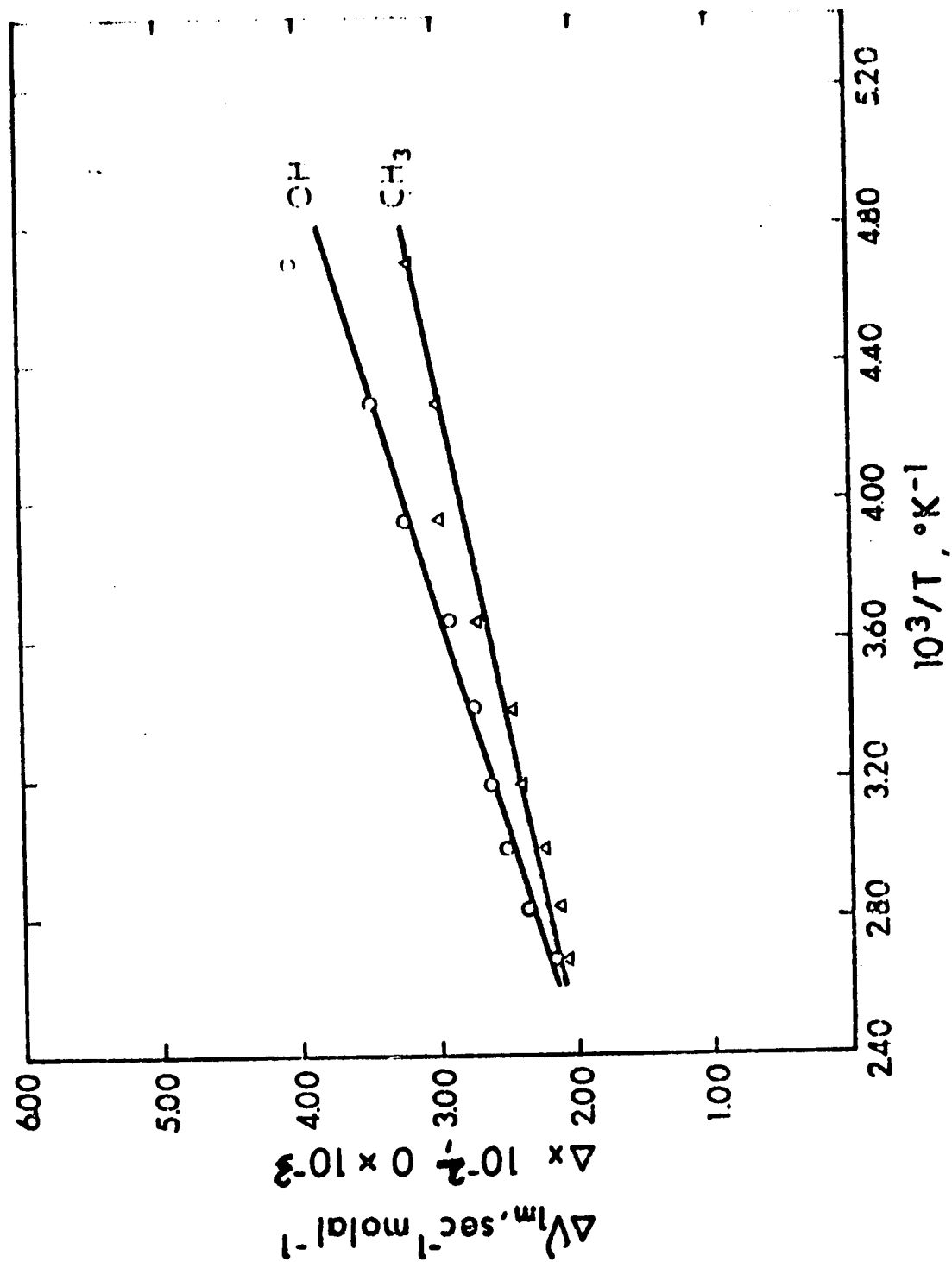


Figure 15: Temperature dependence of the shift normalized to 1 molal at 60 MHz for the protons of methanol containing chromium (II) tetrafluoroborate.

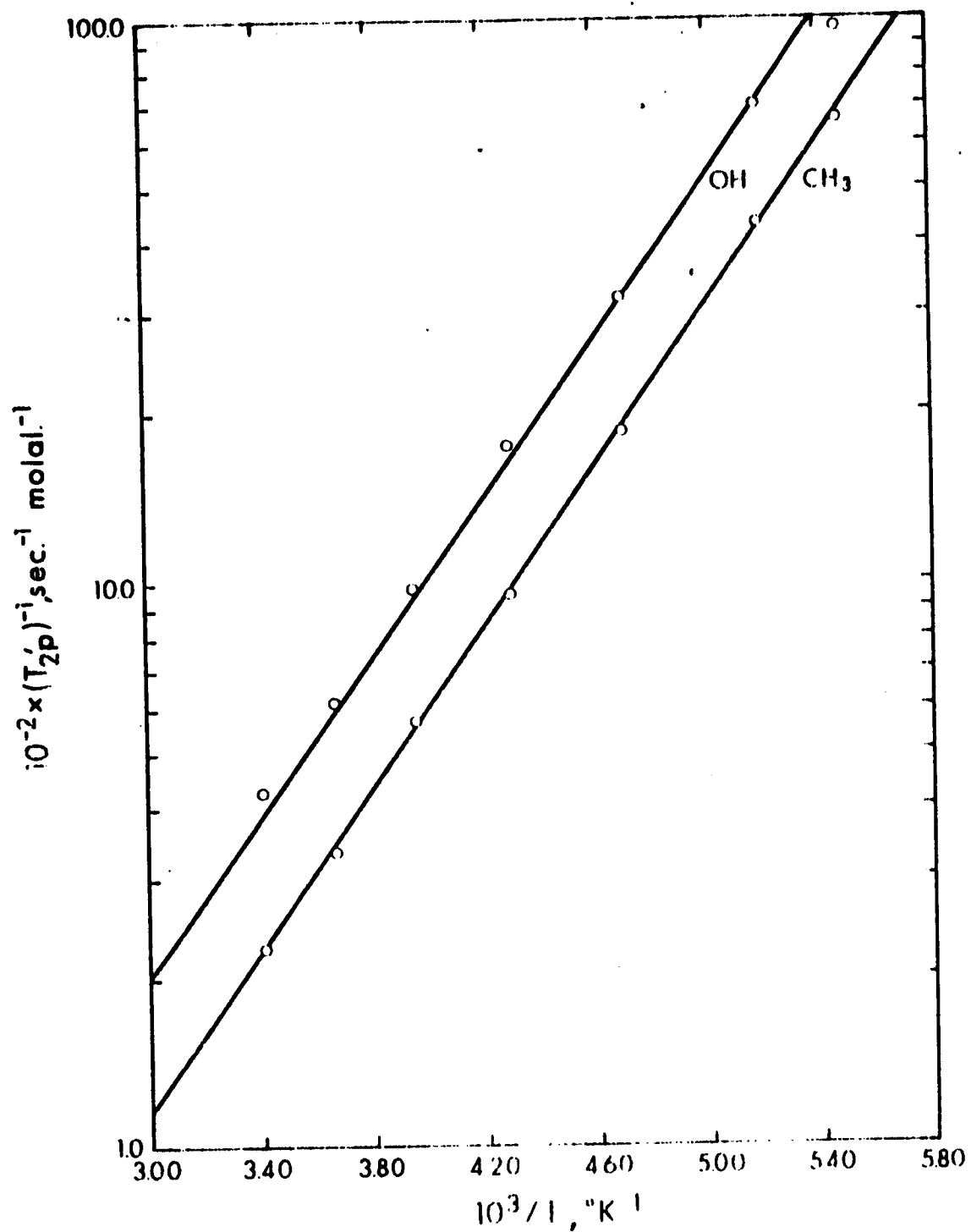


Figure 16: Temperature dependence of $\log (T_{2p}')^{-1}$ at 60 MHz for the protons of methanol containing vanadium (II) tetrafluoroborate.

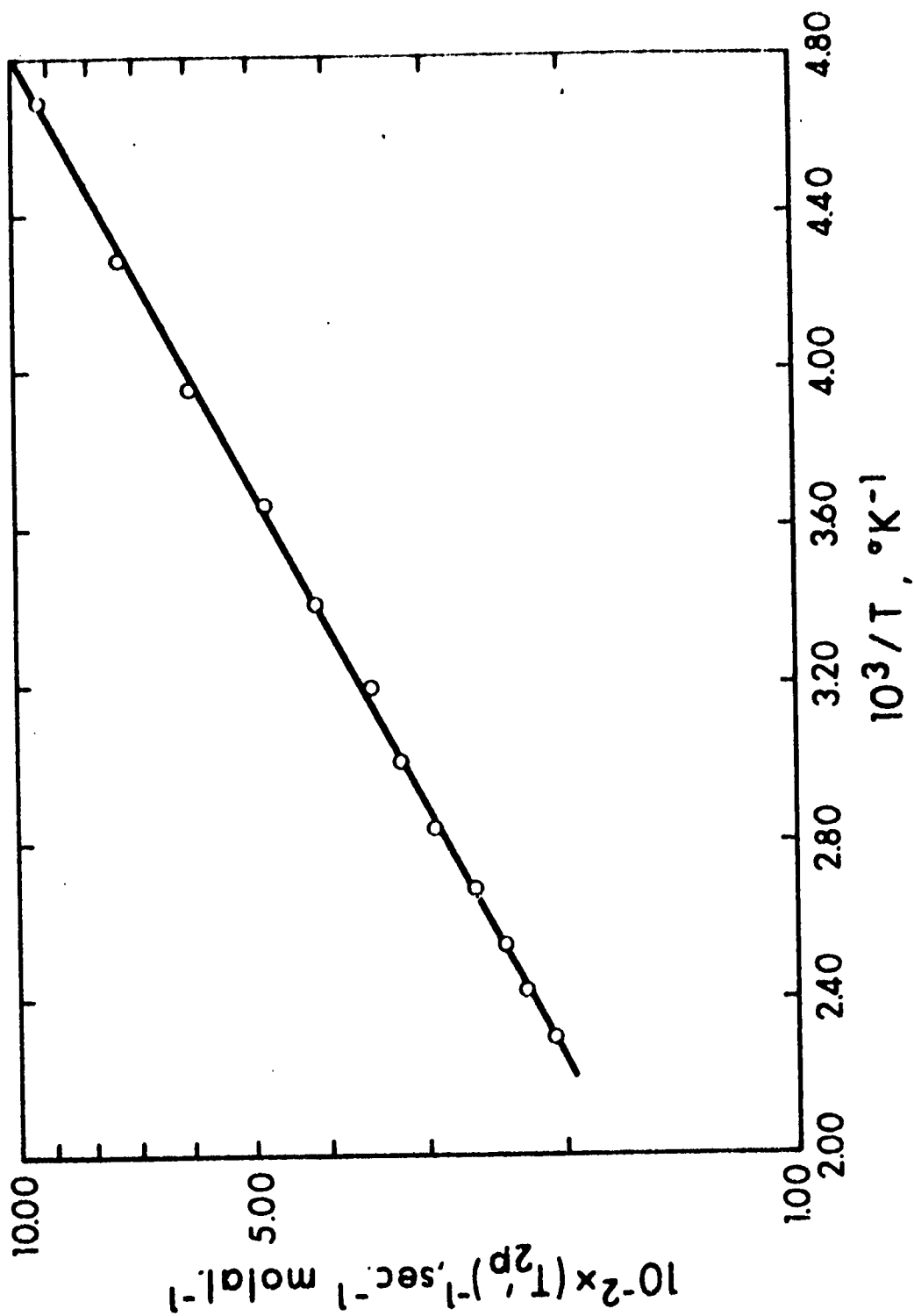


Figure 17: Temperature dependence of $\log (T_{2p})^{-1}$ at 60 MHz for the protons of trimethylphosphate containing chromium (II) tetrafluoroborate.

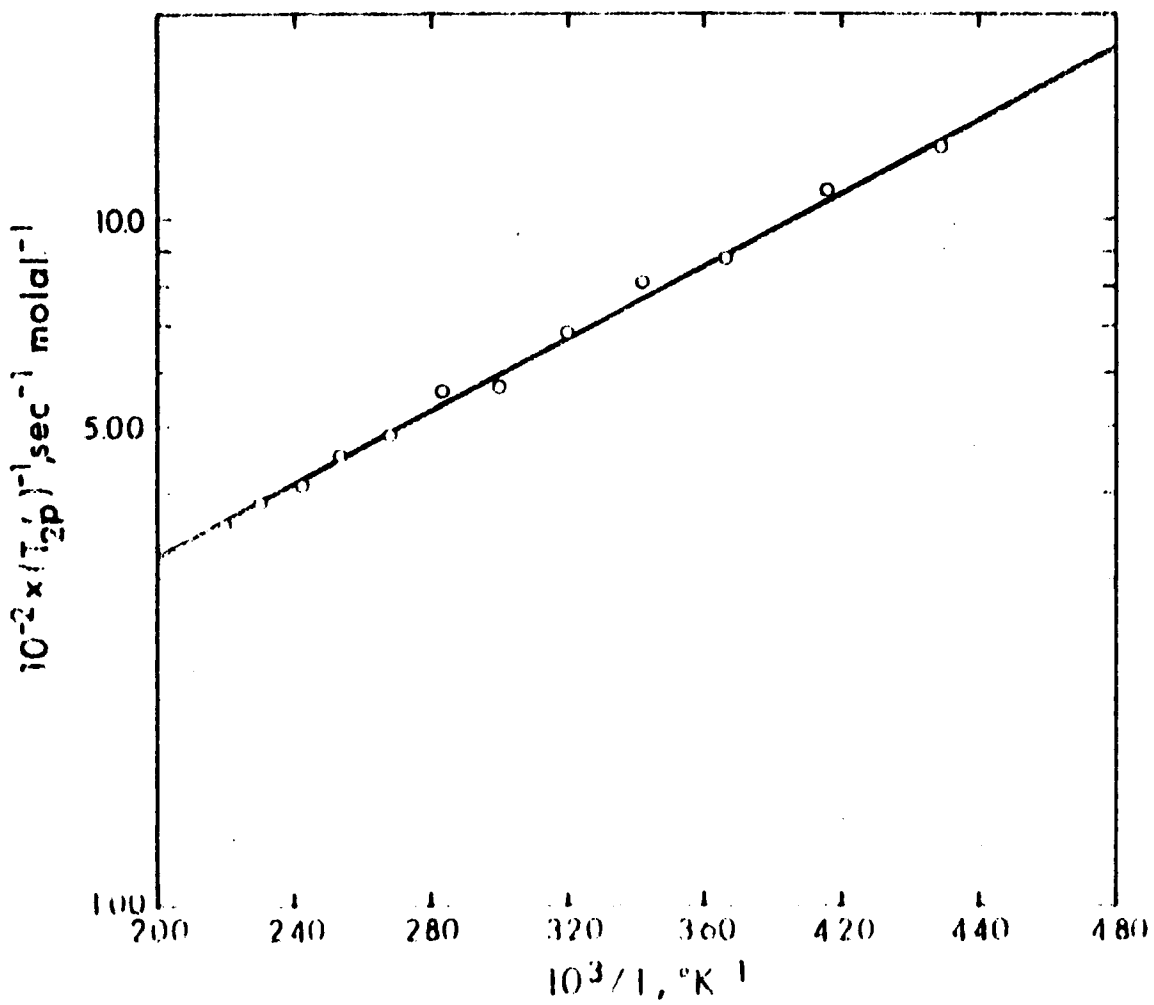


Figure 18: Temperature dependence of $\log (T_{2p})^{-1}$ at 60 MHz for the protons of trimethylphosphate containing vanadium (II) tetrafluoroborate.

was then used in equation (32) to calculate an outer sphere dipolar relaxation contribution to the broadening. This contribution was then subtracted from the total broadening and a reiteration process was carried out on equation (31) to obtain a new τ_c and then a new outer sphere broadening contribution. The iteration was continued until there was complete self consistency. The final value for τ_c was $5.2_5 \times 10^{-12}$ sec. The activation energy (1.32 ± 0.20 kcal mole⁻¹) for this correlation time was obtained from the temperature dependence of $\log (\tau_{2p}')^{-1}$. Inner and outer sphere contributions to $(\tau_{2p}')^{-1}$ at 25°C for the hydroxy proton were $1902.0 \text{ sec}^{-1} \text{ molal}^{-1}$ and $98.0 \text{ sec}^{-1} \text{ molal}^{-1}$ giving the total observed value of $2000.0 \text{ sec}^{-1} \text{ molal}^{-1}$. This correlation time was then used to calculate the inner and outer sphere values of $(\tau_{2p}')^{-1}$ for the methyl proton resonances; they were calculated at 25°C to be $342.0 \text{ sec}^{-1} \text{ molal}^{-1}$ and $87.0 \text{ sec}^{-1} \text{ molal}^{-1}$, respectively, giving a total value of $429.0 \text{ sec}^{-1} \text{ molal}^{-1}$ compared to the observed value of $420.0 \text{ sec}^{-1} \text{ molal}^{-1}$. The hyperfine interaction contributes less than $1 \text{ sec}^{-1} \text{ molal}^{-1}$ to $(\tau_{2p}')^{-1}$ when calculated using the above correlation time and the previously determined coupling constants.

From the definition of τ_c , equation (28), it is possible that it can be interpreted as the complex tumbling time (τ_R),

the electron spin relaxation time (τ_S), or the ligand exchange lifetime (τ_M). A value of $4.1_0 \times 10^{-11}$ sec with an activation energy of 2.91 ± 0.30 kcal mole $^{-1}$ was obtained for τ_R for the vanadyl-methanol complex at 25°C. The large difference between these values and those obtained for the chromium(II) - methanol system indicates that tumbling of the complex is not controlling the electron-proton interaction in the latter system. The lifetime for water ligands on chromium(II) was shown by Meredith (67) to be two orders of magnitude longer than the correlation time obtained here. If the lifetime of the methanol molecule on chromium(II) is assumed to differ by no more than an order of magnitude from the water lifetime as found for nickel(II) and cobalt(II) then $\tau_C \neq \tau_M$. However, it appears that if $\tau_S < 6 \times 10^{-11}$ sec for chromium(II), then the value for $\tau_C = 5.2_5 \times 10^{-12}$ sec obtained here can be associated with the electron spin relaxation time. The small temperature dependence of τ_C is consistent with this interpretation. It may also be possible for an axis interconversion process to be controlling the relaxation of the methanol protons. This process is discussed by Noack and Gordon (69) for Jahn-Teller distorted copper(II) complexes and does not require that the entire complex rotate. It is possible for the metal ion to undergo a change of orientation within the ligand matrix which causes the methanol ligands to experience a change in environment. This process

may be expected to be rapid with a low activation energy which is consistent with the results obtained here.

The arguments applied above can also be used to explain the data for the excess broadening of the trimethylphosphate resonance due to the presence of chromium(II). A correlation time of $4.3_5 \times 10^{-12}$ sec at 25°C was obtained from the iterative process giving an inner and outer sphere contribution to $(T_{2p}')^{-1}$ of $360.4 \text{ sec}^{-1} \text{ molal}^{-1}$ and $39.6 \text{ sec}^{-1} \text{ molal}^{-1}$, respectively. The activation energy for $(T_{2p}')^{-1}$ was also found to be small, $1.26 \pm 0.20 \text{ kcal mole}^{-1}$. Again the value for τ_c and the activation energy do not seem reasonable for a tumbling process because for the vanadyl-trimethylphosphate system $\tau_R = 1.3_2 \times 10^{-10}$ sec and $E_a = 2.25 \pm 0.20 \text{ kcal mole}^{-1}$. The parameters obtained for the chromium(II) - trimethylphosphate were again attributed to the electron spin relaxation with the possibility of axis interconversion.

Excess broadening of the bulk solvent methanol resonance by the vanadium(II) ion was interpreted as due to an outer sphere dipolar relaxation mechanism because inner sphere exchange is normally expected to be slow (70). Equation (32) was used under the assumption that $\omega_e^2 \tau_c^2 \gg 1$ and $r_o = 4.0_0 \text{ \AA}$ for the hydroxy proton of methanol as obtained in the vanadyl-methanol system. A value of $\tau_c = 2.6_8 \times 10^{-11}$ sec was calculated. This value for τ_c and $r_o = 4.8_0 \text{ \AA}$ for the methyl protons gave $(T_{2p}')_{\text{Outer}}^{-1} = 210.0 \text{ sec}^{-1} \text{ molal}^{-1}$ in excellent agreement with the observed value of 210 sec^{-1}

molal⁻¹ at 25°C for the methyl protons (Figure 16). τ_c for vanadium(II) in methanol was taken as the complex tumbling time because of the similarity of the temperature dependence of $(T_{2p}')^{-1}$, $3.26 \pm 0.30 \text{ kcal mole}^{-1}$, compared to the activation energy for the tumbling of the vanadyl complex in methanol ($2.91 \pm 0.30 \text{ kcal mole}^{-1}$), the value for τ_c obtained above also agrees favorably with $\tau_R = 4.1_0 \times 10^{-11} \text{ sec}$ for the vanadyl ion-methanol system.

This same interpretation may be used for the broadening of the proton resonance of trimethylphosphate in the presence of vanadium(II). Using $r_o = 7.5_5 \text{ \AA}$ a value for $\tau_c = 2.4_5 \times 10^{-10} \text{ sec}$ was obtained at 25°C. This value is very close to the tumbling correlation time obtained in the vanadyl ion-trimethylphosphate system, $\tau_R = 1.3_2 \times 10^{-10} \text{ sec}$; however, the activation energy obtained here, $1.21 \pm 0.20 \text{ kcal mole}^{-1}$, is significantly lower than the value obtained in the vanadyl system, $2.40 \pm 0.30 \text{ kcal mole}^{-1}$. Therefore, fast exchange of trimethylphosphate ligands on vanadium(II) is proposed in which case equations (31) and (32), with $\omega_e^2 \tau_c^2 \gg 1$, are required to obtain a correlation time. An iterative method as described above yielded $\tau_c = 2.4_7 \times 10^{-11} \text{ sec}$ giving $(T_{2p}')^{-1}_{\text{Inner}} = 669.0 \text{ sec}^{-1} \text{ molal}^{-1}$ and $(T_{2p}')^{-1}_{\text{Outer}} = 76.0 \text{ sec}^{-1} \text{ molal}^{-1}$ at 25°C. The latter correlation time must be identified with the electron spin relaxation time (τ_s) in order to explain the low activation energy. The

results from the two vanadium(II) systems require that $\tau_S > 2.5 \times 10^{-11}$ sec in methanol, but $\tau_S \approx 2.5 \times 10^{-11}$ sec in trimethylphosphate. There is not sufficient understanding of the factors affecting τ_S to give theoretical justification for this result.

Thus, the electron spin relaxation of chromium(II) can account for the solvent proton resonance line broadening of the methanol and trimethylphosphate which contain this ion. However, it has also been suggested that axis interconversion could also explain the results. The latter interpretation would substantiate existing views that chromium(II) forms Jahn-Teller distorted complexes in solution because it requires that axial and equatorial ligands be in different environments and that the rotation of the metal ion causes the environments to interchange. The similarities in correlation times and temperature dependences of chromium(II) in methanol and trimethylphosphate ($5.2_5 \times 10^{-12}$ sec, 1.32 ± 0.20 kcal mole⁻¹; $2.4_5 \times 10^{-12}$ sec, 1.21 ± 0.20 kcal mole⁻¹, respectively) to these parameters (3.3×10^{-12} sec, 1.7 kcal mole⁻¹) obtained by Hudson (72) for Jahn-Teller distorted copper(II) in copper-doped tris-(2,2'-dipyridine) zinc nitrate indicates that this interconversion process may dominate in relaxing the solvent protons.

The ligand exchange rate on vanadium(II) is expected to

be slow in all cases, (reference 70, p. 151). Vanadium(II) in methanol substantiated this proposal because an outer sphere dipolar relaxation process adequately explains the broadening data. In the vanadium(II) - trimethylphosphate system, however, it was necessary to invoke fast inner sphere exchange to adequately explain the broadening results. This latter mechanism can be justified if the trimethylphosphate ligand is considered to be a bulky ligand which cannot properly form a regular octahedral structure with vanadium(II) in which case steric hinderance would cause rapid exchange of the coordinated ligands with the bulk solvent.

5. Proton Relaxation in Dimethylsulfoxide and Trimethylphosphate by Nickel(II) and Cobalt(II) Perchlorates

This section deals with the temperature dependence of the proton NMR line broadening of dimethylsulfoxide (DMSO) and trimethylphosphate (TMPA) solvents containing nickel(II) perchlorate $\{\text{Ni}(\text{ClO}_4)_2\}$ and cobalt(II) perchlorate $\{\text{Co}(\text{ClO}_4)_2\}$. This work, which is an extension of previous studies on these two paramagnetic ions in nonaqueous solvents, was carried out in order to extend the number of systems in which these two ions and the vanadyl ion can be compared.

The solvent proton relaxation in dimethylsulfoxide solutions of $\text{Ni}(\text{ClO}_4)_2$ shows features which are typical of those observed previously for nickel(II) in water (8), methanol (36), N,N-dimethylformamide (6) and acetonitrile (12). The theory developed by Swift and Connick (8) and recounted in Chapter I, section 2 serves to explain the results for this system. The temperature dependence of $(T_{2p})^{-1}/P_M$ and the chemical shift $(\Delta\omega_{\text{OBS}}/P_M)$ of the bulk solvent protons for solutions of $\text{Ni}(\text{ClO}_4)_2$ in dimethylsulfoxide are given in Figures 19 and 20, respectively.

The temperature dependence of the line broadening for this latter system may be described by a combination of limiting conditions (34-b) and (34-d) of Chapter I, section 2. Then

$$(T_{2p})^{-1}/P_M = \tau_M \Delta\omega_M^2 + (T_{2M})^{-1} \quad (78)$$

$$= \tau_M \Delta\omega_M^2 + C \exp(E_a/RT) \quad (79)$$

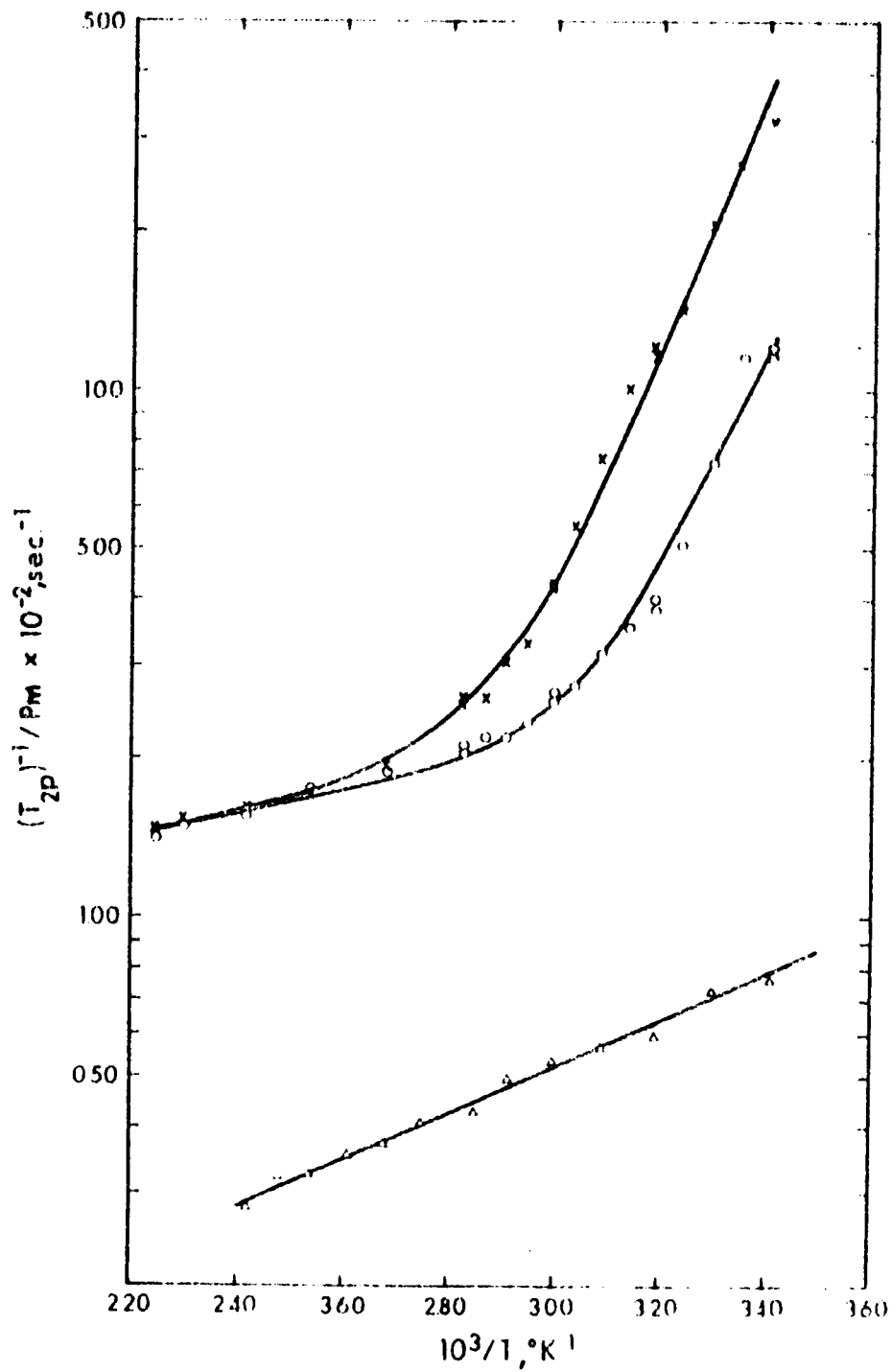


Figure 19: Temperature dependence of $\log (T_{2p})^{-1}/P_M$ for the protons of dimethylsulfoxide at 100 MHz - X, at 60 MHz - O, containing nickel (II) perchlorate and at 60 MHz - Δ , containing cobalt (II) perchlorate.

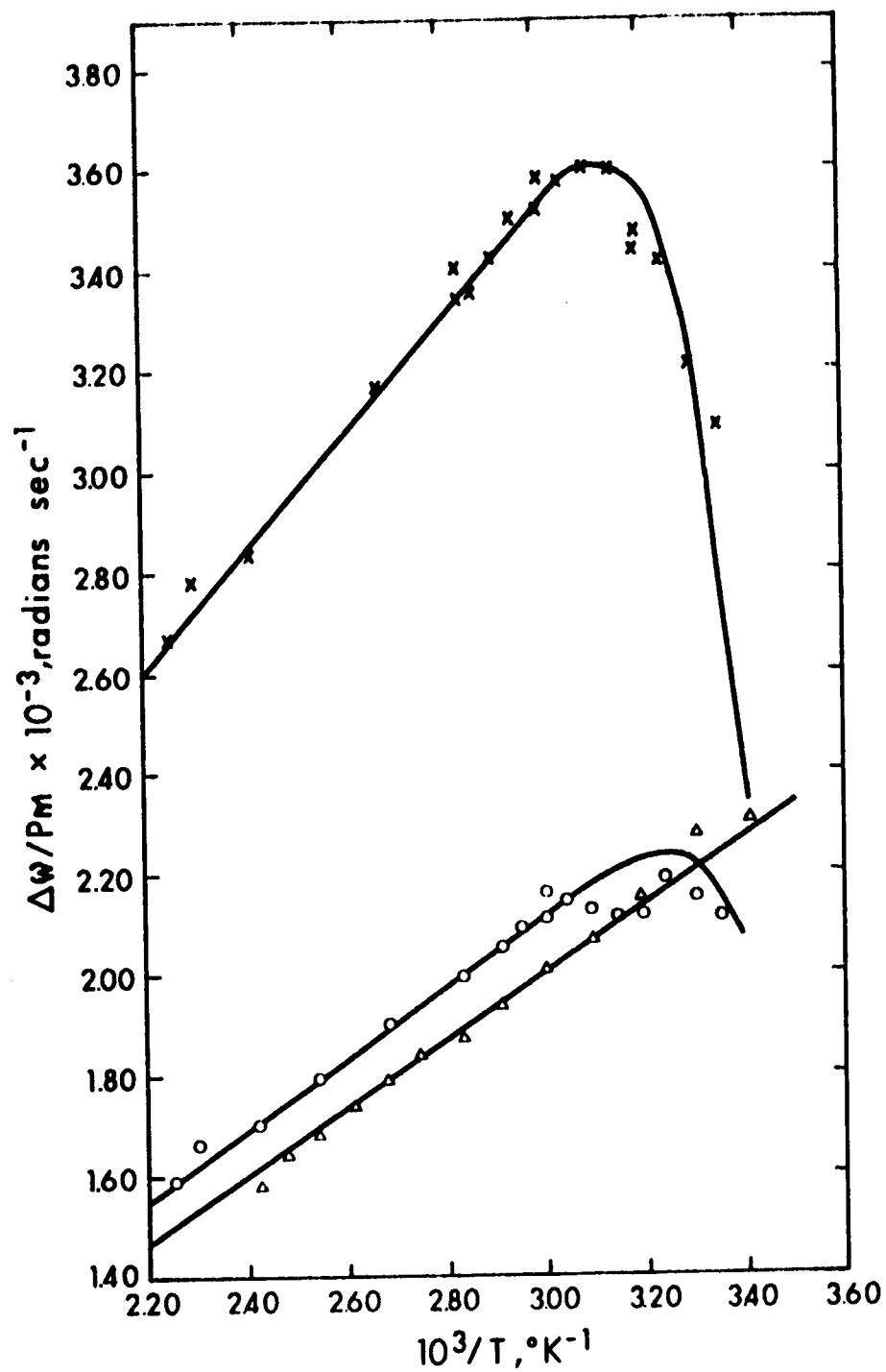


Figure 20: Temperature dependence of the shift of the protons of dimethylsulfoxide at 100 MHz - X, at 60 MHz - O, containing nickel (II) perchlorate, and at 60 MHz - Δ , containing cobalt (II) perchlorate.

The parameters have been defined previously. However, in order to determine the exchange lifetime (τ_M) in equation (79) it is necessary to know $\Delta\omega_M$. The latter may be obtained from the observed chemical shift and equation (11) if $(1/\tau_M)^2 > (\Delta\omega_M)^2 \gg (1/T_{2M}\tau_M)$.

$$\Delta\omega_{\text{OBS}}/P_M = \Delta\omega_M / (1 + \tau_M^2 \Delta\omega_M^2) \quad (80)$$

At high temperatures τ_M is short and $\tau_M^2 \Delta\omega_M^2 \ll 1$; therefore

$$\Delta\omega_{\text{OBS}}/P_M = \Delta\omega_M \quad (81)$$

where $\Delta\omega_M$ is given by equation (21). The temperature dependence of $\Delta\omega_{\text{OBS}}/P_M$ at high temperatures (Figure 20) was fitted to equation (81). The analysis gave $A/h = 7.57 \pm 0.50 \times 10^5$ cps for $\mu_{\text{eff}} = 3.3$ B.M. (77) and a coordination number of 6.

The expression for $\Delta\omega_M$ and the transition state theory expression for τ_M may then be substituted into equation (79) to give

$$\begin{aligned} (\tau_{2p})^{-1}/P_M = (kT/h)^{-1} \exp(\Delta H^\ddagger/RT - \Delta S^\ddagger/R) \left\{ \frac{-2\pi \omega_o \mu_{\text{eff}}}{3kT} \left(\frac{A}{h} \right) \frac{h \sqrt{S(S+1)} \gamma_e}{\gamma_I} \right\}^2 \\ + C \exp(E_a/RT) \quad (82) \end{aligned}$$

The data in Figure 19 were fitted to equation (82) using a nonlinear least squares programme with ΔH^\ddagger , ΔS^\ddagger , C and E_a as adjustable parameters. The results are given in Table VI.

Having determined ΔH^\ddagger and ΔS^\ddagger , it was then possible to fit equation (80) to the shift data in Figure 20 as shown by the solid

line in this figure. The calculated and experimental curves agree well except for the low temperature 60 MHz data. The discrepancy for the latter is due to the overlap of the toluene resonance, which was used as an internal reference, with the broad dimethylsulfoxide resonance giving inaccurate measurements for small shifts.

If $(T_{2M})^{-1}$ is assumed to be due to a hyperfine relaxation process (equation (27), with the approximations that $\omega_I^2 \tau_e^2 \ll \omega_e^2 \tau_e^2$ and $\omega_e^2 \tau_e^2 \gg 1$, then τ_e is calculated to be $1.8_0 \times 10^{-10}$ sec. This value seems much larger than expected from previous studies on nickel(II) (8,12,36). Alternatively, the inner and outer sphere dipolar relaxation may control T_{2M} . If the inner and outer sphere interaction distances are taken as 4.5_0 \AA and 6.7_5 \AA , respectively, as in the vanadyl-dimethylsulfoxide system (Chapter III, section 1), then a correlation time of $9.4_5 \times 10^{-12}$ sec gives exact agreement with the observed $(T_{2M})^{-1}$ at 25°C. The inner and outer sphere contributions to $(T_{2p})^{-1}/P_M$ are 266.0 and 38.0 sec^{-1} . This correlation time is more consistent with the previous values for nickel(II) in various solvents.

There is very poor agreement between the kinetic parameters obtained here (Table VI) and those of Thomas and Reynolds (77) and Blackstaffe and Dwek (78). The temperature range in the latter two studies seems to be too small to properly determine the T_{2M} region at high temperatures. Poor determination of this effect

TABLE VI

The least squares parameters which best fit the broadening data for the $\text{Ni}(\text{ClO}_4)_2$ -dimethylsulfoxide broadening (Figure 19)

Frequency	ΔH^\ddagger , kcal mole ⁻¹	ΔS^\ddagger , e.u.	C, sec ⁻¹	E_a , kcal mole ⁻¹
100 MHz	12.09 ± 0.25	-1.15 ± 0.50	100.8 ± 5.0	0.337 ± 0.500
60 MHz	12.20 ± 0.31	-1.50 ± 0.45	102.0 ± 3.5	0.652 ± 0.200

Errors are quoted as the 95% confidence limits on the least squares fit.

may result in too low an activation energy for exchange. However, there is reasonable agreement between the studies for the values of $(T_{2p})^{-1}/P_M$ at different temperatures. For example, the data of Thomas and Reynolds gives $1.2_7 \times 10^3 \text{ sec}^{-1}$ and $7.3_4 \times 10^2 \text{ sec}^{-1}$ for $(T_{2p})^{-1}/P_M$ at 23°C and 34°C, respectively. These values may be compared to the values of $1.1_8 \times 10^{-3} \text{ sec}^{-1}$ and $6.8_0 \times 10^2 \text{ sec}^{-1}$ interpolated from Figure 19 also at 23°C and 34°C, respectively. Interpolation of the corresponding values from the graphs of Blackstaffe and Dwek shows reasonable agreement as well.

Our hyperfine coupling constant of $7.57 \pm 0.50 \times 10^4 \text{ cps}$ is not in very good agreement with the value of $9.3_0 \times 10^4 \text{ cps}$ calculated from the shift at 40°C reported by Thomas and Reynolds; Blackstaffe and Dwek's value ($8.1_0 \times 10^4 \text{ cps}$) obtained from their high temperature shift does not agree with either of these values. Since a more complete temperature dependence of the shift has been carried out here and found to agree with the line broadening results, it is felt that the value found in this study at least has more experimental basis.

For the solvent proton relaxation of dimethylsulfoxide containing cobalt(II) a plot of $(T_{2p})^{-1}/P_M$ versus the reciprocal of the absolute temperature is shown in Figure 19 and the corresponding shift plot is shown in Figure 20. The slow increase ($E_a = 1.9_6 \text{ kcal mole}^{-1}$) of $(T_{2p})^{-1}/P_M$ with decreasing temperature is typical of a T_{2M} controlled relaxation process.

Thus, the results may be explained by an inner sphere, outer sphere or hyperfine relaxation mechanism or a combination of all these mechanisms. If it is assumed that all the relaxation is due to a hyperfine interaction with an isotropic hyperfine coupling constant of $2.08 \pm 0.50 \times 10^4$ cps, obtained from the temperature dependence of the shift and equation (21) and $\mu_{\text{eff}} = 5.0_1$ B.M. (76), then an unrealistically high value of $\tau_e = 1.7_6 \times 10^{-8} \text{ sec}^{-1}$ is obtained for cobalt(II). Therefore, the T_{2M} relaxation must be due to inner and outer sphere dipolar interactions. If the same interaction distances as in the nickel(II) system are used then a correlation time of $4.4_1 \times 10^{-13} \text{ sec}$ was calculated by the usual iterative procedure. The inner and outer sphere contributions to $(T_{2p})^{-1}/P_M$ are 66.0 sec^{-1} and 8.5_0 sec^{-1} or a total of 74.5 sec^{-1} as observed at 25°C . This correlation time may be identified with the electron spin relaxation time and is in good agreement with the values obtained for cobalt(II) in N,N-dimethylformamide (6), acetonitrile (12) and methanol (36). Substituting this correlation time into the expression for the hyperfine relaxation shows that this process gives negligible contribution to the broadening. From Figure 19 a lower limit of $1.5_3 \times 10^4 \text{ sec}^{-1}$ may be placed on the exchange rate of a single solvent molecule from the coordination sphere of cobalt(II) in dimethylsulfoxide.

It may also be noted that the coupling constant obtained

here, $A/h = 2.08 \pm 0.50 \times 10^4$ cps, does not agree very well with the value of 5.9×10^5 cps reported by Reynolds and Thomas. The reason for this disagreement is not known. In this work the isotropic hyperfine coupling constant was obtained by fitting the observed data to equations (21) and (81) by a nonlinear least squares method.

The temperature dependence of the line broadening of the bulk solvent protons in trimethylphosphate solutions of nickel(II) perchlorate (Figure 21) is also typical of T_{2M} controlled relaxation. The activation energy (E_a) for this relaxation mechanism is 1.0_4 kcal mole⁻¹. A quantitative interpretation of the broadening data again indicates that inner and outer sphere dipolar interaction distances of 4.9_0 \AA and 7.5_5 \AA (Chapter III, section 1) and a correlation time of $3.6_2 \times 10^{-12}$ sec adequately explain the observed value of $(T_{2p})^{-1}/P_M$ at 25°C. The correlation time again is identified with the electron spin relaxation time. Very little contribution from the hyperfine interaction process is predicted with this correlation time.

The variation of the chemical shift with temperature in the nickel(II)-trimethylphosphate system is shown in Figure 22. If the spin only magnetic moment (2.8_3 B.M.) is assumed for nickel(II) then a hyperfine coupling constant of $7.21 \pm 0.45 \times 10^3$ cps is

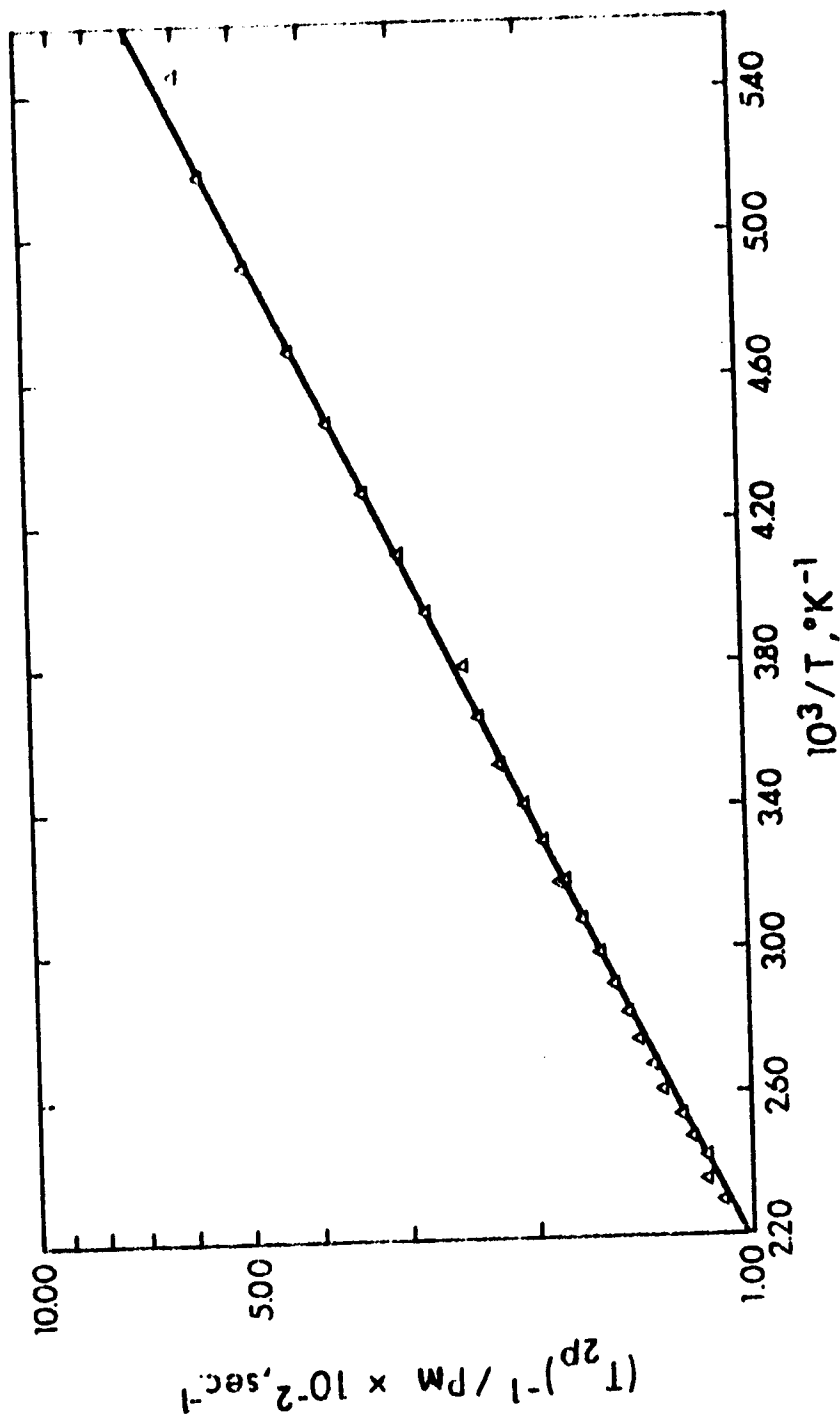


Figure 21: Temperature dependence of $\log (T_{2p})^{-1} / \text{PM}$ at 60 MHz for the protons of trimethylphosphate containing nickel (II) perchlorate.

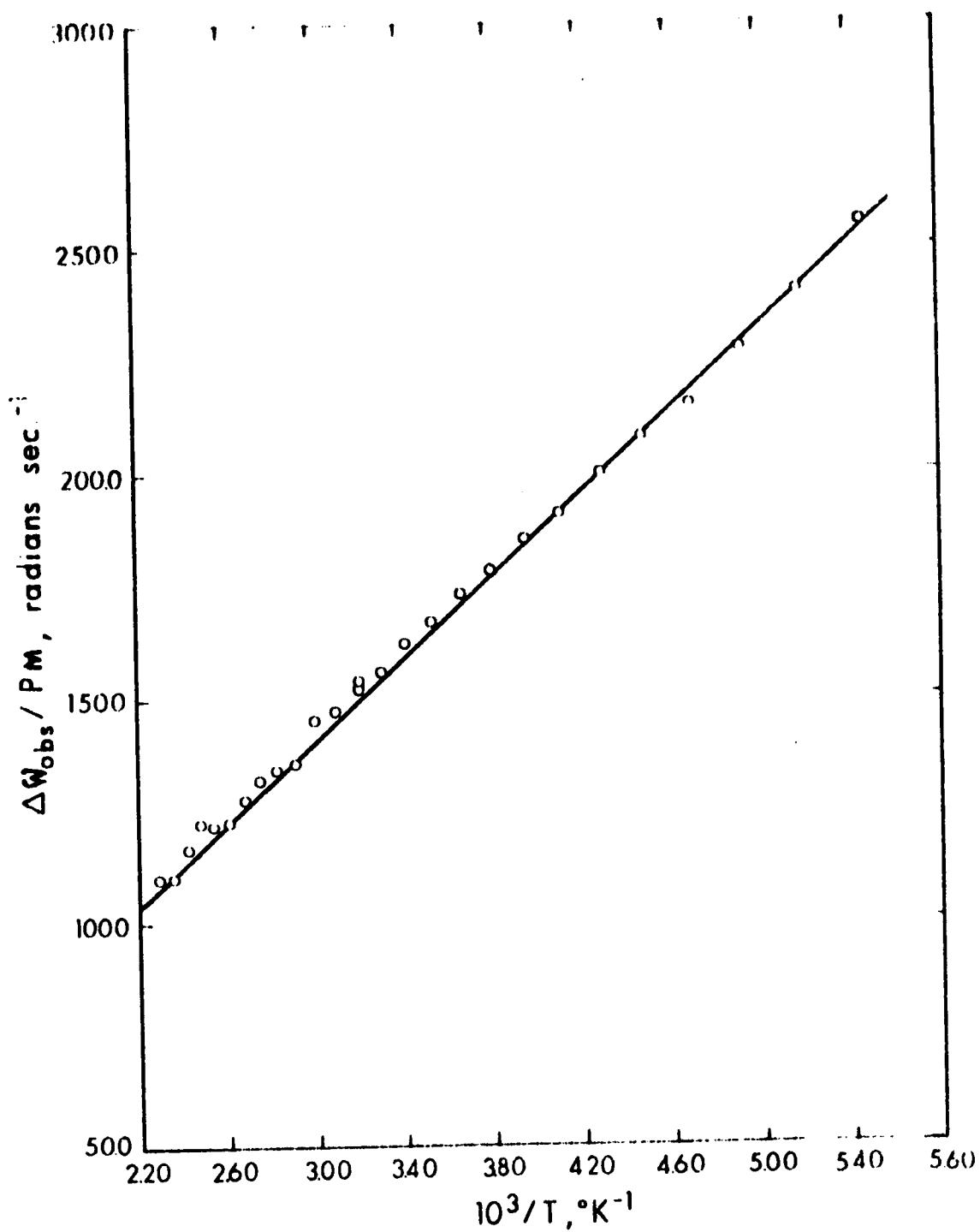


Figure 22: Temperature dependence of the shift at 60 MHz for the protons of trimethylphosphate containing nickel (II) perchlorate.

obtained from a nonlinear least squares fit of the shift data to equations (22) and (81).

The small temperature dependence of the bulk solvent proton relaxation of trimethylphosphate solutions of $\text{Co}(\text{ClO}_4)_2$ is also indicative of a T_{2M} relaxation process. The variation of the line widths with temperature for a 0.49₅ molal solution of $\text{Co}(\text{ClO}_4)_2$ in trimethylphosphate are shown in Table VII; these values will be discussed more thoroughly below.

The most unusual feature of this system is the temperature dependence of the chemical shift. Variation of the shift with temperature is also shown in Table VII. The shift actually changes sign at about 80°C, whereas according to equation (21) or (22) it can be either positive or negative depending on the sign of the coupling constant, but it cannot change sign. Introduction of a pseudocontact shift cannot resolve the anomaly because this shift also has a regular temperature dependence and would not cause the sign change. In order to explain the temperature variation of the shift it is necessary to assume that there are at least two cobalt(II) species in equilibrium in solution and that their relative concentrations change with temperature. Furthermore, to explain the change in sign of the observed shift the hyperfine coupling constant must have a different sign for the two species. In view of the known tendency of cobalt(II) to form tetrahedral complexes

TABLE VII

Calculated and observed NMR results for the cobalt(II)-trimethylphosphate system

Temperature °C	Species Concentration (molal)		SHIFT (a)		BROADENING (a)		
	[A]	[B]	[S]	($\Delta\nu_S$) OBS, cps	($\Delta\nu_S$) CAL, cps	($\Delta\nu_B$) OBS, cps	($\Delta\nu_B$) CAL, cps
140	0.354	0.141	4.88	7.95	3.33	5.7	5.7
120	0.345	0.150	4.86	5.55	2.24	6.5	6.4
100	0.334	0.161	4.83	2.38	0.82	7.0	7.1
80	0.322	0.173	4.81	0.40	-1.03	8.3	8.1
60	0.308	0.187	4.79	-4.75	-3.43	9.2	9.4
40	0.292	0.203	4.75	-7.70	-6.58	11.5	11.2
30	0.282	0.213	4.73	-10.6	-8.50	12.1	12.2
20	0.273	0.222	4.72	-12.8	-10.8	13.6	13.5
10	0.262	0.233	4.69	-15.4	-13.4	14.8	14.8
0	0.250	0.245	4.67	-18.4	-16.4	16.4	16.8

TABLE VII (Cont'd)

Temperature °C	Species Concentration (molal)		SHIFT (a)		BROADENING (a)		
	[A]	[B]	[S]	(Δv_s) OBS, cps	(Δv_s) CAL, cps	(Δv_b) OBS, cps	(Δv_b) CAL, cps
-10	0.238	0.257	4.65	-21.4	-19.5	18.9	18.9
-20	0.225	0.270	4.62	-25.4	-23.4	23.2	21.8
-30	0.210	0.285	4.59	-28.6	-27.9	24.6	24.8
-40	0.195	0.300	4.56	-32.3	-33.1	29.4	29.2
-50	0.178	0.317	4.53	-35.7	-39.6	33.0	34.0
-60	0.162	0.333	4.49	-44.5	-45.8	41.3	40.3
-70	0.146	0.349	4.47			47.6	47.6

(a) The concentration of $\text{Co}(\text{ClO}_4)_2$ in trimethylphosphate is 0.495 molal.

with bulky, weakly bonding ligands (79,80) it seems most probable that the two species are octahedral $\{\text{Co}(\text{TMPA})_6^{2+}\}$ and tetrahedral $\{\text{Co}(\text{TMPA})_4^{2+}\}$ complexes. A spectrophotometric study which is discussed below indicates that the tetrahedral species is favored at high temperatures and the octahedral species at low temperatures. The possibility of octahedral mixed aquo-trimethylphosphate complexes causing the observed results is not consistent with the spectrophotometric study nor is it expected that such species would have coupling constants with opposite signs judging from previous work on mixed aquo-methanol (9,10) and aquo-chloro (81) complexes.

The considerations all indicate the presence of a tetrahedral species and a quantitative description of the shift data may be undertaken. The equilibrium involved may be written as



where A represents the tetrahedral $\text{Co}(\text{TMPA})_4^{2+}$ species, B represents the octahedral $\text{Co}(\text{TMPA})_6^{2+}$ species and S the free solvent. An equilibrium constant is then defined for the above reaction by

$$K = \frac{[\text{B}]}{[\text{A}] [\text{S}]^2} = \exp(-\Delta H/RT + \Delta S/R) \quad (84)$$

where all concentrations are given in molal units.

The observed chemical shift ($\Delta\omega_{\text{OBS}}$) is the sum of the contributions from the tetrahedral species ($\Delta\omega_{\text{A}}$) and octahedral

species ($\Delta\omega_B$)

$$\Delta\omega_{OBS} = P_{MA} \Delta\omega_A + P_{MB} \Delta\omega_B \quad (85-a)$$

$$= P_{MA} \frac{C_A}{T} + P_{MB} \frac{C_B}{T} \quad (85-b)$$

$$= \frac{4[A]}{[S_0] - \{4[A] + 6[B]\}} \left\{ \frac{C_A}{T} \right\} + \frac{6[B]}{[S_0] - \{4[A] + 6[B]\}} \left\{ \frac{C_B}{T} \right\} \quad (85-c)$$

where $[S_0]$ is the molality of the pure solvent. These equations are derived in an obvious way from equations (22) and (81). The constants C_A and C_B depend on the hyperfine coupling constant and other physical constants as seen by comparison to equation (81).

In principle it is possible to determine the concentrations of A and B as a function of temperature by using equation (84) and making use of the concentration conditions

$$[\text{cobalt(II)}]_{TOTAL} = m = [A] + [B] \quad (86)$$

and

$$S = [S_0] - \{4[A] + 6[B]\} \quad (87)$$

The chemical shift versus $(T^\circ K)^{-1}$ data could be fit by a nonlinear least squares computer programme using ΔH , ΔS , C_A and C_B as variables. It was felt, however, that a more meaningful fit of the shift data might be obtained if ΔH and ΔS were determined independently from a spectrophotometric study.

The spectrum of cobalt(II) in trimethylphosphate was recorded at temperatures between 24.1°C and 82.5°C . Bands were observed at $535\text{ m}\mu$ (ϵ , 179), $580\text{ m}\mu$ (ϵ , 191), $630\text{ m}\mu$ (ϵ , 184) and a broad band centred at $1550\text{ m}\mu$ (ϵ , 36). The extinction coefficients are quoted for a spectrum at 24.1°C . Gutmann and Bohunovsky (97) report bands at $505\text{ m}\mu$ and $545\text{ m}\mu$ while Jorgenson (98) reports bands at $464\text{ m}\mu$ and $515\text{ m}\mu$. The spectra reported in both cases are rather typical of octahedral cobalt(II), whereas, the spectrum observed in the present study has features more like tetrahedral cobalt(II) and is similar with but not identical to the spectrum reported recently by Frankel (99) who reports bands at $632\text{ m}\mu$ (ϵ , 235), $600\text{ m}\mu$ (ϵ , 205), $583\text{ m}\mu$ (ϵ , 205) and $552\text{ m}\mu$ (ϵ , 150). It has also been found in this study that one drop of water in 5 ml of cobalt(II)-trimethylphosphate solution produces a solution with a spectrum identical to that reported by Jorgenson. It was concluded that traces of water result in the formation of mixed aquo-TMPA cobalt(II) octahedral complexes.

The results of this study are given in Table VIII. It should be noted that the central peak at $580\text{ m}\mu$ shows a greater relative increase with temperature than the $630\text{ m}\mu$ peak which in turn increases more than the $535\text{ m}\mu$ peak. This effect has been noted previously for tetrahedral cobalt(II) by Katzin (79), and is attributed to the increasing width and overlap of the peaks at higher temperature causing the intensity of the centre peak to

TABLE VIII

Spectrophotometric results for the cobalt(II)-trimethylphosphate system

Temperature °C	Kx10 ² molar ⁻²	Species Concentration (a)		ABSORBANCE (a)		CALCULATED 535mμ
		[A]x10 ³ (molal)	[B]x10 ³ (molal)	OBSERVED 580mμ	535mμ	
24.1	3.53	2.13	3.83	1.32	1.36	1.27
34.0	3.24	2.25	3.71	1.37	1.44	1.33
49.0	2.87	2.42	3.54	1.46	1.55	1.40
60.8	2.62	2.55	3.41	1.52	1.64	1.43
74.0	2.40	2.68	3.28	1.61	1.76	1.48
82.5	2.27	2.76	3.20	1.69	1.85	1.50

(a) Total cobalt(II) concentration is 5.96×10^{-3} molal.

(b) ϵ_A is assumed to be 500 molar⁻¹cm⁻¹.

increase fastest. The procedure of Katzin has been followed in that the least affected peak, that at 535 m μ , has been used to calculate the temperature dependence of the equilibrium constant for tetrahedral-octahedral interconversion. It was assumed that the absorbance of the octahedral species can be neglected at 535 m μ ; this assumption is consistent with numerous previous spectral studies on cobalt(II). The absorbance at 535 m μ , $(Ab)_{535}$, and the molal concentration of the tetrahedral species [A] are related by

$$(Ab)_{535}/\rho = \epsilon_A [A] \quad (88)$$

where ρ is the solvent density and ϵ_A is the molar extinction coefficient of the tetrahedral species. The temperature dependence of the density was calculated from the empirical equation

$$\rho = 1.800 - 2.00 \times 10^{-3} T \quad (89)$$

where T is the temperature in $^{\circ}\text{K}$.

It is easily shown by a combination of equations (84), (86) and (88) that

$$(Ab)_{535}/\rho = \frac{\epsilon_A \times m}{[S_0]^2 \{ \exp(-\Delta H/RT + \Delta S/R) \} + 1} \quad (90)$$

Since the spectrophotometric study was carried out with $m = 5.96 \times 10^{-3}$ molal the solvent concentration is essentially constant and independent of the concentrations of A and B.

The variation of $(Ab)_{535}$ with temperature may be fit to equation (90) by a nonlinear least squares computer programme using ϵ_A , ΔH and ΔS as adjustable parameters. It was found that the best fit of the data to equation (90) gave a value of $1.26 \times 10^3 \text{ molar}^{-1} \text{ cm}^{-1}$ for ϵ_A . This value seems unreasonably high when compared to the extinction coefficients of other similar tetrahedral cobalt(II) species (80, 100).

The sensitivity of the fit of the spectrophotometric data to changes in ϵ_A was determined by systematically lowering ϵ_A and holding it constant while fitting the data to equation (90) using only ΔH and ΔS as variable parameters. It was found that for ϵ_A as low as $350 \text{ molar}^{-1} \text{ cm}^{-1}$ a fit could be obtained for which the calculated and observed values of $(Ab)_{535}$ agreed to within 2%. However, the best fit ΔH and ΔS with ϵ_A set at $350 \text{ molar}^{-1} \text{ cm}^{-1}$ did not produce a fit of the chemical shift data to within the estimated error of $\pm 2 \text{ Hz}$. The disagreement between calculated and observed shifts in this case was generally $\pm 5 \text{ Hz}$. Therefore, a value as low as $350 \text{ molar}^{-1} \text{ cm}^{-1}$ for the extinction coefficient of $\text{Co}(\text{TMPA})_4^{2+}$ does not give an adequate fit of all the data but it is not possible to fix the value accurately between 350 and $1260 \text{ molar}^{-1} \text{ cm}^{-1}$.

Comparison of the extinction coefficients of $\text{Co}((\text{CH}_3)_3\text{NO})_4(\text{ClO}_4)_2$ (80) and $\text{Co}((\text{CH}_3)_3\text{NO})_2\text{Cl}_2$ and $\text{Co}(\text{TMPA})_2\text{Cl}_2$ (100) indicates that the extinction coefficient of $\text{Co}(\text{TMPA})_4(\text{ClO}_4)_2$ should be about $500 \text{ molar}^{-1} \text{ cm}^{-1}$. If this value is chosen

then the fit of the spectrophotometric data gives $\Delta H = -1.5_8$ kcal mole⁻¹ and $\Delta S = -11.9_6$ eu. These values in turn were used to obtain a least squares fit of the shift data to equation (85-c) with C_A and C_B as adjustable parameters. The calculated and observed values (Table VII) agree within the estimated error (± 2 cps) except for the values at -50 , 120 and 140°C for which the difference is about 4 cps. The agreement for these three points does not improve dramatically even for $\epsilon_A \approx 1000$ molar⁻¹ cm⁻¹; therefore, an extinction coefficient of 500 molar⁻¹ cm⁻¹ was assumed to be a reasonable estimate.

The values of C_A and C_B may be used to calculate the hyperfine coupling constants of $-6.2_0 \times 10^4$ cps and $4.8_5 \times 10^4$ cps for the octahedral and tetrahedral species, respectively. The latter were calculated by substituting the effective magnetic moment of 4.9 B.M. in place of $g\sqrt{S(S+1)}$ in equation (21). The negative coupling constant refers to an upfield shift and the positive coupling constant a downfield shift.

It does not seem meaningful to place any errors on ΔH , ΔS and the coupling constants quoted above because they all depend on the rather arbitrary choice of 500 molar⁻¹ cm⁻¹ for the extinction coefficient of the tetrahedral species. Experience in fitting the results has indicated that ΔH and the octahedral coupling constant are the most reliable parameters and may change by a factor of two if the extinction

coefficient falls within the reasonable limits of 350 to 1260 molar⁻¹ cm⁻¹. The inability to fit the data without any assumptions seems impossible because the tetrahedral cobalt(II) species never appears to constitute more than 50% to 70% of the total cobalt concentration. Therefore, it is not possible to reliably determine either the extinction coefficient or coupling constant of the tetrahedral form.

A plot of $\log (T_{2p})^{-1}$ versus $(T^{\circ}K)^{-1}$ shows only a linear increase as the temperature is decreased which is typical of a T_{2M} relaxation process. Therefore:

$$\begin{aligned} (T_{2p})_{OBS}^{-1} &= P_{MA} (T_{2MA})_{INNER}^{-1} + [A] (T_{2MA})_{OUTER}^{-1} \\ &+ P_{MB} (T_{2MB})_{INNER}^{-1} + [B] (T_{2MB})_{OUTER}^{-1}. \end{aligned} \quad (91)$$

P_{MA} , P_{MB} , [A], and [B] can be obtained as before and the T_{2M} terms can be obtained from equations (31) and (32). The inner and outer sphere interaction distances were taken the same as for the nickel(II)-trimethylphosphate system. The only unknowns in equation (91) are the correlation times for the octahedral (τ_{OCT}) and tetrahedral (τ_{TET}) complexes. τ_{OCT} was assumed to be identical for the inner and outer sphere dipolar interaction as well as for the hyperfine interaction for the octahedral species; similar assumptions were made about τ_{TET} . The correlation times were both assumed to have exponential temperature dependences

with τ_0 being the correlation time at infinite temperature. Equation (19) was then fit to the broadening data by a non-linear least squares method, yielding $(\tau_0)_{\text{OCT}} = 2.4_6 \times 10^{-12}$ sec, $(E_a)_{\text{OCT}} = 0.3_7$ kcal mole⁻¹, $(\tau_0)_{\text{TET}} = 1.6_6 \times 10^{-13}$ sec, and $(E_a)_{\text{TET}} = 1.5_4$ kcal mole⁻¹. These parameters give $(\tau)_{\text{OCT}} = 4.5_5 \times 10^{-12}$ sec and $(\tau)_{\text{TET}} = 2.2_0 \times 10^{-12}$ sec at 25°C. The observed and calculated broadenings are given in Table VII.

A general review of the results of this section (Table IX) shows that the only system for which a definite exchange rate could be obtained was the nickel(II)-dimethylsulfoxide system. For all the other systems the data was best analyzed in terms of a fast inner sphere exchange of the ligands on the metal ion leading only to an inner and outer sphere dipolar relaxation of the bulk solvent protons. Since the exchange parameters could be obtained at only the lower temperatures, it is not surprising that no exchange controlled region for the broadening of the bulk solvent was observed in the $\text{Co}(\text{ClO}_4)_2$ -DMSO system because exchange rates on cobalt(II) are about two orders of magnitude faster than on nickel(II) in identical solvents (82). Therefore, low enough temperatures could not be obtained to get exchange control of the broadening in dimethylsulfoxide (m.p. 18.5°) containing cobalt(II). The lower limit of $1.5_3 \times 10^4$ sec⁻¹ at 25°C for the exchange of dimethylsulfoxide on cobalt(II) seems reasonable from comparison to the exchange rate of nickel(II) in this

solvent and other systems of these two metal ions. A more detailed discussion of these latter nickel(II) and cobalt(II) systems and the various factors which may partially determine the exchange parameters in these solvents is given by Stengle and Langford (4).

Comparison of the trimethylphosphate systems of nickel(II) and cobalt(II) to the dimethylsulfoxide systems shows that the former exchange rates are as fast or faster than the latter (Table IX). This behavior may be attributed to the bulkiness of the trimethylphosphate ligand which could cause steric interference in the complex and easy rejection of one ligand as required by a dissociative type mechanism. The proposal that steric hinderance is appreciable in the trimethylphosphate complexes is also substantiated by the presence of a tetrahedral species in the cobalt(II)-trimethylphosphate system. Tetrahedrally coordinated cobalt(II) complexes tend to form only in solvents which are bulky in structure and/or weakly coordinating (80). It may also be renoted that fast solvent exchange best accounted for the results in the vanadyl-dimethylsulfoxide and -trimethylphosphate systems. The correlation between these systems will be extended in Chapter V.

The hyperfine coupling constants which also appear in Table IX warrant some discussion because of the apparent peculiarity of sign change. In this table a downfield shift

TABLE IX

Exchange rates and hyperfine coupling constants for nickel(II) and cobalt(II) in dimethylsulfoxide (DMSO) and trimethylphosphate (TMPA)

Compound	Solvent	k_r, sec^{-1} @ 25°C	A/h, cps	Possible Spin Delocalization Mechanism
$\text{Ni}(\text{ClO}_4)_2$	DMSO	5×10^3	$7.5_7 \times 10^4$	3
$\text{Ni}(\text{ClO}_4)_2$	TMPA	$> 1.8_5 \times 10^2$	$7.1_6 \times 10^3$	1,3
$\text{Co}(\text{ClO}_4)_2$	DMSO	$> 1.5_3 \times 10^4$	$2.0_8 \times 10^4$	3,5
$\text{Co}(\text{ClO}_4)_2$	TMPA (Octahedral)	$> 6.3_0 \times 10^3$	$-6.2_0 \times 10^4$	2,4,5
$\text{Co}(\text{ClO}_4)_2$	TMPA (Tetrahedral)	$> 6.5_5 \times 10^3$	$4.8_5 \times 10^4$	1,3

of the bulk solvent is denoted by a positive coupling constant and an upfield shift is denoted by a negative coupling constant. Only a qualitative explanation of these sign changes will be attempted here. A coupling constant measures the degree of interaction of the magnetic nucleus under observation with the unpaired electrons on the paramagnetic ion. The nature of this interaction can vary as discussed in reference (12). Various types of interaction considered here are:

(1) spin polarization which requires that the electrons on the coordinating atom of the ligand (oxygen in the systems studied in this section) be delocalized by a σ -interaction with the metal ion, thus inducing spin polarization through σ -type bonds on all the atoms of the ligand. This mechanism requires a positive spin density on the hydrogen atoms of trimethylphosphate and a negative spin density on these atoms in dimethylsulfoxide; therefore, this mechanism only accounts for the downfield shift in the nickel(II) and tetrahedral cobalt(II)-trimethylphosphate systems.

(2) σ - π configuration interaction which requires that the spin density in the σ -type orbitals of the coordinated atom induce an opposite spin density in the π -system in the molecule which may transmit spin density to the protons by hyperconjugation. Such a mechanism predicts an upfield shift for the protons in all the complexes studied here. This is only observed for the octahedral cobalt(II)-trimethylphosphate system.

(3) overlap of metal ion e_g -orbitals with a ligand orbital whose wavefunction incorporates at least a slight contribution from every atom in the ligand molecule. Spin is again partially delocalized onto the metal ion causing a downfield shift of the ligand proton resonances. The octahedral cobalt(II)-trimethylphosphate shift is the only one that cannot be explained by this mechanism.

(4) a psuedocontact shift which arises from an anisotropy in the complex gives rise to a small upfield shift. Since this mechanism is usually considered to be negligible in cobalt(II) and nickel(II) due to small anisotropies in these complexes, and since suitable anisotropic parameters are not available for the calculation of the magnitude of this shift in the complexes under consideration here, it was assumed that this mechanism does not dominate in these systems.

(5) t_{2g} - π overlap with configuration interaction requires that there be an overlap of the t_{2g} -orbitals on the metal ion with the ligand π -orbitals which subsequently interact with the σ -orbitals which transmit spin density to the protons by a spin polarization effect. This mechanism adequately accounts for the downfield shift in the cobalt(II)-dimethylsulfoxide complex and the upfield shift in the cobalt(II)-trimethylphosphate octahedral complex. Nickel(II) would not be expected to show this type of interaction because of complete spin pairing in the t_{2g} -orbitals.

It appears from the above discussion that no interaction process between the unpaired electron on the metal and the nuclei accounts for the shift in all systems. However, from consideration of other nickel(II) and cobalt(II) systems (6,8,36) where a σ -type polarization interaction appears to dominate in shifting the resonance of the nucleus, it can be seen that the nickel(II) coupling constant is 1-4 times larger than the cobalt(II) coupling constant in identical solvents. The nickel(II)- and cobalt(II)-dimethylsulfoxide systems also show this same behavior. However, it was found for the nickel(II)- and cobalt(II)-acetonitrile systems (12) that the shift was upfield rather than downfield which could best be accounted for by a σ - π configuration interaction. The coupling constant for the nickel(II)-acetonitrile system was 11 times larger than that for the cobalt(II)-acetonitrile system. It was suggested that possibly a σ -type polarization mechanism was competing with the σ - π interaction and causing a smaller coupling constant in the latter system. The coupling constants for nickel(II) and cobalt(II) in trimethylphosphate indicate a similar duality of coupling mechanisms. In this case it seems that the σ - π interaction is even more important for cobalt(II) and results in a coupling constant of opposite sign to that for nickel(II).

6. Nuclear Magnetic Resonance Line Broadening of
N,N-dimethylformamide Resonances by Vanadium(III)

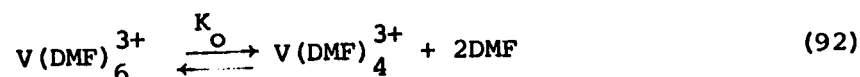
Most of the previous work that has been done on ligand exchange using the NMR line broadening technique has dealt with the divalent first row transition metals. Very little work has been carried out on the trivalent ions due to their instability with respect to hydrolysis and decomposition in most common solvents. The aqueous iron(III) system has been studied recently by Blatt and Connick (84) and also by Zeltmann and Morgan (85). The exchange rates on iron(III) are generally about 10^6 slower than isoelectronic manganese(II) as expected if ligand exchange is an S_N1 process.

Vanadium(III) presents an interesting comparison with theory because it may be expected to exchange by an S_N2 process since it is a d^2 system with an empty low energy t_{2g} orbital. This possibility was first predicted by Taube (86) on the basis of valence bond theory, but is also consistent with crystal field arguments presented by Basolo and Pearson (70). However, the only results available for exchange on vanadium(III) are the thiocyanate system studied by Kruse (reported by Eigen and Wilkins) (87), Sutin, *et al* (88) and Garner and Furman (89) and the aquation rate of $V(N_3)^{2+}$ reported by Espenson (90).

In this study the temperature dependence of the line broadening and shift of the formyl proton in N,N-dimethylformamide (DMF) containing vanadium(III) perchlorate has been studied. The

normal plot of $\log (T_{2p}')^{-1}$ versus the inverse of the absolute temperature was made and is shown in Figure 23; the corresponding shift plot is shown in Figure 24. This system has two unusual features. Firstly, the $(T_{2p}')^{-1}$ data shows a frequency dependent region at low temperatures, and then rises with an unexpectedly high apparent activation energy at high temperatures. This behaviour indicates a chemical exchange region at high temperatures. Secondly, the rapid decrease of the shift as the temperature is raised is not consistent with equation (22) which predicts that the shift goes to zero when $(T^\circ K)^{-1}$ is zero.

These peculiarities show that there must be at least two different vanadium(II) complexes in equilibrium in this system. Due to the similarity of the visible spectrum of the vanadium(III)-DMF system (maxima at 635 m μ , $\epsilon = 28.9$ and 428 m μ , $\epsilon = 40.3$) to the vanadium(III)-aquo system at 25°C (94) it may be concluded that the major species at this and higher temperatures is the octahedral complex. Four (93) and five coordinate (115) vanadium(III) complexes have been isolated. It was arbitrarily assumed that the four coordinate species existed at lower temperatures. This equilibrium can be represented by:



where

$$K_o = \frac{[V(DMF)_4^{3+}]}{[V(DMF)_6^{3+}]} = \frac{[B]}{[A]} = \exp(-\Delta H_o/RT + \Delta S_o/R). \quad (93)$$

B and A represent the tetrahedral and octahedral species, respectively,

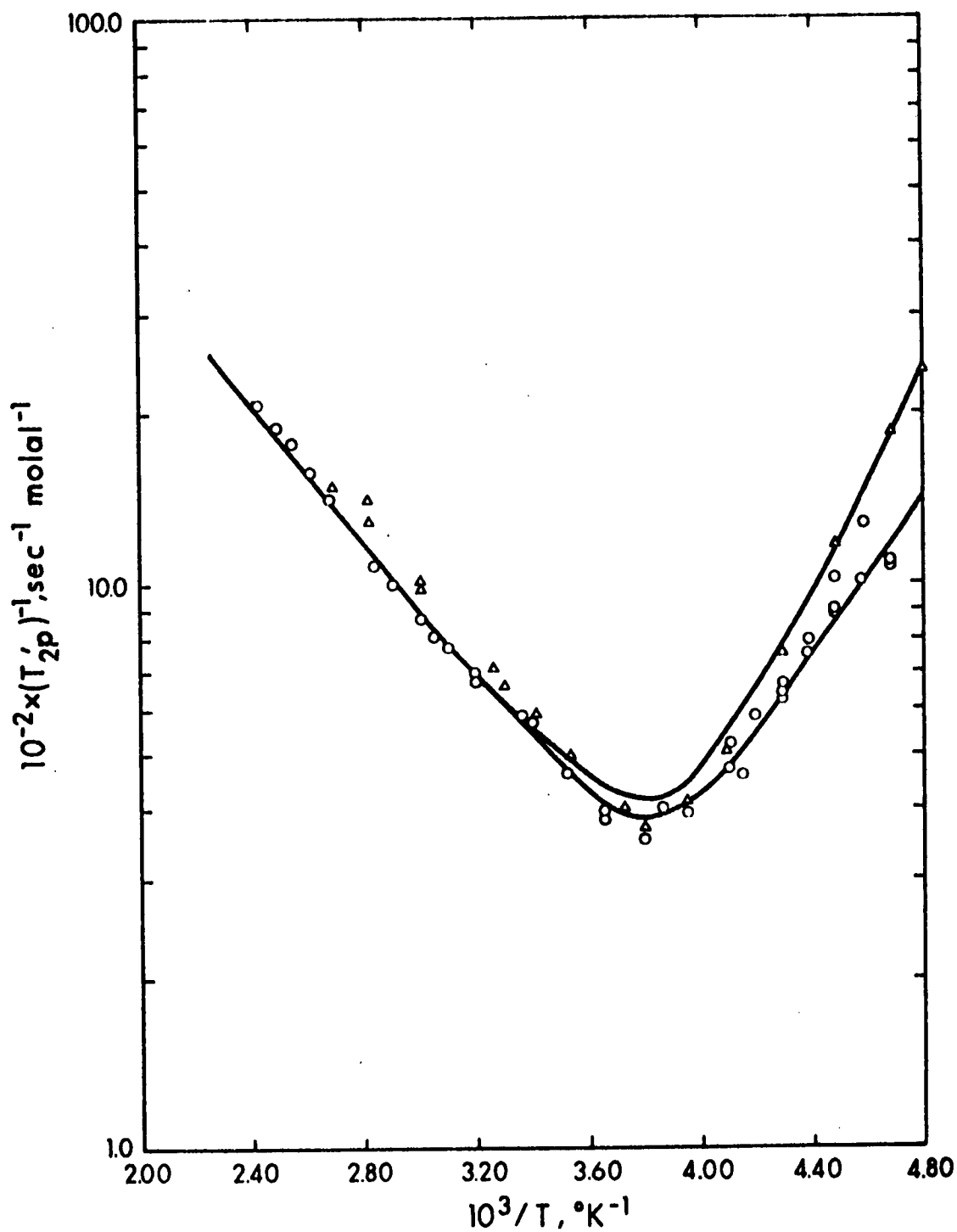


Figure 23: Temperature dependence of $\log (T_{2p}')^{-1}$ at 60 MHz - O and at 100 MHz - Δ for the formyl proton of N,N-dimethylformamide containing vanadium (III) perchlorate.

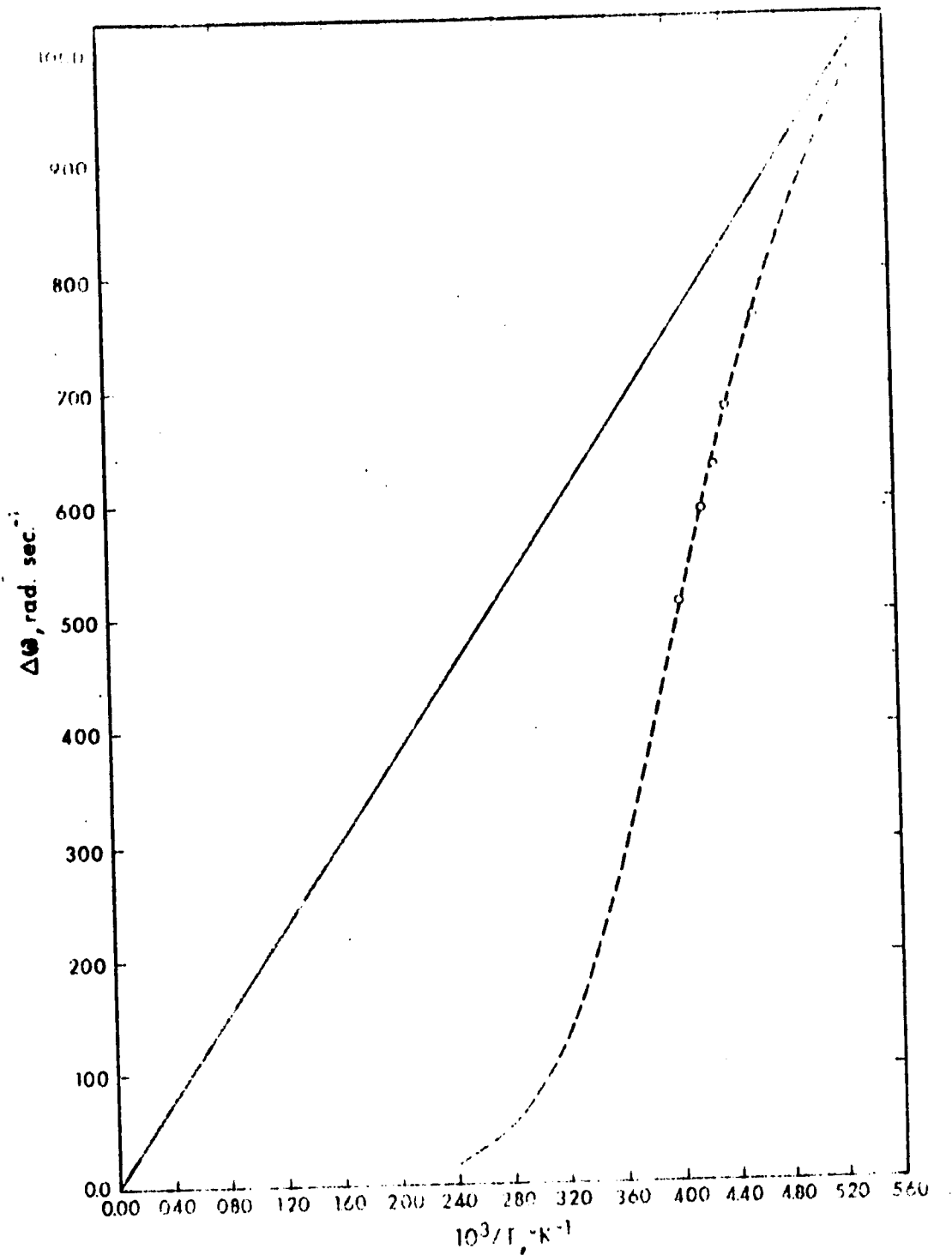


Figure 24: Temperature dependence of the shift normalized to 1 molal for the formyl proton of N,N-dimethylformamide containing vanadium (III) perchlorate: — theoretical molal shift, ----- theoretically calculated shift, O - observed shift.

and the bulk solvent concentration is assumed to be constant (this assumption yields less than 5 percent error in K_o). Since the broadening and shift data are normalized to 1 molal the following relationship holds

$$[A] + [B] = [V^{3+}]_{\text{Total}} = 1.0m \quad (94)$$

The lack of frequency dependence in the high temperature $(T_{2p}')^{-1}$ data and the apparent absence of any chemical shift at high temperatures is consistent with the octahedral exchange being described by condition (34-a). The slight frequency dependence of the low temperature $(T_{2p}')^{-1}$ data and the increased shift at lower temperatures suggests that exchange on the tetrahedral species can be represented by conditions (34-b) and (34-d). Therefore, the broadening and shift are given by equations (96) and (97), respectively.

$$\begin{aligned} (T_{2p}')^{-1} &= P_{MA} [A] / \tau_{MA} + P_{MB} [B] \left\{ \tau_{MB} \Delta\omega_{MB}^2 + (T_{2MB})^{-1} \right\} \quad (95) \\ &= P_{MA} [A] (kT/h) \exp(-\Delta H_A^\ddagger / RT + \Delta S_A^\ddagger / R) \\ &\quad + P_{MB} [B] \left\{ (h/kT) \exp(\Delta H_B^\ddagger / RT - \Delta S_B^\ddagger / R) \times (C_B/T)^2 + C_B' \exp(E_a / RT) \right\} \quad (96) \end{aligned}$$

where $P_{MA} = 6/[DMF]$, $P_{MB} = 4/[DMF]$, ΔH_A^\ddagger and ΔS_A^\ddagger ; ΔH_B^\ddagger and ΔS_B^\ddagger are the activation enthalpy and entropy for exchange on the octahedral and tetrahedral complexes, respectively, C_B contains the known

parameters in equation (22) along with the unknown isotropic hyperfine coupling constant and C_B' contains the parameters which are given in equation (31).

$$\Delta\omega_{\text{OBS}} = P_{\text{MB}} [B] C_B'/T \quad (97)$$

Also from equations (92) and (93):

$$[B] = \frac{K_O}{1+K_O} = \frac{\exp(-\Delta H_O/RT)}{\exp(-\Delta S_O/R) + \exp(-\Delta H_O/RT)} \quad (98)$$

and

$$[A] = 1.0 - \frac{\exp(-\Delta H_O/RT)}{\exp(-\Delta S_O/R) + \exp(-\Delta H_O/RT)} \quad (99)$$

The obvious difficulty in applying the above equations to the data is the large number of unknowns. However, by fitting equation (97) to the shift data by a nonlinear least squares method it was possible to obtain ΔH_O and ΔS_O and $(A/h)_B$; these parameters were found to be -2.11 ± 0.70 kcal mole⁻¹, -8.94 ± 0.40 e.u. and $1.29 \pm 0.10 \times 10^5$ cps, $K_O = 0.40$. These parameters can then be substituted into equation (96), thereby decreasing the number of unknowns to six. The $(T_{2p}')^{-1}$ data was then fit to this equation by a nonlinear least squares method where six parameters were adjusted to give the best fit to the 60 MHz data. The parameters obtained were $\Delta H_A^\ddagger = 6.31 \pm 0.50$ kcal mole⁻¹, $\Delta S_A^\ddagger = -26.9 \pm 2.5$ e.u., $\Delta H_B^\ddagger = 6.82 \pm 0.43$ kcal mole⁻¹, $\Delta S_B^\ddagger = -6.36 \pm 1.50$ e.u.,

$E_a = +1.67 \pm 0.15 \text{ kcal mole}^{-1}$ and $C_B' = 1.43 \pm 0.15 \times 10^2 \text{ sec}^{-1}$
 molal^{-1} . The corresponding parameters for the fit to the 100 MHz
 data are $\Delta H_A^\ddagger = 6.50 \pm 0.50 \text{ kcal mole}^{-1}$, $\Delta S_A^\ddagger = -23.7 \pm 5.2 \text{ e.u.}$,
 $\Delta H_B^\ddagger = 6.53 \pm 0.70 \text{ kcal mole}^{-1}$, $\Delta S_B^\ddagger = -7.10 \pm 0.50 \text{ e.u.}$,
 $E_a = +1.55 \pm 0.90 \text{ kcal mole}^{-1}$, and $C_B' = 1.57 \pm 0.35 \times 10^2 \text{ sec}^{-1}$
 molal^{-1} . The proper frequency dependence was predicted at low
 temperatures (Figure 23).

If the T_{2M} relaxation process is due to an inner sphere
 isotropic hyperfine interaction, equation (31), then it is found
 that C_B' and E_a give $\tau_S = 6.0_0 \times 10^{-9} \text{ sec}$ at 25°C . This electron
 spin relaxation time seems too long for vanadium(III) in
 N,N-dimethylformamide because it was not possible to see an EPR
 spectrum of this system. Therefore, it was assumed that an
 inner and outer sphere dipolar mechanism was causing the relaxation.
 The normal iterative procedure gives $\tau_c = 7.1_0 \times 10^{-12} \text{ sec}$ at 25°C
 which is associated with τ_S because τ_R for this system is expected
 to be of the order of $1.1_2 \times 10^{-10} \text{ sec}$ which is the tumbling
 correlation time for the vanadyl ion in N,N-dimethylformamide.
 This correlation time predicts negligible contribution to $(T_{2p}')^{-1}$
 from the hyperfine interaction process.

The line broadening of the two types of methyl protons in
 N,N-dimethylformamide provides further evidence that the above
 interpretation is correct. The two methyl resonances are
 separated by only 5 Hz in pure N,N-dimethylformamide and, therefore

overlap considerably because they are broadened by the paramagnetic ion. However by using a fairly low vanadium(III) concentration (0.013 molal) and working in the temperature range of minimum broadening (50° to -10°) it has been possible to keep the two peaks at least partially resolved. The individual peaks were resolved on a Dupont 310 Curve Resolver and the line widths determined from these resolved curves (Table LVII).

The values of $(T_{2p})^{-1}$ for the methyl protons approach those of the formyl proton at high temperatures as expected if solvent molecule chemical exchange is controlling the line broadening. At low temperatures the broadening of the methyl proton resonances is less than that of the formal proton again as expected since the broadening depends on $\Delta\omega_M$ and in turn on (A/h) in this region. The hyperfine coupling constant for the methyl protons is expected to be smaller than that of the formyl proton (6). It is not possible to quantitatively analyse the methyl proton broadening because the chemical shift was too small to permit an accurate determination of the hyperfine coupling constant.

The exchange rate for octahedral vanadium(III) in N,N-dimethylformamide at 25°C is $1.7_0 \times 10^2 \text{ sec}^{-1}$. This value is within the expected range when compared to the results of Sutin *et al* (88) for the substitution of thiocyanate on $V(OH_2)_6^{3+}$ in water. The large negative entropy of activation (-26.9 e.u.) is unusual when compared to the values for

cobalt(II) and nickel(II) but is consistent with an S_N2 substitution mechanism for vanadium(III).

Tetrahedral vanadium(III) in N,N-dimethylformamide has an exchange rate of $2.5_5 \times 10^6 \text{ sec}^{-1}$, at 25°C. This value is consistent with Taube's qualitative prediction that tetrahedral vanadium(III) should be labile. The small value of ΔS^\ddagger is also consistent with a predicted S_N1 mechanism.

CHAPTER IV ELECTRON PARAMAGNETIC RESONANCE LINE WIDTH
STUDY OF THE VANADYL ION IN VARIOUS SOLVENTS

Several recent publications (17-28) have dealt with the Electron Paramagnetic Resonance (EPR) spectra of vanadyl complexes in various solvents. The variation in width of the eight hyperfine components of the vanadium(IV) EPR spectrum has been treated in terms of Kivelson's (17) theory with reasonable success (24-28).

The initial purpose of this EPR study on the vanadyl ion in N,N-dimethylformamide (DMF), methanol (CH₃OH), acetonitrile (AN), dimethylsulfoxide (DMSO), trimethylphosphate (TMPA), and trimethylphosphite (TMPI) was to determine the tumbling times (τ_R) of the vanadyl ion-solvent complexes by using Kivelson's EPR theory. The tumbling time could then be used in interpreting the NMR line broadening of the above solvents.

An analysis which is discussed in detail below was carried out to determine the best method of determining τ_R from the EPR theory. The theory was generally found to give an adequate, self-consistent fit of the hyperfine line widths; however, the residual line width (α'') did not agree with the value predicted from the spin-rotational (SR) relaxation theory as given by equation (36). This discrepancy between predicted and observed residual line width led to an investigation of several other vanadyl systems in an attempt to determine how well the residual line width could be accounted for by a spin rotational process.

It was also of interest to investigate how well Kivelson's EPR theory stood up under a wide variation of temperature and solvent viscosity. The systems that were studied were: vanadyl acetylacetonate in ethanol, n-propanol, isopropanol, n-butanol, t-butanol, trichloroethanol, and trifluoroethanol, vanadyl trifluoroacetylacetonate in methanol and vanadyl perchlorate in water. It was found that the residual line width could not be accounted for by the SR -theory but could be interpreted either as an intramolecular dipolar or hyperfine interaction between the unpaired electron and the vanadium nucleus or as an interaction between the unpaired electron and a rapidly exchanging ligand, presumably trans to the vanadyl oxygen.

The EPR theory, which is mentioned above and discussed in Chapter I, section 3, predicts that the hyperfine line width is given by a third order polynomial shown in equation (35). The coefficients (α' , β , γ and δ) are given by the theory (24) and have the general form:

$$j = C_{1j} \tau_R + C_{2j} \left\{ \frac{1}{1 + \omega_e^2 \tau_R^2} \right\} \tau_R + C_{3j} \left\{ \frac{\omega_e^2 \tau_R^2}{1 + \omega_e^2 \tau_R^2} \right\} \tau_R \quad (100)$$

where $j = \alpha'$, β , γ or δ , τ_R is the rotational correlation time for the complex and the constants (C_{ij} , $i = 1-3$) are predicted by the theory and may be calculated if the anisotropic components of the hyperfine coupling constant (A_x , A_y , and A_z) and the g-value (g_x , g_y , and g_z) are known. The latter parameters may

be obtained from the EPR spectrum in a glass.

It is apparent that by fitting the variation of the hyperfine line widths with spin quantum number (m_1) to equation (35) the best fit values of $\alpha = \alpha' + \alpha''$, β , γ and δ may be obtained. Then β , γ and δ may be used in equation (100) to calculate τ_R . In principle all three coefficients (β , γ and δ) should give the same τ_R value, but this ideal is not reached in general. For this reason it was of interest to determine which of the coefficients was least susceptible to errors in the EPR line widths and should, therefore, give the best value for τ_R . A computer programme was drawn up to calculate β , γ and δ from all the line width combinations (6561) if a $\pm 10\%$ error was assumed on each line width. The results showed that γ varied by only $\pm 10\%$, whereas β varied by $\pm 25\%$ and δ varied by a large factor. Therefore, γ was used to calculate τ_R for each combination of lines and the average τ_R was taken as the best value. This value was then used to calculate β and δ , which were used along with the average values of γ and α to recalculate the line widths. These coefficients predicted the original line widths within the estimated $\pm 10\%$ error.

It became apparent in the initial calculations on the vanadyl ion - DMF, CH_3OH , AN, DMSO, TMPA and TMPI systems that the approximation $\omega_e^2 \tau_R^2 \gg 1$ in equation (100) was justified. Therefore, this approximation allows τ_R to be determined from the γ coefficient by solving a quadratic equation. The β and δ

coefficients were calculated from the theoretical expressions for these parameters. The residual line width (α'') was calculated in two ways; first α' was calculated from the theoretical expression for this parameter, then this quantity was subtracted from the average α taken from the least squares fit of equation (35) to all combinations of the EPR hyperfine lines with their errors. Secondly, the contribution to the width of the hyperfine lines from the theoretical α' , β , γ and δ coefficients, obtained from the best τ_R , was determined and the average of the residuals was taken as α'' . The two methods of obtaining α'' agreed identically. However, α'' did not agree well with the residual line width contribution predicted from the SR-theory as can be seen from the results given in Table X. Other results obtained for the above systems are also shown in Table X. Typical glass and solution spectra are shown in Figures 25 and 26, respectively, for the vanadyl ion in N,N-dimethylformamide.

It may be noted that in the initial output from the computer programme that the average values of α , β , γ and δ from the least squares fit of equation (35) to the EPR line width data when the $\pm 10\%$ error on the $m_i = 7/2$ line was considered were identical to the coefficients obtained from the line width data when no error on this line was taken. Therefore, the error on the $m_i = 7/2$ line was dropped from

TABLE X
EPR parameters for vanadyl complexes in various solvents

Compound	Solvent	g_{\parallel}	g_{\perp}	$\langle g \rangle$ OBS	$-A_{\parallel}$ gauss	$-A_{\perp}$ gauss	$-\langle A \rangle$ OBS gauss	$\tau_R \times 10^{10}$ sec @ 25° C	Experimental residual line width (gauss)	Spin rotational line width (gauss)	Hydrodynamic Radius $\overset{\circ}{A}$
$VO(BF_4)_2$	DMSO	1.945	1.978	1.966	194.8	75.9	113.5	1.21	4.20 @ 60°C	0.26 @ 60°C	3.92
$VO(BF_4)_2$	TMPA	1.940	1.977	1.968	202.6	74.5	117.2	1.32	14.54	0.28	3.98
$VO(BF_4)_2$	TMPI	1.944	1.977	1.971	203.0	83.0	121.0	1.10	4.91 @ 60°C	0.31 @ 60°C	5.72
$VO(BF_4)_2$	AN	1.948	1.982	1.974	195.0	76.9	117.0	0.62	7.30	0.44	5.62
$VO(ClO_4)_2$	DMF	1.945	1.977	1.969	192.0	70.2	111.5	1.15	16.89	0.31	5.10
$VO(ClO_4)_2$	MEOH	1.945	1.979	1.969	192.7	75.0	114.5	0.41	12.10	0.78	4.20

(a) The abbreviations for the solvents are as follows:

DMF - N,N-dimethylformamide
 CH₃OH - methanol
 AN - acetonitrile
 DMSO - dimethylsulfoxide
 TMPA - trimethylphosphate
 TMPI - trimethylphosphite

(b) The hydrodynamic radii are calculated from the Debye formula [equation (37)].

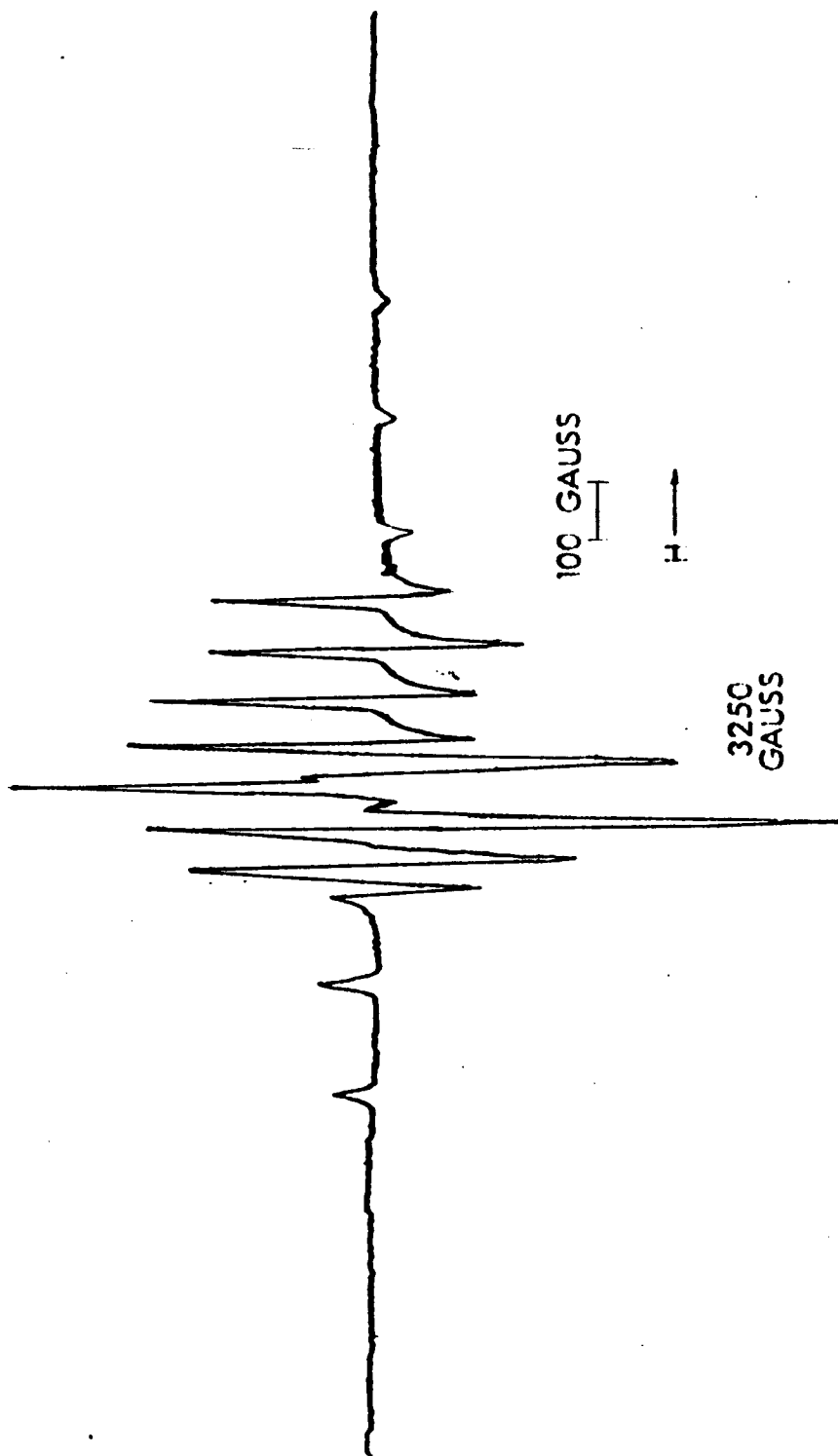


Figure 25: Glass EPR spectrum of 10^{-2} molar vanadyl perchlorate in *N,N*-dimethylformamide at -173°C .

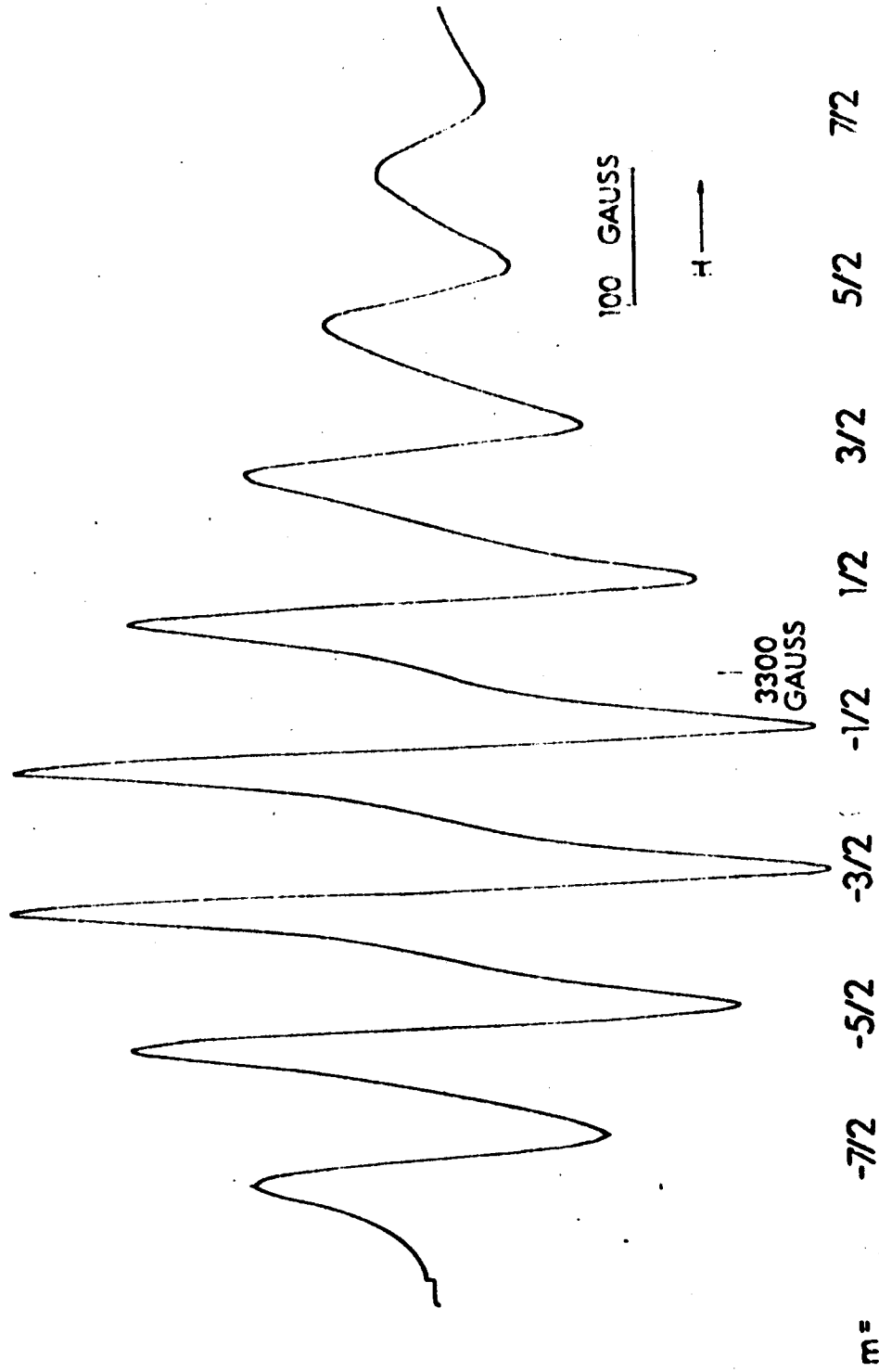


Figure 26: Solution EPR spectrum of 10^{-2} molal vanadyl perchlorate in N,N-dimethylformamide at 25°C .

the computations without loss of generality in order to decrease computer time. This point is also noted in the computer programme in Appendix B.

Since there was considerable disagreement between the observed and calculated residual line widths in the systems listed in Table X additional systems containing vanadyl acetylacetonate and vanadyl trifluoroacetylacetone in various alcohols, as listed above, and vanadyl perchlorate in water were studied to test how well the SR-theory accounted for the residual line width. Alcohol solvents which had various liquid ranges and viscosities were chosen. Viscosities for all the alcohols except trifluoroethanol and trichloroethanol were taken from the Handbook of Physics and Chemistry (46th ed.) and from reference (95). The results of a temperature study on the viscosity and density of trifluoroethanol and trichloroethanol are shown in Table XI.

It was observed in the calculations of these latter systems that the approximation, $\omega_e^2 \tau_R^2 \gg 1$, was no longer justified. In order to eliminate this approximation and still make the equation in τ_R solvable it was necessary to first calculate the correlation time as discussed above; this τ_R could then be used to evaluate $\omega_e^2 \tau_R^2$. The numerical value for $\omega_e^2 \tau_R^2$ could be substituted into the complete theoretical expressions {equation (100)} and a new τ_R could be calculated. $\omega_e^2 \tau_R^2$

TABLE XI

Temperature dependence of the viscosity and density for trichloroethanol and trifluoroethanol

Temperature ± 0.05°C	DENSITY (gm/cc)		VISCOSITY (CENTISTOKES) (a)		
	Trichloroethanol	Trifluoroethanol	Temperature ± 0.10°C	Trichloroethanol	Trifluoroethanol
26.2	1.5440 ± 0.0003	1.3790 ± 0.0002	24.7	14.205 ± 0.005	1.471 ± 0.002
30.0	1.5391 ± 0.0004	1.3725 ± 0.0005	29.8	10.408 ± 0.004	1.264 ± 0.002
35.0	1.5321 ± 0.0001	1.3641 ± 0.0003	35.0	7.851 ± 0.005	1.047 ± 0.004
40.0	1.5248 ± 0.0003	1.3552 ± 0.0001	40.0	6.075 ± 0.003	0.928 ± 0.002
45.0	1.5177 ± 0.0003	1.3469 ± 0.0002	45.0	4.845 ± 0.005	0.800 ± 0.001
50.0	1.5107 ± 0.0001	1.3372 ± 0.0004	50.0	3.911 ± 0.001	0.680 ± 0.000
55.0	1.5031 ± 0.0005	1.3275 ± 0.0010			

(a) The temperature dependences of the viscosity for trifluoroethanol and trichloroethanol have apparent activation energies of 6.3₀ kcal mole⁻¹ and 8.6₀ kcal mole⁻¹, respectively. Errors are given as standard errors for at least three observations.

could be re-evaluated and the same procedure followed to obtain a better value for τ_R ; this iterative process was continued until there was less than 1% improvement in τ_R . It was found that two or three iterations were sufficient to give a correlation time which satisfied these conditions. The final correlation time was generally about 10% smaller than the correlation time used in the initial step of the iteration. τ_R was then used to calculate theoretical values for α' , β and δ . The residual line width was calculated as before. These parameters are given in Tables XIII - XXI for all the systems on which the temperature study was done. The observed coefficients are those which were determined from the average of all the least squares coefficients and the calculated coefficients were obtained by introducing the final τ_R into the theoretical expressions for the coefficients. The calculated and theoretical parameters agree within $\pm 10\%$ except for α'' which will be discussed in detail below. A typical variation of the hyperfine line widths with quantum number and temperature is shown in Figure (27) for vanadyl perchlorate in water; the solid lines indicate the theoretically predicted line widths. The difficulty which McCain and Myers (27) had in determining a suitable τ_R for the vanadyl ion in water was not encountered here.

Tables XIII - XXI also contain the observed and calculated τ_R , the average hyperfine coupling constant, $\langle A \rangle_{\text{OBS}}$, and the average g-value, $\langle g \rangle_{\text{OBS}}$. It should be noted that the isotropic

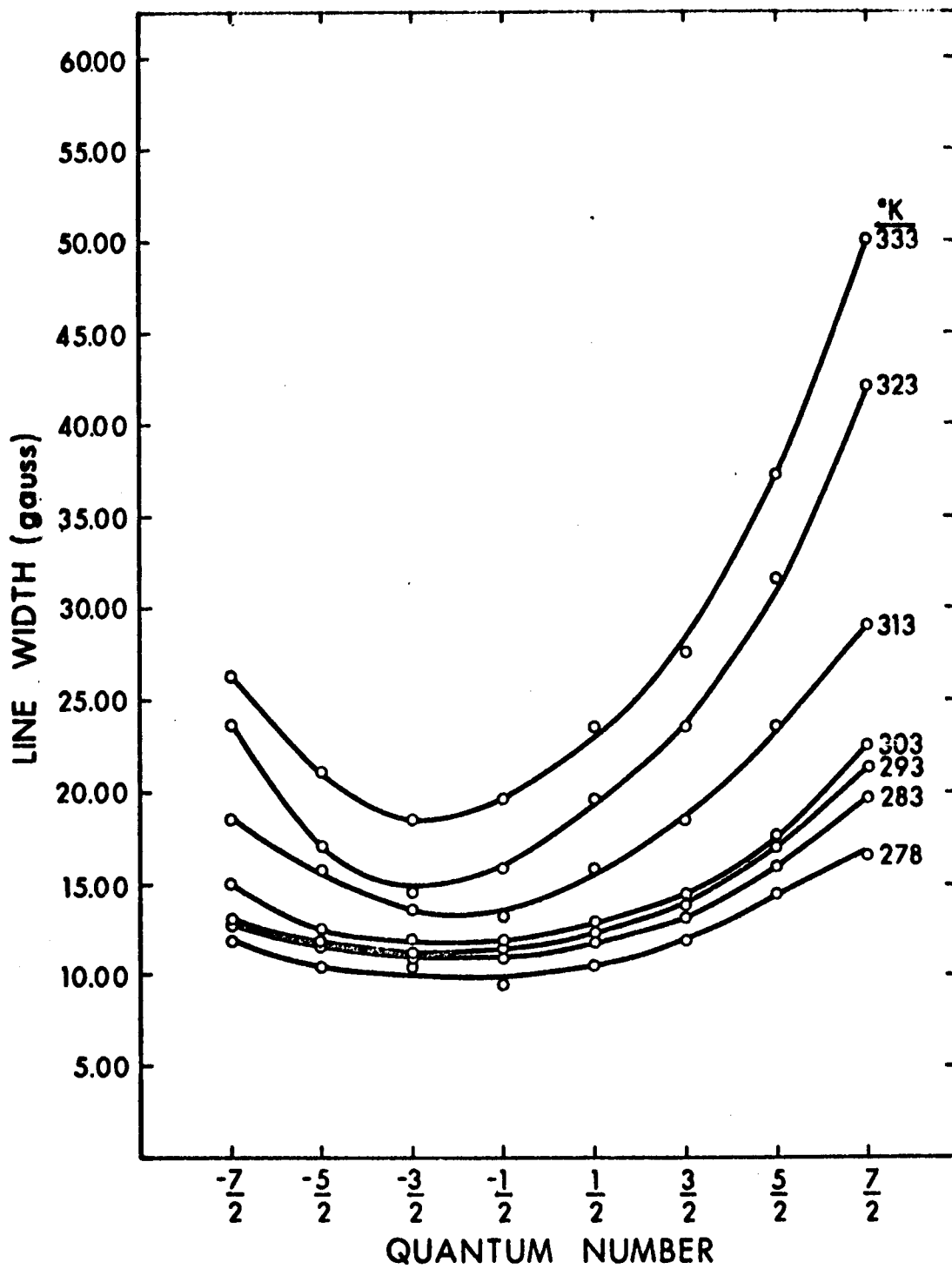


Figure 27: Temperature and quantum number dependence of the EPR hyperfine line width of a solution spectrum of 10^{-3} molal vanadyl perchlorate in water {O - experimental points, — - least mean squares fit.}

TABLE XII

Parameters obtained from the EPR study of vanadyl acetylacetonate-alcohol systems

Solvent	$r^{(a)}$, Å	K	r_{DD} , Å	A/n, cps @ 20°C	$\tau_e \times 10^{10}$, sec @ 20°C
trichloroethanol	3.8 ₀	1.0 ₀	0.34 ₅	2.3 ₆ × 10 ⁸	6.4
n-butanol	3.8 ₀	1.0 ₀	0.35 ₆	2.3 ₇ × 10 ⁸	5.2
n-propanol	3.8 ₀	1.0 ₀	0.44 ₀	2.4 ₂ × 10 ⁸	1.2
ethanol	3.6 ₈	0.9 ₁	0.43 ₁	2.4 ₆ × 10 ⁸	1.6
trifluoroethanol	3.6 ₆	0.8 ₉	0.40 ₅	2.4 ₀ × 10 ⁸	2.4
t-butanol	3.2 ₈	0.6 ₄	0.36 ₄	2.4 ₈ × 10 ⁸	3.4
isopropanol	3.2 ₈	0.6 ₄	0.42 ₀	2.4 ₆ × 10 ⁸	1.9

(a) An error of ± 10% is predicted for these values.

TABLE XIII

EPR Parameters for Vanadyl Perchlorate in Water

Temp. °K	$\eta/T \times 10^3$	$\langle A \rangle$	OBS	$\tau \times 10^{11}$ sec		α' , gauss		β , gauss		γ , gauss		$-\delta \times 10^2$, gauss		α'' , gauss	
				OBS	CAL*	OBS	CAL	OBS	CAL	OBS	CAL	OBS	CAL	OBS	CAL
333.2	1.40	116.40	1.96295	2.35	2.20	2.95	2.96	1.28	1.30	0.340	0.340	0.800	0.725	11.15	11.30
323.2	1.70	116.00	1.96325	2.85	2.65	3.55	3.55	1.58	1.59	0.425	0.425	0.850	0.815	9.45	9.15
313.2	2.10	115.56	1.96330	3.10	3.25	3.60	3.60	1.74	1.78	0.535	0.535	0.900	0.830	8.20	7.50
303.2	2.65	115.12	1.96385	4.17	4.10	3.75	3.75	2.04	2.02	0.685	0.685	0.950	0.845	8.50	6.15
293.2	3.40	114.60	1.96448	4.80	5.30	5.95	6.00	2.40	2.45	0.760	0.770	1.150	1.175	8.60	5.45
283.2	4.60	114.20	1.96548	8.40	7.15	9.80	9.85	3.70	3.66	1.226	1.200	1.775	1.790	9.00	3.15
278.2	5.45	113.50	1.96670	8.80	8.35	10.70	10.73	4.50	4.64	1.450	1.460	1.915	1.900	9.50	2.80

* Hydrodynamic radius: 3.71A°.

TABLE XIV

EPR Parameters for Vanadyl acetylacetonate in Ethanol

Temp. °K	$\eta/T \times 10^3$	$\langle A \rangle$	$\langle g \rangle$	$\tau \times 10^{11}$, sec		α' , gauss		β , gauss		γ , gauss		$-\delta \times 10^2$, gauss		α'' , gauss	
				OBS	CAL*	OBS	CAL	OBS	CAL	OBS	CAL	OBS	CAL	OBS	CAL
353.2	1.10	102.22	1.96835	2.15	1.95	3.20	2.94	0.90	0.94	0.36	0.32	0.745	0.500	8.50	8.70
333.2	1.75	102.24	1.96767	2.68	2.60	3.80	4.10	1.10	1.25	0.46	0.48	0.860	0.810	7.60	7.15
313.2	2.65	101.91	1.96555	4.20	4.00	5.40	5.50	1.40	1.68	0.70	0.69	1.00	1.20	8.60	5.00
293.2	4.10	101.50	1.96630	5.75	6.15	7.82	7.90	2.00	2.24	1.04	1.03	1.55	1.43	11.00	3.60
273.2	6.50	100.06	1.96660	7.95	9.95	10.93	10.90	3.20	3.05	1.48	1.47	2.00	1.88	13.50	2.60
253.2	11.30	99.06	1.96770	16.40	17.00	12.45	12.50	3.64	3.52	1.68	1.68	2.00	2.09	16.00	2.20

* Hydrodynamic radius: 3.68A°.

TABLE XV
EPR Parameters for Vanadyl acetylacetonate in n-Propanol

Temp. °K	$\eta/T \times 10^3$ cp	$\langle A \rangle$ gauss	$\langle g \rangle$ OBS	$\tau \times 10^{11}$, sec		α' , gauss		β , gauss		γ , gauss		$-\delta \times 10^2$ gauss		α'' , gauss	
				OBS	CAL*	OBS	CAL	OBS	CAL	OBS	CAL	OBS	CAL	OBS	CAL
353.2	1.70	100.09	1.96795	2.90	2.80	3.60	4.00	0.80	1.30	0.365	0.465	0.71	0.73	7.90	7.70
343.2	2.20	101.05	1.96783	3.80	3.70	5.00	5.20	1.58	1.60	0.640	0.660	1.00	0.93	5.80	6.00
333.2	2.85	101.46	1.96780	4.30	4.60	5.20	6.80	1.68	2.08	0.860	0.880	1.06	1.20	5.10	4.90
323.2	3.30	102.15	1.96747	5.90	5.80	7.60	8.00	2.40	2.50	1.000	1.040	1.37	1.37	6.40	3.30
313.2	4.46	102.00	1.96735	7.70	7.30	11.20	10.40	3.53	3.28	1.520	1.450	1.89	1.82	7.25	2.65
303.2	5.68	102.10	1.96682	9.10	9.40	11.80	13.60	3.58	4.20	1.890	1.890	1.98	2.31	8.10	2.15
293.2	7.70	102.20	1.96679	14.60	12.50	19.10	18.40	5.62	5.72	2.59	2.59	3.09	3.11	9.10	1.30

* Hydrodynamic radius: 3.80A°.

TABLE XVI

EPR Parameters for Vanadyl acetylacetonate in Isopropanol

Temp. °K	$\eta/T \times 10^3$	$\langle A \rangle$		$\langle g \rangle$		$\tau \times 10^{11}$, sec		α' , gauss		β , gauss		γ , gauss		$-\delta \times 10^2$		α'' , gauss	
		OBS	OBS	OBS	OBS	OBS	CAL*	OBS	CAL	OBS	CAL	OBS	CAL	OBS	CAL	OBS	CAL
353.2	1.45	101.51	1.96957	2.10	2.15	3.00	2.90	0.490	0.800	0.355	0.360	0.40	0.67	8.40	7.85		
343.2	1.85	102.22	1.96853	3.25	2.75	4.05	3.95	1.420	1.160	0.498	0.480	0.83	0.79	5.85	6.25		
333.2	2.45	102.72	1.96825	3.55	3.55	4.40	4.45	1.660	1.540	0.523	0.533	0.70	0.87	4.50	5.15		
313.2	4.30	103.66	1.96750	6.20	6.30	5.55	5.65	1.950	2.090	0.921	0.930	1.34	1.05	5.00	3.25		
303.2	5.80	104.05	1.96715	8.25	8.50	8.25	8.20	3.300	2.950	1.320	1.230	1.40	1.67	6.55	2.70		
293.2	8.20	104.30	1.96685	10.05	12.00	12.30	12.30	4.130	4.240	1.650	1.660	1.83	2.03	10.00	1.75		

* Hydrodynamic radius: 3.28A°.

TABLE XVII

EPR Parameters for Vanadyl acetylacetonate in n-Butanol

Temp. °K	$\eta/T \times 10^3$ cp °K ⁻¹	$\langle A \rangle$ gauss	$\langle g \rangle$ OBS	$\tau \times 10^{11}$, sec		α' , gauss		β , gauss		γ , gauss		$-\delta \times 10^2$ gauss		α'' , gauss	
				OBS	CAL*	OBS	CAL	OBS	CAL	OBS	CAL	OBS	CAL	OBS	CAL
353.2	2.24	102.76	1.96500	3.80	3.70	4.55	4.85	1.69	1.72	0.56	0.55	0.88	0.92	7.3	4.3
343.2	2.71	102.50	1.96575	4.60	4.50	5.90	5.85	2.18	2.05	0.67	0.66	1.37	1.10	8.2	3.7
333.2	3.22	102.70	1.96650	6.15	5.75	7.05	6.90	2.43	2.41	0.92	0.80	1.24	1.28	10.5	3.4
323.2	4.33	102.17	1.96773	7.50	7.20	9.35	9.30	3.20	2.95	1.07	1.07	1.65	1.63	11.3	2.8
313.2	5.70	101.32	1.96865	9.20	9.45	10.00	10.00	3.48	3.47	1.32	1.38	1.64	1.74	13.8	2.4
303.2	7.60	100.04	1.97070	12.00	12.50	10.75	10.85	3.76	3.93	1.82	1.82	1.82	1.83	19.0	2.6
293.2	10.00	97.98	1.97245	21.00	15.00	11.35	11.35	4.32	4.35	2.38	2.42	1.85	1.86	24.3	2.0

* Hydrodynamic radius: 3.80A°.

TABLE XVIII

EPR Parameters for Vanadyl acetylacetonate in t-Butanol

Temp. °K	$\eta/T \times 10^3$	$\langle A \rangle$ OBS	$\langle g \rangle$ OBS	$\tau \times 10^{11}$, sec		α' , gauss		β , gauss		γ , gauss		$-\delta \times 10^2$ gauss		α'' , gauss	
				OBS	CAL*	OBS	CAL	OBS	CAL	OBS	CAL	OBS	CAL	OBS	CAL
353.2	1.55	106.00	1.96775	1.50	1.65	2.65	2.00	1.02	0.70	0.31	0.26	0.63	0.27	11.85	12.00
343.2	2.30	105.88	1.96865	2.40	2.70	2.63	2.65	1.01	1.01	0.30	0.90	0.62	0.60	19.15	9.05
333.2	3.11	105.62	1.96875	3.20	3.40	2.68	3.30	1.02	1.32	0.32	0.54	0.62	0.72	9.40	7.00
323.2	4.50	105.16	1.96900	4.20	4.80	5.00	4.20	1.75	1.72	0.62	0.78	0.96	0.88	10.75	4.60
313.2	7.85	104.70	1.96985	7.20	7.30	5.25	6.10	1.92	2.03	1.19	1.19	1.00	1.16	11.85	4.15
303.2	10.90	103.40	1.97140	11.10	11.50	12.80	13.10	4.54	4.34	1.75	1.91	2.00	2.08	12.50	1.60
293.2	17.10	102.80	1.97175	17.80	19.40	22.40	23.10	7.80	7.90	3.09	2.98	3.08	3.26	14.00	0.90

* Hydrodynamic radius: 3.28A°.

TABLE XIX

EPR Parameters for Vanadyl acetylacetonate in Trifluoroethanol

Temp. $\eta/Tx10^3$ - <A>	OBS	$\tau \times 10^{11}$, sec		α' , gauss		β , gauss		γ , gauss		$-\delta \times 10^2$, gauss		α'' , gauss			
		OBS	CAL*	OBS	CAL	OBS	CAL	OBS	CAL	OBS	CAL	OBS	CAL		
$\circ K$	cp $^\circ K^{-1}$ gauss	<g>													
353.2	1.10	99.17	1.96790	1.70	1.60	2.80	2.70	1.06	1.00	0.32	0.30	0.63	0.52	9.50	9.90
343.2	1.49	99.88	1.96810	2.55	2.20	3.30	3.50	1.28	1.29	0.38	0.40	0.70	0.68	7.25	7.75
333.2	2.05	100.60	1.96834	3.15	3.00	5.30	4.90	1.96	1.68	0.68	0.53	1.00	0.87	5.30	5.40
323.2	2.85	101.54	1.96875	4.65	4.30	5.70	5.80	2.11	2.14	0.74	0.73	1.04	1.07	8.10	4.20
313.2	4.00	101.96	1.96895	5.75	5.90	6.60	6.70	2.38	2.42	0.86	0.88	1.17	1.20	9.50	3.70
303.2	5.80	102.12	1.96905	8.65	8.75	8.60	8.70	3.00	3.10	1.13	1.13	1.45	1.48	9.90	2.85
293.2	8.65	102.20	1.96960	12.50	12.90	13.60	13.60	4.70	4.60	1.80	1.80	2.15	2.17	9.95	1.80

* Hydrodynamic radius: 3.66A $^\circ$.

TABLE XX

EPR Parameters for Vanadyl acetylacetonate in Trichloroethanol

Temp. °K	$\eta/T \times 10^3$	$\langle A \rangle$	OBS	$\langle g \rangle$	OBS	$\tau \times 10^{-11}$, sec		α' , gauss		β , gauss		γ , gauss		$-\delta \times 10^2$, gauss		α'' , gauss	
						OBS	CAL*	OBS	CAL	OBS	CAL	OBS	CAL	OBS	CAL	OBS	CAL
373.2	1.85	104.32	1.96820	2.90	3.00	5.30	5.30	1.85	1.75	0.68	0.68	1.02	0.96	5.45	4.40		
363.2	2.80	104.22	1.96905	4.50	4.70	6.90	7.50	2.55	2.45	0.97	0.97	1.33	1.30	6.05	3.00		
353.2	4.25	103.30	1.96975	7.80	7.70	9.80	10.20	3.30	3.45	1.31	1.28	1.68	1.68	6.60	2.30		
343.2	6.65	101.00	1.97200	11.50	11.00	13.80	14.00	5.55	5.45	1.40	1.42	2.16	2.24	7.25	1.50		
333.2	11.70	99.00	1.97447	16.70	17.50	20.30	19.70	7.40	7.40	2.68	2.24	3.12	3.11	7.55	1.05		
323.2	17.80	97.10	1.97453	27.0	29.5	28.20	29.90	9.95	9.85	3.75	3.80	4.44	4.52	7.80	0.80		

* Hydrodynamic radius: 3.80A°.

TABLE XXI

EPR Parameters for Vanadyl trifluoroacetylacetonate in Methanol

Temp. °K	$\eta/T \times 10^3$	$\langle A \rangle$	OBS	$\langle g \rangle$	$\tau \times 10^{11}$, sec		α' , gauss		β , gauss		γ , gauss		$-\delta \times 10^2$ gauss		α'' , gauss		
					OBS	CAL*	OBS	CAL	OBS	CAL	OBS	CAL	OBS	CAL	OBS	CAL	OBS
333.2	1.13	105.00	1.97055	6.15	6.00	7.60	7.40	1.77	1.77	1.05	0.96	1.37	1.37	1.37	1.37	2.40	2.10
318.2	1.34	106.40	1.96900	6.80	7.00	8.60	8.20	1.84	1.84	1.14	1.10	1.50	1.50	1.47	1.47	2.55	1.90
308.2	1.55	107.60	1.96745	8.50	8.30	8.30	8.70	1.97	1.97	1.16	1.20	1.59	1.59	1.59	1.59	2.50	2.10
298.2	1.85	107.40	1.96625	9.40	9.60	9.30	9.10	2.05	2.06	1.25	1.28	1.72	1.72	1.66	1.66	2.55	2.00
283.2	2.40	107.10	1.96635	9.30	12.50	9.80	9.80	2.05	2.06	1.32	1.35	1.78	1.78	1.79	1.79	3.40	1.90
263.2	3.70	106.90	1.96700	11.30	19.50	11.30	11.30	2.25	2.26	1.56	1.57	1.26	1.26	1.26	1.26	5.05	1.55
243.2	5.85	105.95	1.96800	13.70	30.00	14.20	14.20	3.02	3.00	1.95	1.95	2.50	2.50	2.48	2.48	6.25	1.30

* Hydrodynamic radius: 5.6A°.

coupling constants and g-values vary in a regular way with temperature as observed by Wilson and Kivelson (44) for vanadyl acetylacetonate in toluene. A representative temperature dependence of these parameters is shown in Figures (28) and (29) for vanadyl perchlorate in water. The same view is taken here as by Wilson and Kivelson in that the variation of these parameters is a reflection of the variation in interaction between the solvent and complex as a function of temperature. The observed τ_R 's are the final values obtained from the iterative procedure and the calculated τ_R 's are the values obtained from the Debye formula when a suitable hydrodynamic radius (r) and the temperature dependence of the viscosity are used in equation (37). The calculated τ_R 's fall within a $\pm 10\%$ error of the observed τ_R 's. The hydrodynamic radii are expected to have a $\pm 10\%$ error on them because of the errors on τ_R , the viscosity, and the temperature. The correlation times were found to obey the Debye formula fairly well except for vanadyl trifluoroacetylacetonate in methanol; this system seems anomalous because of the large hydrodynamic radius necessary to explain the correlation time at high temperatures and because of the large deviation between predicted and observed values at low temperatures (Table XXI). It appears that due to the high electronegativity of the fluorine in the trifluoroacetylacetonate ligand association, probably through hydrogen bonding, occurs with the solvent methanol. The correlation time will then

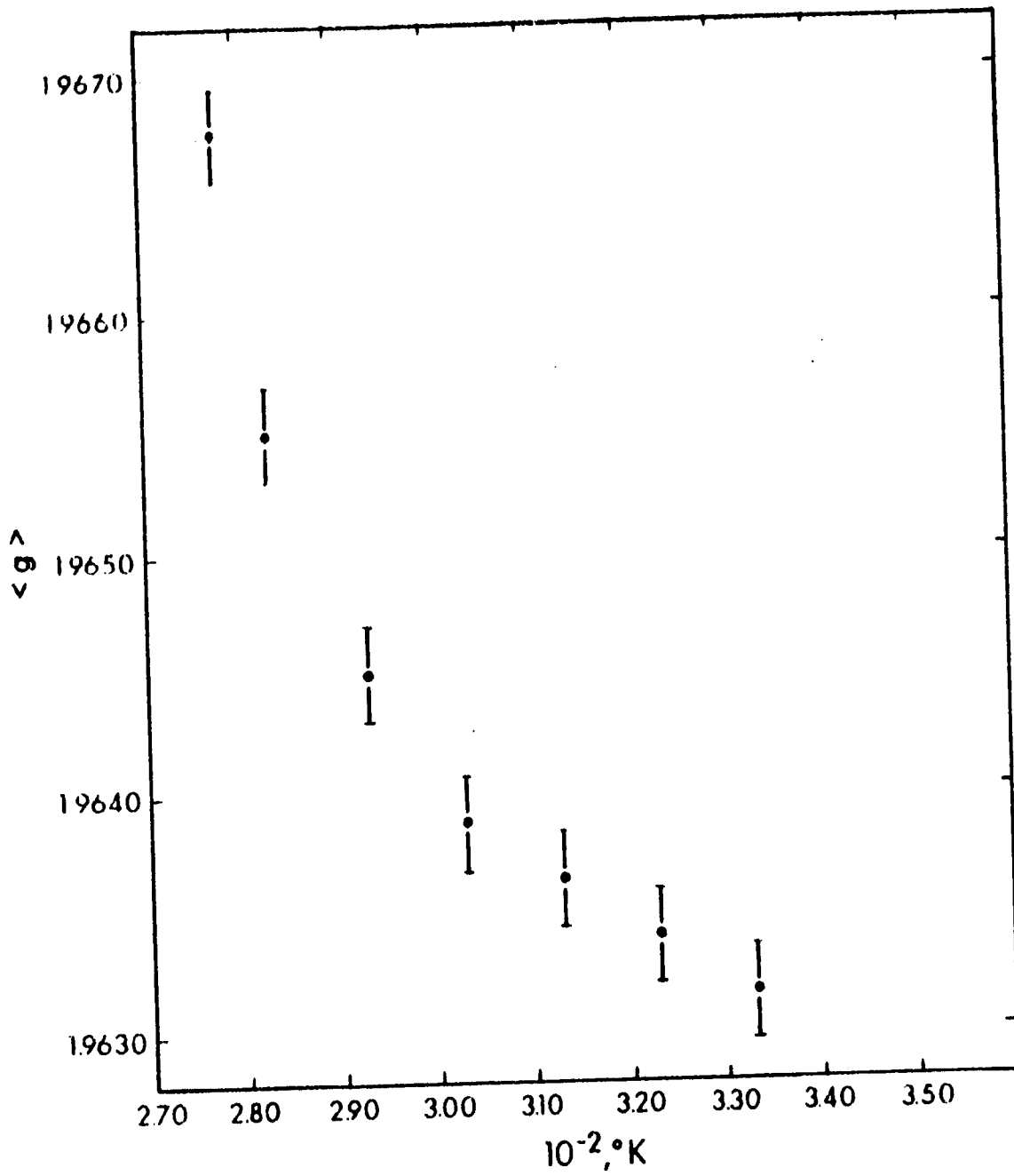


Figure 28: Temperature dependence of the average g -value for a solution of 10^{-3} molal vanadyl perchlorate in water.

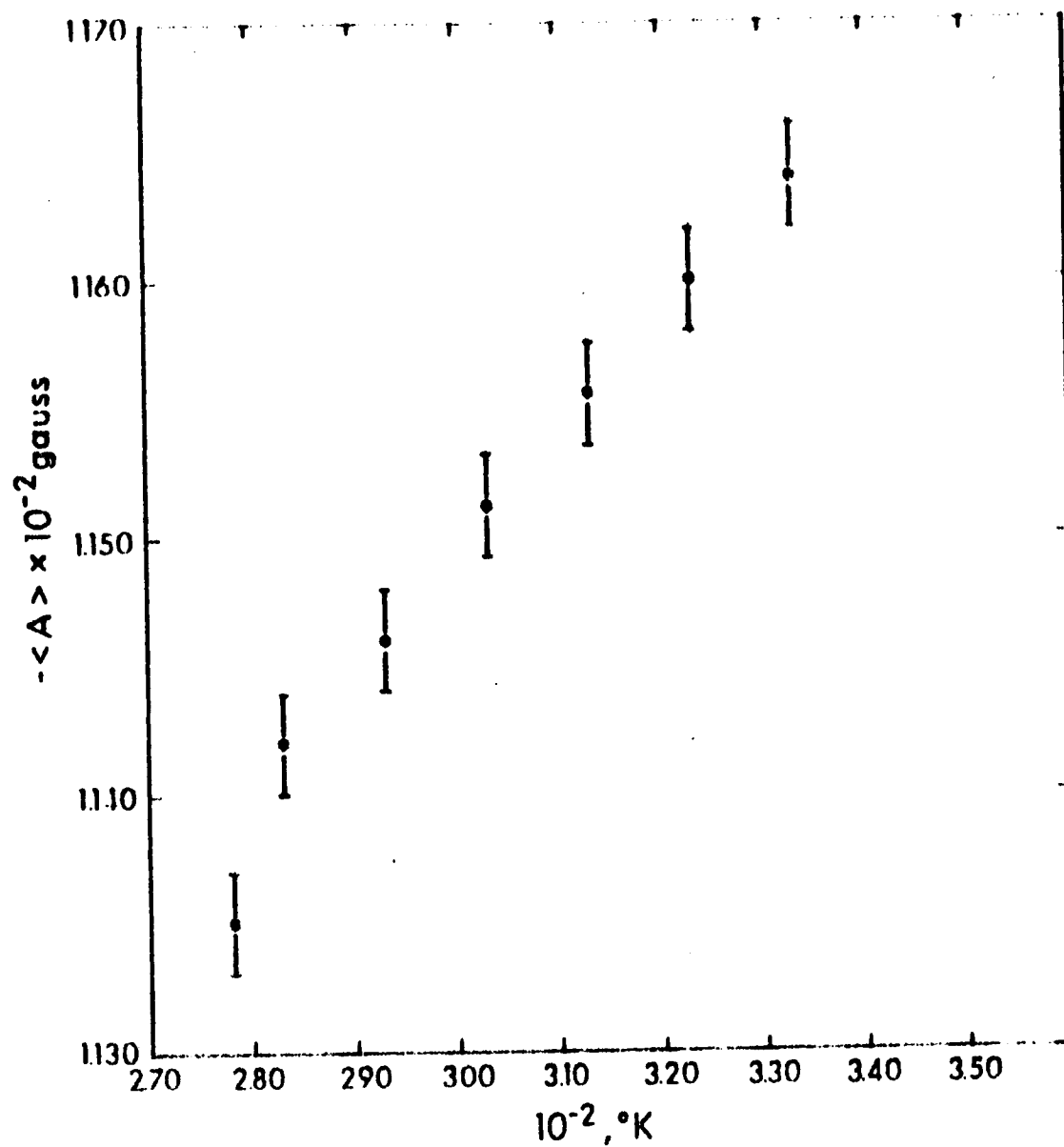


Figure 29: Temperature dependence of the average hyperfine coupling constant of a solution of 10^{-3} molal vanadyl perchlorate in water.

depend strongly on the nature of the associated complex and not necessarily on the hydrodynamic radius of the complex.

It is significant to note that the hydrodynamic radii for $\text{VO}(\text{acac})_2$ in the alcoholic solvents (Tables XIII - XX) does not exceed 3.80\AA . These radii are consistent with the proposal by McClung and Kivelson (96) that $\text{VO}(\text{acac})_2$ has an effective hydrodynamic radius of $r_0 = 3.8 \pm 0.5\text{\AA}$ as determined from diffusion experiments and that:

$$r = \kappa r_0^{1/3} \quad (101)$$

where $0 < \kappa < 1$. Values for r and κ are given in Table XII. κ is a measure of the ratio of the intermolecular torques on the solute molecules to the intermolecular forces on the solvent molecules. It should be emphasized that since $\kappa < 1$ it cannot be associated with a solvation effect which would increase r_0 rather than decrease it as experimentally observed. McClung and Kivelson propose that κ will increase with increased anisotropy of the solvent molecules for a given solute. The results given above appear to substantiate this proposal, that is, *t*-butanol and isopropanol have lower κ 's than the other more anisotropic alcohols. For the other alcohols $r = r_0$ within experimental error; therefore, it may be concluded that the Debye theory applies reasonably well to the $\text{VO}(\text{acac})_2$ complex in the alcohol solvents.

Turning now to the residual line width mentioned above; it is shown by a representative plot of residual line width versus T/η $^{\circ}\text{K}(\text{cp})^{-1}$ for the vanadyl perchlorate-water system (Figure 30) that a spin-rotational mechanism (41) accounts reasonably well for this line width at high temperatures. The line width contribution due to the spin-rotational mechanism is quantitatively expressed by equation (36) and discussed in Chapter I, section 3. The interaction distance required in this expression was set equal to r and all the other parameters were calculated in the computer programme. However, as the temperature was lowered the spin-rotational mechanism no longer adequately explained the residual line width. It was initially assumed that this excess residual line width was due to an inner sphere dipolar interaction between the protons on the rapidly exchanging molecule trans to the vanadyl oxygen and the unpaired electron. However, when the dipolar part of equation (31) with interaction distances similar to the $\text{VO}(\text{acac})_2$ methanol system was applied to the residual line width the correlation times obtained (approx. 10^{-4} sec) were unreasonably long. Therefore, it appears that the excess residual line width is due to some intramolecular interaction between the unpaired electron and the vanadium nucleus. Kivelson mentions the nuclear-electron dipolar interaction but neglects it in his theory for predicting line widths. However, if the dipolar

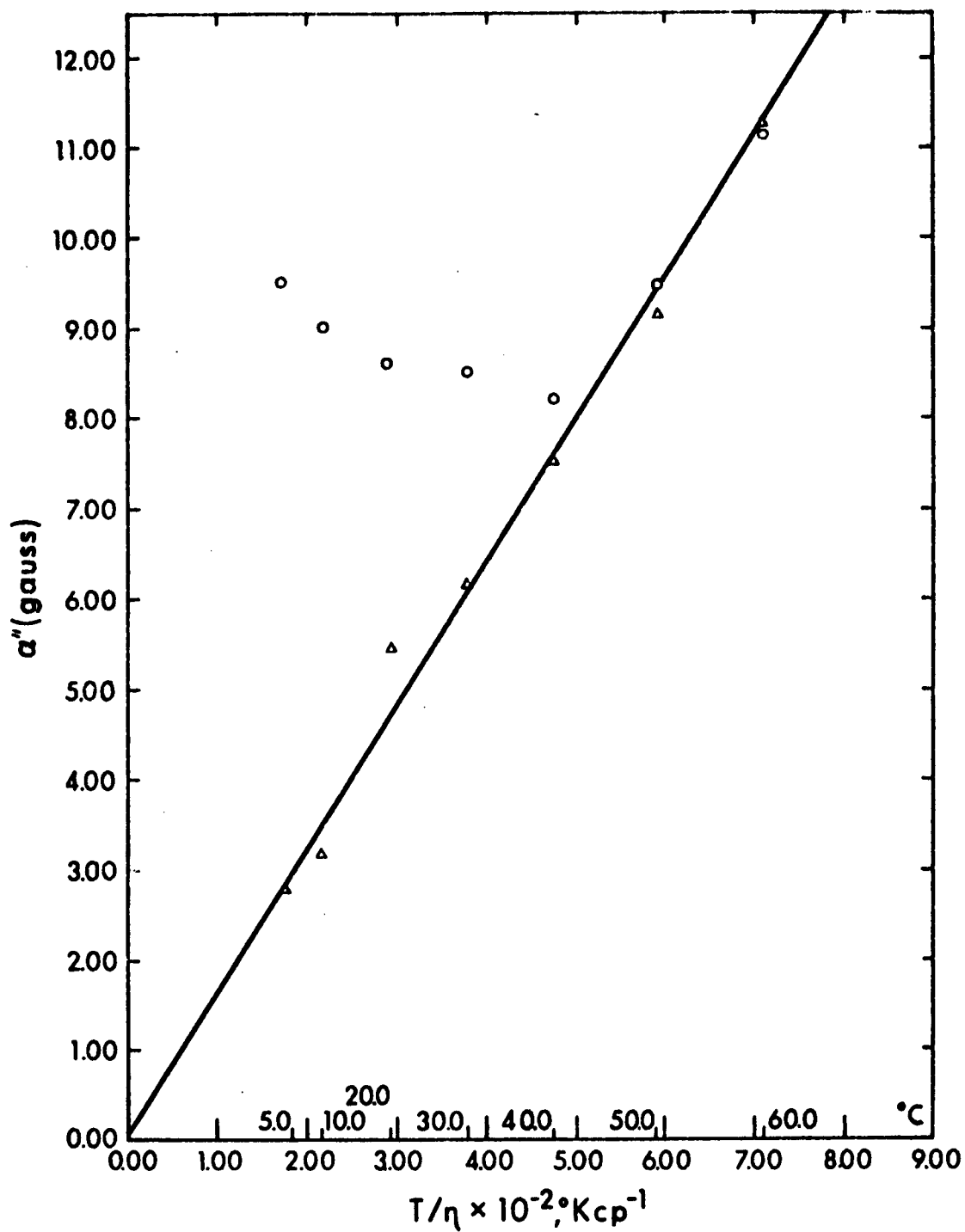


Figure 30: Temperature dependence of the residual line width for a solution of 10^{-3} molal vanadyl perchlorate in water. (Δ - theoretical spin rotational contribution, \circ - experimental points.)

part of equation (31) is used to interpret this intramolecular interaction where γ_I is now the magnetogyric ratio of the vanadium nucleus and τ_C is the correlation time for the nuclear-electron interaction, then an exponential temperature dependence would be expected for the excess residual line width. It was found that a semi-logarithmic plot of the excess residual line width versus $(T^\circ K)^{-1}$ did give a straight line within an estimated $\pm 10\%$ error on the points for all the systems except ethanol. The temperature dependences were all equal to about 6 kcal mole^{-1} which indicates that the same process is being observed in all systems. To quantitatively analyze the results for a dipolar interaction it was assumed that $\tau_C \approx \tau_S \approx 10^{-10}$ sec since this interaction may be associated with the relaxation of the electron. The resulting interaction distances (r_{DD}) are given in Table XII and seem reasonable if r_{DD} is taken as the average distance between the vanadium nucleus and the electron. Slight variations in r_{DD} may be due to the interaction of solvent molecules trans to the vanadyl oxygen which could cause a variation in the average distance of the electron from the vanadium nucleus. The interaction process may equally well be interpreted by a hyperfine contact interaction where the hyperfine coupling constant can be obtained from the isotropic EPR spectrum; these coupling constants are given at $20^\circ C$ in Table XII. The corresponding correlation times at $20^\circ C$ are also given and

are of a reasonable magnitude to be assigned to the electron relaxation time. Unfortunately, the large temperature dependence of the excess residual line width seems inconsistent with these two relaxation processes.

It is conceivable that the excess residual line width is due to a hyperfine interaction process between the unpaired electron and an exchanging ligand trans to the vanadyl oxygen; however, it was not possible to obtain the hyperfine coupling constant for this interaction from the EPR study. This latter relaxation process is more consistent with the large temperature dependence if the interaction correlation time is the ligand exchange time. The difficulty here, however, is that the coupling constant will obviously be large enough to give an appreciable shift of the bulk solvent NMR resonances if a ligand exchange rate of approximately 10^{10} sec^{-1} is assumed. This shift was not observed. It is possible that the residual line width is due to a variation in super hyperfine coupling which has not been resolved, as mentioned by Wilson and Kivelson (26); however, the temperature dependence of this interaction would be expected to parallel the solvent viscosity for all the systems. Therefore, it appears difficult to identify the cause of the excess residual line width explicitly.

The above discussion on the residual line width can also be applied to the systems given in Table X. Results for an intramolecular relaxation process governing the excess

residual line width are given in Table XXII. κ could not be obtained for these complexes because the effective radii, r_o , from diffusion experiments are not available.

The general conclusions from this EPR study are that Kivelson's theory quantitatively predicts the observed hyperfine line widths within the experimental error. The basis for this conclusion is the good agreement between calculated and observed coefficients in equation (35) as a function of temperature and the ability of the theoretical coefficients to predict the original observed EPR hyperfine lines. However, it is necessary to propose relaxation mechanisms in addition to spin-rotational relaxation to explain the total residual line width (α''). The exact nature of these additional mechanisms cannot be definitely established by the results from this study.

TABLE XXII

Parameters obtained from the excess residual EPR line widths for the vanadyl ion-

solvent systems @ 25°C

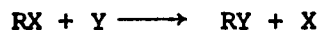
Compound	Solvent (a)	$r_{DD}, \text{\AA}$	A/h, cps	τ_C, sec
$\text{VO}(\text{BF}_4)_2$	DMSO	0.38 ₁	$2.7_4 \times 10^8$	2.8×10^{-10}
$\text{VO}(\text{BF}_4)_2$	TMPA	0.37 ₅	$2.8_4 \times 10^8$	2.7×10^{-10}
$\text{VO}(\text{BF}_4)_2$	TMPI	0.36 ₀	$2.9_3 \times 10^8$	3.3×10^{-10}
$\text{VO}(\text{BF}_4)_2$	AN	0.40 ₇	$2.8_3 \times 10^8$	1.3×10^{-10}
$\text{VO}(\text{ClO}_4)_2$	DMF	0.36 ₄	$2.7_0 \times 10^8$	3.5×10^{-10}
$\text{VO}(\text{ClO}_4)_2$	MEOH	0.39 ₀	$2.7_7 \times 10^8$	2.3×10^{-10}
$\text{VO}(\text{ClO}_4)_2$	H ₂ O	0.36 ₄	$2.7_7 \times 10^8$	6.7×10^{-11}

(a) Solvent abbreviations are given in footnote (a) of Table X.

CHAPTER V. GENERAL DISCUSSION ON LIGAND EXCHANGE
ON TRANSITION METAL IONS

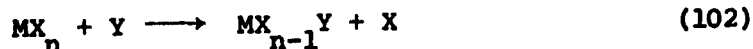
The primary purpose of this work was to determine the rates, activation enthalpies, and activation entropies of chemical reactions with the ultimate goal of obtaining mechanistic information about these reactions. This mechanistic information can be categorized into two types: stoichiometric and intimate (111). An analysis of the mechanistic information in terms of a stoichiometric mechanism involves breaking the reaction into individual elementary steps; whereas, analysis in terms of an intimate mechanism involves consideration of the elementary steps from the point of view of bond breaking or making, electron densities, group polarizabilities, etc. The view held here is that an analysis of the mechanistic information according to the latter category yields more fruitful information about the actual nature of chemical reactions.

There have been several attempts at obtaining mechanistic information in organic chemistry in both aqueous and mixed solvent systems. Hughes and Ingold (112, 113) proposed a qualitative theory for the effects of solvent on reaction rates and Amis (114) has attacked the problem from a more quantitative viewpoint. The organic chemical reactions of interest have been of the type:



where RX and Y are reactants which, in terms of transition state theory, go through an activated complex to give products represented by RY and X. The qualitative and quantitative theories of the factors which affect the reaction mechanism have primarily been concerned with the degree of bond breaking and making in the transition state (S_N1 or S_N2 type mechanisms), charge separation, and the solvating powers of the solvent.

This interest has been carried over into inorganic reactions of the type:



where M is the transition metal with n ligands (X) coordinating in the inner sphere and Y is a substituting ligand which is usually the solvent. It has been shown that both the qualitative and quantitative arguments proposed for the organic systems can be applied with slight modifications to inorganic reactions (5) where the transition metal ion is inert. Typical inert metal ions are cobalt(III), chromium(III), platinum(II) and palladium(II).

In principle similar arguments should be applicable to more labile ligand exchange reactions. Such reactions have been most extensively studied for cobalt(II) and nickel(II) and comparisons are now possible with the vanadyl ion. Results in this general area have been reviewed recently by Langford and Stengle (4).

An understanding of the ligand exchange rates in labile systems requires a knowledge of the effect of changing the metal ion as well as changing the exchanging ligand. Crystal field theory has been used in several attempts to quantitatively explain the former factor. Basolo and Pearson (5) were the first to propose that the relative exchange rates may be explained by the differences in loss of crystal field stabilization on going from the octahedral complex into the transition state for the exchange reaction. This theory predicts qualitatively that the activation enthalpy for exchange should parallel the Dq value and quantitatively that in the case of $Ni^{2+}(d^8)$ there should be a destabilization of $1.8 Dq$ on formation of the most stable transition state the "octahedral wedge." It is apparent from the results for nickel(II) in Table XXIII that even the qualitative predictions of this theory are not followed. For instance the Dq values for CH_3OH , DMF and DMSO are all lower than that of water yet ΔH^\ddagger for water exchange is lower than for the other three solvents.

More recently Spees, Perumareddi and Adamson (101) have proposed a significant variation of the previous crystal field theory, in which they assume that spin pairing of the electrons occurs whenever possible on formation of the transition state. This theory was applied with reasonable success to the aquation reactions of chromium(III) and cobalt(III). However, in this

work attempts to apply the theory to the exchange reactions of nickel(II) and cobalt(II) have been a notable failure. The predicted activation energies are at least a factor of 2 and, with apparently reasonable assumptions, as much as a factor of 4 too large. The nickel(II) methanol system may be used as an example. Spees *et al* predict for a high spin d^8 system that the crystal field contribution to the activation energy for the most favourable intermediate is $(-2.84 Dq + 12B + 3C)$; B and C are the Racah parameters. Interpretation of the visible spectrum of $Ni(CH_3OH)_6^{2+}$ following the method outlined by Lever (102) gives $Dq = 837 \text{ cm}^{-1}$, $B = 949 \text{ cm}^{-1}$. The activation energy is then $(9020 + 3C) \text{ cm}^{-1}$ or $(25.8 + 3C) \text{ kcal mole}^{-1}$. Without considering the term in C the activation enthalpy is already $10 \text{ kcal mole}^{-1}$ greater than the observed value, and if the usual assumption that $C = 4B$ is used then the activation energy is $58 \text{ kcal mole}^{-1}$.

It is apparent that electron pairing costs much more energy than is gained back by increased crystal field stabilization in the transition state and, therefore, no electron pairing is likely to occur. This factor was not obvious in the cases considered by Spees *et al* because the cobalt(III) complexes are completely spin paired in the reactant and in the case of chromium(III) the larger Dq values for the +3 ion were sufficient to cancel the energy change for interelectronic

repulsion. In fact it seems questionable if the original proposal of spin pairing in the transition state can be justified since $10 Dq$ must be less than the pairing energy if the reactant is high spin and the d orbitals in the transition state are always separated by less than $10 Dq$, therefore the electrons should remain unpaired.

More recently Breitschwerdt (103) has revised the calculations of Basolo and Pearson by using a more complete quantum mechanical treatment. The results show the same trends with different d electronic configurations as those of Basolo and Pearson but the absolute value of the crystal field contributions to the activation energy (ΔH_{CF}^\ddagger) are somewhat different. For a C_{4v} square pyramidal transition state, ΔH_{CF}^\ddagger for iron(II), cobalt(II), nickel(II) and manganese(II) are 2.87 Dq, 3.65 Dq, 4.80 Dq and 2.80 Dq, respectively. Breitschwerdt has found that these values give good quantitative predictions of the activation enthalpy for water exchange. However, this version of the crystal field theory also predicts that the activation energy for solvent exchange should parallel the spectroscopic Dq value and as already noted the opposite trend seems to be more generally observed.

The above discussion in this chapter and similar arguments in previous work have emphasized the importance of crystal field effects without paying any heed to the possibility of reactant and transition state solvation. The latter factor

is well recognized but has proven very difficult to calculate because it is always necessary to take the difference between two relatively large solvation energies. It seems reasonable to assume that the total activation energy (ΔH^\ddagger) is made up of a crystal field contribution (ΔH^\ddagger_{CF}) and a solvation contribution (ΔH^\ddagger_{sol}) so that

$$\Delta H^\ddagger = \Delta H^\ddagger_{CF} + \Delta H^\ddagger_{sol} \quad (103)$$

ΔH^\ddagger_{sol} should be a constant for a given solvent complexed to ions of the same charge and exchanging by the same mechanism. If this assumption is correct then only the differences in activation energies for the different metal ions can be predicted by crystal field theory. If ΔH^\ddagger for solvent exchange on nickel(II) is taken as an arbitrary standard then ΔH^\ddagger for other metal ions may be calculated from the value for nickel(II) (Table XXIII) and the predicted differences in crystal field contributions. For example, using the crystal field contributions given by Breitschwerdt (103)

$$(\Delta H^\ddagger)_{Co^{2+}}^{Calc} = (\Delta H^\ddagger)_{Ni^{2+}}^{OBS} + (\Delta H^\ddagger)_{CF Co^{2+}} - (\Delta H^\ddagger)_{CF Ni^{2+}} \quad (104)$$

$$= (\Delta H^\ddagger)_{Ni^{2+}}^{OBS} + 3.65 (Dq)_{Co^{2+}} - 4.80 (Dq)_{Ni^{2+}} \quad (105)$$

Activation enthalpies for cobalt(II) are compared in Table XXIV.

The agreement between calculated and observed values for $(\Delta H^\ddagger)_{Co^{2+}}$

are generally good except for the ammonia system. It was proposed by Glaeser, Dodgen and Hunt (104) that ammonia exchange on cobalt(II) might involve an octahedral-tetrahedral equilibrium and the disagreement found here could be rationalized on this basis. Since the predicted activation enthalpy is lower than the value found it is also necessary to assume that the octahedral-tetrahedral mechanism in this system has a more favorable entropy by about 15 e.u. than the normal exchange mechanism.

As noted previously Breitschwerdt (103) has obtained good agreement between calculated and observed activation energies for water exchange of a number of divalent first row transition metal ions. There is unfortunately very little data for this series of ions in nonaqueous solvents. The recently reported activation enthalpy of 7.4 kcal mole⁻¹ for methanol exchange on manganese(II) (105) is not in good agreement with the predicted value of 11 kcal mole⁻¹. However, the calculated and observed activation enthalpies of 11.3 and 12.0 kcal mole⁻¹ (106), respectively, for the iron(II) methanol system are in reasonable agreement. The calculation in the latter two systems has assumed that D_q for methanol is the same for nickel(II), manganese(II) and iron(II).

It is clear that more experimental values are needed in order to determine if the predictions made here are generally

correct. Assuming the latter is true, it would be very useful to determine the values of $(\Delta H_{sol}^\ddagger)$ and hopefully correlate them with the physical properties of the solvents (Table XXVI). Calculation of $(\Delta H_{sol}^\ddagger)$ requires an absolute knowledge of (ΔH_{CF}^\ddagger) , whereas the activation energies calculated in this work depend only on the difference in crystal field contributions. In any case it appears that $(\Delta H_{sol}^\ddagger)$ decreases in the order $CH_3OH > DMF > DMSO > H_2O > CH_3CN \approx NH_3$. This order, of course, assumes a similar exchange mechanism in all solvents.

The above procedure should be able to predict the exchange enthalpies for solvent exchange on the vanadyl ion as well (Table XXV). However, $(\Delta H_{VO^{2+}}^\ddagger)_{Calc}$ is consistently too high, except for water exchange, regardless of the mechanism of exchange and the $(\Delta H_{CF Ni^{2+}}^\ddagger)$ chosen from Breitschwerdt's results. Therefore, it was concluded that nickel(II) does not provide a good model for comparison to the vanadyl ion in exchange processes. It should be noted, however, that a C_{4V} transition state for water exchange on the vanadyl ion predicts an activation enthalpy of $12.7 \text{ kcal mole}^{-1}$ compared to an observed value of $13.3 \text{ kcal mole}^{-1}$ which suggests that in this case the exchange mechanism is similar to that on nickel(II) and cobalt(II). A small activation entropy is also consistent with this proposal. Since the activation enthalpies (Table XXV) could not be predicted for exchange of other ligands on vanadyl it may be inferred that exchange proceeds

by a different mechanism on this metal ion. From the characteristics of the vanadyl ion observed in this study it appears reasonable that an S_N2 exchange mechanism might be operative. This mechanism may be most easily visualized by considering one rapidly exchanging ligand, trans to the vanadyl oxygen, which allows easy access of the bulk solvent to the planar positions via a S_N2 exchange process. The large negative entropies which do not parallel those of cobalt(II) and nickel(II) also suggest S_N2 exchange processes on the vanadyl ion. Further studies on other transition metal ions are obviously needed to establish a more definite basis for the differences between S_N1 and S_N2 type exchange mechanisms.

TABLE XXIII

Kinetic exchange parameters and spectroscopic parameters
for nickel(II) in various solvents

Complex	k_r, sec^{-1} @ 25°C	$\Delta H^\ddagger, \text{kcal}$ mole^{-1}	$\Delta S^\ddagger, \text{e.u.}$	Dq, cm^{-1}	B, cm^{-1}
$\text{Ni}(\text{H}_2\text{O})_6^{2+}$	$2.7_0 \times 10^4$	11.6 ± 0.5	0.6	870	905
$\text{Ni}(\text{CH}_3\text{OH})_6^{2+}$	$1.0_0 \times 10^3$	15.8	8.0	837	949
$\text{Ni}(\text{DMF})_6^{2+}$	$3.8_0 \times 10^3$	15.0 ± 0.5	8.0 ± 2.0	812	949
$\text{Ni}(\text{CH}_3\text{CN})_6^{2+}$	$3.9_0 \times 10^3$	10.9	-8.8	1104	832
$\text{Ni}(\text{DMSO})_6^{2+}$	$5.2_0 \times 10^3$	12.1 ± 0.3	-1.3 ± 0.5	773	923
$\text{Ni}(\text{TMPA})_6^{2+}$	$>1.8_5 \times 10^2$				
$\text{Ni}(\text{NH}_3)_6^{2+}$	$1.0_0 \times 10^5$	11.0 ± 1.0	2.0 ± 3.0	1095	818

TABLE XXIV

Kinetic exchange parameters and spectroscopic parameters for cobalt(II) in various solvents

Complex	k_r, sec^{-1} @ 25°C	$\Delta H^\ddagger, \text{kcal mole}^{-1}$	$\Delta S^\ddagger, \text{e.u.}$	Dq, cm^{-1}	B, cm^{-1}	$(\Delta H^\ddagger)_{\text{Co}^{2+}}$	Calc
$\text{Co}(\text{H}_2\text{O})_6^{2+}$	$1.1_3 \times 10^6$	8.0	-4.1	861	870		8.0
$\text{Co}(\text{CH}_3\text{OH})_6^{2+}$	$1.8_0 \times 10^4$	13.8	7.2	875	875		13.4
$\text{Co}(\text{DMF})_6^{2+}$	$4.0_0 \times 10^5$	13.6 ± 0.5	12.6 ± 2.0	880	885		13.0
$\text{Co}(\text{CH}_3\text{CN})_6^{2+}$	$1.4_0 \times 10^5$	8.1	-7.5	1100	810		7.2
$\text{Co}(\text{DMSO})_6^{2+}$	$>1.5_3 \times 10^4$						
$\text{Co}(\text{TMPA})_6^{2+}$	$>6.3_0 \times 10^3$						
$\text{Co}(\text{TMPA})_6^{2+}$	$>6.5_5 \times 10^3$						
$\text{Co}(\text{NH}_3)_6^{2+}$	$>7.2_0 \times 10^6$	11.2 ± 0.4	10.2 ± 2.0	1080	794		7.3

TABLE XXV

Kinetic exchange parameters and spectroscopic parameters
for the vanadyl ion in various solvents

Complex	k_x, sec^{-1} @ 25°C	$\Delta H^\ddagger, \text{kcal}$ mole^{-1}	$\Delta S^\ddagger, \text{e. u.}$	Dq, cm^{-1}
$\text{VO}(\text{H}_2\text{O})_5^{2+}$	$7.4_0 \times 10^2$	13.3	-1.5	1600
$\text{VO}(\text{CH}_3\text{OH})_5^{2+}$	$5.6_5 \times 10^2$	$9.4_6 \pm 0.68$	-14.2 ± 2.1	1550
$\text{VO}(\text{DMF})_5^{2+}$	$7.6_5 \times 10^2$	$6.7_7 \pm 1.94$	22.6 ± 5.7	1540
$\text{VO}(\text{CH}_3\text{CN})_5^{2+}$	$2.9_7 \times 10^3$	$6.6_5 \pm 0.29$	-20.3 ± 0.9	1480
$\text{VO}(\text{DMSO})_5^{2+}$	$>1.5_2 \times 10^3$			1430
$\text{VO}(\text{TMPA})_5^{2+}$	$>0.8_4 \times 10^3$			1390
$\text{VO}(\text{TMPI})_5^{2+}$	$<0.3_5 \times 10^3$			1450

TABLE XXVI

Physical properties for some selected solvents

Solvent	Dipole Moment (Debeyes)	Dielectric Constant	Viscosity cp	Density gm/cc
H ₂ O	1.85 (107)	78.54 (107)	1.002 (107)	1.000 (107)
CH ₃ OH	1.70 (107)	32.63 (107)	0.547 (107)	0.795 (107)
DMF	3.82 (110)	36.71 (109)	0.800 (109)	0.945 (107)
CH ₃ CN	3.84 (110)	36.20 (108)	0.345 (108)	0.783 (107)
DMSO	4.30 (110)	46.60 (108)	1.960 (108)	1.101 (107)
TMPA			2.010 (107)	1.200 (107)
TMPI	1.48 (107)		0.570 (107)	1.052 (107)
NH ₃	1.46 (107)	16.9 (107)	0.135 (108)	0.603 (108)

References are given in brackets in the table.

REFERENCES

1. F. Basolo and R.G. Pearson, "*Advances in Inorganic and Radiochemistry*", ed. Emeléus and Sharpe, Academic Press Inc., New York, Volume III (1961).
2. R.G. Wilkins, *Quart. Rev.*, 16, 316 (1962).
3. M. Eigen and R.G. Wilkins, *Advan. Chem. Ser.*, 49, 55 (1965).
4. T.R. Stengle and C.H. Langford, *Coordin. Chem. Rev.*, 2, 349 (1967).
5. F. Basolo and R.G. Pearson, "*Mechanisms of Inorganic Reactions*", 2nd ed., John Wiley and Sons Inc., New York, (1967).
6. N.A. Matwiyoff, *Inorg. Chem.*, 5, 788 (1966).
7. D.K. Ravage, T.R. Stengle and C.H. Langford, *Inorg. Chem.*, 6, 1252 (1967).
8. T.J. Swift and R.E. Connick, *J. Chem. Phys.*, 37, 307 (1962).
See erratum *J. Chem. Phys.*, 41, 2553 (1964).
9. Z. Luz and S. Meiboom, *J. Chem. Phys.*, 40, 1058 (1964).
10. Z. Luz and S. Meiboom, *J. Chem. Phys.*, 40, 1066 (1964).
11. Z. Luz, *J. Chem. Phys.*, 41, 1748 (1964).
12. N.A. Matwiyoff and S.V. Hooker, *Inorg. Chem.*, 6, 1127 (1967).
13. J.S. Babiec, C.H. Langford and T.R. Stengle, *Inorg. Chem.*, 5, 1363 (1966).

14. H.H. Glaeser, H.W. Dodgen and J.P. Hunt, *Inorg. Chem.*, 4, 1061 (1965).
15. J.P. Hunt, S.F. Lincoln, F. Apriele and H.W. Dodgen, *Inorg. Chem.*, 7, 929 (1968).
16. R.B. Jordan, H.W. Dodgen and J.P. Hunt, *Inorg. Chem.*, 5, 1906 (1966).
17. D. Kivelson, *J. Chem. Phys.*, 33, 1094 (1960).
18. R.N. Rogers and G.E. Pake, *J. Chem. Phys.*, 33, 1107 (1960).
19. K. Wüthrich, *Helvetica Chimica Acta*, 48, 779 (1965).
20. D. Kivelson and Sai-Kwing Lee, *J. Chem. Phys.*, 41, 1896 (1964).
21. I. Bernal and P.H. Rieger, *Inorg. Chem.*, 2, 256 (1963).
22. K. De Armond, B.B. Garrett and H.S. Gutowsky, *J. Chem. Phys.*, 42, 1019 (1965).
23. H.A. Kuska and M.T. Rogers, *Inorg. Chem.*, 5, 313 (1966).
24. R. Wilson and D. Kivelson, *J. Chem. Phys.*, 44, 154 (1966).
25. P.W. Atkins and D. Kivelson, *J. Chem. Phys.*, 44, 169 (1966).
26. R. Wilson and D. Kivelson, *J. Chem. Phys.*, 44, 4440 (1966).
27. D.C. McCain and R.J. Myers, *J. Phys. Chem.*, 71, 192 (1967).
28. F.A. Walker, R.L. Carlin and P.H. Rieger, *J. Chem. Phys.*, 45, 4181 (1966).
29. R.K. Wangsness and F. Bloch, *Phys. Rev.*, 89, 728 (1953).
30. F. Bloch, *Phys. Rev.*, 102, 104 (1956).
31. H.M. McConnell, *J. Chem. Phys.*, 28, 430 (1958).

32. J.A. Pople, W.G. Schneider and H.J. Bernstein, "*High Resolution Nuclear Magnetic Resonance*", 1st ed., McGraw-Hill Book Company Inc., (1959).
33. I. Solomon, *Phys. Rev.*, 99, 559 (1955).
34. I. Solomon and N. Bloembergen, *J. Chem. Phys.*, 25, 261 (1956).
35. R.E. Connick and D. Fiat, *J. Chem. Phys.*, 44, 4103 (1966).
36. Z. Luz and S. Meiboom, *J. Chem. Phys.*, 40, 2686 (1964).
37. Share Library nonlinear least squares programme SDA 3094, (1964).
38. W.D. Ellis, Ph.D. Thesis, University of Alberta, (1968).
39. P.S. Hubbard, *Phys. Rev.*, 131, 1155 (1963).
40. V. Gutmann and H. Laussegger, *Monatsh. Chemie*, 98, 439 (1967).
41. K. Wüthrich and R.E. Connick, *Inorg. Chem.*, 6, 583 (1967).
42. J. Reuben and D. Fiat, *Inorg. Chem.*, 6, 579 (1967).
43. C.J. Ballhausen and H.B. Gray, *Inorg. Chem.*, 1, 111 (1962).
44. A.B.P. Lever, "*Advances in Chemistry Series*", (American Chemical Society, 1967), Vol. 62, p. 431.
45. K.J. Coskran, T.J. Hutteman and J.G. Verkade, *Ibid.*, p. 590.
46. B. Duffin, *Acta. Cryst.*, B24, 396 (1968).
47. V.S. Mastryikov, L.V. Vilkov, P.A. Akiskin, *Acta. Cryst.*, A128, 16 (1963).

48. J.D. Dunitz and J.S. Rollet, *Acta. Cryst.*, 23, 581 (1967).
49. M.J. Bennett, F.A. Cotton, and D.W. Weaver, *Acta. Cryst.*, 23, 581 (1967).
50. C.J. Balhausen, B.F. Djurinskig, and K.J. Watson, *J. Amer. Chem. Soc.*, 90, 3305 (1968).
51. K. Wüthrich and R.E. Connick, *Inorg. Chem.*, 7, 1377 (1968).
52. J. Koskikallio, *Suomen Kemistilehti*, B30, 111, 157 (1957).
53. F.J.C. Rossotti and H.S. Rossotti, *Acta. Chem. Scand.*, 9, 1177 (1955).
54. T. Shedlovsky and R.L. Kay, *J. Phys. Chem.*, 60, 151 (1956).
55. A.E. Martell and L.G. Sillen, "Stability Constants of Metal Complexes", Special Publication No. 17, The Chemical Society, London (1964).
56. R.G. Pearson and J.W. Moore, *Inorg. Chem.*, 5, 1528 (1966).
57. R. Hausser and G. Laukien, *Z. Physik*, 153, 394 (1959).
58. A.D. Cavouras, Master Thesis, Washington State University, (1966).
59. T.J. Swift, T.A. Stephenson and G.R. Stein, *J. Amer. Chem. Soc.*, 89, 1611 (1967).
60. E. Grunwald, C.T. Jumper and S. Meiboom, *J. Amer. Chem. Soc.*, 84, 4664 (1962).
61. R.L. Carlin and F.A. Walker, *J. Amer. Chem. Soc.*, 87, 2128 (1965).

62. L. De Maeyer and K. Kustin, *Ann. Rev. Phys. Chem.*, 14, 5 (1963).
63. R.P. Dodge, D.H. Templeton and A. Zalkin, *J. Chem. Phys.*, 35, 55 (1961).
64. R.L. Livingston and G. Vaughan, *J. Amer. Chem. Soc.*, 78, 2711 (1956).
65. F.A. Cotton and J.J. Wise, *Inorg. Chem.*, 6, 913 (1967).
66. H.M. McConnell and R.E. Robertson, *J. Chem. Phys.*, 29, 1361 (1958).
67. G.W. Meredith, Ph.D. Thesis, University of California (1965).
68. H. Taube, private communication.
69. M. Noack and G. Gordon, *J. Chem. Phys.*, 48, 2689 (1968).
70. A. McAuley and J. Hill, *Quart. Rev.*, 23, 18 (1969).
71. J.A. Jackson, J.F. Lemons and H. Taube, *J. Chem. Phys.*, 38, 836 (1968).
72. A. Hudson, *Mol. Phys.*, 10, 575 (1966).
73. R.E.D. McClung and D. Kivelson, *J. Chem. Phys.*, 49, 3380 (1968).
74. J.S. Griffith, "*The Theory of Transition Metal Ions*", Cambridge at the University Press, p. 281 (1961).
75. B.N. Figgis, "*Introduction to Ligand Fields*", Interscience Publishers, p. 218 (1967).
76. F.A. Cotton and R. Francis, *J. Amer. Chem. Soc.*, 82, 2986 (1960).

77. S. Thomas and W.L. Reynolds, *J. Chem. Phys.*, 46, 4164 (1967).
78. S. Blackstaffe and R.A. Dwek, *Molec. Phy.*, 15, 279 (1968).
79. L.I. Katzin, *J. Chem. Phys.*, 35, 467 (1961).
80. D.W. Herlocker and R.S. Drago, *Inorg. Chem.*, 7, 1479 (1968).
81. A.H. Zeltman, N.A. Matwiyoff and L.O. Morgan, *J. Phys. Chem.*, 72, 121 (1968).
82. S. Ooi and Q. Fernando, *Chem. Comm.*, 532 (1967).
83. H.M. McConnell and R.E. Robertson, *J. Chem. Phys.*, 29, 1361 (1958).
84. E.C. Blatt and R.E. Connick, Proceedings of the 8th International Congress on Coordination Chemistry, Vienna, p. 284 (1964).
85. L.O. Morgan and A.H. Zeltmann, *J. Phys. Chem.*, 70, 2877 (1966).
86. H. Taube, *Chem Rev.*, 50, 69 (1952).
87. M. Eigen and R.G. Wilkins, "Advances in Chemistry Series", Vol. 39, American Chemical Society (1965).
88. B.R. Baker, N. Sutin and T.J. Welsh, *Inorg. Chem.*, 6, 1948 (1967).
89. S.C. Furman and C.S. Garner, *J. Amer. Chem. Soc.*, 73, 4528 (1951).
90. J.H. Espenson, *J. Amer. Chem. Soc.*, 89, 1276 (1967).

91. G.W.A. Fowles and P.T. Greene, *J. Chem. Soc.*, (London), 1869 (1967).
92. G.W.A. Fowles and P.G. Lanigan, *J. Less Common Metals*, 6, 396 (1964).
93. R.J.H. Clark, R.S. Nyholm and D.E. Scaife, *J. Chem. Soc.*, (London), 1296 (1966).
94. E.L. Martin and K.E. Bentley, *Anal. Chem.*, 34, 354 (1962).
95. H.J.V. Tyrrell, "*Diffusion and Heat Flow in Liquids*", Butterworth and Company, Ltd., (1961).
96. R.E.D. McClung and D. Kivelson, *J. Chem. Phys.*, 49, 3380 (1968).
97. V. Gutmann and O. Bohunovsky, *Monatsh. für Chemie*, 99, 740 (1968).
98. C.K. Jorgensen, *Acta. Chem. Scand.*, 8, 1495 (1954).
99. L.S. Frankel, *J. Chem. Phys.*, 50, 943 (1969).
100. M. Baaz, V. Gutmann, G. Hampel and J.R. Masaguer, *Monatsh. für Chemie.*, 93, 1416 (1962).
101. S.T. Spees, J.R. Perumareddi and A.W. Adamson, *J. Amer. Chem. Soc.*, 90, 6626 (1968).
102. A.B.P. Lever, "*Werner Centennial*", Advances in Chemistry Series, Vol. 62, ed. R.F. Gould, American Chemical Society, p. 430 (1967).
103. K. Breitschwerdt, *Ber. der Buns.*, 72, 1046 (1968).
104. H.H. Glaeser, H.W. Dodgen and J.P. Hunt, *Inorg. Chem.*, 4, 3148 (1966).

104. H. Levanon and Z. Luz, *J. Chem. Phys.*, 49, 2031 (1968).
106. F.W. Breivogel, private communication.
107. *Handbook of Chemistry and Physics*, 46th edition.
108. T.C. Waddington, "Nonaqueous Solvent Systems", Academic Press Inc. (London) Ltd., 1st ed. (1965).
109. *Dupont Product Information Bulletin* (1967).
110. A.J. Parker, *Quarterly Reviews* (London), 163 (1962).
111. C.H. Langford and H.B. Gray, "Ligand Substitution Processes", W.A. Benjamin, Inc., New York (1965).
112. C.K. Ingold, "Structure and Mechanism in Organic Chemistry", Cornell University Press, Ithaca, New York (1953).
113. E.D. Hughes, C.K. Ingold, and R.I. Reed, *J. Chem. Soc.*, 2400 (1950).
114. E.S. Amis, "Solvent Effects on Reaction Rates and Mechanisms", Academic Press, New York (1966).
115. P.C. Crouch, G.W.A. Fowles, and R.A. Walton, *J. Chem. Soc. (A)*, 2172 (1968).
116. M.D. Zeidler, *Ber. Bunsenges. Physik. Chem.*, 69, 659 (1965).

APPENDIX A

Tables XXVII to XXXIII of this appendix give the proton magnetic resonance line widths at half height as a function of temperature for the pure solvents used in this study. The data was chosen for a representative run at 60 MHz and was reproduced to ± 1.0 cps for other runs at both 60 MHz and 100 MHz. Tables XXXIV to LVII give the observed line widths at half height of the bulk solvent proton magnetic resonance and the corresponding $(T_{2p})^{-1}$ as a function of temperature for solutions containing various transition metal ions. The figures in the thesis to which these tables correspond are also indicated.

TABLE XXVIITemperature dependence of the water proton line width at 60 MHz

T° C	Line width at half height (sec ⁻¹)
100	1.00
90	1.00
80	1.10
70	1.20
60	1.30
50	1.35
40	1.45
30	1.50
20	1.60
10	1.75

TABLE XXVIII

Temperature dependence of the formyl proton line width
of N,N-dimethylformamide at 60 MHz

T° C	Line width at half height (sec ⁻¹)
140	1.00
130	1.10
120	1.20
110	1.25
100	1.30
90	1.40
80	1.50
70	1.55
60	1.60
50	1.70
40	1.75
30	2.00
20	2.50
10	2.75
0	3.00
-10	3.05
-20	3.50
-30	3.75
-40	4.25
-50	4.50

TABLE XXIX

Temperature dependence of the hydroxy and methyl proton
line widths of methanol at 60 MHz

T° C	Line width at half height (sec ⁻¹)	
	<u>Hydroxy</u>	<u>Methyl</u>
80	0.80	0.75
70	0.80	0.80
60	0.80	0.80
50	0.80	0.80
40	0.80	0.80
30	0.85	0.85
20	0.85	0.85
10	0.90	0.85
0	0.90	0.90
-10	0.95	1.00
-20	0.95	1.00
-30	1.00	1.00
-40	1.00	1.00
-50	1.05	1.05
-60	1.10	1.05
-70	1.10	1.10
-80	1.15	1.10

TABLE XXX

Temperature dependence of the methyl proton line width
of acetonitrile at 60 MHz

T° C	Line width at half height (sec ⁻¹)
80	1.00
70	1.05
60	1.10
50	1.10
40	1.15
30	1.20
20	1.25
10	1.30
0	1.30
-10	1.40
-20	1.45
-30	1.50
-40	1.50

TABLE XXXI

Temperature dependence of the methyl proton line width
of dimethylsulfoxide at 60 MHz

<u>T° C</u>	<u>Line width at half height (sec⁻¹)</u>
180	1.00
170	1.00
160	1.00
150	1.00
140	1.00
130	1.00
120	1.10
110	1.10
100	1.15
90	1.15
80	1.20
70	1.30
60	1.30
50	1.35
40	1.40
30	1.40
20	1.70

TABLE XXXII

Temperature dependence of the methyl proton line width
of trimethylphosphate at 60 MHz

<u>T° C</u>	<u>Line width at half height (sec⁻¹)</u>
180	1.00
160	1.00
140	1.00
120	1.00
100	1.00
80	1.05
60	1.05
40	1.07
20	1.10
0	1.15
-20	1.15
-40	1.20
-60	1.20
-80	1.25

TABLE XXXIII

Temperature dependence of the methyl proton line width
of trimethylphosphite at 60 MHz

<u>T° C</u>	<u>Line width at</u> <u>half height (sec⁻¹)</u>
110	1.00
100	1.00
80	1.05
60	1.05
40	1.10
20	1.10
0	1.15
-20	1.20
-40	1.30
-60	1.40
-80	1.50

TABLE XXXIV

Proton line broadening for 0.0907 molal (1), 0.0276 molal (2), and 0.0547 molal (3) solutions of VO(ClO₄)₂ in N,N-dimethylformamide (Figure 1). Frequency: 60 MHz. *Frequency: 100 MHz.

T°, C	$\frac{10^3}{T}, K^{-1}$	FORMYL PROTON LINE BROADENING			
		$\Delta\nu_{OBS}, sec^{-1}$	$10^{-2} \times (T_{2p}')^{-1}, sec^{-1} molal^{-1}$		
150	2.36	13.9 (2)		15.85	
140	2.42	15.0 (2)		17.05	
130	2.48	15.6 (2)		17.75	
120	2.54	16.1 (2)		18.30	
110	2.61	16.0 (2)		18.20	
100	2.68	14.3 (2)		16.28	
90	2.75	12.9 (2)		14.68	
80	2.83	18.6 (3)		10.38	
70	2.91	15.2 (3)		8.73	
60	3.00	13.2 (3)		7.60	
60	3.00	23.0 (1)		7.97	
50	3.09	19.6 (1)		6.79	
40	3.19	16.1 (1)		5.56	
30	3.30	11.9 (1)	12.7 (1)*	4.11,	4.40*
20	3.41	3.0 (2)		3.39	
10	3.53	2.9 (2)	9.2 (1)*	3.30,	3.20*

TABLE XXXIV (Cont'd)

FORMYL PROTON LINE BROADENING				
T°, C	$\frac{10^3}{T}, K^{-1}$	$\Delta\nu_{OBS}, sec^{-1}$	$10^{-2} \times (T_{2p}')^{-1}, sec^{-1} molal^{-1}$	
10	3.53	2.7 (2)	3.14	
0	3.66	2.6 (2)	2.96	
0	3.66	5.3 (3)	3.06	
-10	3.80	5.5 (3)	9.0 (1)*	3.14, 3.11*
-20	3.95	6.1 (3)	3.52	
-30	4.11	11.8 (1)	12.7 (1)*	4.08, 4.40*
-35	4.20	13.3 (1)	4.62	
-40	4.29	14.5 (1)	5.02	
-45	4.38	15.4 (1)	5.34	
-50	4.48	17.0 (1)	17.9 (1)*	5.87, 6.20*
-50	4.48	16.8 (1)	5.81	

TABLE XXXV

Proton line broadening of a 0.0851 molal solution
of VO(ClO₄)₂ in acetonitrile (Figure 2). Frequency 60 MHz

PROTON LINE BROADENING			
T°, C	$\frac{10^3}{T}, K^{-1}$	$\Delta\nu_{OBS}, sec^{-1}$	$10^{-2} \times (T_{2p}')^{-1}, sec^{-1} molal^{-1}$
80	2.83	80.5	2.97
70	2.91	60.5	2.23
60	3.00	50.5	1.87
50	3.09	38.0	1.40
40	3.19	26.0	9.59
30	3.30	18.0	6.64
20	3.41	12.5	4.61
10	3.53	7.5	2.77
0	3.66	4.5	1.66
-10	3.80	3.5	1.29
-20	3.95	2.5	0.92
-30	4.11	2.5	0.92
-40	4.29	3.0	1.11
-50	4.48	3.6	1.33
-60	4.68	4.2	1.55

TABLE XXXVI

Proton line broadening of a 0.1563 molal solution of
VO(BF₄)₂ in trimethylphosphite (Figure 3). Frequency: 60 MHz.

PROTON LINE BROADENING			
T°, C	$\frac{10^3}{T}, ^\circ\text{K}^{-1}$	$\Delta\nu_{\text{OBS}}, \text{sec}^{-1}$	$10^{-2} \times (T_{2p}')^{-1}, \text{sec}^{-1} \text{molal}^{-1}$
120	2.54	4.1	0.82
100	2.68	4.8	0.97
80	2.83	5.3	1.07
70	2.91	5.9	1.18
60	3.00	6.5	1.31
40	3.19	7.3	1.47
20	3.41	9.1	1.83
0	3.66	11.5	2.31
-20	3.95	15.0	3.02
-40	4.29	21.0	4.22

TABLE XXXVII

Proton line broadening of a 0.0632 molal solution of
VO(BF₄)₂ in dimethylsulfoxide (Figure 3). Frequency 60 MHz.

PROTON LINE BROADENING			
T°, C	$\frac{10^3}{T}, ^\circ\text{K}^{-1}$	$\Delta\nu_{\text{OBS}}, \text{sec}^{-1}$	$10^{-2}(\tau_{2p}')^{-1}, \text{sec}^{-1} \text{molal}^{-1}$
180	2.20	1.30	0.65
160	2.30	1.60	0.80
140	2.42	1.90	0.95
120	2.54	2.30	1.15
100	2.68	2.90	1.44
80	2.83	3.80	1.89
60	3.00	5.20	2.59
40	3.19	7.10	3.53
20	3.41	10.00	4.97

TABLE XXXVIII

Proton line broadening of 0.0726 molal (1) and
0.0363 molal (2) solutions of VO(BF₄)₂ in trimethylphosphate
(Figure 3). Frequency: 100 MHz.

PROTON LINE BROADENING				
T°, C	$\frac{10^3}{T}, ^\circ\text{K}^{-1}$	$\Delta\nu_{\text{OBS}}, \text{sec}^{-1}$	$10^{-2} \times (T_{2p}')^{-1}, \text{sec}^{-1} \text{molal}^{-1}$	
180	2.20	2.90 (1)	1.26	
160	2.30	3.30 (1)	1.43	
140	2.42	3.60 (1)	1.56	
120	2.54	4.20 (1)	1.82	
100	2.68	5.30 (1)	2.29	
80	2.83	5.60 (1)	2.42	
60	3.00	7.70 (1)	3.90 (2)	3.31, 3.38
40	3.19	9.50 (1)	4.80 (2)	4.10, 4.15
20	3.41	12.60 (1)	5.35	
0	3.66	15.60 (1)	6.74	
-20	3.95	21.20 (1)	10.30 (2)	9.16, 8.90
-40	4.29	30.00 (1)	13.00	

TABLE XXXIX

Proton line broadening of 0.123 molal (1) and 0.101 molal (2) solutions of $\text{VO}(\text{ClO}_4)_2$ in

methanol (Figure 4). Frequency: 100 MHz. *Frequency: 60 MHz.

T, °C	$10^3 \frac{1}{T}, \text{K}^{-1}$	PROTON LINE BROADENING			$10^{-2} \times (\tau_{2p})^{-1}, \text{sec}^{-1} \text{ molal}^{-1}$	CH ₃
		OH	$\Delta\nu_{\text{OBS}}, \text{sec}^{-1}$	CH ₃		
80	2.83			38.0*		11.80*(2)
70	2.91			25.0*		7.75*(2)
60	3.00	14.5		15.4, 16.7	45.0(2)	4.80(2), 5.20*(1)
50	3.09	76.0*, 76.5		9.65, 9.65*	23.6*(2), 23.8(2)	3.00(2), 3.00*(2)
40	3.19	74.5, 59.0		10.0, 7.70, 7.70*	19.0(1), 18.3(2)	2.55(1), 2.40(2), 2.40*(2)
30	3.30	38.6, 37.0*		6.80, 6.75*	12.0(2), 11.5*(2)	2.12(2), 2.10*(2)
20	3.41	19.3		5.30*, 6.55, 5.80	6.00(2)	1.65*(2), 1.67(1), 1.80(2)
10	3.53	19.1, 19.3*		5.30*, 5.38	5.95(2), 6.00*(2)	1.65*(2), 1.67(2)
5	3.59	18.8		6.47	4.80(1)	1.65(1)
0	3.66	16.0*, 16.5, 14.5		5.90*, 6.00, 5.31	4.05(1)*, 4.20(1), 4.50(2)	1.50*(1), 1.53(1), 1.65(2)
-10	3.80	18.8		7.65	4.80(1)	1.95(1)
-20	3.95	21.0*, 21.2		9.21*, 9.45	5.35(1)*, 5.40(1)	2.35*(1), 2.40(1)
-40	4.29	26.9		13.0	8.35(2)	4.05(2)
-60	4.68	46.6		21.2	14.50(2)	6.60(2)

TABLE XL

Proton line broadening of a 0.067 molal solution of
VO(acac)₂ in methanol (Figure 5). Frequency: 60 MHz.

T°, C	$\frac{10^3}{T}, ^\circ\text{K}^{-1}$	PROTON LINE BROADENING			
		$\Delta\nu, \text{sec}^{-1}$		$10^{-2} \times (T_{2p}')^{-1}, \text{sec}^{-1} \text{molal}^{-1}$	
		OH	CH ₃	OH	CH ₃
70	2.91		1.04		0.49
60	3.00		1.17		0.55
40	3.19	129.0	1.53	60.50	0.72
30	3.30	70.0	1.81	32.80	0.85
20	3.41	41.3	2.08	19.40	0.98
10	3.53	21.0	2.45	9.85	1.15
0	3.66	17.4	3.00	8.15	1.41
-20	3.95	15.4	4.50	7.25	2.12
-40	4.29	20.3	7.05	9.55	3.30
-60	4.68	36.6	13.00	17.20	6.10
-70	4.92	50.0	18.50	23.50	8.70

TABLE XLI

Proton line broadening of a 0.2186 molal solution of
VO(tfac)₂ in methanol (Figure 6). Frequency: 60 MHz.

T°, C	$\frac{10^3}{T}, ^\circ\text{K}^{-1}$	PROTON LINE BROADENING			
		$\Delta\nu_{\text{OBS}}, \text{sec}^{-1}$		$10^{-2} \times (T_{2p}')^{-1}, \text{sec}^{-1} \text{molal}^{-1}$	
		OH	CH ₃	OH	CH ₃
80	2.83	491.0		70.50	
70	2.91	349.0		50.10	
60	3.00	249.0		35.80	
50	3.09	153.0		22.00	
40	3.19	92.4		13.25	
30	3.30	46.8		6.72	
20	3.41	30.0	10.0	4.31	1.44
10	3.53	27.0	11.5	3.88	1.65
0	3.66	30.0	14.0	4.31	2.01
-10	3.80	36.0	16.0	5.16	2.30
-20	3.95	42.5	20.0	6.10	2.87
-30	4.11	53.0	24.5	7.61	3.52
-40	4.29	68.0	32.0	9.76	4.59
-50	4.48	87.0	42.0	12.50	6.03
-60	4.68	110.0	54.0	15.80	7.75

TABLE XLII

Proton line broadening of a 0.0073 molal solution of
VO(acac)₂ in trichloroethanol (Figure 7). Frequency: 100 MHz.

T°,C	$\frac{10^3}{T}, ^\circ\text{K}^{-1}$	PROTON LINE BROADENING			
		$\Delta\nu_{\text{OBS}}, \text{sec}^{-1}$		$10^{-2} \times (T_{2p}')^{-1}, \text{sec}^{-1} \text{molal}^{-1}$	
		OH	CH ₂	OH	CH ₂
80	2.83	42.5	0.9	18.4	0.39
70	2.91	36.4	1.3	15.7	0.56
60	3.00	31.4	2.1	13.6	0.91
50	3.09	28.6	3.1	12.4	1.34
40	3.19	33.0	5.9	14.3	2.55
30	3.30	42.5	11.0	18.4	4.76
20	3.41	61.0	19.5	25.4	8.45

TABLE XLIII

Proton line broadening of a 0.0613 molal solution of
VO(acac)₂ in trifluoroethanol (Figure 8). Frequency: 60 MHz.

PROTON LINE BROADENING					
T°, C	$\frac{10^3}{T}, ^\circ\text{K}^{-1}$	$\Delta\nu_{\text{OBS}}, \text{sec}^{-1}$		$10^{-2} \times (T_{2p}')^{-1}, \text{sec}^{-1} \text{molal}^{-1}$	
		OH	CH ₂	OH	CH ₂
80	2.83	6.5		3.33	
70	2.91	8.5		4.36	
60	3.00	12.0		6.15	
50	3.09	15.5	5.2	7.95	2.24
40	3.19	23.0	8.1	11.80	3.00
30	3.30	31.0	11.7	15.90	4.90
20	3.41	45.0	16.3	23.05	6.00
10	3.53	70.0	25.8	35.90	9.55
0	3.66	110.0	36.1	56.40	15.00
-10	3.80	125.0	54.6	89.60	22.00
-20	3.95	300.0	103.5	154.0	39.00
-30	4.11	580.0	175.5	298.0	64.00
-40	4.29	800.0		410.0	

TABLE XLIV

Proton line broadening of 0.175 molal (1) and 0.069 molal (2)
solutions of copper acetylacetonate in methanol (Figure 10).

Frequency: 60 MHz.

T°, C	$\frac{10^3}{T}, ^\circ\text{K}^{-1}$	PROTON LINE BROADENING			
		$\Delta\nu_{\text{OBS}}, \text{sec}^{-1}$		$10^{-2} \times (T_{2p}')^{-1}, \text{sec}^{-1} \text{molal}^{-1}$	
		OH	CH ₃	OH	CH ₃
40	3.19	24.3 (1)	7.77 (1)	4.35	1.39
20	3.41	31.5 (1)	9.73 (1)	5.65	1.74
0	3.66	43.8 (1)	12.20 (1)	7.85	2.18
-20	3.95	60.9 (1)	19.40 (1)	10.90	3.47
-40	4.29	38.7 (2)	11.55 (2)	17.60	5.25
-60	4.69	62.0 (2)	18.25 (2)	28.20	8.30
-60	4.69	62.1 (2)	19.10 (2)	28.30	8.70
-80	5.18	124.0 (2)	38.70 (2)	56.50	17.60
-90	5.46	162.0 (2)	50.30 (2)	74.00	22.90

TABLE XLV

Proton line broadening and shift for a 0.0175 molal solution of $\text{Cu}(\text{ClO}_4)_2$ and

1.56 molar H_3PF_6 in methanol (Figure 11). Frequency: 60 MHz.

T°, C	$10^3 \frac{^\circ\text{K}^{-1}}{T}$	PROTON LINE BROADENING				PROTON LINE SHIFT			
		$\Delta\nu_{\text{OBS}}, \text{sec}^{-1}$	$10^{-3} \times (T_{2p}')^{-1}, \text{sec}^{-1} \text{molal}^{-1}$	$\Delta\nu_s, \text{sec}^{-1}$	$10^{-3} \times \Delta\omega, \text{rad sec}^{-1} \text{molal}^{-1}$	CH_3	OH	CH_3	OH
80	2.83	5.5	16.5	0.99	2.96	11.3	17.3	4.05	6.22
70	2.91	6.0	17.0	1.08	3.06	11.5	17.9	4.15	6.43
60	3.00	6.5	18.0	1.17	3.25	11.8	18.3	4.44	6.60
50	3.09	6.5	19.5	1.17	3.60	12.1	18.9	4.36	6.81
40	3.19	7.5	22.5	1.35	4.10	12.4	19.4	4.45	6.98
40	3.19	7.5	22.5	1.35	4.10	12.4	19.6	4.45	7.03
20	3.41	9.0	26.5	1.62	4.80	13.2	20.7	4.75	7.45
0	3.66	12.5	36.0	2.25	6.45	14.1	22.1	5.06	7.93
-20	3.95	15.5	47.0	2.78	8.20	14.9	23.4	5.35	8.44
-40	4.29	21.5	62.0	3.86	11.10	16.0	25.4	5.75	9.16

TABLE XLVI

Proton line broadening of 0.0151 molal (1) and 0.00999 molal (2)
solutions of $\text{Cu}(\text{ClO}_4)_2$ in methanol (Figure 11). Frequency: 60 MHz.

T°, C	$\frac{10^3}{T}, ^\circ\text{K}^{-1}$	PROTON LINE BROADENING			
		$\Delta\nu_{\text{OBS}}, \text{sec}^{-1}$		$10^{-3} \times (T_{2p}')^{-1}, \text{sec}^{-1} \text{molal}^{-1}$	
		OH	CH ₃	OH	CH ₃
70	2.91	5.02 (1)	5.06 (1)	1.05	1.06
60	3.00	5.98 (1)	5.75 (1)	1.25	1.20
50	3.09	7.90 (1)	6.03 (1)	1.65	1.26
40	3.19	9.20 (1)	6.27 (1)	1.92	1.31
30	3.30	11.50 (1)	6.80 (1)	2.40	1.42
20	3.41	16.50 (1)	7.61 (1)	3.45	1.59
10	3.53	22.20 (1)	9.43 (1)	4.65	1.95
0	3.66	17.20 (2)	6.85 (2)	5.40	2.15
-10	3.80	20.40 (2)	7.50 (2)	6.40	2.35
-20	3.95	22.00 (2)	8.35 (2)	6.90	2.62
-30	4.11	26.20 (2)	9.40 (2)	8.25	2.95
-40	4.29	32.40 (2)	11.75 (2)	10.20	3.69
-50	4.48	40.00 (2)	13.60 (2)	12.60	4.28
-60	4.69	45.00 (2)	16.70 (2)	14.10	5.25
-70	4.92	56.40 (2)	19.10 (2)	17.40	6.00
-80	5.18	69.00 (2)	26.20 (2)	21.60	8.25

TABLE XLVII

Proton line shift of 0.0151 molal (1) and 0.00999 molal (2)
solutions of $\text{Cu}(\text{ClO}_4)_2$ in methanol (Figure 12). Frequency: 60 MHz.

T°, C	$\frac{10^3}{T}, ^\circ\text{K}^{-1}$	PROTON LINE SHIFT			
		$\Delta\nu_s, \text{sec}^{-1}$		$10^{-3} \times \Delta\omega, \text{rad sec}^{-1} \text{molal}^{-1}$	
		CH_3	OH	CH_3	OH
60	3.00	10.2 (1)	12.4 (1)	4.28	5.20
40	3.19	10.7 (1)	14.8 (1)	4.48	6.20
20	3.41	11.3 (1)	16.3 (1)	4.75	6.82
0	3.66	8.0 (2)	12.2 (2)	5.01	7.61
-20	3.95	8.6 (2)	13.4 (2)	5.40	8.40
-30	4.11	8.9 (2)	14.0 (2)	5.58	8.78
-40	4.29	9.2 (2)	14.6 (2)	5.81	9.18

TABLE XLVIII

Proton line broadening and shift for a 0.1503 molal solution of $\text{Cr}(\text{BF}_4)_2$ in methanol.

(Figures 14 and 15). Frequency: 60 MHz.

T°, C	$\frac{10^3}{T}, \text{K}^{-1}$	PROTON LINE BROADENING			PROTON LINE SHIFT				
		$\Delta\nu_{\text{OBS}}, \text{sec}^{-1}$	$10^{-2} \times (\tau_{2p})^{-1}, \text{sec}^{-1} \text{molal}^{-1}$	$\Delta\nu_s, \text{sec}^{-1}$	$10^{-2} \times \Delta\omega, \text{rad sec}^{-1} \text{molal}^{-1}$	OH	CH ₃		
100	2.68	64.0	11.6	13.45	2.44	51.5	5.00	21.6	2.10
90	2.75	66.0	12.3	13.85	2.58				
80	2.83	68.0	13.0	14.25	2.73	55.5	5.05	23.30	2.13
70	2.91	70.5	14.4	14.80	3.03				
60	3.00	70.5	14.9	14.80	3.13	59.5	5.30	25.00	2.23
50	3.09	81.5	16.0	17.15	3.36				
40	3.19	88.3	17.7	18.55	3.71	62.5	5.70	26.2	2.40
20	3.41	99.5	19.5	20.90	4.09	65.5	5.85	27.4	2.46
0	3.66	122.5	24.3	25.75	5.10	69.5	6.40	29.2	2.68
-20	3.95	152.0	30.0	30.90	6.28	76.5	7.05	32.1	2.96
-40	4.29	201.0	38.8	42.25	8.15	82.5	7.15	34.6	3.00
-60	4.69	257.0	51.5	54.00	10.88	96.0	7.60	40.4	3.20

TABLE XLIX

Proton Line broadening of a 0.1523 molal solution of
 $V(BF_4)_2$ in methanol (Figure 16). Frequency: 60 MHz.

T° C	$\frac{10^3}{T}, ^\circ K^{-1}$	PROTON LINE BROADENING			
		$\Delta\nu_{OBS}, sec^{-1}$		$10^{-2} \times (T_{2p}')^{-1}, sec^{-1} molal^{-1}$	
		OH	CH ₃	OH	CH ₃
-90	5.46	470.0	320.0	97.0	66.0
-80	5.18	340.0	210.0	70.0	43.2
-60	4.69	155.5	90.0	32.0	18.50
-40	4.29	84.3	46.0	17.4	9.50
-20	3.95	47.0	27.5	9.70	5.69
- 0	3.66	29.5	16.3	6.10	3.36
20	3.41	20.5	11.0	4.24	2.26

TABLE I

Proton line broadening of a 0.5285 molal solution of
Cr(BF₄)₂ in trimethylphosphate (Figure 17). Frequency: 60 MHz.

T°, C	$\frac{10^3}{T}, ^\circ\text{K}^{-1}$	PROTON LINE BROADENING	
		$\Delta\nu_{\text{OBS}}, \text{sec}^{-1}$	$10^{-2} \times (T_{2p})^{-1}, \text{sec}^{-1} \text{molal}^{-1}$
-80	5.18	203.0	12.10
-60	4.69	155.4	9.21
-40	4.29	123.8	7.35
-20	3.95	100.6	5.99
0	3.66	80.8	4.80
20	3.41	59.0	4.13
40	3.19	54.1	3.51
60	3.00	54.1	3.22
80	2.83	49.0	2.92
100	2.68	43.7	2.60
120	2.54	40.1	2.38
140	2.42	37.8	2.25
160	2.30	35.0	2.08

TABLE LI

Proton line broadening of a 0.967 molal solution of
 $V(BF_4)_2$ in trimethylphosphate (Figure 18). Frequency: 60 MHz.

T°, C	$\frac{10^3}{T}, ^\circ K^{-1}$	PROTON LINE BROADENING	
		$\Delta\nu_{OBS}, sec^{-1}$	$10^{-2} \times (T_{2p}')^{-1}, sec^{-1} molal^{-1}$
-40	4.29	39.4	12.80
-20	3.95	33.8	11.00
0	3.66	27.0	8.77
20	3.41	25.0	8.13
40	3.19	21.0	6.82
60	3.00	17.5	5.70
80	2.83	17.4	5.65
100	2.68	15.0	4.87
120	2.54	14.1	4.59
140	2.42	12.6	4.10
160	2.30	11.9	3.86
180	2.20	11.1	3.60

TABLE LII

Proton line broadening of 0.219 molal (1) and 0.181 molal (2) solutions of $\text{Ni}(\text{ClO}_4)_2$ in dimethylsulfoxide (Figure 19).

T° C	$\frac{10^3}{T}, \text{K}^{-1}$	PROTON LINE BROADENING			
		$\Delta\nu_{\text{OBS}}, \text{sec}^{-1}$	60 MHz $(P_M)^{-1}(\tau_{2p})^{-1}, \text{sec}^{-1}$	$\Delta\nu_{\text{OBS}}, \text{sec}^{-1}$	100 MHz $(P_M)^{-1}(\tau_{2p})^{-1}, \text{sec}^{-1}$
20	3.41	42.0 (1)	1155.0	116.5 (1)	3210.0
		35.5 (2)	1200.0		
25	3.35	42.5 (1)	1170.0	110.5 (1)	2690.0
30	3.30	26.5 (1)	730.0	74.5 (1)	2050.0
35	3.24	18.5 (1)	510.0	51.3 (1)	1415.0
40	3.19	17.5 (1)	482.0	41.8 (1)	1160.0
		15.0 (2)	507.0	15.0 (2)	1200.0
45	3.14	13.0 (1)	356.0	36.0 (1)	1000.0
50	3.09	11.5 (1)	317.0	26.8 (1)	740.0
55	3.04	10.0 (1)	275.0	20.0 (1)	553.0

TABLE LII (Cont'd).

T° C	PROTON LINE BROADENING				
	$\frac{10^3 \text{ } ^\circ\text{K}^{-1}}{T}$	60 MHz	100 MHz		
	$\Delta\nu_{\text{OBS}}, \text{sec}^{-1}$	$(P_M)^{-1} (\tau_{2p})^{-1}, \text{sec}^{-1}$	$\Delta\nu_{\text{OBS}}, \text{sec}^{-1}$	$(P_M)^{-1} (\tau_{2p})^{-1}, \text{sec}^{-1}$	
60	3.00	9.5 (1)	261.0	15.3 (1)	422.0
		7.8 (2)	261.0	12.7 (2)	430.0
65	2.95	8.5 (1)	234.0	12.0 (1)	330.0
70	2.91	8.0 (1)	220.0	11.0 (1)	304.0
75	2.87	8.0 (1)	220.0	8.7 (1)	260.0
80	2.83	7.5 (1)	206.0	8.0 (1)	259.0
		6.3 (2)	211.0	6.4 (2)	254.0
100	2.68	5.8 (1)	191.5	5.8 (1)	194.0
120	2.54	5.3 (1)	175.0	5.3 (1)	174.5
140	2.42	4.8 (1)	158.5	4.8 (1)	158.5
160	2.30	4.5 (1)	150.0	4.5 (1)	150.0
170	2.25	4.3 (1)	142.0	4.3 (1)	144.0

TABLE LIII

Proton line shift of 0.219 molal (1) and 0.181 molal (2) solutions of

Ni(ClO₄)₂ in dimethylsulfoxide (Figure 20).

T°, C	$\frac{10^3}{T}, K^{-1}$	PROTON LINE SHIFT			
		60 MHz		100 MHz	
		$\Delta\nu_S, sec^{-1}$	$\frac{\Delta\omega}{P_M}, rad. sec^{-1}$	$\Delta\nu_S, sec^{-1}$	$\frac{\Delta\omega}{P_M}, rad. sec^{-1}$
20	3.41				
25	3.35	38.4 (1)	2110.0	56.0 (1)	3090.0
30	3.30	39.0 (1)	2150.0	58.0 (1)	3410.0
35	3.24	39.6 (1)	2190.0	59.3 (1)	3260.0
40	3.19	38.5 (1)	2120.0	60.5 (1)	3440.0
45	3.14	38.4 (1)	2110.0	51.4 (2)	3470.0
50	3.09	39.7 (1)	2130.0	63.8 (1)	3590.0
55	3.04	40.0 (1)	2140.0	64.4 (1)	4000.0
				64.8 (1)	3570.0

TABLE LIII (Cont'd).

T°,C	PROTON LINE SHIFT					
	$10^3 \frac{^{\circ}\text{K}^{-1}}{\text{T}}$	60 MHz		100 MHz		
	$\Delta\nu_s, \text{sec}^{-1}$	$\frac{\Delta\omega, \text{rad. sec}^{-1}}{\text{P}_M}$	$\Delta\nu_s, \text{sec}^{-1}$	$\frac{\Delta\omega, \text{rad. sec}^{-1}}{\text{P}_M}$	$\Delta\nu_s, \text{sec}^{-1}$	$\frac{\Delta\omega, \text{rad. sec}^{-1}}{\text{P}_M}$
60	3.00	38.4 (1)	2110.0	63.8 (1)	3510.0	
		32.0 (2)	2160.0	53.0 (2)	3580.0	
65	2.95	38.0 (1)	2090.0	63.5 (1)	3500.0	
70	2.91	37.4 (1)	2050.0	62.0 (1)	3420.0	
75	2.87	36.4 (1)	2010.0	61.0 (1)	3360.0	
80	2.83	36.3 (1)	1995.0	60.7 (1)	3340.0	
		30.0 (2)	2030.0	50.5 (2)	3400.0	
100	2.68	28.5 (1)	1900.0	47.5 (1)	3170.0	
120	2.54	27.0 (1)	1795.0	45.0 (1)	3000.0	
140	2.42	25.5 (1)	1700.0	42.5 (1)	2840.0	
160	2.30	25.0 (1)	1665.0	41.8 (1)	2780.0	
170	2.25	24.0 (1)	1595.0	40.0 (1)	2670.0	

TABLE LIV

Proton line broadening and shift of 0.413 molal (1) and 0.356 molal (2) solutions of $\text{Co}(\text{ClO}_4)_2$ in dimethylsulfoxide (Figures 19 and 20). Frequency: 60 MHz.

T°, C	$\frac{10^3}{T}, \text{K}^{-1}$	PROTON LINE BROADENING			PROTON LINE SHIFT	
		$\Delta\nu_{\text{OBS}}, \text{sec}^{-1}$	$(T_{2p})^{-1}/P_M, \text{sec}^{-1}$	$\Delta\nu_S, \text{sec}^{-1}$	$\Delta\omega/P_M, \text{rad. sec}^{-1}$	
20	3.41	5.93 (1)	77.4	88.0 (1)	2300.0	
30	3.30	4.64 (2)	73.0	73.0 (2)	2280.0	
40	3.19	4.60 (1)	60.2	82.5 (1)	2150.0	
50	3.09	3.64 (2)	57.1	66.0 (2)	2070.0	
60	3.00	4.08 (1)	53.3	77.0 (1)	2010.0	
70	2.91	3.17 (2)	49.9	62.0 (2)	1940.0	
80	2.83	3.30 (1)	43.0	72.0 (1)	1875.0	
90	2.75	2.60 (2)	41.0	58.6 (2)	1840.0	
100	2.68	2.90 (1)	37.8	68.5 (1)	1790.0	
110	2.61	2.26 (2)	35.6	55.4 (2)	1740.0	
120	2.54	2.50 (1)	32.7	64.5 (1)	1685.0	
130	2.48	2.04 (2)	32.1	52.3 (2)	1640.0	
140	2.42	2.17 (1)	28.4	60.5 (1)	1580.0	

TABLE IV

Proton line broadening and shift of 0.137 molal (1), 0.244 molal (2) and 0.432 molal (3) solutions of $\text{Ni}(\text{ClO}_4)_2$ in trimethylphosphate (Figures 21 and 22). Frequency: 60 MHz.

T°, C	PROTON LINE BROADENING			PROTON LINE SHIFT	
	$\frac{10^3}{T}, ^\circ\text{K}^{-1}$	$\Delta\nu_{\text{OBS}}, \text{sec}^{-1}$	$(T_{2p})^{-1}/P_M, \text{sec}^{-1}$	$\Delta\nu_S, \text{sec}^{-1}$	$\Delta\omega/P_M, \text{rad. sec}^{-1}$
160	2.30	20.0 (3)	110.0	10.00 (3)	110.0
150	2.36	9.5 (2)	116.0	4.50 (2)	110.0
140	2.42	21.0 (3)	115.5	10.60 (3)	117.0
130	2.48	10.0 (2)	122.0	4.80 (2)	122.5
120	2.54	22.7 (3)	125.0	11.10 (3)	122.0
110	2.61	11.0 (2)	134.0	4.80 (2)	122.5
100	2.68	24.9 (3)	137.0	11.60 (3)	127.5
90	2.75	11.7 (2)	143.0	5.40 (2)	132.0
80	2.83	26.9 (3)	148.0	12.20 (3)	134.0
70	2.91	12.7 (2)	155.0	5.50 (2)	134.5
60	3.00	29.5 (3)	162.0	13.20 (3)	145.5

TABLE LV (Cont'd).

T°, C	PROTON LINE BROADENING			PROTON LINE SHIFT		
	$10^3 \frac{^{\circ}\text{K}^{-1}}{\text{T}}$	$\Delta\nu_{\text{OBS}}, \text{sec}^{-1}$	$(T_{2p})^{-1} / P_M, \text{sec}^{-1}$	$\Delta\nu_S, \text{sec}^{-1}$	$\Delta\omega/P_M, \text{rad. sec}^{-1}$	
50	3.09	14.0 (2)	171.0	6.00 (2)	147.0	
40	3.19	33.3(3) 14.7(2)	183.0	13.90(3) 6.20(2)	153.0 151.5	
30	3.30	15.2 (2)	183.0 180.0	6.20 (2)	151.5	
20	3.41	15.7 (2)	192.0	6.40 (2)	156.0	
10	3.53	8.3 (1)	201.0	3.35 (1)	162.0	
0	3.66	18.2 (2)	222.0	6.80 (2)	166.5	
-10	3.80	9.8 (1)	237.0	3.57 (1)	173.0	
-20	3.95	20.2 (2)	247.0	7.40 (2)	179.0	
-30	4.11	11.5 (1)	278.0	3.82 (1)	185.0	
-40	4.29	24.6 (2)	300.0	7.90 (2)	191.0	
-50	4.48	13.8 (1)	334.0	4.14 (1)	200.0	
		30.6 (2)	374.0	8.50 (2)	208.0	

TABLE IV (Cont'd).

T°, C	PROTON LINE BROADENING			PROTON LINE SHIFT	
	$\frac{10^3}{T}, \text{K}^{-1}$	$\Delta\nu_{\text{OBS}}, \text{sec}^{-1}$	$(T_{2p})^{-1}/P_M, \text{sec}^{-1}$	$\Delta\nu_S, \text{sec}^{-1}$	$\Delta\omega/P_M, \text{rad. sec}^{-1}$
-60	4.69	17.4 (1)	422.0	4.45 (1)	215.0
-70	4.92	39.4 (2)	481.0	9.30 (2)	227.0
-80	5.18	23.2 (1)	560.0	4.95 (1)	240.0
-90	5.46	49.2 (2)	600.0	10.40 (2)	255.0

TABLE LVI

Proton line broadening and shift of a 0.495 molal solution of

Co(ClO₄)₂ in trimethylphosphate. Frequency: 60 MHz.

T°, C	PROTON LINE BROADENING			PROTON LINE SHIFT	
	$\frac{10^3}{T}, \text{K}^{-1}$	$\Delta\nu_{\text{OBS}}, \text{sec}^{-1}$	$(T_{2p})^{-1}/P_M, \text{sec}^{-1}$	$\Delta\nu_S, \text{sec}^{-1}$	$-\Delta\omega_1 \text{ molar}^{-1} \text{ rad. sec}^{-1} \text{ molal}^{-1}$
140	2.42	5.7	17.5	7.95	-100.0
120	2.54	6.5	20.0	5.55	- 70.0
100	2.68	7.0	21.6	2.38	- 30.0
80	2.83	8.3	25.6	0.40	5.0
60	3.00	9.2	28.3	-4.75	60.0
40	3.19	11.2 11.5	34.5	-7.55 -7.95	95.0 100.0
		11.7	36.0 35.4	-7.85	99.0
30	3.30	12.2 12.0	37.5 37.0	-10.6	134.0
20	3.41	13.7 13.5	42.1 41.5	-12.7 -12.9	160.0 162.0
10	3.53	14.7 15.0	45.2 46.1	-15.4	194.0

TABLE LVI (Cont'd).

T°,C	$10^3 \frac{^{\circ}\text{K}^{-1}}{\text{T}}$	PROTON LINE BROADENING			PROTON LINE SHIFT	
		$\Delta\nu_{\text{OBS}}, \text{sec}^{-1}$	$(T_{2p})^{-1} / P_M, \text{sec}^{-1}$	$\Delta\nu_S, \text{sec}^{-1}$	$-\Delta\omega_1 \text{ molal}^{\text{rad.}} \text{ sec}^{-1} \text{ molal}^{-1}$	
0	3.66	16.2 16.5	49.8 50.8	-18.4	232.0	
-10	3.80	18.9	58.1	-21.4	270.0	
-20	3.95	23.2	71.4	-25.4	320.0	
-30	4.11	24.6	75.7	-28.6	360.0	
-40	4.29	29.4	90.5	-32.3	406.0	
-50	4.48	33.0	102.0	-35.7	450.0	
-60	4.69	41.3	127.0	-44.5	524.0	
-70	4.92	47.6	146.5			

TABLE LVII

Proton line broadening of 0.150 molal (1), 0.160 molal (2), and 0.120 molal (3) solutions of

$\text{V}(\text{ClO}_4)_3$ in N,N -dimethylformamide (Figure 23).

FORMYL PROTON LINE BROADENING

T°, C	$10^3 \frac{^\circ K^{-1}}{T}$	$\Delta\nu_{\text{OBS}}, \text{sec}^{-1}$	$10^{-2} \times (T_{2p}')^{-1}, \text{sec}^{-1} \text{ molal}^{-1}$	$\Delta\nu_{\text{OBS}}, \text{sec}^{-1}$	$10^{-2} \times (T_{2p}')^{-1}, \text{sec}^{-1} \text{ molal}^{-1}$	100 MHz	
						60 MHz	
140	2.42	99.5	20.8 (1)				
130	2.48	91.0	19.0 (1)				
120	2.54	86.0	18.0 (1)				
110	2.61	75.5	15.7 (1)				
100	2.68	68.0	14.2 (1)	71.7		15.0 (1)	
80	2.83	52.7	11.0 (1)	62.2		13.0 (1)	
70	2.91	48.0	10.0 (1)				
60	3.00	44.5	8.7 (2)	47.0 48.0		9.2(2), 10.0(1)	
55	3.05	40.7	8.02 (2)				

TABLE LVII (Cont'd).

T°, C	$\frac{10^3}{T}, \text{K}^{-1}$	$\Delta\nu_{\text{OBS}}, \text{sec}^{-1}$	FORMYL PROTON LINE BROADENING		
			$10^{-2} \times (T_{2p})^{-1}, \text{sec}^{-1} \text{molal}^{-1}$	$\Delta\nu_{\text{OBS}}, \text{sec}^{-1}$	$10^{-2} (T_{2p})^{-1}, \text{sec}^{-1} \text{molal}^{-1}$
			60 MHz		100 MHz
50	3.09	39.3		7.7 (2)	
40	3.19	32.0, 35.2		6.7(1), 6.9(2)	
35	3.25				36.2
30	3.30				33.6
25	3.36	30.1		5.9 (2)	
20	3.41	29.1		5.7 (2)	30.1
10	3.53	23.5		4.6 (2)	25.5
0	3.66	18.7, 19.9, 15.3		3.9(1), 3.9(2), 4.0(3)	20.9
- 5	3.73				15.3
-10	3.80	13.3		3.5 (3)	14.2
-20	3.95	15.3		4.0 (3)	15.7

TABLE LVII (Cont'd)

T° C	FORMYL PROTON LINE BROADENING				10 ⁻² x (T _{2p}) ⁻¹ , sec ⁻¹ molal ⁻¹	10 ⁻² x (T _{2p}) ⁻¹ , sec ⁻¹ molal ⁻¹
	10 ³ , °K ⁻¹	Δν _{OBS} , sec ⁻¹	10 ⁻² x (T _{2p}) ⁻¹ , sec ⁻¹ molal ⁻¹	Δν _{OBS} , sec ⁻¹		
			60 MHz			100 MHz
-30	4.11	18.0, 19.9	4.7(3), 5.2(3)	19.1		5.0 (3)
-35	4.20	22.2	5.8 (3)			
-40	4.29	24.1, 24.5,	6.3(3), 6.4(3), 6.7(3)	28.8		7.5 (3)
		25.7, 24.9	6.5(3)			
-45	4.38	28.7, 30.2	7.5(3), 7.9(3)			
-50	4.48	42.0, 34.5, 38.3	8.8(1), 9.0(3), 10.0(3)	44.7		11.7 (3)
-55	4.58	48.0	10.0 (1)	71.0		18.5 (3)
-60	4.69	51.8, 42.2	10.8(1), 11.0(3)			
-65	4.80			92.0		24.0 (3)

TABLE LVII (Cont'd)

T°, C	$\frac{10^3}{T}, K^{-1}$	METHYL PROTON LINE BROADENING			
		$\Delta\nu_{OBS}, sec^{-1}$	100 MHz, 0.013 molal V(ClO ₄) ₃	$10^{-2} \times (T_{2p}')^{-1}, sec^{-1} molal^{-1}$	
		Methyl (1)	Methyl (2)	Methyl (1)	Methyl (2)
50	3.09	3.27	3.08	7.90	7.45
40	3.19	2.70	2.81	6.55	6.80
30	3.30	2.36	2.46	5.70	5.95
20	3.41	2.05	1.86	4.95	4.50
10	3.53	1.72	1.82	4.15	4.40
0	3.66	1.41	1.47	3.40	3.55
-10	3.80	1.26	1.32	3.05	3.20
-30	4.11	1.34	1.45	3.25	3.50

TABLE LVIII

Proton line shift of a 0.085 molal solution of
 $\text{V}(\text{ClO}_4)_3$ in N,N-dimethylformamide (Figure 24)

T°, C	$\frac{10^3}{T}, ^\circ\text{K}^{-1}$	$\Delta\nu_S, \text{sec}^{-1}$	$\Delta\omega, \text{rad. sec}^{-1}$	molal^{-1}
-25	4.03	6.9	510	
-35	4.20	8.0	590	
-40	4.29	8.5	628	
-45	4.38	9.2	680	
-55	4.58	10.1	750	

APPENDIX B

This appendix gives the IBM 360/67 compiler output of the Fortran version of the EPR computer programme used in this study. The programme has been divided up into several sections and the operations in each section have been briefly outlined in "Comment Statements". Compiling time for this programme was 0.8 minutes on level H and normal calculating time was about 3 minutes. For a more detailed discussion of the actual computations of the programme see Chapter IV of this thesis.

PROGRAMME FOR COMPUTING A CORRELATION TUMBLING TIME FROM EPP
HYPERFINE LINES.

THE FOLLOWING CONDITIONS APPLY TO THE LEAST SQUARES ANALYSIS.

N IS THE NUMBER OF OBSERVATIONS
 TOL IS THE ALLOWABLE VALUE OF THE STANDARD ERROR
 LAST IS THE VALUE OF THE HIGHEST ORDER OF THE POLYNOMIAL TO BE FITTED
 IS4=1 FOR ONE DATA SET
 IS4=2 FOR MULTIPLE DATA SETS
 LAST DATA SET MUST END WITH A 999 CARD COL.1-3.
 III=1 FOR WEIGHTED INPUT
 III=2 FOR UNWEIGHTED INPUT
 ISS2=1 FOR INTERMEDIATE OUTPUT
 ISS2=2 FOR FINAL OUTPUT ONLY
 ISS3=1 FOR OUTPUT OF OBSERVED AND CALCULATED VALUES
 ISS3=2 FOR NO OUTPUT

CISS3 ONLY USED IF ISS2=1

NSA002
 NSA003
 NSA004
 NSA005
 NSA006
 NSA007
 NSA008
 NSA009
 NSA010
 NSA011
 NSA012
 NSA013
 NSA014

VALUES FOR TEMPERATURE (°K), ESTIMATED HYDRODYNAMIC RADIUS
(ANGSTROMS) AND VISCOSITY (POISE) ARE READ IN.

922 READ(5,927,END=821) TFMP,RAD,ETA
 927 FORMAT (3F20.8)

NSA015
 NSA016

VALUES FOR THE OPERATING FREQUENCY (CYCLES), THE MAGNETIC FIELD
(GAUSS) AND ESTIMATED VALUE FOR THE TUMBLING TIME (SECL).

910 READ(5,910) V,B0, TG
 910 FORMAT(3F20.0)
 UN=1
 DOUBLE PRECISION X(200),Y(200),A(16,16),SUMX(31),SUMY(15),W(200),C
 1,S1,S2,S3,B,TOL
 INTEGER Z2,Z3

NSA017
 NSA018
 NSA019
 NSA020
 NSA021
 NSA022

REAL LWP(7),LWN(7),LW(8),LINE
 DIMENSION LINE(119)
 REAL LV(8),LWR(8),LWS(8),LVW(8),LVX(8),RR(8)
 REAL TA(300),TAUM(30),TAUT(30),ALSEC(30),ALPSEC(30),ALNSEC(30),
 1ALTOL(30),HSEC(30),BPSEC(30),BNSEC(30),BTOL(30),DSEC(30),DPSEC(30),
 2,DNSEC(30),DTOL(30),GSEC(30),GPSEC(30),GNSEC(30),GTOL(30),
 3GVCCS(30),GVCC(5),AVCC(30),BMA(5)
 REAL E(4),Z(4),DA(4),TAU(4),CA(4),CB(4),MS(4),HM(8)
 REAL YR(8,3),TAUR(6561),TAUG(6561)

NSA023
 NSA024
 NSA025
 NSA026
 NSA027
 NSA028
 NSA029
 NSA030
 NSA031

LINE WIDTHS IN GAUSS ARE READ IN, THE LINE WIDTH OF THE HIGHEST
MAGNETIC FIELD FIRST.

929 READ(5,929) HM(1),HM(2),HM(3),HM(4),HM(5),HM(6),HM(7),HM(8)
 FORMAT(8F10.0)
 READ(5,901)APA,GPA

NSA032
 NSA033
 NSA034

THE PARALLEL COUPLING CONSTANT (GAUSS) AND THE PARALLEL G-VALUE
ARE READ IN.

901 FOPMAT(2F20.0)
 READ(5,937) DIFG,DIFA

NSA036

IF THERE ARE TWO PARALLEL COUPLING CONSTANTS AND G-VALUES THE
DIFFERENCE BETWEEN THEM ARE READ IN, RESPECTIVELY, OTHERWISE ZERO
IS READ IN.

DIFG IS A NEGATIVE NUMBER AND DIFA IS A POSITIVE NUMBER.

937 FOPMAT(2F20.8)

NSA037

CALCULATING AVERAGE HYPERFINE COUPLING CONSTANT FROM SOLUTION
SPECTRUM

$BMA(1) = (HM(1) - HM(8)) / 3.5$
 $BMA(2) = (HM(2) - HM(7)) / 2.5$
 $BMA(3) = (HM(3) - HM(6)) / 1.5$

NSA039
 NSA040

NSA042
 NSA043
 NSA044

NSA045
NSA046
NSA047
NSA048
NSA049
NSA050
NSA051

BMA(4)=(HM(4)-HM(5))/0.5
BMAV=(BMA(1)+BMA(2)+BMA(3)+BMA(4))/8.0
GS=2.0023
H=1.054E-27
RM=9.273E-21
AVCO(UN)=BMAV*GS*RM/H
BSH=2.0*3.1415*H*V/(GS*BM)

NSA052

CALCULATING AVERAGE G-VALUE FROM SOLUTION SPECTRUM

GVC0(1)=GS+GS*(BSH-0.5*(HM(8)+HM(1)))/(0.5*(HM(8)+HM(1)))-2.0*AVCO
1(UN)**2*H**2*(3.5*(3.5+1.0)-3.5**2)/(GS*RM**2*(HM(1)+HM(8))**2)
GVC0(2)=GS+GS*(BSH-0.5*(HM(7)+HM(2)))/(0.5*(HM(7)+HM(2)))-2.0*AVCO
1(UN)**2*H**2*(3.5*(3.5+1.0)-2.5**2)/(GS*BM**2*(HM(2)+HM(7))**2)
GVC0(3)=GS+GS*(BSH-0.5*(HM(6)+HM(3)))/(0.5*(HM(6)+HM(3)))-2.0*AVCO
1(UN)**2*H**2*(3.5*(3.5+1.0)-1.5**2)/(GS*BM**2*(HM(3)+HM(6))**2)
GVC0(4)=GS+GS*(BSH-0.5*(HM(5)+HM(4)))/(0.5*(HM(5)+HM(4)))-2.0*AVCO
1(UN)**2*H**2*(3.5*(3.5+1.0)-0.5**2)/(GS*BM**2*(HM(4)+HM(5))**2)
GVCOS(UN)=(GVC0(1)+GVC0(2)+GVC0(3)+GVC0(4))/4.0
AVCO(UN)=RMAV
WRITE(6,943)

THIS TITLE MAY BE CHANGED TO IDENTIFY THE SYSTEM.

943 FORMAT(1H1, ' VANADYL PERCHLORATE IN WATER ',//)
WRITE (6,930) TEMP,AVCO(UN),GVCOS(UN),ETA,RAD
930 FORMAT(' TEMP=',E20.8,' AVCO=',E20.8,' GVCOS=',E20.8,' ETA= ',E20.
18,' RAD= ',E20.8)

NSA064
NSA065
NSA066
NSA067

CALCULATING GPEX AND GPEY

GPEX=(3.0*GVCOS(UN)-GPA+DIFG)/2.0
GPEY=(3.0*GVCOS(UN)-GPA-DIFG)/2.0

NSA069
NSA070
NSA071
NSA072

CALCULATING APEX AND APEY

NSA076
NSA077
NSA078
NSA079
NSA080

```

APEX=(3.0*AVCD(UN)-APA+DIFA)/2.0
APEY=(3.0*AVCD(UN)-APA-DIFA)/2.0
WRITE (6,031) APA,APEX,APEY,GPA,GPEX,GPEY
031 FORMAT(1, APA=,E16.8, APEX=,E16.8, APEY=,E16.8, GPA=,F16.8,
1, GPEX=,F16.8, GPEY=,E16.8)
    
```

NSA081
NSA082

APA,GT,APF AND GPF .GT. GPA
CALCULATING CONSTANTS REQUIRED IN THEORETICAL EXPRESSIONS.

NSA083
NSA084
NSA085
NSA086
NSA087
NSA088
NSA089
NSA090
NSA091
NSA092
NSA093
NSA094
NSA095
NSA096
NSA097
NSA098
NSA099
NSA100
NSA101

```

SA=0.0
SRA=0.0
SC=0.0
SD=0.0
ISA=0
JL=0
JU=0
SR=0.0
SG=0.0
IM=3.5
RAD = RAD*1.0E-8
G=(GPA+GPEX+GPEY)/3.0
DG=GPA-(GPEX+GPEY)/2.0
BS=-G*2.0*(APA-(APEX+APEY)/2.0)*BM/(3.0*H)
AS=-G*(APA+APEX+APEY)*BM/(3.0*H)
DN=2.0*3.1416*V
CR=(APEX-APEY)/4.0*G*BM/H
DV=(GPEX-GPEY)*BM/(2.0*H)
IF(DM**2*TG**2 .GT. 1.0) GO TO 801
    
```

NSA102
NSA103
NSA104

CASE 1 W**2*TG**2.LI.1.0

R1 =RM#DG#RD/H
R2=IM*(IM+1.0)

EVALUATING THEORETICAL BETA TERMS.

NSA105
NSA106
NSA107
NSA108
NSA109
NSA110
NSA111

U1=7.0*RS*R1/15.0
U2=-14.0*R1**2*AS/(45.0*QM)
U3=-7.0*RS**2*P2*AS/(20.0*QM)
U4=RS**2*(2.0*R2-1.0)*AS/(8.0*QM)
U5=16.0*CR*BO*DV/15.0
U6=4.0*CR*DV*RO/ 5.0
E(2)=U1+U2+U3+U4+U5+U6

EVALUATING THEORETICAL GAMMA TERMS.

NSA112
NSA113
NSA114
NSA115
NSA116
NSA117
NSA118
NSA119

V1=RS**2/10.0
V2=-2.0*RS*R1*AS/(5.0*QM)
V3=16.0*CR**2/15.0
V4=-2.0*CR**2/5.0
V5=4.0*CR**2/ 5.0
V6=-2.0*CR**2/15.0
V7=-4.0*CR**2/5.0
E(3)=V1+V2+V3+V4+V5+V6+V7

EVALUATING THEORETICAL ALPHA TERMS.

NSA121
NSA122
NSA123
NSA124
NSA125
NSA126
NSA127
NSA128
NSA129
NSA130

T1=7.0*R1**2/45.0
T2=RS**2**P2/4.0
T3=-P1*HS**P2*AS/(QM*15.0)
T4=4.0*DV**2**BO**2/15.0
T5=2.0*CR**2**R2/5.0
T6=DV**2**RO**2/5.0
T7=2.0*CR**2**R2/15.0
T8=4.0*CR**2**P2/5.0
E(1)=T1+T2+T3+T4+T5+T6+T7+T8
GO TO 902

NSA131

NSA132

CASE 2 W**2*TG**2.GI.1.L.C

801 R1 =R4*RG*RD/H

EVALUATING THEORETICAL BETA TERMS.

P2=IM*(IM+1.C)
 U1= 4.C*R1*BS/15.C
 U2= -8.C*P1**2*AS/(45.C*OM)
 U3=R1*RS/(5.C*OM**2)
 U4 = -4.C*P1**2*AS/(15.C*OM**3)
 U5= -RS**2*P2*AS/(2.C*OM**3)
 U6= -BS**2*P2*AS/(5.C*OM)
 U7= 3.C*BS**2*(2.C*P2-1.C)*AS/(4.C*OM)
 U8= BS**2*(2.C*P2-1.C)*AS/(2.C*OM**3)
 U9=16.C*CP*RO*OV/15.C
 U10=4.C*CP*DV*RO/(5.C*OM**2)
 CA(2)=U1+U2+U6+U7+U9

NSA133
 NSA134
 NSA135
 NSA136
 NSA137
 NSA138
 NSA139
 NSA140
 NSA141
 NSA142
 NSA143
 NSA144

EVALUATING THEORETICAL GAMMA TERMS.

CB(2)=U3+U4+U5+U8+U10
 V1= RS**2/R.C
 V2= -7.C*RS*R1*AS/(30.C*OM)
 V3=-BS**2/(40.C*OM**2)
 V4=BS**2*AS/(8.C*OM**3)
 V5=-BS*P1*AS/(6.C*OM**3)
 V6=-2.C*BS*R1/(5.C*OM**2)
 V7=16.C*CP**2/15.C
 V8=-2.C*CR**2/5.C
 V9=4.C*CR**2/(5.C*OM**2)
 V10=-2.C*CR**2/(15.C*OM**2)
 V11=-4.C*CR**2/(5.C*OM**2)
 CA(2)=V1+V2+V7+V8
 CB(2)=V3+V4+V5+V6+V9+V10+V11

NSA145
 NSA146
 NSA147
 NSA148
 NSA149
 NSA150
 NSA151
 NSA152
 NSA153
 NSA154
 NSA155
 NSA156
 NSA157
 NSA158

EVALUATING THEORETICAL ALPHA TERMS.

```

T1=4.0*R1**2/45.0
T2=3.0*R2**2/40.0
T3=P1**2/(15.0*OM**2)
T4=7.0*B3**2*R2/(40.0*OM**2)
T5=-5.0*B3**2*R2**AS/(40.0*OM**3)
T6=-R1*R2**AS/(30.0*OM)
T7=-P1*R2**AS/(30.0*OM**3)
T8=4.0*DV**2*B0**2/15.0
T9=2.0*CR**2*P2/5.0
T10=DV**2*H0**2/(5.0*OM**2)
T11=2.0*CR**2*R2/(15.0*OM**2)
T12=4.0*CR**2*R2/(5.0*OM**2)
CA(I)=T1+T2+T6+T8+T9
CB(I)=T3+T4+T5+T7+T10+T11+T12
800 IN=5
    IOUT=6
    III=2
    ISS2=1
    IS3=1
    IS4=2
    1 READ (IN,?) N,TOL, LAST
    2 FORMAT (I3,E14.8,I3)
    5 DO 40 J=1,N
      GO TO (20,20),III
    20 READ(IN,?) X(I),YR(I,1)
    3  FORMAT (F12.0,I2X,F12.0)
      GO TO 40
    30 READ (IN,4) X(I),Y(I),W(I)
    4  FORMAT (3E14.8)
    40 CONTINUE
      DO 201 KM=1,8

```

NSA160
NSA161
NSA162
NSA163
NSA164
NSA165
NSA166
NSA167
NSA168
NSA169
NSA170
NSA171
NSA172
NSA173
NSA174
NSA175
NSA176
NSA177
NSA178
NSA179
NSA180

NSA181
NSA182
NSA183
NSA184
NSA185
NSA186
NSA187
NSA188
NSA189
NSA190

EVALUATING THE LINE WIDTHS WITH THE TEN PERCENT ERROR ON THEM FROM THE OBSERVED LINE WIDTHS.

```

201 YR(KM,2)=1.1*YR(K4,1)
    Y4(KM,3)=0.0*YR(KM,1)
    DO 202 K1=1,3
    DO 203 K2=1,3
    DO 204 K3=1,3
    DO 205 K4=1,3
    DO 206 K5=1,3
    DO 207 K6=1,3
    DO 208 K7=1,3
NSA191
NSA192
NSA193
NSA194
NSA195
NSA196
NSA197
NSA198
NSA199

```

NOTE: THE ERROR IS OMITTED ON THIS LINE BECAUSE THE AVERAGE OF THE COEFFICIENTS FOR THE TWO ERROR CASES IS IDENTICAL TO THOSE FOR THE OBSERVED LINE ITSELF.

```

DO 209 K8=1,1
Y(1)=YR(1,K1)
Y(2)=YR(2,K2)
Y(3)=YR(3,K3)
Y(4)=YR(4,K4)
Y(5)=YR(5,K5)
Y(6)=YR(6,K6)
Y(7)=YR(7,K7)
Y(8)=YR(8,K8)
GO TO (70,50) , III
NSA200
NSA201
NSA202
NSA203
NSA204
NSA205
NSA206
NSA207
NSA208
NSA209

```

BEGINNING OF LEAST SQUARES ANALYSIS TO FIT ABOVE DATA TO A THIRD ORDER POLYNOMIAL.

```

50 DO 60 I=1,N
60 W(I)=1.
70 SUMX(1)=0.
    SUMX(2)=0.
    SUMX(3)=0.
NSA210
NSA211
NSA212
NSA213
NSA214

```

NSA215
NSA216
NSA217
NSA218
NSA219
NSA220
NSA221
NSA222
NSA223
NSA224
NSA225
NSA226

```

SUMY(1)=C.
SUMY(2)=C.
DO 100 I=1,N
SUMX(1)=SUMX(1)+W(I)
SUMX(2)=SUMX(2)+W(I)*X(I)
SUMX(3)=SUMX(3)+W(I)*X(I)*X(I)
SUMY(1)=SUMY(1)+W(I)*Y(I)
SUMY(2)=SUMY(2)+W(I)*X(I)*Y(I)
NCRD=1
01 L=NCRD+1
KK=L+1
DO 101 I=1,L

```

NSA227
NSA228
NSA229
NSA230
NSA231
NSA232
NSA233
NSA234
NSA235
NSA236
NSA237
NSA238
NSA239
NSA240
NSA241
NSA242
NSA243
NSA244
NSA245
NSA246
NSA247
NSA248
NSA249

```

DO 100 J=1,L
IK=J-1+I
100 A(I,J)=SUMX(IK)
101 A(I,KK)=SUMY(I)
DO 140 I=1,L
A(KK,I)=-1.
KKK=I+1
DO 110 J=KKK,KK
110 A(KK,J)=C.
C=1./A(I,I)
DO 120 II=2,KK
DO 120 J=KKK,KK
120 A(II,J)=A(II,J)-A(I,J)*A(II,I)*C
DO 140 II=1,L
DO 140 J=KKK,KK
140 A(II,J)=A(II+1,J)
S2=C.
DO 160 J=1,N
S1=C.
S1=S1+A(1,KK)
DO 150 I=1,NCRD
150 S1=S1+A(I+1,KK)*X(J)*#I
160 S2=S2+(S1-Y(J))*(S1-Y(J))

```



```

NSA250
NSA251
NSA252
NSA253
NSA254
NSA255
NSA256
NSA257
NSA258
NSA259
NSA260
NSA261
NSA262
NSA263
NSA264
NSA265
NSA266
NSA267
NSA268
NSA269
NSA270
NSA271
NSA272
NSA273
NSA274
NSA275
NSA276
NSA277
NSA278
NSA279
NSA280
NSA281
NSA282
NSA283
NSA284
NSA285

R=N-L
S2=(S2/R)**.5
GO TO (163,161),ISS2
161 IF(NORD-LAST)162,163,162
162 IF(S2-TOL)163,163,171
163 IF(NORD.LT.3) GO TO 805
805 CONTINUE
210 DO 806 J=1,L
J=J-1
IF (I-1) 164,11,164
11 IF(NORD.LT.3) GO TO 806
164 IF(NORD.LT.3) GO TO 808
808 CONTINUE
806 CONTINUE
GO TO (167,165),IS3
165 IF(NORD-LAST)166,167,166
166 IF(S2-TOL)167,167,171
167 DO 807 I=1,N
SI=C.
SI=A(1,KK)
DO 168 J=1,NORD
SI=SI+A(J+1,KK)*X(I)**J
S3=Y(I)-SI
IF (I-1) 169,14,169
14 IF(NORD.LT.3) GO TO 807
169 IF(NORD.LT.3) GO TO 809
809 CONTINUE
807 CONTINUE
IF(NORD-LAST)170,173,173
170 IF(S2-TOL)173,173,171
171 NORD=NORD+1
J=2*NORD
SUMX(J)=C.
SUMX(J+1)=C.
SUMY(NORD+1)=C.
DO 172 I=1,N

```

```

NSA286
NSA287
NSA288
NSA289
NSA290
NSA291
NSA292
NSA293
NSA294
NSA295
NSA296
NSA297
NSA298
NSA299
NSA300
NSA301
NSA302
NSA303
NSA304
NSA305
NSA306
NSA307
NSA308
NSA309
NSA310
NSA311
NSA312
NSA313
NSA314
NSA315
NSA316
NSA317
NSA318

SUMX(J)=SUMX(J)+X(I)**(J-1)*W(I)
SUMX(J+1)=SUMX(J+1)+X(I)**J*W(I)
172 SUMY(NORD+1)=SUMY(NORD+1)+Y(I)*X(I)**NORD*W(I)
GO TO 21
173 CONTINUE
200 DO 29 I= 1,4
201 A(I,5)= A(I,5) *1.7221*G*BM/(2.0*H)
ISA=ISA+1
SA=SA+A(1,5)
SBA=SBA+A(2,5)
SC=SC+A(3,5)
SD=SD+A(4,5)
IF(OM**2*TG**2 .GT. 1.0) GO TO 16
DO 21 K=2,3
21 TAU(K)= A(K,5)/ E(K)
JL=JL+1
JU=JU+1
TAUB(JL)=TAU(2)
TAUG(JU)=TAU(3)
SR=SR+TAUB(JL)
SG=SG+TAUG(JU)
GO TO 813
16 DO 26 K=2,3
MS(K)= (A(K,5)**2-4.0*CA(K)*CB(K))
IF(MS(K).LT. 0.0) GO TO 803
Z(K)= SQRT( MS(K))
36 TAU(K)= (A(K,5)+Z(K))/(2.0*CA(K))
JL=JL+1
JU=JU+1
TAUR(JL)=TAU(2)
TAUG(JU)=TAU(3)
SR=SR+TAUB(JL)
SG=SG+TAUG(JU)

```

ALL POSSIBLE LEAST SQUARES FITS ARE CARRIED OUT ON THE OBSERVED EPR LINES AND A CORRELATION TIME FROM THE GAMMA AND BETA COEFFICIENTS IS EVALUATED.

NSA319
NSA320
NSA321
NSA322
NSA323
NSA324
NSA325
NSA326
NSA327
NSA328
NSA329

803 CONTINUE
209 CONTINUE
208 CONTINUE
207 CONTINUE
206 CONTINUE
205 CONTINUE
204 CONTINUE
203 CONTINUE
202 CONTINUE
INTJU=JII
INTJL=JL

AVERAGE GAMMA TUMBLING TIME.

NSA330

TAUAV=SG/FLOAT(INTJU)

AVERAGE BETA TUMBLING TIME.

NSA331

TAUAVB=SR/FLOAT(INTJL)

EVALUATION OF AVERAGE EXPERIMENTAL COEFFICIENTS.

NSA332
NSA333
NSA334
NSA335
NSA336
NSA337
NSA338
NSA339
NSA340

ALPHAV=SA/FLOAT(ISA)
BETAV=SPA/FLOAT(ISA)
GAMAV=SC/FLOAT(ISA)
DELAV=SD/FLOAT(ISA)
PM=2.0*H/(1.7321*G*BM)
ALPHAV=ALPHAV*PM
BETAV=BETAV*PM
GAMAV=GAMAV*PM
DELAV=DELAV*PM

NSA341
CALCULATING IMPROVED TAU FROM GAMMA USING THE ENTIRE THEORETICAL
 EXPRESSIONS.

```

GAM1=BS**2/5.0
GAM2=-4.0*BS*BM*DG*BO*AS/(OM*H*15.0)
GAM3=16.0*CR**2/15.0
GAM4=-3.0*BS**2/40.0
GAM5=-2.0*CR**2/5.0
GAM6=3.0*BS**2/20.0
GAM7=-BS*PN*DG*BO*AS/(5.0*H*OM)
GAM8=-2.0*HS*RM*DG*BO*AS/(5.0*H*OM)
GAM9=4.0*CP**2/5.0
GAM10=-BS**2/40.0
GAM11=-2.0*CR**2/15.0
GAM12=-BS**2*AS/(40.0*OM)
GAM13=-3.0*BS**2/20.0
GAM14=-4.0*CR**2/5.0
GAM15=3.0*BS**2*AS/(20.0*OM)
GAM16=2.0*BM*DG*BO*BS*AS/(15.0*H*OM)
GAM17=-BM*DG*BO*BS*AS/(10.0*H*OM)
GAM18=BS*BM*DG*BO*AS/(10.0*H*OM)
GAM19=-BM*DG*BO*BS*AS/(15.0*H*OM)
TA(1)=TAUAV
GAMV=GAM1+GAM2+GAM3+GAM4+GAM5+GAM16+GAM17
GAMX=GAM6+GAM7+GAM9+GAM10+GAM11+GAM13+GAM14+GAM18+GAM19
GAMY=GAM8+GAM15+GAM12
DO816I=1,100
TA(I+1)=GAMAV/((GAMV+GAMX/(1.0+OM**2*TA(I)**2)+GAMY*OM**2*TA(I)**2
1/((1.0+OM**2*TA(I)**2)**2))*PM)
TAUM(UN)=TA(I+1)
IF(ABS(TA(I+1)-TA(I)).LT.TA(I)/100.0) GO TO 815
816 CONTINUE

```

NSA342
 NSA343
 NSA344
 NSA345
 NSA346
 NSA347
 NSA348
 NSA349
 NSA350
 NSA351
 NSA352
 NSA353
 NSA354
 NSA355
 NSA356
 NSA357
 NSA358
 NSA359
 NSA360
 NSA361
 NSA362
 NSA363
 NSA364
 NSA365
 NSA366
 NSA367
 NSA368
 NSA369
 NSA370

PREDICTED TUMBLING TIME FROM DEBEYE FORMULA.

```

R15 TAUT(UN)=4.C*3.1415927*ETA*RAD**3/(1.3805E-16*TEMP*3.C)
WRITE(6,920) TAUAVB,TAUAV,ALPHAV
920 FORMAT(' TAUAVB ',E20.8,' TAUAV= ',E20.8,' ALPHAV= ',E20.8)
WRITE(6,924) BETAV,GAMAV,DELAV
924 FORMAT(' BETAV= ',E20.8,' GAMAV= ',E20.8,' DELAV= ',E20.8)
WRITE(6,932)TAUIM(UN),TAUT( UN),I
932 FORMAT(' TAUIM(UN)= ',E20.8,' TAUT(UN)= ',E20.8,' I= ',I4)
TAUAV=TAUIM(UN)
ALPHAV=ALPHAV/PM
IF(OM**2*TG**2 .LT. 1.0) GO TO 27

```

```

NSA371
NSA372
NSA373
NSA374
NSA375
NSA376
NSA377
NSA378
NSA379
NSA380

```

EVALUATING RESIDUAL LINE WIDTH FROM AVERAGE EXPERIMENTAL ALPHA (CASE 2).

```

25 RS=(ALPHAV-CA(1)*TAUAV-CB(1)/TAUAV)*2.C*H/(1.7321*G*BM)

```

```

NSA381
NSA382

```

CALCULATING DELTA CASE 2

```

DEL=BS**2*AS*TAUAV/(20.C*CM)+BS**2*AS/(10.C*OM**3*TAUAV)
BETA=CA(2)*TAUAV+CB(2)/TAUAV
GAMMA= CA(3)*TAUAV+CB(3)/TAUAV
BETA=BETA*PM
GAMMA=GAMMA*PM
DEL=DEL*PM
WRITE(6,907) RS,DEL,BETA,GAMMA
907 FORMAT(' RS= ',E20.8,' DEL= ',E20.8,' BETA= ',E20.8,' GAMMA= ',E20.8//)
GO TO 28

```

```

NSA383
NSA384
NSA385
NSA386
NSA387
NSA388
NSA389
NSA390
NSA391

```

EVALUATING RESIDUAL LINE WIDTH FROM AVERAGE EXPERIMENTAL ALPHA (CASE 1).

```

27 RS=(ALPHAV-E(1)*TAUAV)*2.C*H/(1.7321*G*BM)

```

```

NSA392

```

NSA393
NSA394
NSA395
NSA396
NSA397
NSA398
NSA399
NSA400
NSA401
NSA402

CALCULATING DELTA CASE 1

DEL=TAUAV*RS**2*AS/(10.C*DM)

BETA=F(2)*TAUAV

GAMMA=F(3)*TAUAV

BETA=BETA*PH

GAMMA=GAMMA*PM

DEL=DEL*PM

WRITE(6,908) PS,DEL,BETA,GAMMA

908 FORMAT(' PS=',E20.8,' DEL=',E20.8,' BETA=',E20.8,' GAMMA=',E20.8//)

28 CONTINUE

EVALUATING SPIN-ROTATIONAL RESIDUAL LINE WIDTH.

DFLGZ=(GPA-2.C*23)**2

DELGX=(GPEX-2.C*23)**2

DELGY=(GPEY-2.C*23)**2

RSSR=(DELGZ+DELGX+DELGY)/(9.C*TAUIM(UN))*2.C*3.1415

RSSP=R.SSR*PM

WRITE(6,929) RSSR

929 FORMAT(' RSSR= ', E20.8)

ALPHAV=ALPHAV*PM

DC 813 N1=1,4

MI=N1*2-1

LWP(MI)=ALPHAV+BETA/2.C*FLOAT(MI)+GAMMA /4.C*FLOAT(MI)**2+DEL/8.C

1*FLOAT(MI)**3

813 LWN(MI)=ALPHAV-BETA/2.C*FLOAT(MI)+GAMMA /4.C*FLOAT(MI)**2-DEL/8.C

1*FLOAT(MI)**3

LW(1)=LWP(7)

LW(2)=LWP(5)

LW(3)=LWP(3)

LW(4)=LWP(1)

LW(5)=LWN(1)

LW(6)=LWN(3)

LW(7)=LWN(5)

LW(8)=LWN(7)

NSA403
NSA404
NSA405
NSA406
NSA407
NSA408
NSA409
NSA410
NSA411
NSA412
NSA413
NSA414
NSA415
NSA416
NSA417
NSA418
NSA419
NSA420
NSA421
NSA422
NSA423
NSA424

```

WRITE(6,926)
926 FORMAT(' QUANTUM NUMBER          OBSERVED LINE WIDTH          CALC
1. LINE WIDTH ')
NSA425
NSA426
NSA427

DO 814 LI=1,8
L2=LI-1
NSA428
NSA429
NSA430
QN=FLOAT(7-2*L2)/2.0
NSA431
WRITE(6,925) QN,YR(LI,1),LW(LI)
NSA432
925 FORMAT(6X,1F4.1,22X,1E11.4,15X,1E11.4)
814 CONTINUE
NSA433
DG=ABS(DG)
NSA434
BS=ABS(BS)
NSA435
AS=ABS(AS)
NSA436
CR=ABS(CR)
NSA437
DV=ABS(DV)
NSA438

```

CALCULATION OF SECULAR PSEUDOSECULAR, AND NONSECULAR FUNCTIONS OF BETA USING THE BEST TUMBLING TIME FROM GAMMA.

```

PS1=4.0*(PM*DG*BO/H)**2/45.0
NSA440
PS2=4.0*(DV*BO)**2/15.0
NSA441
PS3=-2.0*BM*DG*BO*BS*R2*AS/(15.0*H*OM)
NSA442
PS3=-PS3
NSA443
PS4=3.0*BS**2*R2/40.0
NSA444
PS5=2.0*CR**2*R2/5.0
NSA445
PS6=BM*DG*BO*BS*R2*AS/(10.0*H*OM)
NSA446
PS6=-PS6
NSA447
PS7=(BM*DG*BO/H)**2/(15.0*(1.0+OM**2*TAU1M(UN)**2))
NSA448
PS8=(DV*BO)**2/(5.0*(1.0+OM**2*TAU1M(UN)**2))
NSA449
PS9=BS**2*R2/(40.0*(1.0+OM**2*TAU1M(UN)**2))
NSA450
PS10=2.0*CR**2*R2/(15.0*(1.0+OM**2*TAU1M(UN)**2))
NSA451
PS11=BS**2*R2*AS*(OM*TAU1M(UN))**2/(40.0*OM*(1.0+(OM*TAU1M(UN))**
NSA452
12)**2)
NSA453
PS11=-PS11
NSA454
PS12=3.0*BS**2*R2*AS/(20.0*OM*(1.0+OM**2*TAU1M(UN)**2))
NSA455
PS12=-PS12
NSA456

```

PS12=-BS*BM*DG*BO*R2*AS/(10.C*H*OM*(1.C+OM**2*TAUIM(UN)**2)) NSA457
 PS13=-PS13 NSA458
 PS14=BM*DG*BO*BS*R2*AS/(15.C*H*OM*(1.C+OM**2*TAUIM(UN)**2)) NSA459
 PS14=-PS14 NSA460
 PS15=4.C*CR**2*R2/(5.C*(1.C+OM**2*TAUIM(UN)**2)) NSA461
 PS16=-3.C*BS**2*R2*AS*OM**2*TAUIM(UN)**2/(20.C*OM*(1.C+OM**2* TAUIM(UN)**2)**2) NSA462
 PS16=-PS16 NSA463
 PS17=4.C*BS*BM*DG*BO/(15.C*H) NSA464
 PS18=-8.C*(BM*DG*BO/H)**2*AS/(45.C*OM) NSA467
 PS18=-PS18 NSA468
 PS19=16.C*CR*DV*BO/15.C NSA469
 PS19=-PS19 NSA470
 PS20=-BS**2*R2*AS/(5.C*OM) NSA471
 PS20=-PS20 NSA472
 PS21=3.C*BS**2*(2.C*R2-1.C)*AS/(40.C*OM) NSA473
 PS21=-PS21 NSA474
 PS22=BS*BM*DG*BO/(5.C*H*(1.C+OM**2*TAUIM(UN)**2)) NSA475
 PS23=-2.C*(BM*DG*BO/H)**2*AS*OM**2*TAUIM(UN)**2/(15.C*OM*(1.C+OM**2*TAUIM(UN)**2)**2) NSA476
 PS23=-PS23 NSA477
 PS24=-2.C*(BM*DG*BO/H)**2*AS/(15.C*OM*(1.C+OM**2*TAUIM(UN)**2)) NSA478
 PS24=-PS24 NSA479
 PS25=4.C*CR*DV*BO/(5.C*(1.C+OM**2*TAUIM(UN)**2)) NSA480
 PS25=-PS25 NSA481
 PS26=-BS**2*R2*AS*OM**2*TAUIM(UN)**2/(20.C*OM*(1.C+OM**2*TAUIM(UN)**2)**2) NSA482
 PS26=-PS26 NSA483
 PS27=-3.C*BS**2*R2*AS*OM**2*TAUIM(UN)**2/(10.C*OM*(1.C+OM**2*TAUIM(UN)**2)**2) NSA484
 PS27=-PS27 NSA485
 PS30=-3.C*BS**2*R2*AS/(20.C*OM*(1.C+OM**2*TAUIM(UN)**2)) NSA486
 PS30=-PS30 NSA487
 PS31=BS**2*(2.C*R2-1.C)*AS/(20.C*OM*(1.C+OM**2*TAUIM(UN)**2)) NSA488
 PS31=-PS31 NSA489
 NSA490
 NSA491
 NSA492
 NSA493

NSA494
NSA495

CALCULATION OF SECULAR, PSEUDOSFCULAR, AND NONSECULAR FUNCTIONS OF
DELTA USING THE BEST TUMBLING TIME FROM GAMMA.

NSA496
NSA497

PS32=-3.0*BS**2*AS*OM**2*TAUIM(UN)**2/(10.0*OM*(1.0+OM**2*TAUIM(UN)**2)**2)

NSA499
NSA500

PS33=BS**2*AS*(OM*TAUIM(UN)**2/(20.0*OM*(1.0+(OM*TAUIM(UN)**2)**2))

NSA501

PS33=-PS33

NSA502

PS34=3.0*BS**2*AS*OM**2*TAUIM(UN)**2/(10.0*OM*(1.0+OM**2*TAUIM(UN)**2)**2)

NSA503

TAUIM(UN)**2)

NSA504

PS34=-PS34

NSA505

PS35=3.0*BS**2*AS/(20.0*OM*(1.0+OM**2*TAUIM(UN)**2))

NSA506

PS35=-PS35

NSA507

PS36=-BS**2*AS/(10.0*OM*(1.0+OM**2*TAUIM(UN)**2))

NSA508

PS36=-PS36

NSA509

PS37=BS**2*AS/(5.0*OM)

NSA510

PS37=-PS37

NSA511

PS38=-3.0*BS**2*AS/(20.0*OM)

NSA512

PS38=-PS38

NSA513

ALSEC(UN)=(PS1+PS2+PS3)*TAUIM(UN)

NSA514

ALPSEC(UN)=(PS4+PS5+PS6)*TAUIM(UN)

NSA515

ALNSEC(UN)=(PS7+PS8+PS9+PS10+PS11+PS12+PS13+PS14+PS15+PS16)*TAUIM(UN)

NSA516

ALSEC(UN)=ALSEC(UN)*PM

NSA517

ALPSEC(UN)=ABS(ALPSEC(UN))*PM

NSA518

ALNSEC(UN)=ABS(ALNSEC(UN))*PM

NSA519

ALTOL(UN)=ALSEC(UN)+ALPSEC(UN)+ALNSEC(UN)

NSA520

RSEC(UN)=(PS17+PS18+PS19+PS20)*TAUIM(UN)*PM

NSA521

BNSEC(UN)=(PS22+PS23+PS24+PS25+PS26+PS27+PS30+PS31)*TAUIM(UN)*PM

NSA522

RPSEC(UN)=(PS21)*TAUIM(UN)*PM

NSA523

BPSEC(UN)=ARS(BPSEC(UN))

NSA524

BNSEC(UN)=ARS(BNSEC(UN))

NSA525

BTCL(UN)=BSEC(UN)+BPSEC(UN)+BNSEC(UN)

NSA526

NSA527
NSA528
NSA529
NSA530
NSA531
NSA532
NSA533
NSA534
NSA535
NSA536
NSA537
NSA538
NSA539
NSA540
NSA541
NSA542
NSA543

```

DSEC(UN)=PS37*TAU1M(UN)
DNSFC(UN)=(PS32+PS33+PS34+PS35+PS36)*TAU1M(UN)
DPSEC(UN)=(PS38)*TAU1M(UN)
DSEC(UN)=DSEC(UN)*PM
DNSEC(UN)=DNSEC(UN)*PM
DPSEC(UN)=DPSEC(UN)*PM
DTOL(UN)=DSEC(UN)+DIHSEC(UN)+DPSEC(UN)
UNK=1.0/(1.0+OM**2*TAU1M(UN)**2)
UMF=UNK*OM**2*TAU1M(UN)**2
GSEC(UN)=GAM1+GAM2+GAM3+GAM16
GPSEC(UN)=GAM4+GAM5+GAM17
GNSEC(UN)=(GAM6+GAM7+GAM8*UMF+GAM9+GAM10+GAM11+GAM12*UMF+GAM13+
1GAM14+GAM15*UMF+GAM18+GAM19)*UNK
GSEC(UN)=GSEC(UN)*TAU1M(UN)
GPSEC(UN)=GPSEC(UN)*TAU1M(UN)*PM
GNSEC(UN)=GNSEC(UN)*TAU1M(UN)*PM
GSEC(UN)=GSEC(UN)*PM

```

NSA544
NSA545
NSA546
NSA547
NSA548
NSA549
NSA550
NSA551
NSA552
NSA553
NSA554
NSA555
NSA556
NSA557
NSA558
NSA559
NSA560

```

GTOL(UN)=GSFC(UN)+GNSEC(UN)+GPSEC(UN)
WRITE(6,933) ALSEC(UN),ALPSEC(UN),ALNSFC(UN),ALTOL(UN)
933 FORMAT(' ALSEC(UN)=',E20.8,' ALPSEC(UN)=',E20.8,' ALNSFC(UN)=',
1E20.8,' ALTOL(UN)=',E20.8)
WRITE(6,934) RSEC(UN),RPSEC(UN),BNSFC(UN),BTOL(UN)
934 FORMAT(' RSEC(UN)=',E20.8,' BPSEC(UN)=',E20.8,' BNSFC(UN)=',E20.8,
1,' BTOL(UN)=',E20.8)
WRITE(6,938) GSEC(UN), GPSEC(UN), GNSEC(UN), GTOL(UN)
938 FORMAT(' GSEC(UN)=',E20.8,' GPSEC(UN)=',E20.8,' GNSEC(UN)=',
1E20.8,' GTOL(UN)=',E20.8)
WRITE(6,935) DSEC(UN),DPSEC(UN),DNSEC(UN),DTOL(UN)
935 FORMAT(' DSEC(UN)=',E20.8,' DPSEC(UN)=',E20.8,' DNSEC(UN)=',E20.8,
1,' DTOL(UN)=',E20.8)
DO 817 N2=1,4
MJ=N2*2-1
LWR(MJ)=ALTOL(UN)+BTOL(UN)/2.0*FLOAT(MJ)+GTOL(UN)/4.0*FLOAT(MJ)**2+NSA559
1+DTOL(UN)/8.0*FLOAT(MJ)**3

```

```

817 LWS(MJ)=AL(TOL(UN)-BTOL(UN))/2.C*FLOAT(MJ)+GTOL(UN)/4.C*FLOAT(MJ)**
      12-DTOL(UN)/8.C*FLOAT(MJ)**3
      LV(1)=LWR(7)
      LV(2)=LWR(5)
      LV(3)=LWR(3)
      LV(4)=LWR(1)
      LV(5)=LWS(1)
      LV(6)=LWS(3)
      LV(7)=LWS(5)
      LV(8)=LWS(7)
      DO 818 IP=1,8
818 PR(IP)=YR(IP,1)-LV(IP)
      RS1=ALPHAV-AL(TOL(UN)
NSA561
NSA562
NSA563
NSA564
NSA565
NSA566
NSA567
NSA568
NSA569
NSA570
NSA571
NSA572
NSA573

```

EVALUATING THE RESIDUAL LINE WIDTH FROM THE AVERAGE OF THE
RESIDUAL LINE WIDTHS OBTAINED AFTER THE THEORETICAL CONTRIBUTIONS
OF THE ALPHA, BETA, GAMMA AND DELTA TERMS HAD BEEN SUBTRACTED.

```

      RS2=(RR(1)+RR(2)+RR(3)+RR(4)+RR(5)+RR(6)+RR(7)+RR(8))/8.C
      DO 819 JP=1,8
      LVW(JP)=LV(JP)+RS2
819 LVX(JP)=LV(JP)+RS1
      WRITE(6,942) PSI
842 FORMAT(' PSI= ',E20.8)
      WRITE(6,940)
840 FORMAT(' Q.N. OBS. LINEWIDTH      RS2      CALC. LINEWIDTH 2  CALC
      1. LINEWIDTH 1. ')
      DO 820 L3=1,8
      L4=L3-1
      QS=FLOAT(7-2*L4)/2.C
      WRITE(6,941) QS,YR(L3,1),RR(L3),LVW(L3),LVX(L3)
841 FORMAT(' 2X,1F4.1,4X,1E11.4,2X,1E11.4,6X,1E11.4,9X,1E11.4)
820 CONTINUE
      GO TO 822
821 STOP
      END
NSA574
NSA575
NSA576
NSA577
NSA578
NSA579
NSA580
NSA581
NSA582
NSA583
NSA584
NSA585
NSA586
NSA587
NSA588
NSA589
NSA590
NSA591

```